



A University of Sussex PhD thesis

Available online via Sussex Research Online:

<http://sro.sussex.ac.uk/>

This thesis is protected by copyright which belongs to the author.

This thesis cannot be reproduced or quoted extensively from without first obtaining permission in writing from the Author

The content must not be changed in any way or sold commercially in any format or medium without the formal permission of the Author

When referring to this work, full bibliographic details including the author, title, awarding institution and date of the thesis must be given

Please visit Sussex Research Online for more information and further details

**INVESTIGATING THE DEREGLATION OF HOST CELL GENES BY EPSTEIN-
BARR VIRUS NUCLEAR ANTIGENS**

By

Hildegonda F. Veenstra

Summited in total fulfilment of the requirements of the degree of

Doctor of Philosophy

Department of Biochemistry

School of Life Sciences

University of Sussex

September 2019

Declaration

I hereby declare that this thesis has not been and will not be, submitted in whole or in part to another University for the award of any other degree.

Hildegonda F Veenstra

UNIVERSITY OF SUSSEX

Hildegonda F. Veenstra

PhD in Biochemistry

INVESTIGATING THE DEREGLATION OF HOST CELL GENES BY EPSTEIN-BARR VIRUS
NUCLEAR ANTIGENS

SUMMARY

Epstein-Barr virus (EBV) immortalises B-lymphocytes and is associated with the development of various human malignancies. The EBV transcription factors, Epstein-Barr nuclear antigens (EBNA)2, 3A, 3B and 3C drive B cell immortalisation through epigenetic reprogramming of cellular genes.

Pathway analysis showed the B-cell receptor (BCR) signalling pathway to be enriched for EBNA-bound genes. We identified EBNA binding sites at promoter-proximal elements near BCR genes *CD79A* and *CD79B* and confirmed they are repressed by EBNA2. We found EBNA2 disrupts binding of transcription activator EBF1 at the *CD79B* promoter, correlating with decreased levels of acetylated histone H3, an active chromatin mark. *NFATC1* and *NFATC2*, downstream effectors of the BCR signalling pathway, were also identified as EBNA target genes. We confirmed EBNA3B and 3C as negative regulators of *NFATC1* and *NFATC2*, and EBNA2 as a negative regulator of *NFATC1*. However, we could not confirm direct binding by the EBNAs indicating repression may result from upstream deregulation. BCR stimulation results in release of the second messenger calcium. We found that Ca^{2+} release following BCR activation is significantly reduced in the presence of EBNA2.

We also investigated how EBNA2 activates oncogene *MYC* and how EBNA3A and 3C silence pro-apoptotic gene *BCL2L11*; two key genes involved in growth regulation and lymphoma development. We found EBNA2 activation of *MYC* induced chromatin restructuring of the 3Mb *MYC* locus differently from 'normal' B cell activation via CD40; EBNA2 activation increased upstream, whereas CD40 activation increased downstream enhancer-promoter interactions. Additionally, EBNA2 recruits SWI/SNF to the *MYC* promoter where it is required to establish enhancer-promoter interactions. At *BCL2L11* we showed EBNA3A and 3C disrupt enhancer-promoter interactions leading to PRC2 recruitment across the enhancer hub and deposition of the H3K27me3 silencing mark.

Taken together these data shed light on the pathways and mechanisms through which EBV immortalises B cells and promotes lymphoma development.

Dedication

I dedicate this work to my late father Gauke Eize Veenstra. You gave me the drive and motivation to pursue my passion in science and for that I am thankful. I love you and I wish you were still with us.

Acknowledgements

I would like to thank Professor Michelle West for her endless support, patience and guidance throughout my studies. I would also like to thank all the West, Sinclair and Mancini lab members past and present, in particular Sarika, Yaqi, Jake, Rajesh, Leanne, Barak and Rob for all their help and support. A special thank you to David and Helen who have taught me so much and were always there to offer help, advice and a shoulder to cry on!

A big thank you to my partner Ben, for supporting me through all the ups and downs, and to my Mum for encouraging and believing in me. A special thank you to my brother Sjoerd for making me laugh and keeping me entertained.

Publication arising from this work

Wood, C.D., [Veenstra, H.](#), Khasnis, S., Gunnell, A., Webb, H.M., Shannon-Lowe, C., Andrews, S., Osborne, C.S. & West, M.J., 2016. *MYC* activation and *BCL2L1* silencing by a tumour virus through the large-scale reconfiguration of enhancer-promoter hubs. *eLife*, 5, e18270

Abbreviations

3C	Chromosome Conformation Capture
4C	Circularised Chromosome Conformation Capture
BCR	B cell Receptor
BL	Burkitt's Lymphoma
B2M	β -microglobulin
ChIP	Chromatin Immunoprecipitation
Seq	Sequencing
Cp	C Promoter
CTD	C-terminal Domain
DBD	DNA binding domain
DLBCL	Diffuse Large B cell Lymphoma
EBER	EBV encoded RNA
EBF-1	Early B cell Factor 1
EBNA	Epstein-Barr Nuclear antigen
EZH2	Enhancer of Zeste homolog 2
GAPDH	Glyceraldehyde 3-phosphate dehydrogenase
GC	Germinal Centre
GTF	General Transcription Factor
H3Ac	Histone H3 Acetylation
H3K27Ac	Histone H3 Lysine 27 Acetylation
H3K27Me3	Histone H3 Lysine 27 Tri-methylation
HAT	Histone Acetyltransferase
HDAC	Histone Deacetylase
HIV	Human immunodeficiency virus
HL	Hodgkin's Lymphoma
HMT	Histone methyltransferase
IM	Infectious mononucleosis
LCL	Lymphoblastoid Cell Line
LMP	Latent membrane protein
NFAT	Nuclear Factor of activated T cells
OriP	Origin of replication
PCR	Polymerase Chain Reaction
PIC	Pre-initiation complex
PLC γ 2	Phospholipase C gamma 2
Pol II	RNA polymerase II
PTLD	Post-transplant lymphoproliferative Disease
Qp	Q promoter
QPCR	Quantitative Polymerase Chain Reaction
RBPJ κ	Recombination signal binding protein for immunoglobulin Kappa J region
TAD	Transactivation Domain
TAF	TBP associated factor
TBP	TATA-box binding protein
TF	Transcription factor
Wp	W promoter

Table of Contents

1. Introduction.....	1
1.1 Regulation of transcription	1
1.1.1 RNA Polymerase II recruitment and regulation.....	1
1.1.2 Chromatin structure and its regulation	4
1.1.3 Transcriptional regulation through long range enhancers	10
1.2 B cell development.....	14
1.2.1 Early B cell development.....	14
1.2.2 B cell maturation	20
1.3 B cell Receptor Signalling	21
1.3.1 BCR signal initiation	24
1.3.2 BCR signal propagation	25
1.3.3. NFAT family of transcription factors	26
1.4 Epstein Barr Virus	28
1.4.1 EBV infection of B cells <i>in vitro</i>	29
1.4.2 EBV latent gene expression.....	30
1.4.3 EBV persistence <i>in vivo</i>	33
1.4.4 EBNA1	34
1.4.5 EBNA2	35
1.4.6 EBNA3 Family	37
1.4.7 LMP1	40
1.4.8 LMP2	41
1.4.9 Diseases associated with EBV.....	42
1.5 Aims	46
2. Materials and Methods	47
2.1 Cell Culture.....	47
2.1.1 Media and supplements.....	47
2.1.2 Cell line maintenance.....	48
2.1.3 Freezing Cells	50
2.1.4 Thawing Cells	50
2.1.5 Haemocytometer cell counting	50
2.1.6 Harvesting cells.....	51
2.1.7 Transient Transfection	51
2.1.8 siRNA knockdown	53

2.1.9	Actinomycin D mRNA stability assay.....	53
2.2	Biochemistry	53
2.2.1	Reagents and Buffers.....	54
2.2.2	Preparation of total cell lysate	54
2.2.3	SDS-PAGE	55
2.2.4	Western Blot.....	55
2.2.5	Stripping a Western Blot	56
2.2.6	Dual Luciferase Assay.....	56
2.3	Molecular Biology.....	56
2.3.1	Reagents and Buffers	57
2.3.2	RNA isolation	58
2.3.3	cDNA Synthesis.....	58
2.3.4	Q-PCR	59
2.3.5	Chromatin Immunoprecipitation (ChIP).....	60
2.3.6	Circularised Chromatin Conformation Capture (4C).....	62
2.3.7	Chromatin Conformation Capture (3C).....	66
2.3.8	Agar plates.....	68
2.3.9	Bacterial Cell Transformation	68
2.3.10	Glycerol Stocks.....	68
2.3.11	Caesium Chloride (CsCl) DNA Preparation	68
3.	Transcriptional regulation of <i>CD79A</i> and <i>CD79B</i> by EBNA2	71
3.1	Introduction	71
3.2	<i>CD79A</i> and <i>CD79B</i> are repressed by EBNA2	80
3.3	Promoter-proximal EBNA2 binding overlaps with EBF-1 and RBPJk binding sites at <i>CD79A</i> and <i>CD79B</i>	82
3.4	EBNA2 hinders EBF-1 mediated activation of <i>CD79B</i> in Luciferase reporter assays.....	87
3.5	<i>CD79B</i> repression by EBNA2 occurs at a transcriptional level	93
3.6	EBNA2 activation disrupts EBF-1 binding and histone acetylation at the <i>CD79B</i> promoter.	94
3.7	EBNA2 activation leads to reduced NFAT activation <i>in vivo</i>	99
3.8	Conclusion.....	102
4.	Regulation of the B-cell receptor signalling molecules <i>NFATC1</i>, <i>NFATC2</i> and <i>PLCy2</i> by EBV transcription factors.	103
4.1	Introduction	103
4.2	<i>NFATC1</i> is repressed by EBNA2 at the mRNA level	109

4.3 <i>NFATC1</i> and <i>NFATC2</i> are repressed by EBNA3B and EBNA3C at the mRNA and the protein level.....	113
4.4 EBNA2 and EBNA3 binding is not detected at <i>NFAT</i> regulatory sites.	125
4.5 EBNA2 regulation of <i>PLCγ2</i> is cell line specific.....	132
4.6 Conclusion.....	133
5. EBV latent proteins regulate cellular genes <i>MYC</i> and <i>BCL2L11</i> through large scale reorganisation of enhancer-promoter interactions.	137
5.1 Introduction	137
5.2 EBV infection leads to <i>MYC</i> upregulation in primary B-cells.	140
5.3 EBV infection of naïve B-cells results in a different pattern of chromatin reorganisation to that induced by physiological B-cell activation.....	141
5.4 The SWI/SNF ATPase BRG1 is required for <i>MYC</i> upstream enhancer-promoter interactions.	144
5.5 Inhibition of EZH2 by UNC1999 results in de-repression of the <i>BCL2L11</i> enhancer hub	147
5.6 Conclusion.....	150
6. Discussion.....	154
6.1 Deregulation of the BCR signalling pathway by the EBNA2 and EBNA3 proteins.....	154
6.2 Survival implications for EBV.....	163
6.3 Regulation of cellular genes by EBNA2 and EBNA3 proteins through reorganisation of long distance enhancer-promoter interactions.	166
6.4 Future work.....	171
7. Bibliography	172
8. Appendices.....	187
8.1 Cell line summary	187
8.2 Plasmids used for transient transfections	189
8.3 Antibodies used for Western Blot	190
8.4 Antibodies used for CHIP-QPCR.....	190
8.5 Q-PCR Primers used for mRNA analysis.....	191
8.6 Q-PCR Primers used for CHIP-QPCR.....	192
8.7 PCR primers used for 4C and 3C.....	193
8.8 The 4C technique workflow	194
8.9 3C technique workflow.....	195

1. Introduction

1.1 Regulation of transcription

Transcription of protein coding genes in eukaryotes is carried out by a conserved initiation complex consisting of RNA Polymerase II (Pol II) and general transcription factors (GTFs) and begins at promoter DNA. Transcription regulation is important for every aspect of cellular function; from growth and differentiation to cell survival and apoptosis. The strict regulation of gene transcription is necessary to ensure the cell is able to correctly differentiate, maintain cell identity and respond to environmental changes. Transcription factors bind to DNA within gene regulatory elements, such as promoters and enhancers of genes under their control. They are attracted to these genes via specific DNA-binding motifs, or interaction with other TFs or chromatin. Once bound TFs either activate or repress transcription activation by recruiting cellular machinery required for gene transcription, chromatin remodelling, or histone modification (reviewed in Stadhouders et al., 2019).

Regulation occurs at different stages in the transcription cycle; however regulation at the initiation stage is key to controlling gene expression. Regulation at this stage involves both Pol II recruitment and the opening up of chromatin to enable the polymerase to access the DNA template.

1.1.1 RNA Polymerase II recruitment and regulation

Eukaryotic Pol II alone is unable to bind promoter DNA and transcription initiation depends on the assembly of a complex between Pol II and the GTFs, TFIIB, TFIID, TFIIE,

TFIIF and TFIIH to form the Preinitiation complex (PIC). The first step in the assembly of the PIC is the binding of TFIID to the TATA-element; a regulatory sequence located roughly 30 bp upstream of the transcription start site (TSS) in humans. The TFIID complex comprises a sequence-specific TATA box-binding protein (TBP) along with 13-14 TBP-associated factors (TAFs) (reviewed in (Haberle and Stark, 2018)). Many eukaryotic genes do not contain a TATA-box, and at TATA-less promoters TBP binds to the initiator (Inr) motif suggesting that the overall function and composition of the PIC is similar at TATA and TATA-less promoters (Blair et al., 2012, Haberle and Stark, 2018). The binding of TBP to the TATA-element induces a bend in the DNA, bringing the regions upstream and downstream of the TATA element in closer proximity and providing a platform for interactions with other transcription factors (Nikolov et al., 1992). The TBP-DNA interactions can be stabilised by the binding of TFIIA (K Lee et al., 1992). The initial binding by TFIID and TFIIA is followed by TFIIB binding and Pol II recruitment. TFIIB binds to TFIIA and the DNA region upstream and downstream of the TATA element. Like TFIIA, TFIIB has a stabilising effect on the TBP-TATA interactions at promoters with suboptimal binding conditions (reviewed in Haberle and Stark, 2018). Once TFIIB is bound it recruits the TFIIF-Pol II complex, followed by recruitment of TFIIE and TFIIH to complete the PIC. TFIIF helps Pol II target TSS sequences and prevents non-specific Pol II DNA interactions. It also helps stabilise TFIIB within the PIC, stimulates phosphodiester bond formation and early RNA synthesis and suppresses Pol II pausing. In addition, it also helps stabilise the transcription bubble (reviewed in Sainsbury et al., 2015). TFIIE interacts directly with Pol II and is involved in promoter melting. The TFIIH complex contains a protein kinase and a bi-directional helicase essential for transcription initiation and promoter clearance. The TFIIH ATP-dependent

helicase subunits XPD/Ssl2 unwind the DNA and together with TFIIE they form the open promoter complex required for transcription initiation. TFIIE also stimulates the kinase activity of TFIIH, which catalyses the phosphorylation of the carboxy-terminal repeat domain (CTD) of the largest subunit of Pol II, essential for promoter clearance, transcription initiation and elongation (reviewed in Svejstrup et al., 1996). The PIC dissociates after Pol II has left the promoter.

Transcription initiation by Pol II is directly regulated by a multi-subunit mediator complex and association with mediator is required for successful PIC formation. Mediator consists of 26 polypeptides in humans and many of its core polypeptides are highly conserved (reviewed in Allen and Taatjes, 2015). Mediator interacts with activators and binds directly to the CTD of Pol II. Mediator was initially identified as a co-activator of transcription that acts as a “molecular bridge” to enable contacts between DNA-binding TF and Pol II and the GTF (Myers et al., 1999). Mediator plays key roles in PIC assembly by facilitating the recruitment of Pol II to the promoter and Pol II re-initiation by allowing the binding of another Pol II enzyme after transcription initiation and promoter escape (Allen and Taatjes, 2015). In addition to being a co-activator of transcription, mediator is also involved in negative gene regulation through its reversible association with protein kinase Cyclin-dependent kinase 8 (CDK8). While the precise mechanism of repression by mediator-CDK8 complexes is unclear, the binding of CDK8 and Pol II to mediator appear to be mutually exclusive. Therefore, CDK8 is able to block transcription initiation (Näär et al., 2002). Further functions of mediator include the enabling of long-range enhancer-promoter interactions and may also include maintaining nucleosome free regions at key regulatory sites (Ansari et al., 2014, Kagey et al., 2010).

1.1.2 Chromatin structure and its regulation

DNA in eukaryotic cells is tightly wrapped around nucleosomes and densely packed into a structure called chromatin. A single nucleosome consists of an octamer containing two copies of each core histone protein H2A, H2B, H3 and H4. A basic unit of chromatin consists of the core nucleosome with ~147bp of DNA wrapped twice around it and each nucleosome is separated by a 10-60bp of linker DNA. This gives rise to a chromatin fibre that is ~10nm in diameter and is also known as a “beads-on-a-string” arrangement (reviewed in Peterson and Laniel, 2004). This arrangement is then folded in to more condensed zig-zag formation to form ~30nm thick fibres through nucleosomal interactions (Staynov, 2000). The 30nm fibres undergo higher levels of super-coiling in vivo (Daban, 2000). Although condensed chromatin precludes the transcription machinery from accessing DNA promoter elements, as well as impeding DNA replication and repair, it does provide an opportunity for gene regulation.

Highly condensed chromatin is usually associated with gene repression. Chromatin structure has to be dynamic in order to accommodate transcription and DNA replication and repair and while the core nucleosome is quite compact, each histone has a highly conserved, unstructured N-terminal histone tail that protrudes out from the nucleosome core. The histone tails contain multiple amino acid residues that are targets for covalent post-translational modifications by specific enzymes that can establish ‘active’ and ‘repressive’ marks. These post-translational modifications form the basis of a histone ‘code’ where patterns of histone marks are interpreted by cellular factors leading to a specific biological response (Peterson and Laniel, 2004). A further layer of regulation is added by ‘cross talk’ between different histone modifications to fine tune control through competitive antagonism between

modifications, or interdependence of different modifications (Bannister and Kouzarides, 2011). Some histone markers may be epigenetically inherited (Huang et al., 2013).

There are at least eight different types of modifications found on histone tails, but the major ones include acetylation, methylation, phosphorylation and ubiquitination. Histone marks can affect the chromatin structure in different ways; two well-characterised mechanisms involve the disruption of contacts between nucleosomes, or between histones and DNA leading the unravelling of chromatin by affecting the charge on the histone tail or the recruitment of non-histone proteins, such as chromatin modellers. Both mechanisms serve to modify the chromatin structure and regulate processes such as transcription, DNA replication and repair (reviewed in Kouzarides, 2007).

1.1.2.1 Histone Acetylation

Acetylation of lysine residues on histone tails is localised at the 5' end and promoter regions of genes and is generally associated with regions of active transcription (Workman, 2006). Since the discovery of histone acetylation in 1964 (Allfrey et al., 1964) acetylation of lysine residues has been shown to be highly dynamic and regulated by two different families of enzymes; the histone acetyl transferases (HATs) and histone deacetylases (HDACs).

HATs catalyse the transfer of an acetyl group from the co-factor acetyl CoA to the lysine residues of histone tails. Acetylation can occur at multiple lysine residues where the distinct pattern of acetylation either provides binding sites for the recruitment of gene activators or repressors, or the accumulation of acetylated lysine residue alters

the net charge on the nucleosome changing the folding properties and structure of the chromatin rendering the DNA more or less accessible (Kurdistani et al., 2004). There are two types of HAT; Type A and Type B. Type B HATs are cytoplasmic and acetylate newly formed histone H4 at K5 and K21 as well as certain sites within H3. This pattern of acetylation is important for chromatin assembly, after which it is removed (Parthun, 2007). Type A HATs are nucleosomal and can be classified into three different families; GNAT, MYST and CBP/p300 (Sterner and Berger, 2000). Each family of HATs acetylates selected lysine residues; GNAT family members PCAF and GCN5 can acetylate H3 (K9, K14 and K18) and CBP/p300 can acetylate lysine residues on all four histones, H3 (K14, K18 and K27), H4 (K5, K8), H2A (K5) and H2B (K12, K15) (Kouzarides, 2007). CBP/P300, GCN5 and PCAF also contain a bromodomain for acetyl-lysine recognition (Haynes et al., 1992). Type A HATs are often found in large multi-protein complexes. In these complexes the non-catalytic subunits play an important role in regulating the activity and substrate specificity of catalytic subunits (Yang and Seto, 2007).

Deacetylation of acetylated lysine residues is carried out by HDACs and is associated with gene repression. HDACs have been classified into three distinct families; Class I (HDAC1, 2, 3, 8) and Class II (HDAC4, 5, 6, 7, 9, 10) histone deacetylases and Class III NAD –dependent enzymes of the Sir family (HDAC11) (Yang and Seto, 2008). HDACs are involved in a number of signalling pathways and HDAC1 and HDAC2 interact with each other to form the catalytic core in a number of repressive complexes, such as Co-REST (co-repressor of RE1 silencing transcription factor) and NuRD (Nucleosome remodelling and deacetylating) (Grozingler and Schreiber, 2002). HDACs show low substrate specificity and they often appear to deacetylate multiple lysine residues,

although this has been difficult to confirm *in vivo* as HDACs are typically part of a much larger multiprotein complex (reviewed in Yang and Seto, 2007).

There is considerable interplay between HATs and HDACs and other regulators. This interplay can occur through a number of different mechanisms. For example, acetylation of a lysine residue can preclude or promote other histone modifications. This mechanism has been well studied in fission yeast, where deacetylation primes lysine residues for methylation and subsequent heterochromatin formation (Yamada et al., 2005). Hypo-acetylation is also a prerequisite for heterochromatin formation and gene silencing in mammals (Zaratiegui et al., 2007). Acetylation of a specific lysine residue can also affect modification of neighbouring serine residues, for example H3K9 acetylation promotes H3S10 phosphorylation (Li et al., 2006). Lastly as HATs and HDACs act as part of a larger complex they are often involved in other catalytic activities, for example PCAF and P300 possess intrinsic E3 and E4 ubiquitin ligase activity, GCN5 is associated with Ubiquitin protease 8, and Lysine-specific demethylase 1 and HDAC1/2 are present in the same multiprotein complex, while HDAC3 is associated with a Jumonji demethylase (reviewed in Yang and Seto, 2007).

1.1.2.2 Histone methylation

Histone methyltransferases catalyse the transfer of one, two or three methyl groups to specific lysine or arginine residues on histone proteins. Lysine methylation is associated with both transcriptional activation and repression. Lysine methyltransferases have more specificity than acetyltransferases. Each methyltransferase usually modifies a specific lysine residue on a single histone (Bannister and Kouzarides, 2005). Methylation of H3K4, H3K36 and H3K79 is

associated with transcriptional activation and H3K36 and H3K79 methylation is associated with active genes. Methylation of H3K9, H3K27 and H4K20 is linked to repression of transcription. H3K9me has been implicated in the formation of silent heterochromatin. Repression by H3K9me involves recruitment of methyltransferase SUV39H1/H2 and HP1 to the promoters of repressed genes which leads to the compaction of chromatin through interactions with other co-repressors such as RB (retinoblastoma protein) and KAP1 (KRAB –associated protein 1) (reviewed in Kouzarides, 2007). Tri-methylation of H3K27 is catalysed by the polycomb repressive complex 2 (PRC2) through its SET-domain containing subunit EZH2 resulting in chromatin compaction and gene silencing (Shi et al., 2017). EZH2 closely associates with zinc-finger protein SUZ12 and the WD40 protein EED to form the core complex necessary for PRC2 catalytic function (reviewed in Laugesen et al., 2016). Deregulation of EZH2 has been identified as a driver of tumorigenesis. EZH2 is over-expressed several cancer types, such as lung, breast, colon as well as sarcomas and lymphomas. These high levels of EZH2 expression often correlate with advanced cancers and poor prognosis. Therefore the catalytic activity of PRC2 is now an important target for therapeutic treatments (reviewed in Shi et al., 2017).

Methyl groups can be removed from histones by specific demethylases. 20 human lysine residue demethylases (KDMs) have been identified and they can be grouped into two subfamilies based on sequence homology and catalytic activity. The KDM1 (or lysine specific demethylase, LSD) subfamily are related to the monoamine oxidases and use the co-substrate Flavin Adenine dinucleotide (FAD) during catalysis of demethylation (reviewed in Thinnes et al., 2014). For example, KDM1A catalyses the removal of mono and di-methylated H3K4. The second subfamily is the JmjC domain

containing KDMs (KDM2-7) which catalyse demethylation of mono-, di- and trimethylated lysines at multiple sites using 2-oxoglutarate (2-OG) and dioxygen as co-substrates and Fe(II) as a co-factor (Walport et al., 2012). KDM1A is overexpressed in leukaemia and solid tumours and the JmjC KDMs are also overexpressed in various types of cancer cell (Shi, 2007, Hayami et al., 2011, Harris et al., 2012, Hoffmann et al., 2012) making them important therapeutic targets.

Arginine methylation, like lysine methylation is associated with transcriptional activation or repression. Arginine can be mono-, or di-methylated and is catalysed by protein arginine methyltransferases (PRMTs) which are recruited to the gene promoters by transcription factors. Arginine methylation cannot be reversed by enzymes. It is instead removed through deimination, a process that involves the conversion of a mono-methylated arginine to a citrulline. In mammals this conversion is catalysed by PADI4, however the PADI4 reaction does not regenerate an unmodified arginine. Deimination in effect, counters the activation effects of arginine methylation as citrulline prevents arginine residues from being methylated (Cuthbert et al., 2004, Wang et al., 2004).

1.1.2.3 ATP- Dependent Chromatin Remodellers

Chromatin remodelling involves the dynamic modification of chromatin structure to allow transcription factors access to gene promoters and other regulatory elements. Chromatin remodelling can involve histone tail modifications as previously described, or it can involve the action of chromatin remodelling complexes that use the energy released from ATP-hydrolysis to move histones along, or eject histones to expose the DNA and enable binding of transcription factors to gene promoters (Becker and Hörz,

2002). ATP-dependent chromatin remodelling complexes belong to the SF2 superfamily and Snf2 family of DNA and RNA helicases and can be divided into four subfamilies: imitation switch (ISWI), chromodomain helicase DNA-binding (CHD), switch/sucrose non-fermentable (SWI/SNF) and INO80 and SWR1 family. Each subfamily is recruited through transcriptional activators or through their individual domains and each subfamily uses distinct enzymatic mechanisms to reorganise chromatin structure, move or eject nucleosomes. For example, the SWI/SNF remodeller contains a C-terminal bromodomain facilitating recruitment to acetylated promoter elements marked for activation by HATs and specialises in repositioning or ejecting nucleosomes and evicting histone dimers (reviewed in Clapier et al., 2017). The ISWI family are characterised by a C-terminal SANT domain next to a SLIDE domain which together form a recognition domain able to bind to unmodified histone tails and DNA. ISWI specialises in optimising nucleosome spacing to facilitate chromatin compression and gene repression (Corona and Tamkun, 2004). A characteristic feature of the CHD family is an N-terminal tandem chromodomain. CHD remodellers slide or eject nucleosomes and are associated with both activation and repression of transcription (Denslow and Wade, 2007). INO80 remodellers form a large complex and are characterised by a split ATPase domain with a long insertion in the middle. INO80 promotes transcription and SWR1 is involved restructuring chromatin by removing damaged H2A histones; it removes H2A-H2B dimers and replaces them with a dimer containing a H2A variant, H2A.Z-H2B (van Attikum et al., 2007).

1.1.3 Transcriptional regulation through long range enhancers

Complex metazoan genomes contain regulatory DNA elements that can be categorised into two main groups; enhancers and silencers. Enhancers are modular DNA elements

that contain binding sites for TFs. They activate their target genes by interacting with the gene promoter, often over great distances. Recruitment of the PIC to the core promoter located near the TSS is sufficient to initiate transcription. However, transcription driven by the promoter, in the absence of enhancer elements is often weak and constitutive enhancers provide responsive regulation and enable high level transcription (Shlyueva et al., 2014). Silencers suppress gene expression by binding repressors or by acting as insulators to confine specific regions within chromatin boundaries. The interplay between gene promoters, enhancers, silencers and epigenetic modifications is used to fine-tune gene expression during development and differentiation (Kolovos et al., 2012).

The first enhancer was identified over 35 years ago as a 72bp sequence of the SV40 virus genome. It was able to enhance transcription of a reporter gene in HeLa cells by over a hundred fold (Banerji et al., 1981). Shortly after the initial discovery, more enhancer elements were identified in the immunoglobulin heavy chain locus (Neuberger, 1983, Gillies et al., 1983, Banerji et al., 1983). A functional hallmark of enhancers is their ability to act independently of distance and orientation to their target genes (Shlyueva et al., 2014). Enhancers recruit specific TFs through their DNA motifs. The bound TF will recruit co-activators or co-repressors depending on the status of the enhancer or the gene promoter. Active enhancers tend to be devoid of nucleosomes so that the DNA is accessible to TFs, whereas the nucleosomes flanking the active enhancer often contain histone tail modifications such as H3K4me and H3K27ac, typical markers of active chromatin. Enhancers can be located up to 2Mb upstream or downstream from the promoter. Chromatin looping brings the enhancer and promoter into close proximity of one another allowing active enhancers to interact

with its target promoter by binding to the PIC, or tethering elements near the promoter to influence the rate of transcription. These interactions have been shown using chromatin conformation capture (3C) and its successors 4C, 5C and Capture Hi-C (Riethoven, 2010). Another feature of enhancers is that they are able to maintain their function independently of promoter context, for example, enhancers placed into a reporter construct will still be able to activate the promoter. Enhancers can contribute additively to gene expression, or their contribution can be partly redundant (Shlyueva et al., 2014). In addition to enhancers, there are also regulatory sites that have been characterised as super-enhancers. A super-enhancer can be defined as clusters of enhancer sites bound by multiple transcription factors including a high density of mediator and chromatin regulators, or are enriched for active chromatin marks and like enhancers they can regulate gene transcription (Khan et al., 2018). Super-enhancers can act as switches to determine cell identity and fate (Whyte et al., 2013).

The functional opposite of activating enhancers are silencers. Silencers are DNA elements that confer downregulation of gene expression. Two classes of silencers have been identified. Firstly, silencer elements, which are short, position independent motifs bound with negative transcription factors that actively interfere with PIC assembly. These elements are normally found upstream of the TSS. Secondly, negative regulatory elements (NREs), which are position-dependent elements that passively prevent the binding of TF to their regulatory motifs. They are found both upstream and downstream of the TSS and within introns and exons (reviewed in Riethoven, 2010).

Enhancers and silencers can act on more than one gene often at large distances, which can lead to unwanted interactions. Erroneous interaction can be blocked by regulatory

DNA elements called insulators. There are two types of chromatin insulator; barrier insulators and enhancer-blocking insulators. Barrier insulators lie on the border between open chromatin (euchromatin) and closed chromatin (heterochromatin) to prevent the spread of heterochromatin to neighbouring domains thereby preventing heterochromatin mediated silencing (Riethoven, 2010). Enhancer-blocking insulators interfere with the interaction between enhancers and promoters and protect the gene against inappropriate activation (Gaszner and Felsenfeld, 2006). Various studies have shown that enhancer-blocking activity is dependent on transcription factor CTCF binding to the insulator element (reviewed in Phillips and Corces, 2009). CTCF insulator function has been well characterised in the chicken β -globulin locus and in the imprinted IGF2/H19 locus in human and mouse. The β -globulin gene region and its dedicated enhancer are flanked by CTCF insulators separating them from neighbouring heterochromatin to prevent heterochromatisation (Bell et al., 1999, Saitoh et al., 2000). Enhancer blocking by CTCF is demonstrated at the IGF2/H19 locus, where CTCF binds to the imprinted control regions (ICR) of the maternal allele blocking access of a distal enhancer to the IGF2 promoter, effectively silencing its expression. The ICR on the paternal allele is methylated which prevents CTCF binding, and allows the distal enhancer to interact with the IGF2 promoter to activate expression (reviewed in Ghirlando et al., 2012). These studies show that CTCF insulators play an important role in gene regulation.

CTCF is also a key regulator of 3D chromatin structure and acts as a looping factor establishing chromatin loops that can prevent long-range enhancer-promoter interactions by isolating them on separate loops, or establishing loop formation that can bring enhancers and promoters in closer proximity to each other. High throughput

3C analysis by Dixon et al (2012) has shown that the genome can be divided into topologically associated domains (TADs) where CTCF demarcated individual TAD boundaries. They showed that contacts within each TAD were strong, but contacts between different TADs were weak, consistent with the ability of CTCF to block interactions (Dixon et al., 2012). In a separate study where CTCF was depleted they observed a reduction of intradomain contacts and an increase in interdomain interactions, implicating CTCF in the formation and regulation of long range chromatin interaction (Zuin et al., 2014). Cohesin has been shown to co-localise with CTCF and is essential for the stabilisation of loop formation mediated by CTCF and for CTCF insulator function (Ghirlando et al., 2012).

1.2 B cell development

Cell-fate decisions are largely driven by sequential activation of lineage specific transcription factors. The transcriptional control of early B-cell development has been well-studied and is important in understanding the mechanism of EBV driven immortalisation of B-cells.

1.2.1 Early B cell development

B cells derive from Haematopoietic stem cells. (HSCs). HSCs are multipotent and self-renewing and they develop into other blood cells. HSCs differentiation and lineage commitment begins in the bone marrow and whether they develop into myeloid cells or lymphoid cells, such as B cells or T cells, depends on a carefully orchestrated pattern of gene expression. There are many TFs involved in B cell development and the focus

here will be on those crucial for driving B-cell lineage decisions that are relevant to this work in relation to EBV TF function and B cell immortalisation.

1.2.1.1 PU.1

The E2F family transcription factor PU.1 is required for the development of both myeloid and lymphoid cells. PU.1 expression is essential for the generation of multipotent progenitor cells from HSCs as it regulates the expression of factors required to guide B cells through key developmental checkpoints (Hagman, 2015). For example, in the absence of PU.1, the interleukin-7 receptor- α (IL-7R α) is not expressed. IL-7R α is involved in the regulation of lymphocyte development and is crucial for the differentiation of common lymphoid progenitors (CLPs) into early B lymphoid progenitors (BLPs) (Miller et al., 2002). In early progenitors branching into lymphoid lineages is regulated by TFs such as PU.1, Runx1, Ikaros and E2A (Figure 1.1). This expression of a subset of genes required to make cell fate decisions is known as lineage priming. The role of PU.1 in lineage priming involves its action as a pioneer factor to induce nucleosome remodelling to allow deposition of H3K4me, a marker of poised transcriptional enhancers (Heinz et al., 2010). The poised enhancers will be activated by other temporally regulated TF's further downstream in the B cell development process (Hagman, 2015). Lineage fate decisions by PU.1 are dose dependent; low levels of PU.1 promote B cell development, and high levels of PU.1 promote myeloid cell development (DeKoter and Singh, 2000). Levels of PU.1 are controlled through transcriptional repression of *SPI1* (the gene encoding PU.1) by Gfi1, or by lengthening of the cell cycle in myeloid cells to allow PU.1 levels to accumulate (Kueh et al., 2013)). Along with PU.1, Ikaros is also essential for the generation of lymphoid lineages. Ikaros null mice fail to produce any B, T or NK cells suggesting

Ikaros acts in early lymphoid progenitors. Also, in the absence of Ikaros lymphoid primed multipotent progenitors (LMPP) do not differentiate into common lymphoid progenitors (CLP), but instead show a pattern of gene expression that promotes myeloid cell development. Ikaros drives expression of Gfi1. Gfi1 represses PU.1 expression in MPPs which results in low levels of PU.1 promoting B cell development. Without Ikaros to mediate repression, PU.1 levels increase and drive myeloid cell development (Spooner et al., 2009). Like, PU.1 the action mechanism of Ikaros involves transcriptional priming needed for cell fate decisions. Genes activated by Ikaros include, *Sox4*, *Immunoglobulin* genes and *Notch1*. Repression by Ikaros is mediated by the recruitment of the Mi-2/NuRD complex. The transcription factor E2A, formed from the heterodimerisation of the basic helix-loop-helix proteins E12 and E47, is expressed in MPPs and is essential for the development of MPPs into CLPs (Borghesi et al., 2005). The importance of E2A was shown in studies using E2A deficient mice as these mice completely lacked B cells (Zhuang et al., 1994). E2A primes downstream regulators for activation in LMPPs and CLPs, including *EBF-1*.

1.2.1.2 EBF-1

Early B cell factor (EBF1) drives B cell specification and commitment and is essential for the rearrangement and expression of *Ig* genes and for the expression of *PAX5* (Gao et al., 2009). In EBF-1 null mice, only B cell development is affected and cells arrest at an early pre-pro B stage of differentiation (Lin and Grosschedl, 1995). EBF-1 regulates B cell specific genes such as *CD79A* and *CD79B* in co-operation with partner proteins such as E2A and Pax5 (reviewed in Hagman, 2015).

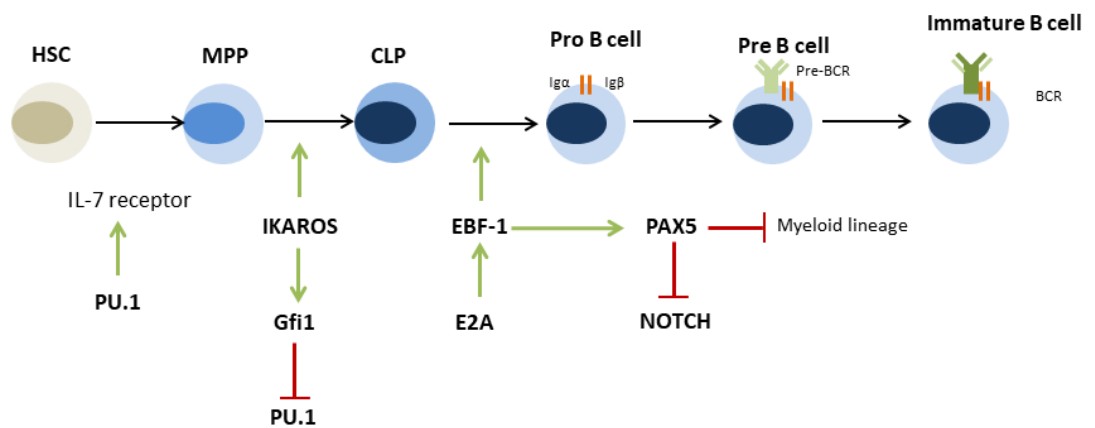


Figure 1.1 Key transcription factors driving B cell lymphogenesis. B cell development is driven by sequence specific activation and repression of lineage determining TF such as PU.1, E2A, EBF-1 and Notch. Transcription factors are shown in bold. HSC (haematopoietic stem cell), MPP (multipotent progenitor), CLP (common lymphoid progenitor), BCR (B cell receptor) (Adapted from Fiedler and Brunner 2012).

It has the ability to activate and repress gene transcription by facilitating chromatin remodelling by SWI/SNF complexes (Gao et al., 2009). In pro-B cells, active genes bound by EBF-1 show enrichments of H3K4Me3 and H3Ac, whereas genes where EBF-1 has dissociated show enrichment for repressive marker H3K27Me and are bound by the repressive Mi-2/NuRD complex (Gao et al., 2009). EBF-1 therefore acts as a pioneer factor and is able to modulate the epigenetic landscape (Boller et al., 2016). Like E2A, EBF-1 interacts with other DNA binding proteins to modulate transcription. For example, it has been shown to interact with Runx1 at the *CD79A* promoter (Maier et al., 2004) and the co-operation between EBF-1 and Pax 5 at the *CD79A* promoter is clearly defined. Activation of the *CD79A* promoter begins in early B cell progenitors with the recruitment of an EBF-1, Runx1 (and its partner CBF β) and E2A complex to the distal end of the promoter. The complex begins demethylation of the distal CpG islands which opens up the chromatin for Pax5 binding. SWI/SNF is recruited to facilitate demethylation and the collaborative action of EBF-1, Pax5 and partners mediates the removal of Mi-2/NuRD complexes, which maintained hyper-methylation of lysine residues on histone tails (H3K4 and H3K27) at the *CD79A* promoter. Once Pax5 is bound to open chromatin it recruits Ets-1 to the promoter to drive transcription (Gao et al., 2009). Pax5 expression is driven by EBF-1 in the pro/pre BCR stages of differentiation. In the absence of Pax5 B cells fail to develop beyond pre-pre B cells and pro-B cells. The arrested cells fail to express B cell specific genes such as *CD79A* and *CD19*. Pax 5, like EBF-1 is required for B cell lineage commitment and development into immature B cells by driving the formation of the pre-BCR complex and Ig rearrangement and signalling (reviewed in Hagman, 2015).

1.2.1.3 Notch/RBPJ κ

The transcription factor RBPJ κ (also known as CSL, CBF-1, Suppressor of hairless, Lag-1) is a highly conserved DNA binding protein and plays a key role in haematopoietic cell fate decisions as part of the canonical Notch signalling pathway (Miele, 2011, Smith et al., 2005). The Notch signalling pathway is initiated by a transmembrane Notch receptor interacting with any one of its ligands from the Delta-like (DLL1, DLL3, DLL4) or Jagged (JAG1 and JAG2) protein families. In canonical Notch signalling, the binding of a ligand to the Notch receptor results in a γ -secretase mediated cleavage of the Notch receptor, which releases the Notch intracellular domain (NICD). The NICD translocates to the nucleus where it forms a complex with RBPJ κ and activates transcription (reviewed in Bray, 2016). In the absence of active Notch, RBPJ κ acts as a transcriptional repressor as part of a complex with co-repressors. Once bound with NICD RBPJ κ recruits a co-activator complex that includes Mastermind (MAML1-3) to drive transcription (Pannuti et al., 2010). However, Notch signalling is responsible for a wide range of biological outcomes and other mechanism of regulation do exist. In the haematopoietic system, Notch/RBPJ κ signalling can influence CLPs lineage decisions to become B cells or T cells in a dose dependent manner (Smith et al., 2005). For example, transgenic mice with constitutively active NICD go on to display an abnormal lymphoid development pattern where CLPs preferentially differentiate into T cells as opposed to B cells (Pui et al., 1999). Whereas disruption of the *Notch* gene results in a significant reduction of T cell numbers and an increase in B cell development (Radtke et al., 1999, Wilson et al., 2001).

1.2.2 B cell maturation

The development pathway from immature B cell to memory B cell is also tightly regulated. During the pro/pre-B cell stages the cells develop into immature B cells that express surface Immunoglobulins (sIg) needed to express the pre-B cell receptor (pre-BCR) on pre-B cell plasma membrane and the BCR on immature B cell plasma membrane. Many developing B cells become apoptotic during the pre-B cell stage as they undergo positive selection for inappropriate heavy chain rearrangement and immature B cell will enter apoptosis if their IgM surface receptor recognised self-antigens (negative selection). Self-reacting antibodies must be eliminated to prevent autoimmune disease. The immature B cells (IgM^+) expressing competent BCR complexes will migrate from the bone marrow to the peripheral lymphoid system where immature B cell undergo further transitions to become mature naïve B cells ($\text{IgM}^+/\text{IgD}^+$) (Ollila and Vihinen, 2005). The mature naïve B cells will circulate around the blood stream until they encounter an antigen. Once they encounter an antigen they will locate to the lymphoid organs where they form Germinal Centres.

Germinal centres (GCs) are transient structures that form in lymph nodes and recruit mature B cells that have been activated by antigen receptor stimulation. Here the naïve B cell transform into CD77^+ centroblasts (CBs) that proliferate in the GC “dark zone”. The CBs undergo somatic hypermutation (SHM) of the Ig variable region genes so that every clone has a slightly different BCR binding specificity. The CBs then develop into CD77^- noncycling centrocytes (CCs) in the “light zone”. The CCs with increased affinity for the antigen are retained through positive selection. The CCs expressing high affinity antibody mutants will eventually differentiate into plasma cells or memory B cells (Krautler et al., 2017, Klein et al., 2003).

Like the early stages of B cell development, the transition from naïve B cell to memory B cell is orchestrated by tightly regulated transcription patterns. Klein et al (2003) tracked the expression of roughly 12,000 genes in B cells during the GC reaction. They found that 457 genes are differentially expressed between naïve B cells and CB. Interestingly, *MYC*, synonymous with proliferation, was not expressed in CBs. B cell lines and Burkitt Lymphoma biopsies contain high levels of *MYC mRNA*, however in CB the level of *MYC* expression is lower than that in resting B cells suggesting that *MYC* is actively suppressed in CB. DNA repair, pro-apoptotic genes were found to be upregulated in CBs, and anti-apoptotic and cytokines and chemokines genes were downregulated in the transition from naïve B cell to CB. The gene expression profile between $CD77^+$ CBs and $CD77^-$ CCs was largely similar, whereas the transition from CC to memory B cell involved 267 genes. They found that memory B cells regained a gene expression pattern similar to that of naïve B cells implying that post GC memory cells return to quiescence (Klein et al., 2003).

1.3 B cell Receptor Signalling

The expression of a functional BCR is required for B cell development and survival, as pre-B cells with defective pre-BCRs arrest at the pre-B cell stage and the removal of the BCR in mature B cells results in cell death (Kitamura et al., 1991, Kitamura et al., 1992, Lam et al., 1997). The activation of a functional BCR leads to the initiation of the BCR signalling pathway. The B-cell receptor (BCR) signalling pathway is involved in controlling growth and apoptosis in both normal and malignant B-cells and has been implicated in the pathogenesis of chronic lymphocytic leukaemia (CLL) and a variety of

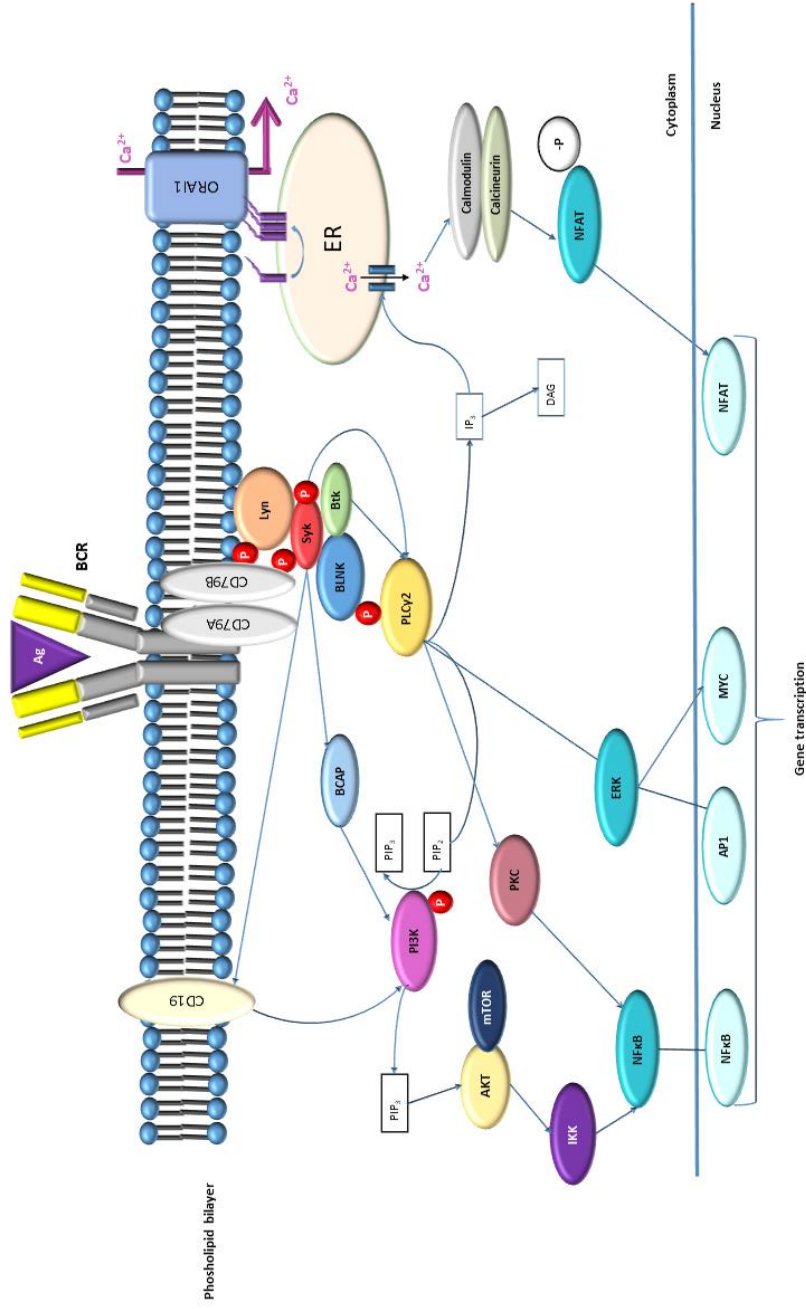


Figure 1.2. A schematic representation of the BCR signalling pathway. Antigen binding triggers BCR activation resulting in phosphorylation of the CD79B ITAM by tyrosine kinases Lyn and Syk initiating a downstream cascade of signalling pathways, including the PI3K-Akt, NFκB, ERK/MAPK, and Ca^{2+} signalling pathways.

other lymphomas such as Diffuse large B-cell lymphoma and Follicular lymphoma (Young and Staudt, 2013).

The B cell receptor (BCR) plays an essential role in B cell development and function (Geisberger et al., 2006, Reth, 1992). It comprises a surface immunoglobulin (IgM) non-covalently bonded to a heterodimer composed of CD79A (Ig α) and CD79B (Ig β) that mediates signal transduction (Wienands, 2000, van Noesel et al., 1991) (Figure 1.2). Both CD79A/B are required for BCR cell surface expression and BCR signal initiation (Clark et al., 1992). B cell development, maturation and VDJ homologous recombination are also dependent on CD79A and CD79B. The human gene CD79A (also known as mb-1) is located on chromosome 19 (Torres et al., 1996, Hermanson et al., 1988). The CD79A promoter contains transcription factor motifs that include AP-1, AP-2, NF-kB and EBF-1. The gene *B29* (*CD79B*) located on chromosome 17 encodes for CD79B (Omori and Wall, 1993). It shares a high degree of homology for transcription factor binding sites with *CD79A* (Hermanson et al., 1989, Travis et al., 1991). Multiple studies have shown that EBV is involved in the regulation of *CD79A* and *CD79B*. A study using SCID mice showed that *CD79A* and *CD79B* were significantly downregulated upon EBV infection (Mori et al., 1994). Two further independent microarray studies using LCLs and EBV negative BL cells conditionally expressing EBNA2 or LMP1 have also shown *CD79B* to be repressed (Maier et al., 2006, Cahir-McFarland et al., 2004). Further experiments showed that LMP1 represses both *CD79A* and *CD79B* in germinal centre B cells (Vockerodt et al., 2008).

1.3.1 BCR signal initiation

The BCR is activated when surface IgM is ligated by an antigen. This leads to BCR aggregation and phosphorylation of the immunoreceptor tyrosine-based activation motifs (ITAMs) tyrosine residues located on each of the cytoplasmic tails of CD79A and CD79B by the tyrosine kinase LYN (Kurosaki, 1999). This phosphorylation initiates the formation of the signalosome composed of the BCR, the kinases SYK, BTK and LYN, the adaptor proteins GRB2, CD19 and B-cell linker (BLNK), and signalling components such as guanine exchange factor proteins VAV (1-3), PLC γ 2 and PI3K (Figure 1.2). The signalosome facilitates progressive ITAM phosphorylation by Lyn and recruitment of SYK to doubly phosphorylated tyrosine residues via its SH2 domain resulting in recruitment of downstream effector molecules and initiation of various different signalling pathways (Johnson et al., 1995, Pao et al., 1998). Syk deficient B cells show defective BCR-mediated activation of downstream signalling pathways, while LYN activation and ITAM phosphorylation remains intact suggesting SYK is an essential link between BCR initiation and downstream signal transduction (Takata et al., 1994). SYK initiates signal transduction through the phosphorylation and interaction with adaptor molecule B cell linker (BLNK), which acts as a scaffold for signalling molecules such as Grb2 and PLC γ 2 (Fu et al., 1998).

Despite significant homology, the contribution of the CD79A and CD79B ITAM regions is not equal. Studies have shown that truncation to the CD79A cytoplasmic domain arrested development at the pre-B cell stage, whereas truncation of the CD79B cytoplasmic domain arrested development at the immature B cell stage. It is thought that CD79B may play an important role in BCR surface expression and that CD79A is more involved in protein tyrosine kinase activation. CD79A and CD79B are therefore

not functionally redundant and each regulate distinct regulatory activities (Dal Porto et al., 2004).

Protein tyrosine kinase LYN is able to positively and negatively regulate BCR signal initiation. As previously discussed LYN phosphorylates the CD79A and CD79B ITAM tyrosines following BCR activation. However, it also phosphorylates the immunoreceptor tyrosine-based inhibitory motif (ITIM) on inhibitory co-receptors FcγRIIB and CD22, which recruit tyrosine phosphatases and repress the BCR response (Nishizumi et al., 1998). Studies have suggested that the positive role of LYN can be carried out by other Src-family kinases, while LYN is absolutely required for attenuation of BCR initiation (Nishizumi et al., 1998). Another positive regulator of BCR initiation is CD45 (or B220), a transmembrane tyrosine phosphatase, which ensures LYN is in its de-repressed phosphorylation state ready to respond to BCR activation. CD45 is not essential for mature B cell survival, but it does regulate B cell maturation and in its absence B cells develop abnormal signalling patterns (Benatar et al., 1996). Whereas the kinase Csk acts as a negative regulator by keeping the Src-family of protein tyrosine kinases repressed and inactive (Hata et al., 1994).

1.3.2 BCR signal propagation

BCR signal propagation leads to the induction of signalling pathways that are crucial for the proliferation and survival of B cells, such as the PI3K-AKT, MAPK, NF-κB, and Calcium signalling pathways. The PI3K-AKT and MAPK pathways are involved in cell survival and the NF-κB pathway has been shown to protect cells from apoptotic signals (Niuro and Clark, 2002). This section will focus on the Calcium signalling pathway and the activation of NFAT transcription factors as it is most relevant to the work in this

thesis. After signal initiation by LYN, PLC γ 2 is recruited to the plasma membrane by adaptor molecule BLNK through its SH2 domain and activated through dual phosphorylation by protein tyrosine kinase BTK and SYK. BLNK is essential for signal propagation; in the absence of BLNK PLC γ 2 fails to translocate to the membrane resulting in impaired BCR signalling (Dal Porto et al., 2004). Activated PLC γ 2 cleaves membrane bound PIP $_2$ to generate second messengers IP $_3$ and DAG. Generation of IP $_3$ induces release of calcium from the endoplasmic reticulum, depleting intracellular calcium stores, which in turn induces activation of the stromal interaction molecule (STIM). STIM activation promotes opening of calcium release-activated channels (CRAC) in the plasma membrane leading to an influx of Ca $^{2+}$ ions and a sustained increase in cytoplasmic calcium levels. The increased levels of calcium activate the calcium/calmodulin-dependent serine/threonine phosphatase Calcineurin which dephosphorylates specific serine residues on Nuclear Factor of Activated T cell (NFAT) transcription factors, exposing their nuclear localisation signals resulting in translocation to the nucleus. Once in the nucleus, NFATs are involved in regulating cell cycle progression, apoptosis, growth and proliferation (reviewed by (Mognol et al., 2016)). The activation of calcineurin is a rate limiting factor for NFAT activity.

1.3.3. NFAT family of transcription factors

The NFAT family consists of five members; NFATC1 (also known as NFAT2 and NFATc), NFATC2 (also known as NFAT1 and NFATp), NFATC3 (also known as NFAT4 and NFATx), NFATC4 (NFAT3) and NFAT5. Unlike NFATC1-4, NFAT5 is not regulated by calcium flux and NFATC1-3 are the only family members expressed in lymphoid cells (Medyouf and Ghysdael, 2008). For the purpose of this work the focus will be on NFATC1 and NFATC2. The calcium regulated NFAT isoforms share a conserved Rel-homology region

(RHR) and a NFAT homology region (NHR) which contains the Calcineurin binding site needed for activation and relocation to the nucleus. NFAT family members differ in their C and N-terminal activation domains. NFATs interact with DNA either as homodimers or heterodimers. Cooperation with binding partners can result in stronger DNA binding affinity. Well known binding partners are AP1, required for T-cell activation, GATA4 and FOXP3, which have both been implicated in cell activation and proliferation (Mancini and Toker, 2009). NFATC1 and NFATC2 have been shown to differentially regulate the cell cycle, where NFATC1 activates genes involved in cell cycle progression and NFATC2 acts as an inhibitor. For example, NFATC2 directly downregulates cyclin A2 expression, while NFATC1 upregulates cyclin A2 (Carvalho et al., 2007, Karpurapu et al., 2008). NFATC1 also upregulates cyclin D1 and cyclin D3 expression and ectopic expression of NFATC2 inhibits CDK4 promoter activity (Karpurapu et al., 2010, Baksh et al., 2000). NFATC1 also has been implicated in the upregulation of anti-apoptotic gene A1, member of the Bcl-1 family. Whereas, NFATC2 is involved in the upregulation of pro-apoptotic genes such as TNF- α and TRAIL (reviewed in Mognol et al., 2016).

Deregulation of calcium/NFAT signalling has been reported in solid tumours, lymphomas and leukaemias (Medyouf and Ghysdael, 2008). Active NFATC1 has been found in Burkitt's Lymphoma, diffuse large B cell lymphoma and aggressive T cell lymphoma (Pham et al., 2005, Marafioti et al., 2005, Medyouf et al., 2007). In contrast, NFATC2 appears to exhibit tumour suppressor activity, as NFATC2 null mice were more susceptible to tumour development than wild type mice and a separate study showed that NFATC2 null mice developed spontaneous B cell lymphomas (Robbs et al., 2008).

Taken together, the opposing activities of NFATC1 and NFATC2 suggest NFATC1 acts an oncogene and NFATC2 functions as a tumour suppressor.

1.4 Epstein Barr Virus

Epstein-Barr Virus (EBV) was first discovered in 1964 in cells obtained from an African Burkitt's Lymphoma biopsy (Epstein et al., 1964). It is a gamma herpesvirus which preferentially infects B lymphocytes. Like all herpesviruses, EBV is a double-stranded DNA virus capable of establishing a productive lytic cycle and a latent (dormant) cycle allowing the virus to persist undetected in infected hosts. EBV infects 90% of the population worldwide and infection is usually asymptomatic in healthy individuals that have been infected as children, although primary exposure to EBV often during adolescence can cause infectious mononucleosis. EBV has been consistently linked to B cell cancers such as Burkitt's lymphoma, Hodgkin's lymphoma and lymphoproliferative disease in immunosuppressed hosts. In addition to B cell cancers it is also associated with various epithelial tumours such as nasopharyngeal carcinoma and gastric cancer (Young and Rickinson, 2004). While the mechanisms through which EBV drives lymphomagenesis still needs to be fully elucidated, the ability of EBV to effectively immortalise human B-cells *in vitro* turning them into permanently growing lymphoblastoid cell lines (LCLs) clearly underlies its oncogenicity (Young and Rickinson, 2004).

There are two natural variants of EBV, classified as type 1 and type 2, based primarily on sequence differences in EBNA2 and the EBNA3 family of genes (Palser et al., 2015). Type 1 EBV, also known as type A, was sequenced from strain B95-8 originally derived

from a lymphoblastoid cell line and type 2, also known as type B, was sequenced from the AG876 strain derived from an African Burkitt's lymphoma cell line (reviewed in Tzellos and Farrell, 2012). Type 1 EBV is prevalent worldwide, whereas Type 2 EBV is found in sub-Saharan Africa and New Guinea where type 1 and type 2 are equally abundant. While both variants activate B cells upon infection, type 1 EBV strains have been shown to be more efficient at immortalising B cells *in vitro* than type 2 EBV strains (Cohen et al., 1989).

1.4.1 EBV infection of B cells *in vitro*

EBV is able to efficiently immortalise B cells from peripheral blood to form lymphoblastoid cell lines (LCLs) (Henle et al., 1967). In LCLs the EBV viral genome is maintained as a circular episome in the host cell nucleus where it directs a programme of viral gene expression which includes six EBV nuclear antigens (EBNAs 1, 2, 3A, 3B, 3C and Leader protein (LP)) and three latent membrane protein (LMPs 1, 2A, 2B). The expression of these EBV genes drives continued proliferation and survival of LCLs. However, only EBNA1, 2, 3A and 3C and LMP1 have been shown to be essential for B cell immortalisation, and while EBNA-LP is an important driver of proliferation it is not essential for B cell transformation (Young and Rickinson, 2004).

The expression of the full pattern of latent viral proteins is known as latency III and is observed only in B-cells. Several functional RNAs are also expressed during latency III including Epstein-Barr small encoded RNAs (EBERs) and micro RNAs (miRNAs). Latency I and II, found in Burkitt's lymphoma (BL) and Hodgkin lymphomas respectively, represent a more restricted pattern of latent viral gene expression (Figure 1.4).

1.4.2 EBV latent gene expression

The EBV genome consists of a circular double stranded DNA episome roughly 172kb in size. The total genome consists of around 90 genes, however only selected genes are expressed during B cell transformation. There are several promoters contained within the EBV genome that are involved in the expression of EBV latent proteins, the Qp; Wp, Cp, and LMP promoters (Figure 1.3). The C and W promoter are located close together in the genome and are involved in the expression of all EBNA proteins (Murray and Young, 2001). EBNA proteins are encoded by individual mRNAs generated by differential splicing of the same long transcript expressed from either the C or W promoter. After initial EBV infection the W promoter is switched on by B cell TFs leading to expression of EBNA-LP and EBNA2 (Bell et al., 1998). Initial expression of EBNA2 activates Cp and initiates the switch from W to C usage for EBNA mRNA production (Puglielli et al., 1996). EBNA2 also activates expression from a bidirectional promoter sequence that controls LMP1 and LMP2. This pattern of latent gene expression is known as latency III. During latency I only EBNA1 and EBER RNAs are expressed and in latency II EBNA1 and EBER RNAs are expressed together with LMP1 and LMP2. In the absence of EBNA2 in latency I and II EBNA1 is expressed from the Q promoter (reviewed in Murray and Young, 2001). The ability of EBV to scale down its gene expression profile allows EBV to persist in memory B cells undetected and is discussed in more detail below.

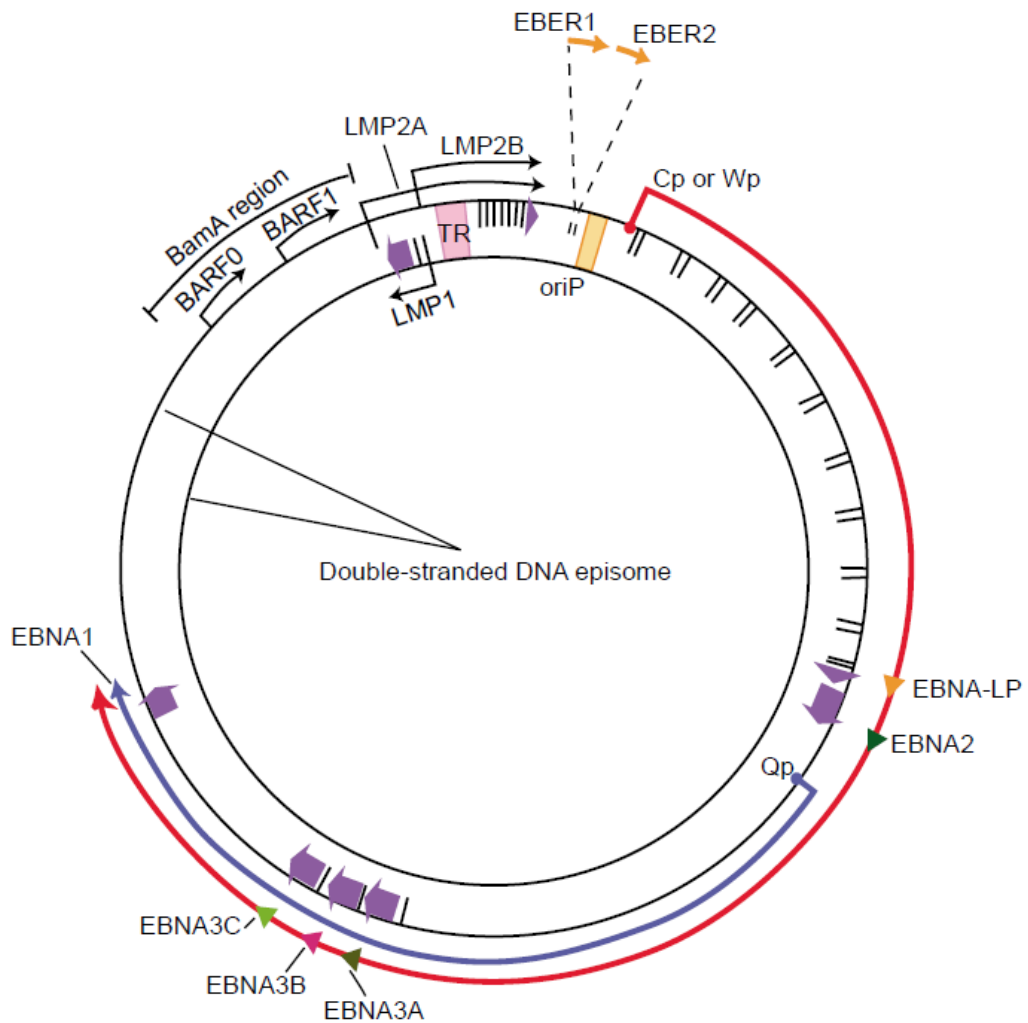


Figure 1.3. The EBV genome. A simplified map of the EBV genome showing selected latent genes on a double stranded viral DNA episome. The purple arrows represent coding exons for each latent gene and the direction in which they are transcribed. The mRNA for the EBNA and BHRF1 genes are all spliced from the same long primary transcript starting at Cp or Wp as indicated by the red arrow. The blue arrowed line represents the EBNA1 transcript starting from Qp during latency I and II. Abbreviations: EBER, Epstein-Barr small encoded RNA; OriP, origin of replication; Cp, C promoter; Wp, W promoter; Qp, Q promoter; EBNA, Epstein-Barr nuclear antigen; LP, Leader protein; LMP, latent membrane protein (adapted from (Murray and Young, 2001)).

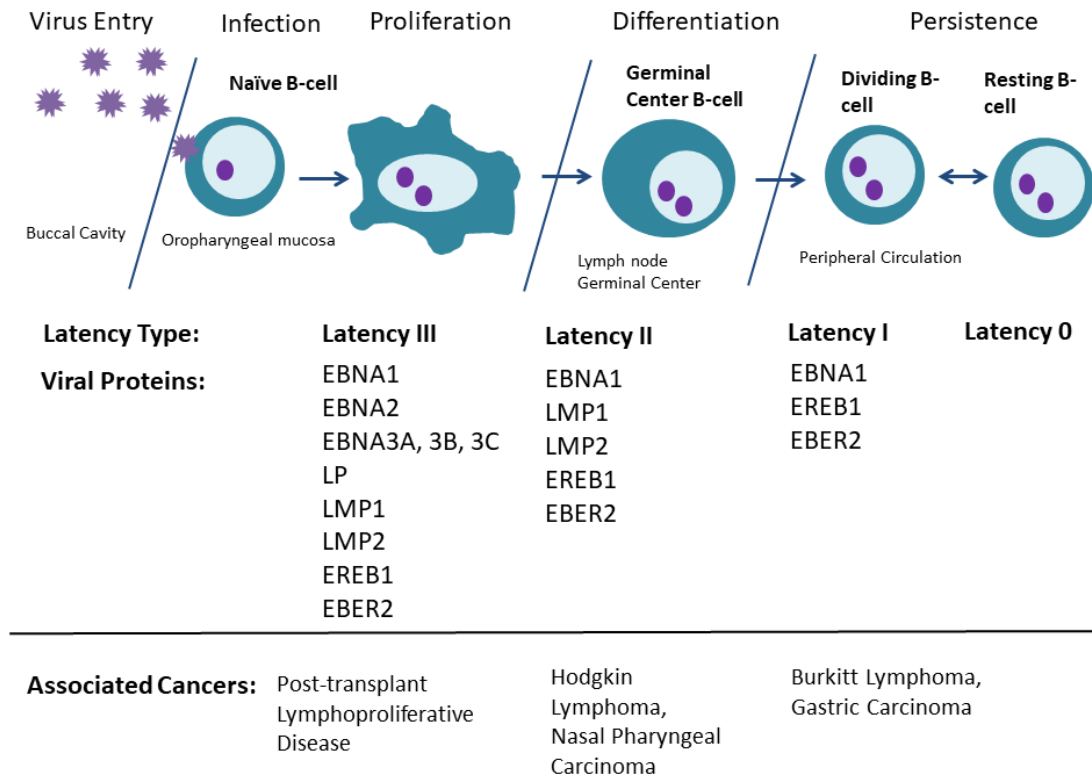


Figure 1.4. The EBV life cycle in vivo. A schematic showing the EBV life cycle *in vivo*. Purple stars represent virus particles, purple dots represent the EBV episome within the B cell nucleus. Latency type, EBV protein expression and associated cancers corresponding to each stage in B cell development/gene expression pattern are outlined underneath. (Figure adapted from Heslop, 2009)

1.4.3 EBV persistence *in vivo*

After initial infection the EBV episome circularises and activates the latency III programme of gene expression driving growth and proliferation in naïve B cells (Adams and Lindahl, 1975). EBV gains entry to the B cell pool through interaction of the viral glycoprotein gp350/220 with the B cell specific complement receptor CD21 (CR2) (Fingerroth et al., 1984). Viral entry into B cells also involves the viral glycoproteins gp25 and gp42/38 in a complex with gp85. This complex allows interaction between EBV and major histocompatibility complex class II (MHC II) which act as a co-receptor for entry into the B cell (Knox and Young, 1995).

While proliferating B cells grow out into LCLs *in vitro*, they cannot persist *in vivo* due to the strong cytotoxic CD8⁺ T cell response initiated in response to lytic and latent cycle viral proteins (Young and Rickinson, 2004). EBV infected (latency III expressing) naïve B cells are thought to migrate to the lymph nodes where they undergo the germinal centre (GC) reaction leading to differentiation into memory or plasma B cells (Figure 1.4). To allow differentiation to occur EBNA2 expression needs to be downregulated to stop rapid proliferation. EBV infected cells facilitate this downregulation by switching to a latency II gene expression programme. The latency II gene expression programme protects the infected B cells from apoptosis as the continued expression of EBNA1, LMP1 and LMP2 drives cell survival (Thorley-Lawson and Allday, 2008). When the infected cells leave the GC as memory B cells EBV gene expression has been further reduced to latency I, characterised by low levels of EBNA1 and some EBER RNAs, or latency 0 where no EBNA1 is expressed (only in resting cells). By reducing viral protein expression the virus can evade detection and persist in memory B cells for the lifetime of the host. When the memory cells enter the cell cycle to divide EBNA1 expression is

switched on as it is required for segregation and maintenance of the viral genome in daughter cells (Babcock et al., 1998). It is clear that by switching latent gene expression programmes during B cell development EBV is able to persist in memory B cells undetected.

1.4.4 EBNA1

EBNA1 is a DNA binding protein that plays an essential role in latent virus biology. It is required for the maintenance and replication of the viral genome in B cells as they multiply. EBNA1 binds with high specificity and affinity to the EBV latent origin of replication (oriP) as a homodimer through a DNA binding domain located in its C terminus. Cellular DNA replication machinery is recruited to oriP by EBNA1 and other co-factors resulting in replication of the EBV genome alongside host chromosomes each cell cycle. The EBNA1 N terminus binds loosely to random sites on the cell chromosome to avoid degradation by the cell and to ensure EBV genomes are distributed into daughter cells during mitosis (Westhoff Smith and Sugden, 2013). EBV genomes can be eliminated from EBV positive BL cell lines *in vitro* through the inhibition of EBNA1 DNA binding (Li et al., 2010). EBNA1 is also able to activate transcription by binding to the viral LMP and C promoters. It has also been shown to activate transcription of cellular gene *NOX2* (Gruhne et al., 2009). EBNA1 proteins contain a glycine-alanine (Gly-Ala) repeat sequence which makes EBNA1 resistant to proteasomal degradation which in turn avoids presentation of EBNA1 epitopes to cytotoxic T cells. This makes EBNA1 undetectable to T cells and allows for its continued expression throughout all stages of latent gene expression. (Levitskaya et al., 1997). Additionally, the Gly-Ala sequence is thought to induce translational stress leading to indirect activation of *MYC* expression through PI3-kinase mediated signalling. This is

supported by evidence that some EBNA1 containing lymphoma cells are sensitive to PI3K δ inhibition (Gnanasundram et al., 2017). It is also thought that EBNA1 interaction with USP7 (a ubiquitin-specific protease) can alter p53 or MDM2 levels in cells and that EBNA1 can regulate anti-apoptotic activity by inducing survivin in BL cell lines indicating that the role of EBNA1 extends beyond maintenance of the EBV genome in infected B cells (Frappier, 2012, Kennedy et al., 2003).

1.4.5 EBNA2

EBNA2 is a transcriptional activator and is crucial for B-cell transformation. After initial EBV infection only EBNA-LP and EBNA2 are expressed from the viral W promoter (Young and Rickinson, 2004). EBNA2 drives activation of the upstream viral C promoter to produce a long message, that when differentially spliced produces transcripts for all the EBNA proteins required for LCL immortalisation (Woisetschlaeger et al., 1991). EBNA2 also activates expression of all three LMP proteins from their respective promoters (Wang et al., 1990).

EBNA2 drives B-cell proliferation and transformation through epigenetic reprogramming (White et al., 2010). EBNA2 does not bind DNA directly, but forms complexes with B-cell and viral DNA binding proteins such as RBP-Jk and PU.1 thereby enabling access to gene regulatory elements (Johannsen et al., 1995, Grossman et al., 1994, Ling et al., 1993, Waltzer et al., 1994). RBPJk is the downstream target of the Notch signalling pathway and is activated by binding of the NICD (as discussed in section (1.2.1.3)). Studies have shown that EBNA2 can functionally replace the NICD and activate RBPJk in its absence rendering the Notch receptor redundant (Sakai et al., 1998). A recent study has shown EBNA2 binding sites are enriched for EBF-1 motifs and

that EBNA2 can bind EBF-1 to form a complex in B cells suggesting EBF-1 may also be a potential DNA binding partner for EBNA2 (Glaser et al., 2017). EBNA2 activates transcription by recruiting the basal transcription machinery including TFIIB, TAF40, TFIIE, and TFIIH (Tong et al., 1995b, Tong et al., 1995a). Activation of transcription initiation by EBNA2 also involves association with histone acetyltransferases (HATs) (Wang et al., 2000) and chromatin remodelling complexes, such as SWI/SNF.

EBNA2 frequently targets cellular and viral genes that drive proliferation. EBNA2 drives expression of EBV *LMP1* and *LMP2* and results in the induction of cell-surface expression of activation molecules CD21 and CD23. It also up-regulates anti-apoptotic proteins such as BCL2 and activates signalling pathways by acting through the tumour necrosis factor receptor/CD40 pathway sending growth and differentiation signals downstream to B-cells (Young and Rickinson, 2004, Peng and Lundgren, 1992). EBNA2 is also known to upregulate oncogene *MYC* (Kaiser et al., 1999). *MYC* is master transcription factor and is involved in the regulation of many cellular processes including cell-cycle progression, proliferation, differentiation and survival (Dang et al., 2006). *MYC* is frequently deregulated in cancer leading to aberrant expression of its downstream targets resulting in uncontrolled proliferation and tumorigenesis. EBNA2 exploits *MYC* oncogenic capabilities by upregulating its transcription leading to uncontrolled growth and cell immortalisation (Kaiser et al., 1999).

EBNA-LP interacts with EBNA2 and while it is not required for immortalisation *in vitro*, it is required for the efficient outgrowth of LCLs (Allan et al., 1992). EBNA2 and EBNA-LP alone can induce G0 to G1 transition through the upregulation of cyclin D2 when

transiently transfected into primary B cells (Sinclair et al., 1994). The co-operation of EBNA2 and EBNA-LP can also upregulate LMP1.

1.4.6 EBNA3 Family

The EBNA3 family of proteins consists of three members; EBNA3A, EBNA3B and EBNA3C. All three family members have a similar gene structure, share partial sequence homology and are arranged in tandem in the EBV genome. Studies using recombinant EBV have shown that EBNA3A and 3C are essential for efficient B cell transformation and immortalisation *in vitro*, whereas EBNA3B is not required (Tomkinson et al., 1993). More recent work showed that it is possible to establish EBNA3A negative LCLs under specific conditions with feeder cells in the culture (Hertle et al., 2009, Skalska et al., 2010).

Like EBNA2, EBNA3A, 3B and 3C act as transcription factors (TFs) and drive B-cell proliferation and transformation through epigenetic reprogramming (Young and Rickinson, 2004). The EBNA3 proteins are not able to bind DNA directly and like EBNA2 they form complexes with cellular DNA binding proteins such as RBP-J κ , PU.1 and CBF β enabling access to gene regulatory elements (Johannsen et al., 1995). As EBNA2 and EBNA3 proteins bind RBPJ κ in a mutually exclusive way, the EBNA3 proteins can negatively regulate EBNA2 mediated gene activation by blocking the EBNA2/RBPJ κ interaction. As EBNA3 proteins can inhibit EBNA2 mediated activation of the viral Cp and LMP2A promoter it suggests that the EBNA3 proteins could form a negative feedback loop limiting expression of all RBPJ κ /EBNA2 activated genes, including their own expression (reviewed in Allday et al., 2015).

The EBNA3 proteins have been best studied as repressors. They can individually or together regulate genes that control growth and survival through polycomb-mediated epigenetic silencing (White et al., 2010, McClellan et al., 2012, Hertle et al., 2009, Paschos et al., 2009, Paschos et al., 2012). An example of EBNA3A mediated reprogramming of the cellular genome is the silencing of neighbouring chemokine genes *CXCL10* and *CXCL9*. Both *CXCL10* and *CXCL9* and their receptors in NK and T cells are critical for the host cell's ability to control EBV infection. EBNA3A is able to silence *CXCL10* and *CXCL9* by associating with intragenic enhancer elements located between these genes and displacing EBNA2, thereby impairing enhancer activity and leading to polycomb-mediated deposition of H3K27me3. The silencing of *CXCL10* and *CXCL9* by EBNA3A may help EBV infected to escape immune surveillance (Harth-Hertle et al., 2013, McClellan et al., 2012).

EBNA3A and EBNA3C can also work co-operatively, for example by driving polycomb-mediated silencing of *BCL2L11*, (Anderton et al., 2008). Here, EBNA3A and EBNA3C mediated gene silencing is associated with recruitment of polycomb repressor complex 1 and 2 (PRC1,2) and the deposition of H3K27Me3 (McClellan et al., 2012, McClellan et al., 2013, Paschos et al., 2009). The Bcl-2-like protein 11, also known as BIM is part of the BH3-only protein family and is encoded by the *BCL2L11* gene. It is a pro-apoptotic protein and an important regulator of cellular apoptotic pathways (Willis and Adams, 2005). *BCL2L11* is highly expressed in hematopoietic cells and has been shown to be critical for apoptosis during B lymphocyte development (Strasser, 2005) (O'Reilly et al., 2000). In normal B cells the expression of *BCL2L11* is tightly regulated. Its transcription can be activated by various TFs including E2F1, MYC, Smad1/3 and Runx1-3, and repressed by YY1, PU.1 and PINCH-1. PU.1 mediated silencing of *BCL2L11* involves PU.1

binding to the promoter, recruitment of the PCR2 and deposition of H3K27me3 (reviewed in Sionov et al., 2015). The EBV protein family EBNA3 are able to silence *BCL2L11* by exploiting this repression mechanism to prevent apoptosis triggered by EBNA2 mediated upregulation of MYC (Paschos et al., 2009, Anderton et al., 2008, McClellan et al., 2012)

EBNA3A and 3C are also responsible for the transcriptional silencing of cyclin-dependent kinase inhibitors p16^{INK4A} and p14^{ARF}, potent cell cycle regulators and tumour suppressors that are encoded by the *CDKN2A* gene. Silencing of *CDKN2A* by EBNA3A and 3C, together with cellular co-repressor CtBP, aids B cell transformation and outgrowth by overcoming a p16 (INK4a) and p14^{ARF} driven proliferation block (Maruo et al., 2011, Skalska et al., 2010). Here, EBNA3C and EBNA3A recruit Sin3A repressive complexes (Sin3A, HDAC1 and 2, and RBPJk) to the *CDKN2A* regulatory locus to remove histone acetylation marks, and recruit Polycomb repressor complexes leading to the deposition of H3K27Me3. The combined actions of EBNA3A and EBNA3C induce repression of p16^{INK4A} and p14^{ARF} allowing EBV to drive cell cycle entry for viral replication (Skalska et al., 2013). Studies using B cells containing an inducible EBNA3C-estrogen receptor (ER)-fusion protein (EBNA3C-ER) showed that polycomb mediated repression of *BCL2L11* and *CDKN2A* expression can be reversed in the absence of EBNA3C (Skalska et al., 2010, Paschos et al., 2012).

Unlike EBNA3A and EBNA3C, EBNA3B is not essential for B cell transformation *in vitro*. EBNA3B has been identified as a tumour suppressor by upregulating chemokine *CXCL10* and having a growth inhibitory role. Studies have shown that NOD/SCID/IL2 γ ^{null} mice with reconstituted human immune components infected with an EBNA3B

knockout EBV (EBNA3BKO) developed diffuse large B cell lymphoma –like tumours, whereas mice infected with WT EBV, or an EBNA3B revertant EBV developed less aggressive B cell tumours. Failure to express EBNA3B caused B cells to proliferate more rapidly and secrete less of the T cell chemoattractant CXCL10 leading inefficient T cell recruitment *in vitro* and a reduction of T cell mediated killing *in vivo* (White et al., 2012). Similar gene expression profiles and phenotypic characteristics have been found in a small number of B cell lines derived from human lymphomas encoding a truncated version of EBNA3B (Gottschalk et al., 2001). It is thought that the role of EBNA3B *in vivo* may be to trigger the switch from latency III to latency II during the germinal centre reaction by de-repressing genes such as CXCL1, IL10 and IL19, which mediate essential T cell interaction as part of the germinal centre reaction and B cell differentiation (White et al., 2010, White et al., 2012).

1.4.7 LMP1

LMP1 function is associated with at least four signalling pathways, including NF- κ B, JNK/AP1, p38/MAPK and JAK/STAT (reviewed in Murray and Young, 2001). The LMP1 C-terminus contains two activation regions, known as C-terminal activating region 1 and 2 (CTAR1 and CTAR2). CTAR1, located near the membrane is essential for B cell transformation and CTAR2, located at the extreme end of the C-terminus is required for the long term outgrowth of EBV infected B cells (Izumi and Kieff, 1997). In a normal immune response T cells will activate CD40 signal transduction in B cells using its CD40 ligand located on the cell surface. LMP1 mimics the CD40 receptor, a member of the tumour necrosis factor receptor (TNFR) super family, on the surface of infected B cells. LMP1 acts as a constitutively active CD40 (Kieser and Sterz, 2015). LMP1 mediated activation of NF- κ B occurs through interactions between CTAR1 and CTAR2 with

TRADD and TRAF proteins respectively (Izumi and Kieff, 1997, Devergne et al., 1996). Activation of the NF- κ B transcription factor results in the expression of the anti-apoptotic gene *Bcl2* (Kieser and Sterz, 2015). Activation of JNK signalling cascade occurs through the CTAR2 region, and p38/MAPK and JAK/STAT activation occurs through both CTAR1 and 2 regions (Eliopoulos et al., 1999a, Eliopoulos et al., 1999b, Gires et al., 1999). Activation of these signalling pathways results in the induction of various anti-apoptotic proteins and cytokines.

1.4.8 LMP2

The LMP2 gene encodes two distinct proteins; LMP2A and LMP2B. The LMP2 proteins are not essential for B cell transformation *in vitro*. However, LMP2A expression in transgenic mice prevents normal B cell development by allowing immunoglobulin negative B cells to accumulate in peripheral lymphoid organs, implicating LMP2A as a driver of proliferation and survival of B cells in the absence of a functional BCR (Young and Rickinson, 2004). The N-terminal domain of the LMP2A proteins contains eight tyrosine residues that together form an immunoreceptor tyrosine-based activation motif (ITAM) (Fruehling and Longnecker, 1997). Like the ITAM motif present in BCR components CD79A and CD79B, the LMP2A ITAM motif interacts with, and is phosphorylated by protein tyrosine kinases (PTK) LYN and SYK. In normal mature B cells, phosphorylation of the ITAM on CD79A and CD79B activates a BCR mediated signalling cascade leading to B cell proliferation and differentiation. However, PTK interaction with the LMP2A ITAM appears to negatively regulate their activity (Fruehling and Longnecker, 1997). The negative impact of LMP2A on PTK activity leads to a reduction in BCR-mediated Ca^{2+} release, tyrosine phosphorylation and activation of the EBV lytic cycle in B cells (Miller et al., 1995). This suggests that LMP2A may play

an important role in maintaining EBV latency in favour of activation of the lytic cycle. LMP2B has been implicated as a modulator of LMP2A (Scholle et al., 1999).

1.4.9 Diseases associated with EBV

EBV infects 90% of the world population with the majority of infected hosts not developing EBV-related disease. Nonetheless, EBV is implicated in the development of approximately 1.5% of all cancers world-wide. EBV-associated cancers are mainly B cell lymphomas and epithelial cell carcinoma reflecting the cell types known to be infected by the virus (outlined in Table 1.1). The most commonly EBV-associated lymphoma is African Burkitt's lymphoma, followed by Hodgkin's lymphoma (30% of cases), most lymphomas in immunosuppressed hosts, Diffuse large B cell lymphoma in the elderly (5-10% of cases) and some NK and T cell lymphomas. EBV-associated epithelial cell carcinomas include nasopharyngeal carcinoma and gastric carcinoma (reviewed in Farrell, 2019). Since this work has a B cell focus, the B cell lymphomas will be covered in more detail below.

1.4.9.1 Burkitt's Lymphoma

EBV was first discovered in Burkitt's Lymphoma (BL) biopsies from sub-Saharan Africa (Epstein et al., 1964), where BL is endemic and mostly EBV associated. World-wide 20% of sporadic BL cases and 60% of immunodeficiency-associated BL are EBV positive (Mbulaiteye et al., 2014). Burkitt's lymphoma is also common in HIV infected adults in the developed world and often arises as the first AIDS-associated illness. In 30-40% of these cases the tumours are EBV-associated (Young and Rickinson, 2004). A defining feature of BL, regardless of its origin is the chromosomal translocation of *MYC* on chromosome 8 to an immunoglobulin (IG) gene. These translocations often involve the

Cancer	Latency pattern expressed
B cell lymphoma	
Post-transplant lymphoma	III
Burkitt's lymphoma	I
Hodgkin's lymphoma	II
Diffuse Large B cell lymphoma	II or III
T cell lymphoma	
NK cell and T cell lymphoma	II
Carcinoma	
Nasopharyngeal carcinoma	II
Gastric carcinoma	II

Table 1.1 Summary of EBV-associated cancers and latency pattern expression. During latency III the following EBV genes are expressed; *EBNA1*, *EBNA2*, *EBNA3A*, *3B* and *3C*, *EBNA-LP*, *LMP1*, *LMP2A*, *EBER1*, *EBER2*, *BHRF1* *miRNAs*, *BART* *miRNAs*. During Latency II *EBNA1*, *LPM1*, *LMP2AEBER1*, *EBER2* and *BART* *miRNAs* are expressed. During Latency I only *EBNA1*, *EBER1*, *EBER2* and *BART* *miRNAs* are expressed. Abbreviations used *miRNA*, microRNA; NK, natural killer.

IG heavy chain locus on chromosome 14, or the lambda or kappa light chain loci on chromosomes 2 or 22. The most common translocation is t(8:14) and occurs in 85% of BL cases (Boerma et al., 2009). The location of the *MYC*/IG breakpoint varies between endemic BL and sporadic BL. It usually sits far 5' of *MYC* in endemic BL, whereas breakpoints in sporadic BL are situated in the first exon or intron, alluding to different mechanism involved in their generation (Neri et al., 1988, Shiramizu et al., 1991). The translocation of *MYC* to highly active regulatory regions of the IG loci drives constitutively high levels of *MYC* expression and leads to uncontrolled growth of BL cells. In addition to the *MYC* translocation, many Burkitt's tumours have TP53 mutations and defects in the p53-ARF pathway (Lindstrom and Wiman, 2002) . EBV positive BL cells show a highly restricted Latency I program of viral gene expression where they only express EBNA1. It is thought that EBV has an initiating role where growth-transformed infected B cells establish a pool of cells that are at vulnerable to developing *MYC* translocations (Polack et al., 1996).

1.4.9.2 Hodgkin's Lymphoma

Hodgkin's Lymphoma (HL) is characterised by malignant Reed-Sternberg cells, which are surrounded by non-malignant B cells. Approximately 40% of classic HL cases worldwide are EBV associated. EBV-positive HL tumours display the latency II viral gene expression programme, so express only EBNA1, LMP1 and LMP2. LMP1 and LMP2 are highly expressed in EBV-positive Reed-Sternberg cells. These cells are thought to derive from GC B cells and in EBV associated cases they often have defective rearrangements of their surface BCR. The inability to signal through the BCR would normally result in apoptosis. However, in EBV infected B cells, LMP1 and LMP2 mimic CD40 and the BCR respectively, independently of ligand binding, activating CD40 and

BCR signalling and driving the survival of Reed-Sternberg cells (reviewed in Farrell, 2019).

1.4.9.3 Lymphomas in immunosuppressed hosts

Immunocompromised patients are at risk of developing B cell lymphomas. One of the best-studied examples is post-transplant lymphoma (PTL). PTL typically develops within the first year post transplant and is almost always EBV positive. Tumour cells express the latency III programme of viral gene expression and grow out in the absence of adequate T cell immune surveillance (Young et al., 1989). Late onset PTLs tend to be monoclonal tumours. Some of these tumours mimic the latency III phenotype of early onset disease; others are EBNA2 and LMP1 negative, or EBNA2 negative and LMP1 positive. It is possible that these tumours have evolved from EBV transformed B cells through inherited genetic changes that mean they no longer require EBNA2 or LMP1 (Timms et al., 2003, Capello et al., 2003).

1.4.9.4 Diffuse Large B Cell Lymphoma

Diffuse Large B Cell Lymphoma (DLBCL) is the most common type of malignant lymphoma. It is more common in elderly patients and EBV associated cases often have a poor prognosis (Ok et al., 2013, Lu et al., 2015). Roughly 10% of DLBCL cases in Asia are EBV associated, as opposed to 5% of cases in the West (Lu et al., 2015). Recent gene expression studies showed that BCL2 expression is frequently upregulated in DLBCL. However, none of these cases were associated with EBV and the link between EBV and DLBCL remains poorly understood. There is some evidence of EBNA3B mutations in DLBCL, which is consistent with a study that showed deletion of EBNA3B cause DLBCL-like disease in transgenic mice (White et al., 2012). This suggests that

EBNA3B could act as a tumour suppressor and mutations of EBNA3B could result in an aggressive oncogenic virus (Farrell, 2019).

1.5 Aims

The overall aim of this project was to study aspects of cellular gene deregulation relevant to B cell transformation by Epstein-Barr encoded transcription factors.

Specific aims were to:

- 1) Study the transcriptional regulation of the B cell Receptor signalling pathway by the EBNA2 and EBNA3 transcription factors and examine the impact on downstream signalling.

- 2) Investigate EBNA2 mediated activation of the oncogene MYC and the silencing of pro-apoptotic gene BCL2L11 by EBNA3A and EBNA3B by long-range control elements.

2. Materials and Methods

2.1 Cell Culture

Reagents and buffers used in tissue culture were all purchased from ThermoFisher Scientific unless otherwise specified.

2.1.1 Media and supplements

100x Penicillin-Streptomycin-L-Glutamine (PSG) 50 mg/ml containing 10,000 units of penicillin, 10,000 µg of streptomycin, and 29.2 mg/ml of L-glutamine. PGS was stored in 5ml aliquots at -20°C (Invitrogen)

RPMI 1640 without L-glutamine stored at 4°C(Invitrogen)

Dulbecco's Phosphate Buffered Saline without Calcium Chloride and Magnesium Chloride (Invitrogen)

Fetal Bovine Serum (FBS) Pre-screened for endotoxins (≤ 5 EU/ml) and haemoglobin (≤ 10 mg/dl) levels, and heat inactivated at 56°C for 30 min . Stored at -20°C (Gibco)

Freezing media: 80% FBS and 20% DMSO

2 mM β -estradiol in DMSO (Sigma)

Hygromycin B (50 mg/ml) (Invitrogen)

100x Glutamax containing 200 mM L-alanyl-L-glutamine dipeptide in 0.85% NaCl (Gibco)

1 mM Sodium Pyruvate (Sigma)

50 µM Thioglycerol (Sigma)

2.1.2 Cell line maintenance

All cell lines were passaged twice weekly unless stated otherwise and cultured in 75 cm² flasks (Nunc) at 5% CO². A summary table outlining the characteristics of the cell lines used can be found in appendix 8.1.

2.1.2.1 Burkitt's Lymphoma cell lines

The BL31 and BL2 series of cell lines derive from the EBV-negative Burkitt's lymphoma (Lenoir et al., 1985). BL31 and BL2 cell lines infected with wild-type recombinant EBV or EBNA 3A, 3B and 3C knock-out and revertant EBV (kindly provided by Prof M. Allday) (Anderton et al., 2008). These lines were cultured in RPMI-1640 medium (Invitrogen) supplemented with 10% fetal bovine serum, 5% penicillin-streptomycin, glutamine, 1 mM sodium pyruvate (Sigma) and 50 µM thioglycerol (Sigma). Hygromycin B (Invitrogen) was added at a concentration of 100 µg/ml to all BLs containing recombinant hygromycin B-resistant EBV.

The EBV-positive latency III BL cell line Mutu III (clone 48) derives from the Mutu I BL cell-line (Gregory et al., 1990). Mutu I cells display the latency I pattern of EBV gene expression. Mutu III cell clones arose spontaneously during culture of Mutu I cells and display the latency III pattern of EBV gene expression. The latency III expressing Mutu III cell line was cultured in RPMI-1640 medium (Invitrogen) supplemented with 10% FBS and 5% PSG.

The BJABK3 cell line derives from EBV-negative B cell lymphoma cell line (BJAB) (Klein et al., 1974) transfected with a plasmid expressing a conditionally-active oestrogen receptor (ER)- EBNA2 fusion protein (Kempkes et al., 1995a). This cell line

was cultured in RPMI-1640 medium (Invitrogen) supplemented with 10% FBS and 5% PSG. 1 μ M β -estradiol was added to the culture media to activate ER-EBNA2.

The BL41K3 cell line derives from the EBV-negative Burkitt's Lymphoma cell line BL41 (Lenoir et al., 1985) transfected with a plasmid expressing a conditionally active oestrogen receptor (ER)- EBNA2 fusion protein (Kempkes et al., 1995a). This cell line was cultured in RPMI-1640 medium (Invitrogen) supplemented with 10% FBS and 5% PSG. 1 μ M β -estradiol was added to the culture media to activate ER-EBNA2.

The DG75 cell line derives from human EBV-negative Burkitt's Lymphoma cells from a biopsy taken in 1975 (Ben-Bassat et al., 1977). This cell line was cultured in RPMI-1640 medium (Invitrogen) supplemented with 10% FBS and 5% PSG.

The DG75 CBF1KO cell line is a derivative of DG75 cells where the CBF1/RBPJ κ gene has been inactivated by homologous recombination (Maier, 2005). These cells were cultured in RPMI-1640 medium (Invitrogen) supplemented with 10% FBS and 5% PSG.

The BJABK3, BL41K3, DG75 and DG75 CBF-1 KO cell lines were a kind gift from Bettina Kempkes.

2.1.2.2 Lymphoblastoid Cell Lines

The EBV-immortalised LCL GM12878 is an ENCODE Tier 1 cell line (Coriell Cell Repositories). The GM12878 cell line was cultured in RPMI-1640 medium (Invitrogen) supplemented with 10% FBS and 5% PSG.

The ER-EB 2.5 LCL is an EBV-immortalised LCL expressing a conditionally-active oestrogen receptor (ER)-EBNA2 fusion protein and was provided by Prof B. Kempkes

(Kempkes et al., 1995). ER-EB 2.5 LCLs were cultured in RPMI-1640 medium without phenol red (Invitrogen) supplemented with 10% FBS, 5% PSG and in the presence of 1 μ M β -estradiol. For β -estradiol withdrawal ER-EB 2.5 cells were cultured in the absence of β -estradiol for 4 days, and 1 μ M β -estradiol was re-added for 4, 8, 17 or 24 h prior to cell harvest.

2.1.3 Freezing Cells

40 ml of confluent cells were pelleted and resuspended in 2 ml freezing media. Following resuspension, cells were aliquoted into 2x 1.5 ml cryogenic vials (Nunc) and frozen at -80°C in a Mr. Frosty freezing container (Nalgene) containing isopropanol. After at least 24 h at -80°C the vials were transferred to liquid nitrogen storage.

2.1.4 Thawing Cells

Vials were taken out of liquid nitrogen and gently thawed by hand. Once cells started to thaw the 1 ml vial was added to 10 ml pre-warmed conditioned media and placed in the incubator at 37°C and 5% CO_2 overnight.

2.1.5 Haemocytometer cell counting

15 μ l of cells were added to 15 μ l of Trypan Blue, mixed, and counted using a Neubauer haemocytometer. The haemocytometer is divided into 9 equally spaced squares. Cells in the 4 corner squares were counted. The total number of cells was then divided by 4 to get the average cell number and multiplied any dilution factor. To establish the concentration of cells the following formula was used:

$$\text{Cells/ml} = \text{average cell count} \times 10^4$$

2.1.6 Harvesting cells

Cells were pelleted by centrifugation for 10 min at 403 x g at 4°C using a Sorvall legend RT centrifuge with swing bucket rotor (ThermoFisher). The pellet was washed once in half the original culture volume of PBS, counted using the haemocytometer, and pelleted by centrifugation. The pelleted cells were then resuspended in PBS at the required concentration and aliquoted in 1 ml Eppendorf tubes. Cells were pelleted by centrifugation for 2 min at 2408 x g and the supernatant removed. Cell pellets were immediately frozen in dry ice and stored at -80°C.

2.1.7 Transient Transfection

2.1.7.1 Bio-Rad electroporation

DG75 or DG75-CBF-1 KO cells were diluted 1:2 24 h prior to electroporation. Cells were pelleted by centrifugation at 403 x g for 10 min at 4°C and the supernatant was kept as conditioned media. The cells were washed in cold serum free media, counted and re-pelleted at 403 x g and resuspended at 2×10^7 cells/ml in cold serum free media. DNA (see appendix for list of plasmid DNA used) was mixed in Eppendorf tubes in a total volume of 50 μ l. 1×10^7 cells (0.5 ml) were added to Eppendorf tubes containing the required plasmid DNA mix at room temperature, gently mixed and transferred to electroporation cuvettes (4 mm gap, VWR). Samples were electroporated at 260 V and 950 μ F using a Bio-Rad Gene Pulser II. Immediately after electroporation 1 ml of conditioned media was added to the cuvettes and the contents of the cuvettes was transferred into a small upright flask containing 10 ml of pre-warmed conditioned media and incubated at 37°C with 5% CO₂ for 48 h. The cells were then harvested by pelleting at 403 x g for 10 min at 4°C and washed in 10 ml PBS. 1 ml of cells was

transferred to an Eppendorf tube and cells pelleted by centrifugation at 2408 x g for 2 min using a bench top centrifuge before being snap frozen and stored at -80°C until used for Western blot analysis. The remaining 9 ml of cells were pelleted at 403 x g for 10 min, resuspended in 1 ml PBS, and re-pelleted at 2408 x g for 2 min, the supernatant was removed and the pellet snap frozen and stored at -80°C until used for Dual Luciferase assay.

2.1.7.2 Neon Transfection System

BL41K3 cells were diluted 1:2 24 h prior to electroporation. Cells were pelleted by centrifugation at 403 x g for 10 min at 4°C and the supernatant was discarded and the cells were resuspended at 1×10^6 cells/ml in PBS to wash out the media. Cells were re-pelleted and resuspended at 1×10^6 cells/100 μ l of Buffer T. DNA (5 μ g NFAT3 plasmid) was mixed in Eppendorf tubes in a total volume of 20 μ l. 100 μ l (1×10^6 cells) was added to Eppendorf tubes containing DNA at room temperature and gently mixed. The samples were electroporated using the Neon Transfection System using 1 pulse of 1300 V for 30 msec, using a 100 μ l Neon tip. Immediately after electroporation the cells were transferred to a 6-well plate containing 2 ml of pre-warmed conditioned media (RPMI, 10%FCS and 1X Glutamax) per well and incubated at 37°C with 5% CO₂ for 48 h. For EBNA2 function assays after 5 h 1 μ M β -estradiol was added to activate ER-EBNA2. The samples were incubated at 37°C with 5% CO₂ for a further 19 h. 24 h after transfection 10 μ g/ml anti-IgM (Merck) was added to crosslink the BCR. The cells were harvested 48 h after transfection. The cells were pelleted at 403 x g for 10 min at 4°C and washed in 1 ml PBS. 100 μ l of cells transferred to an Eppendorf tube, pelleted by centrifugation at 2408 x g for 2 min using a bench top centrifuge. The supernatant was removed, snap frozen and stored at -80°C until needed for RNA analysis. The

remaining 900 μ l of cells were pelleted at 403 x g for 5 min, the supernatant was aspirated and the pellet snap frozen and stored at -80°C until used for Dual Luciferase assay.

2.1.8 siRNA knockdown

200 nM ON-TARGETplus Human SMARCA4 (BRG1) siRNA (Dharmacon, GE Healthcare) or ON-TARGETplus siRNA non-targeting siRNA #1(Dharmacon, GE Healthcare) were transfected into 5×10^6 GM12878 cells using the Neon transfection system and 1 pulse of 1300 V for 30 msec. The transfected cells were incubated at 37°C with 5% CO₂ for 72 h in normal media without antibiotics.

2.1.9 Actinomycin D mRNA stability assay

ERE2.5 cells were withdrawn from β -estradiol for 4 days prior to Actinomycin D treatment. ERE2.5 cells (10 ml) was transferred to a small upright flask. Duplicate samples were set up for each time point (0, 2, 4, 8 and 24 hrs) +/- EBNA2. 1 μ M β -estradiol was added to the +EBNA2 samples and samples were incubated at 37°C with 5% CO₂ for 2 h. After 2 h, 0.5 μ g/ml of Actinomycin D was added to all samples and cells were incubated at 37°C with 5% CO₂ and harvested after 0, 2, 4, 8, and 24 h. Pellets were snap frozen and stored at -80°C until used for mRNA analysis.

2.2 Biochemistry

Reagents and buffers used were all purchased from ThermoFisher Scientific unless otherwise specified.

2.2.1 Reagents and Buffers

1x GSB (Gel Sample Buffer) 50 mM Tris, 4% SDS, 5% 2-Mercaptoethanol (Sigma), 10% Glycerol, 1 mM EDTA and 0.01% Bromophenol Blue

1x SeeBlue™ Plus2 Pre-stained Protein Standard containing 10 protein ranging from 4-250 kD (Invitrogen, Cat. No LC5925).

SDS-PAGE running buffer: 20x NuPAGE™ Mops running buffer (Invitrogen, Cat. No. NP0001)

PBS-Tween Wash buffer: 100 PBS tablets (Thermo Fisher Cat No. 18912014), 10 ml Tween 20 (Thermo Fisher Cat. No. P9416) in 10 L dH₂O.

Transfer Buffer: 1 L methanol, 75 g glycine, 15 g Tris Base in 4 L of dH₂O

ECL solution I: 20 µl of 25 mM luminal, 8.8 µl coomarcic acid, 200 µl Tris pH8.5 made up to 2 ml dH₂O

ECL solution II: 1.28 µl of 30% H₂O₂, 200 µl Tris pH8.5 made up to 2 ml dH₂O

2.2.2 Preparation of total cell lysate

To prepare the total cell lysate, cells were washed in PBS, counted and resuspended at 1×10^6 cells/100 µl 1x GSB. The samples were sonicated on ice for 5 pulses at 25% amplitude for 10 s at 10 second intervals using a Vibra-Cell VC 750 sonicator (Sonics). After sonication the samples were boiled for 10 min at 95°C, vortexed and spun briefly for 30 s before being stored at -20°C.

2.2.3 SDS-PAGE

Samples (15 µl) were loaded on a pre-cast 4-20% NuPage Bis-Tris gel (Thermo Fisher) alongside 5 µl SeeBlue™ Plus2 marker and resolved using a 1x MOPS-SDS-page running buffer. Electrophoresis was carried out for 50min at 200 V and maximum mA.

2.2.4 Western Blot

After separation by SDS-Page the proteins were then transferred to 0.45 µm Amersham Protran nitrocellulose membrane (GE Healthcare) in transfer buffer using a wet transfer system (Bio-Rad) at 85 V for 90 min with cooling. The membrane was stained with Ponceau stain (Sigma) to verify the transfer had been successful. The stain was rinsed off with dH₂O followed by a PSB-Tween wash. The membrane was blocked using 5% milk (2.5 g milk powder in 50 ml PBS-Tween) for 1-2 h at room temperature.

Once blocked the blot was incubated with the appropriate primary antibody diluted in milk overnight at 4°C on a rocker (Appendix 8.3) for list of antibodies and dilutions used). The next day the blot was washed 3 times for 10 min with PBS-Tween at room temperature. The blot was then incubated for 1 h with a horseradish peroxidase-conjugated secondary antibody appropriately diluted in 5% milk (Appendix 8.3) at room temperature, followed by 3 times 10 min washes with PBS-Tween. Any excess liquid was then drained from the blot and it was briefly incubated with a total volume of 4 ml enzymatic chemiluminescence (ECL) solution (equal volumes of ECL solution I and II). The membrane was exposed to the Odyssey Fc Imager (Licor) using the chemiluminescence channel to visualise the protein and the 700 channel to visualise the markers.

2.2.5 Stripping a Western Blot

To strip and re-probe Western blots the membrane was rinsed in PBS-Tween and then washed 2 times for 10 min in PBS-Tween. The blot was incubated with Restore™ Western Blot Stripping Buffer (ThermoFisherScientific Cat. No 21059) at room temperature for 15 min on a rocker. After incubation the stripping buffer was poured off and the blot rinsed with PBS-Tween and washed 3 times in PSB-Tween for 5 min. The blot was then blocked for 1-2 h in 5% milk and Western blot carried out as described above.

2.2.6 Dual Luciferase Assay

The cell pellets harvested from cells transfected using either the Bio-Rad or Neon transfection system were defrosted and lysed in 90 µl of 5x Passive Lysis Buffer (Promega). The lysed cells were centrifuged briefly to clear the lysate of any debris and 10 µl aliquots of the cleared lysate were assayed in duplicate in a 96-well plate with 50 µl of Luciferase Assay Reagent LARII (firefly) read sequentially every 10 s, followed by 50 µl of Stop and Glo (renilla) also read every 10 s (Dual-Luciferase® assay, Promega). The firefly luciferase signal was adjusted for transfection efficiency using the Renilla luciferase signal from the control plasmids pRL-CMV or pRL-TK.

2.3 Molecular Biology

Reagents and buffers used were all purchased from Thermo Fisher Scientific unless otherwise specified and all solutions were made using sterile Milli-Q water.

2.3.1 Reagents and Buffers

ChIP Cell Lysis Buffer: 85 mM KCl, 0.5% NP-40, and 5 mM PIPES pH 8. 1 mM PMSF and 1 EDTA-free protease inhibitor cocktail mini-tablet (Roche) added prior to use.

SDS Lysis Buffer: 1% SDS, 10 mM EDTA, 50 mM Tris pH 8.0.

IP Dilution Buffer: 0.01% SDS, 1.1% Triton X-100, 1.2 mM EDTA, 16.7 mM Tris pH 8.0, 167 mM NaCl. 1 mM PMSF and 1 EDTA-free protease inhibitor cocktail mini-tablet (Roche) added prior to use.

Low salt wash buffer: 0.1% SDS, 1% Triton X-100, 2 mM EDTA, 20 mM Tris pH 8.0, 150 mM NaCl.

High salt wash buffer: 0.1% SDS, 1% Triton X-100, 2 mM EDTA, 20 mM Tris pH 8.0, 500 mM NaCl.

LiCl wash buffer: 250 mM LiCl, 1% NP-40, 1% Na-deoxycholate, 1 mM EDTA, 10 mM Tris pH 8.0.

TE Buffer: 10 mM Tris pH 8.0, 1 mM EDTA

Elution buffer: TE buffer, 5 mM EDTA, 1% SDS.

Proteinase K: dissolved in dH₂O and stored as 20 mg/ml aliquots at -20°C).

10x TBE: 108 g Tris base, 55 g Boric Acid and 9.3 g EDTA dissolved in 1 L dH₂O

4C Lysis buffer: 50 mM Tris pH7.5, 150 mM NaCl, 5 mM EDTA, 0.5% NP-40, 1% Trito-X, 50x protease inhibitors.

Proteinase K: dissolved in dH₂O and stored as 10 mg/ml aliquots at -20°C).

NEB Enzymes: NlaIII, DpnII

3C Lysis buffer: 10 mM Tris pH7.7, 10 mM NaCl, 5 mM MgCl₂, 0.01 mM EDTA, 1x complete protease inhibitor

Agar: 5 g agar in 400 ml LB.

Ampicillin (Sigma): 100 mg/ml dissolved in filter-sterilised dH₂O using a 0.2 µm filter (Nalgene), aliquoted and stored at -20°C.

Luria Broth (LB): 10 g tryptone (Oxoid), 5 g yeast extract (Oxoid), 10 g NaCl, made up to 1 litre in dH₂O followed by autoclaving.

CsCl Prep Solution I: 50 mM glucose, 25 mM Tris-HCl pH 8.0, 10 mM EDTA (Sigma).
Stored at 4°C

CsCl Prep Solution II: 200 mM NaOH, 1% SDS. This buffer is made up fresh at the start of the experiment.

CsCl Prep Solution III: 300 ml 5 M KAC, 57.5 ml glacial acetic acid, 142.5 ml dH₂O.

CsCl saturated butanol: 100 g Caesium chloride (Invitrogen) in 200 ml dH₂O and 200 ml butanol.

2.3.2 RNA isolation

RNA was extracted from 5×10^6 cells using TRIreagent (Sigma) and purified using RNeasy columns (Qiagen) according to the manufacturer's guidelines. Following RNA purification the RNA concentration was determined by placing 2 µl of the RNA sample on the NanoDrop 2000c (ThermoFisher Scientific).

2.3.3 cDNA Synthesis

cDNA was synthesised from purified RNA using the ImProm-II reverse transcription system using random primers (Promega). 1 µg of RNA was incubated with 1 µl of Random Primer and Milli-Q water in a total volume of 5 µl at 70°C for 5 mins, followed

by 5 min on ice. For reverse-transcription 15 µl of master mix containing 4.5 µl nuclease free water, 4 µl Improm-II 5x reaction buffer, 4 µl MgCl₂, 1 µl dNTP mix, 0.5 µl RNAsin ribonuclease inhibitor and 1 µl Improm-II Reverse Transcriptase was added to each sample. cDNA was synthesised under the following conditions; 25°C for 5 min (primer annealing), 42°C for 60 min (extension); 70°C for 15 min (enzyme denaturation). cDNA samples were stored at -20°C until needed.

Alternatively, for low cell numbers (1×10^5 cells) cDNA was synthesised directly from the cells using the Power SYBR® Green Cells-to-CT™ kit (Life technologies) according to manufacturer's instructions.

2.3.4 Q-PCR

Q-PCR was carried out using an Applied Biosystems StepOnePlus PCR machine. Each real-time PCR reaction (total volume 15 µl) contained 3 µl cDNA, 7.5 µl GoTaq QPCR mastermix (Promega) and 0.15 µM of each primer. The DNA was amplified under the following conditions: heating to 95°C for 10 min followed by 40 cycles of heating to 95°C for 15 s and 60°C for one minute. Serial dilutions of cDNA were used to generate standard curves for each primer set (Appendix 8.5 and 8.6 for primers).

For cDNA analysis, samples were analysed using absolute quantification, or relative quantification (ddCT). For absolute quantification standard curves were generated using an appropriate cDNA sample. Transcript levels were determined using cDNA specific primers for the gene in question. GAPDH, Actin, or β-2-Microglobulin transcript levels were used as a normalisation control. For relative quantification (ddCT), Q-PCR was carried out using the Power SYBR® Green Cells-to-CT™ kit (Life technologies) according to the manufacturer's specifications. Transcript levels were determined

using cDNA specific primers for the gene in question with GAPDH as the endogenous control.

For ChIP analysis, input control samples were serially diluted 4-fold to generate the standard curve for each primer set.

2.3.5 Chromatin Immunoprecipitation (ChIP)

2.3.5.1 Chromatin Preparation

For the EREB2.5 cell line, cells were washed and re-suspended at 5×10^5 cells/ml in medium without β -estradiol in four separate flasks. After 4 days of withdrawal, a 0 control sample was taken and β -estradiol then added and chromatin prepared 4, 8, and 24 h later.

For Mutu III and BL31 WT Bac cell lines, cells were diluted to 2×10^5 cells/ml 48 h prior to chromatin preparation.

Prior to crosslinking all cell lines were re-suspended at 1×10^7 cells in fresh media. Cells were crosslinked by adding formaldehyde to the media to a final concentration of 1% from a 36.5% stock and incubated at room temperature for 15 min on a rocker. Glycine was added to a final concentration of 0.125 M to quench the reaction. Cells were pelleted by centrifugation at $403 \times g$ for 10 min at 4°C and washed with PBS once before being resuspended in $300 \mu\text{l}$ Cell lysis buffer per 1×10^7 cells. The cells were lysed on ice for 10 min. The nuclei were pelleted at $6093 \times g$ for 5 min at 4°C and resuspended in $200 \mu\text{l}$ SDS lysis buffer per 1×10^7 cells. The chromatin was then sonicated in Eppendorf tubes on ice for 10 times 10 s pulses at 30% output to reduce

DNA length to 200-600 bp. The sonicated chromatin was pooled, aliquoted into Eppendorf tubes and stored at -80°C.

25 µl of sonicated chromatin was analysed to determine the DNA length. 75 µl of elution buffer was added and the sample incubated overnight at 65°C to reverse the crosslinks. 75 µl of TE buffer and 1.25 µl of 20 mg/ml proteinase K was then added to digest the protein and the sample incubated 50°C for 2 h. The DNA was purified using a Qiagen Gel Extraction kit and eluted in 40 µl dH₂O. The size of the chromatin was determined by running a sample on a 1.5% agarose TBE gel.

2.3.5.2 Protein A sepharose Bead Preparation

To preblock protein beads, 100 µl of 50% protein A Sepharose beads per IP reaction were washed 3 times with IP dilution buffer and resuspended in 50 µl of IP dilution buffer per IP reaction. Beads were then incubated with 0.05% BSA at 4°C for a minimum of 2 h with rotation.

2.3.5.3 Chromatin Immunoprecipitation

Chromatin was pre-cleared using preblocked beads by diluting 100 µl chromatin per IP 1:10 with IP dilution buffer containing protease inhibitors, adding 45 µl of preblocked protein A beads per IP reaction and incubating samples for 45 min at 4°C with rotation. The sample was centrifuged at 1452 x g for 5 min to remove the beads. The supernatant was aliquoted into fresh Eppendorf tubes and 40 µl was removed and stored at -20°C to be used as input control. The remaining chromatin was incubated with rotation overnight at 4°C with specific antibodies (Appendix 8.4), or an IgG anti-mouse control antibody. Secondary antibodies were added as required and incubated for a further 2 h at 4°C with rotation.

To collect the precipitated complexes 45 μ l of preblocked Protein A sepharose beads were added to each IP sample and samples rotated at 4°C for 3 h. The samples were then washed for 10 min with rotation at 4°C once with 1 ml each of the following wash buffers: low salt wash buffer, high salt wash buffer, LiCl wash buffer. Samples were then washed twice in 1 ml TE buffer. After the final wash samples were centrifuged at 857 x g for 1 min at 4°C and the supernatant was discarded. The immunocomplexes were eluted in 150 μ l Elution buffer at 65°C for 20 min. The beads were removed and the DNA-protein complexes were incubated overnight at 65°C to reverse the crosslinks alongside the input control samples. 45 μ g of proteinase K and 150 μ l of TE were added and samples incubated at 50°C for 2 h to digest the protein. The DNA was purified using a Qiagen Gel Extraction Kit and DNA was eluted in 110 μ l dH₂O.

2.3.6 Circularised Chromatin Conformation Capture (4C)

Cells were fixed in 2% formaldehyde for 10 min, the reaction was quenched using 1 M glycine. Cells were pelleted at 403 x g for 8 min at 4°C using Sorvall Legend RT centrifuge with swing bucket rotor (ThermoFisher) and the supernatant removed. Pellets were resuspended in 5 ml cold lysis buffer, incubated for 10 min on ice and spun at 773 x g for 5 min at 4°C and supernatant removed. Cells were stored at -80°C until needed.

Pellets were resuspended in 440 μ l Milli-Q water and 60 μ l of 10x RE buffer (NEB CutSmart) was added. Samples were placed at 37°C and 7.5 μ l of 20% SDS was added followed by incubation for an hour with shaking at 900 rpm in a thermomixer (Eppendorf). 75 μ l of 20% Triton X-100 was then added and samples incubated for a further hour with shaking. A 5 μ l aliquot from each sample was taken as an undigested control. To begin the first digestion 200 U of Nla III (NEB) were added to the samples

and samples incubated for 4 h at 37°C with shaking. A further 200 U of NlaIII (NEB) were then added and the samples incubated overnight under the same conditions. Finally another 200 U of Nla III was added and samples incubated for a further 4 h. A 5 µl aliquot was taken from each sample as a digested control. To reverse the crosslinks and digest the protein 90 µl of 10 mM Tris-HCL pH 7.5 and 5 µl of Proteinase K (10mg/ml) were added to the 5 µl samples and incubated at 65°C for 1 h. Before proceeding to the ligation step the digestion efficiency was determined by running samples on a 0.6% agarose gel after reversing the crosslinks using Proteinase K.

Nla III was then inactivated by heating at 65°C for 20 min. The samples were transferred to a 50 ml falcon tube and 700 µl of 10x ligation buffer (Roche) and Milli-Q water (up to 7 ml) was added, followed by the addition of 10 µl ligase (Roche 5 U/µl). Ligation was carried out overnight at 16°C. A 100 µl aliquot was taken from each sample as a ligation control. Ligation efficiency was determined by running the samples on a 0.6% agarose TBE gel after reversing the crosslinks as described above.

After successful ligation, 30 µl Proteinase K (10mg/ml) was added to the samples to digest the protein followed by overnight incubation at 65°C to reverse the crosslinks. The overnight incubation was followed by addition of 15 µl RNase A (20mg/ml) (Invitrogen) and incubation for a further 45 min at 37°C. DNA was purified using phenol-chloroform extraction and ethanol precipitation and then dissolved in 150 µl of 10 mM Tris-HCL (pH 7.5) at 37°C.

For the secondary RE digestion 50 μ l of 10x Dpn II restriction buffer was added to each sample along with 50 U of Dpn II enzyme (Roche). Samples were made up to 500 μ l using Milli-Q and incubated overnight at 37°C. A 5 μ l aliquot was taken from each sample as a digested control. Before proceeding to the ligation the digestion efficiency was determined by running the controls out on a 0.6% agarose TBE gel.

After successful secondary RE digestion, the RE was inactivated by incubating at 65°C for 25 min after which the samples were transferred to a 50 ml falcon tube and 1.4 ml of 10x ligation buffer (Roche) and 20 μ l of ligase (Roche) were added. Volume made up 14 ml using Milli-Q. Ligation was carried out at 16°C overnight. A 100 μ l aliquot was taken from each sample as a ligation control. Ligation efficiency was checked by running the samples on a 0.6% agarose TBE gel.

After ligation, DNA was isolated using ethanol precipitation. The resulting pellet was dissolved in 150 μ l 10mM Tris-HCl (ph 7.5) at 37°C. DNA samples were purified using the QIAquick PCR purification kit, using three columns per sample. The concentration of the samples was measured using a NanoDrop 2000c (ThermoFisher Scientific).

Next, the 4C template was prepared for sequencing; The PCR reaction mixture was prepared by combining 80 μ l of 10x PCR buffer (Roche), 16 μ l of 10 mM dNTPs, 1.12 nmol 75nt P5 sequencing primer and 1.12 nmol 40nt reverse P7 primer, 3.2 μ g of 4C template was added along with 11.2 μ l Expand Long Template Polymerase (Roche) and Milli-Q water up to 800 μ l. 16 individual 50 μ l PCR reactions were carried out for each sample. The PCR reactions used forward primers that included a 5' overhang of the

Illumina sequence adaptor P5 and a unique barcode for each sample and a common reverse primer, MYCP7, that also included a 5' of the Illumina sequence adaptor P7 (Appendix 8.7). The DNA was amplified using the following conditions; heating to 94°C for 2 min , 94°C for 10 s , 55°C for 1 min, 68°C for three min for 29 cycles followed by 68°C for five min. Upon completion of the PCR program the 16 reactions were pooled and the samples were purified using the High Pure PCR product Purification kit (Roche), which separates non-used adaptor primers and PCR product. The sample DNA quantity was determined using a NanoDrop 2000c (ThermoFisher Scientific). The quality of the 4C PCR product was determined by analysing 300 ng of purified PCR product on a 1.5% agarose TBE gel.

2.3.6.1 Bioanalyser (4C)

Prior to sequencing the 4C library, the samples were quantified using a 2100 Agilent bioanalyser. To establish the molarity of the samples 8.5 ng/ul of each sample was loaded in to a well on an Agilent High Sensitivity DNA chip and assayed. The data obtained from the electropherogram were analysed using Agilent 2100 Expert software. Samples too concentrated for Illumina sequencing were diluted to 10 nM in 10 µl prior to sequencing.

2.3.6.2 4C –sequencing and data analysis

4C-sequencing and data analysis was performed at the Babraham Institute. The data extraction used a custom script to remove and separate embedded barcodes, and to remove reads from the restriction fragment neighbouring the bait region where no digestion had occurred. The reads were mapped to the Homo sapiens GRCh37 genome assembly using bowtie 2 v2.2.7 and default parameters and were filtered to retain only

those uniquely mapping reads with $\text{MAPQ} \geq 42$. For absolute quantitation, the genome was divided into 10 kb windows and quantitated with read counts normalised to the data set with the highest read coverage. For relative quantitation, the genome was divided into windows containing 50,000 reads across all samples. Read counts for each region were quantitated in each individual data set and the raw counts were corrected for the total read count to normalise data. Interaction count differences were calculated by subtracting the normalised counts from one data set from another data set. The 4C data is available via GEO accession GSE82150 (Wood et al., 2016). A simplified flow diagram of the 4C process can be found in Appendix 8.8

2.3.7 Chromatin Conformation Capture (3C)

Cells were passed through a 70 μm cell strainer to obtain a single-cell suspension. 1×10^7 cells were fixed in 1% formaldehyde with 10% FCS and incubated for 10 min at room temperature while tumbling. The crosslinking reaction was quenched with 0.125 M glycine and centrifuged for 8 min at 230 g at 4°C to collect the cells. The pellet was taken up in 5 ml of cold lysis buffer and lysed for 10 min on ice. The nuclei were collected by centrifuging for 10 min at 400 g at 4°C and then resuspended in 0.5 ml 1.2x restriction enzyme buffer (NEB) containing 0.3% SDS and incubated for 1 h at 37°C with shaking at 900 rpm. 50 μl of 20% Triton X-100 was added to the nuclei and samples incubated for 1 h at 37°C while shaking at 900 rpm. 400 U of Hind III (NEB) was added and samples incubated at 37°C while shaking at 900 rpm overnight. The reaction was stopped by the addition of 40 μl of 20% SDS and incubated at 80°C for 25 min while shaking at 900 rpm. The digested nuclei were transferred to a 50 ml falcon tube and 6.125 ml of 1.15X ligation buffer (NEB) was added along with 375 μl of 20% Triton X-100. The sample was then incubated for 1 h at 37°C while shaking gently at 225 rpm.

Following the incubation, 100 U T4 DNA ligase (NEB) were added and samples incubated at 16°C for 4 h followed by 30 min at room temperature. 300 µg of Proteinase K (Roche) was added and samples or the sample incubated overnight at 65°C to reverse cross links. RNA was removed by adding 300 µg RNase and incubating for 45 min at 45°C. Following phenol-chloroform extraction the DNA was ethanol precipitated and analysed by PCR using primers designed to amplify over the ligated junctions (Appendix 8.7). As a positive control for the ligation products GeneArt Strings DNA fragments (Invitrogen) were designed to represent the each of the three anticipated ligation products and analysed by PCR using the same 3C primers. The PCR product was visualised and quantified using a LiCOR imaging system following agarose gel electrophoresis and staining with GelRed (Biotium). The interaction frequencies were determined by dividing the 3C library signal for each ligation junction by the signal from the positive control sample. A simplified flow diagram of the 3C process can be found in Appendix 8.9.

2.3.7.1 Polymerase Chain Reaction (PCR) for 3C

PCR was carried out using the ProFlex™ System from Applied Biosystems. Each PCR reaction (total volume 25 µl) contained 1 µl template DNA, 5 µl GC buffer (NEB), 0.5 µl dNTPs, 1.25 µl of each primer, 0.25 µl High-Fidelity Phusion DNA Polymerase (NEB) and 15.75 µl Milli-Q water. The DNA was amplified under the following conditions: heating to 98°C for 30 s followed by 35 cycles of heating to 98°C for 10 s , 55°C for 30 s and 72°C for 30 s , followed by a final extension phase at 72°C for 10 min.

2.3.8 Agar plates

Agar was melted in the microwave and left to cool. Ampicillin (selection antibiotic) was added at a final concentration of 100 µg/ml and gently mixed. Once mixed the plates were poured, left to set on the bench and later stored at 4°C

2.3.9 Bacterial Cell Transformation

100 ng of plasmid DNA was added to 50 µl of competent E.coli DH5α cells, samples were mixed and incubated on ice for 20 min. The cells were heat-shocked at 42°C for 45 s and placed on ice for 2 min. 250 µl of LB (without antibiotics) was added and cells incubated for 40 min at 37°C with shaking at 225 rpm. 25 µl of transformed cells were plated onto an agar plate with the appropriate selection antibiotic and incubated overnight at 37°C to allow colonies to grow.

2.3.10 Glycerol Stocks

Competent E.coli DH5α cells were transformed with plasmid DNA and streaked onto an agar plate containing the appropriate antibiotic. The plate was left to grow overnight at 37°C. One colony was picked and inoculated into 10 ml of LB (containing the appropriate antibiotic) and incubated overnight at 37°C with gentle shaking at 225 rpm. Following overnight incubation, 850 µl of culture was added to 150 µl of glycerol in a cryogenic vial to make a 15% glycerol stock. The vials were stored at -80°. The glycerol stocks were used for long-term storage.

2.3.11 Caesium Chloride (CsCl) DNA Preparation

A single colony of DH5α transformed cells containing the plasmid of interest was picked, inoculated into 5 ml of LB containing the appropriate antibiotics and incubated at 37°C for 6 hours with gentle shaking at 225 rpm. The 5 ml culture was

then transferred to a large conical flask with 400 ml LB containing the appropriate antibiotics and incubated at 37°C overnight with shaking (225 rpm).

The cells were pelleted by centrifugation at 3951 x g for 10 min at 4°C using a JA-10 rotor (Beckman) in a Beckman Coulter Avanti J-20 XP centrifuge. The cell pellet was resuspended in 14 ml of Solution I. 28 ml of Solution II was added to the cell suspension to lyse the cells and mixed well by gently swirling. 22 ml of Solution III was added followed by mixing and incubation on ice for 5 min. The cell debris was pelleted by centrifugation at 7903 x g for 10 min at 4°C and the supernatant was filtered through a cheesecloth into a fresh bottle. 36 ml of isopropanol was added to the samples and incubated for 10 min at room temperature to precipitate the DNA. The samples were centrifuged at 2580 x g for 10 min at 4°C in a Heraeus Mega Fuge 8R centrifuge. The pellets were resuspended in 6 ml Milli-Q water and 4 ml of 5M NH₄ acetate was added to precipitate the RNA. The samples were left to incubate on ice for 1 hour. The precipitated RNA was pelleted by centrifugation at 2580 x g for 15 min at 4°C and the supernatant was mixed with 30 ml of 100% ethanol to precipitate DNA. The samples were left at room temperature for 5-10 min before the DNA was pelleted by centrifugation at 2580 x g for 10 min at 4°C. The supernatant was discarded and the DNA was resuspended in 4 ml Milli-Q water. 4.3 g CsCl and 100 µl Ethidium Bromide (10mg/ml) was added to each sample. The solution was transferred to Beckman Optiseal centrifuge tubes, ensuring there were no air bubbles, and placed in Beckman VTi 65.2 rotor with a spacer and torqued screw seal. The samples were centrifuged overnight at 227,640 x g in a Beckman Optima LE-80K ultracentrifuge. During ultracentrifugation plasmid DNA was separated from chromosomal DNA using the CsCl gradient.

The following morning a 19G needle was used to extract the plasmid DNA. The Ethidium bromide was removed by several extractions using an equal volume of CsCl saturated butanol. Once the Ethidium Bromide had been removed the DNA was diluted by adding 3 volumes of Milli-Q water and the DNA was precipitated with 2 volumes of ethanol. Following a 1 hour incubation at -20°C, the DNA was pelleted by centrifugation at 2580 x g for 20 min at 4°C, air dried for 10 min and resuspended in 0.5 ml of nuclease free H₂O. The concentration of plasmid DNA was then determined using a NanoDrop 2000c (ThermoFisher Scientific)

3. Transcriptional regulation of *CD79A* and *CD79B* by EBNA2

3.1 Introduction

EBV is able to deregulate the expression of host cell genes from several growth and survival pathways to transform and immortalise B cells. EBV nuclear antigens EBNA2 and EBNA3 play a key role in driving B cell transformation and immortalisation. To determine where EBNA2 and EBNA3 proteins bind in the B cell genome to target and deregulate host cell gene expression, a previous PhD student in our lab (Michael McClellan) carried out ChIP-sequencing (ChIP-seq) for EBNA2 and EBNA3 proteins. He used the EBV positive Burkitt's Lymphoma (BL) cell line Mutu III, which expresses all EBV latent proteins (McClellan et al., 2013). An EBNA2-specific monoclonal antibody was used for the EBNA2 ChIP-seq and a polyclonal antibody raised against EBNA3C was used for EBNA3C ChIP-seq. During the experiments it was discovered that the EBNA3C antibody cross reacts with EBNA3A and EBNA3B so the sites mapped could not distinguish between individual EBNA3 proteins and were termed EBNA3 protein binding sites (McClellan et al., 2013). Significant binding peaks for EBNA2 and EBNA3 proteins were identified using the peak calling algorithm MACS with a p-value cut off of $<10^{-7}$ (Zhang et al., 2008).

To link EBNA binding sites to potential host cell target genes three different criteria were used (Figure 3.1). The first criterion was the most stringent; it selected host cell genes that had significant promoter-proximal EBNA binding. Promoter-proximal binding sites are sites that are within 2kb of the gene transcription start site. There is a high probability that genes with promoter-proximal EBNA binding sites are regulated by EBNA proteins. The second criterion was less stringent and selected genes that

were closest to the top most significant EBNA binding sites (irrespective of distance). For EBNA3, the top 300 most significant binding sites were used for analysis. For EBNA2, a total of 526 sites were used for analysis (as these all shared the lowest p-value). Criterion two was based on the assumption that the most significant binding sites are likely to represent active gene regulatory elements. The third and final criterion identified target genes that were closest to any significant EBNA binding site, again irrespective of distance.

Pathway analysis of these gene lists using the bioinformatic tool DAVID, was carried out by Prof. Michelle West. Analysis of the promoter-proximal-EBNA2 and EBNA3-bound gene list found that the B-cell Receptor (BCR) signalling pathway was the only significantly enriched pathway using the widely-used cut off of Bonferonni <0.01 (Table 3.1). Analysis of the genes closest to the top most significant EBNA2 binding sites showed that, again, the BCR signalling pathway was the only significantly enriched pathway (Table 3.1). Analysis of the genes closest to the top EBNA3 binding sites did not show significant enrichment for any pathways. Combining the first two criteria identified 25 unique BCR signalling pathway genes that may be potential targets for EBNA2 and EBNA3 proteins (*IFITM1, NFKBIA, CD72, RASGRP3, CD22, PIK3AP1, NFATC4, INPP5D, PIK3R1, NFATC1, PIK3R2, SYK, PTPN6, CR2, VAV3, LYN, PIK3CD, VAV2, PRKCB, MAPK1, CD19, CD81, PLCG2, CD79B, CD79A*). The position of these genes along the BCR signalling pathway is shown in Figure 3.2.

Pathway analysis of the genes identified using the third criterion identified the BCR signalling pathway as the second most significantly enriched pathway for both EBNA2 and EBNA3 bound sites. The most significantly enriched pathway for EBNA2 was the T-

cell receptor signalling pathway, although many genes in these two pathways overlap. The most significantly enriched pathway for using this criterion for EBNA3 binding was JAK/STAT signalling. All three criteria combined identified 63 unique genes in the BCR signalling pathway that could be potential target genes of EBNA2 and EBNA3 proteins.

The B cell receptor (BCR) plays an essential role in all stages of B cell development and function (Geisberger et al., 2006, Reth, 1992). The ligand-binding subunit is a surface immunoglobulin (IgM) and its signal transduction subunits are Ig α and Ig β (also known as *CD79A* and *CD79B*) (Wienands, 2000, van Noesel et al., 1991) (Figure 3.3). *CD79A* and *CD79B* proteins are expressed in virtually all mature and immature B-cells (Mason et al., 1995, Mason et al., 1992). Both *CD79A* and *CD79B* are required for BCR cell surface expression and signalling leading to B cell activation (Clark et al., 1992). Antigen binding to the surface immunoglobulin triggers activation of the BCR resulting in signal transduction down various signalling pathways including, the calcium signalling, PIK3-AKT and MAPK pathways leading to the activation of transcription factors including NFAT, NF- κ B, AP-1 and MYC resulting in the activation of gene transcription. The focus of this project was on the calcium signalling pathway and its components (Figure 3.2), while the PIK3-AKT pathway was studied by Dr. Sarika Khasnis as part of her PhD project (Khasnis, 2018).

Published microarray studies from our own and other laboratories were studied by Dr Michael McClellan for previous evidence of EBNA2 and EBNA3-dependent regulation of the BCR signalling target genes we identified as potential targets by ChIP-seq. His findings are summarised in table 3.2 (Chen et al., 2005), (Maier et al., 2006),

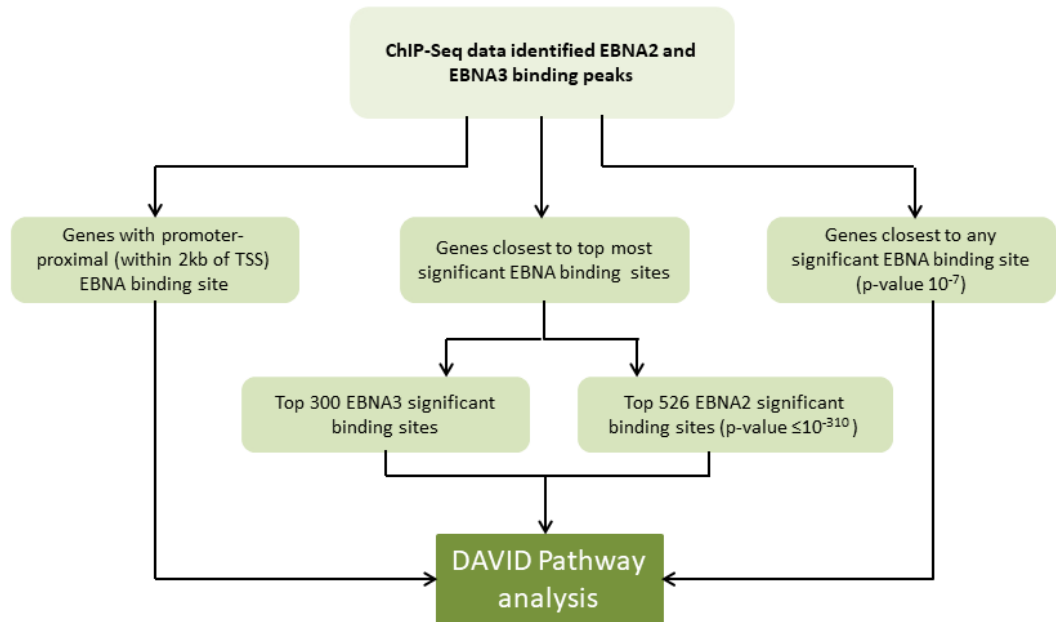


Figure 3.1. Flow chart outlining the methodology used to identify EBNA bound genes from the ChIP-seq data generated by the West laboratory. The host cell genes were selected using three different criteria; genes with promoter proximal peaks, genes closest to top most significant EBNA peaks, and genes closest to any significant EBNA binding peak. Pathway analysis of these genes was carried out using the bioinformatics tool DAVID.

Signalling Pathway	P-value	Genes	Bonferroni	Benjamini	FDR
EBNA2 Promoter-Proximal					
B cell receptor signalling pathway	1.39E-05	PTPN6, CD19, RASGRP3, NFKBIA, CD22, CD79B, NFATC4, CD79A, CD72, PIK3RI, SYK	0.001759	0.001759	0.016079
EBNA3 Promoter-Proximal					
B cell receptor signalling pathway	1.87E-06	PTPN6, VAV3, NFKBIA, CD72, PRKCB, MAPK1, CD19, RASGRP3, CD22, NFATC4, CD79B, CD79A, PIK3R1, SYK	2.82E-04	2.82E-04	2.23E-03
EBNA2 Top Significant					
B cell receptor signalling pathway	2.61E-09	PTPN6, CR2, IFITM1, LYN, PIK3CD, VAV2, CD19, CD81, PLCG2, CD22, CD79B, PIK3AP1, NFATC4, CD79A, INPP5D, NFATC1, PIK3R2	3.50E-07	3.50E-07	3.06E-06
EBNA2 closest					
B cell receptor signalling pathway	1.95E-12	HRAS, NFKB1, BTK, FOS, PIK3CA, PIK3AP1, SYK, AKT2, PIK3CG, BCL10, LYN, PIK3CB, RELA, LOC646626, PIK3CD, PRKCB, CARD11, MAPK1, JUN, CD81, IFITM1, NFKBIE, GRB2, PPP3R1, NFKBIA, CD72, LOC407835, KRAS, RASGRP3, DAPP1, RAC2, SOS1, RAC1, PPP3CB, NFAT5, PPP3CC, CD22, NFATC4, PIK3R5, PPP3CA, INPP5D, PIK3R3, NFATC2, NFATC3, PIK3R1, NFATC1, PIK3R2, BLNK, PTPN6, VAV3, CR2, MAP2K1, MAP2K2, MALT1, VAV2, VAV1, CD19, GSK3B, PLCG2, CD79B, CD79A, IKKBK	3.37E-10	1.87E-10	2.42E-09
EBNA3 closest					
B cell receptor signalling pathway	3.96E-10	NFKBIA, CD72, LOC407835, FOS, KRAS, RASGRP3, DAPP1, RAC2, SOS1, PPP3CC, CD22, NFATC4, PIK3AP1, PPP3CA, INPP5D, PIK3R3, NFATC3, AKT3, PIK3R1, NFATC1, BLNK, SYK, PIK3CG, PTPN6, BCL10, VAV3, CR2, LYN, PIK3CB, MAP2K2, LOC646626, VAV2, PRKCB, CARD11, MAPK1, CD19,	7.40E-08	3.70E-08	4.90E-07

Table 3.1. David analysis using ChIP-seq data from Mutu III cells shows enrichment of the BCR signalling pathway. Enrichment of the BCR signalling pathway for genes with promoter proximal (within 2Kb) EBNA2 and EBNA3 binding sites, genes closest to the top most significant EBNA2 binding site, or genes close to any significant EBNA2 or EBNA3 binding site (McClellan *et al.*, 2013).

(Spender et al., 2006), (Zhao et al., 2006), (Hertle et al., 2009), (White et al., 2010), (Zhao et al., 2011a). His analysis showed that some BCR genes had previously been identified as regulated genes by gene expression arrays, confirming the validity of our approach. For many genes however, regulation had not been confirmed in follow-up experiments or in other cell lines.

CD79A and *CD79B* were identified as potential BCR pathway target genes for EBNA2 and EBNA3 proteins. *CD79A* and *CD79B* were identified as genes with a top significant promoter-proximal EBNA2 peak and a promoter-proximal EBNA3 peak (Table 3.1). Consistent with this, our ChIP-seq analysis mapped EBNA2 and EBNA3 binding peaks proximal to the *CD79A* and the *CD79B* promoter (Figures 3.4 and 3.5). Microarray data from other laboratories had previously identified *CD79A* and *CD79B* as genes whose expression was regulated by these EBNA3 proteins. A microarray study by White et al (2010) using the EBV negative Burkitt's Lymphoma cell line (BL31) infected with recombinant wild-type EBV or EBNA3 knock-out viruses found *CD79A* and *CD79B* to be negatively regulated by EBNA3B and EBNA3C. However, microarray studies by carried out in a LCL background did not detect regulation of *CD79A* and *CD79B* by the EBNA3 family of proteins (White et al., 2010, Hertle et al., 2009, Skalska et al., 2013). These published microarray data were consistent with a TaqMan gene expression study carried out by Dr Khasnis in our lab, suggesting regulation of *CD79A* and *CD79B* by the EBNA3 family is cell line specific.

CD79A and *CD79B* were also identified as EBNA2 regulated genes in a microarray study by Maier et al. (2006) in a lymphoma background. This study found that *CD79A* was

Unique BCR targeted genes	EBNA3A		EBNA3B		EBNA3C			EBNA3s			EBNA2				EBNA2 top significant	EBNA2 promoter proximal	EBNA3 promoter proximal
	1	2	3	4	5	6	7	8	9	10	11	12	13	14			
	0	0	0	0	0	0	0	0	0	0	0	0	0	0			
CR2	0	0	0	0	0	0	0	0	0	0	0	0	0	0	0	0	0
CD22	0	0	0	0	0	0	0	0	0	0	0	0	0	0	0	0	0
CD72	0	0	0	0	0	0	0	0	0	0	0	0	0	0	0	0	0
CD79B	0	0	0	0	0	0	0	0	0	0	0	0	0	0	0	0	0
CD79A	0	0	0	0	0	0	0	0	0	0	0	0	0	0	0	0	0
LYN	0	0	0	0	0	0	0	0	0	0	0	0	0	0	0	0	0
NFATC1	0	0	0	0	0	0	0	0	0	0	0	0	0	0	0	0	0
NFATC2	0	0	0	0	0	0	0	0	0	0	0	0	0	0	0	0	0
PIK3R5	0	0	0	0	0	0	0	0	0	0	0	0	0	0	0	0	0
VAV2	0	0	0	0	0	0	0	0	0	0	0	0	0	0	0	0	0
VAV3	0	0	0	0	0	0	0	0	0	0	0	0	0	0	0	0	0
BLNK	0	0	0	0	0	0	0	0	0	0	0	0	0	0	0	0	0
CD19	0	0	0	0	0	0	0	0	0	0	0	0	0	0	0	0	0
IFITM1	0	0	0	0	0	0	0	0	0	0	0	0	0	0	0	0	0
PIK3AP1	0	0	0	0	0	0	0	0	0	0	0	0	0	0	0	0	0
PIK3R3	0	0	0	0	0	0	0	0	0	0	0	0	0	0	0	0	0
PPP3CA	0	0	0	0	0	0	0	0	0	0	0	0	0	0	0	0	0
PTPN6	0	0	0	0	0	0	0	0	0	0	0	0	0	0	0	0	0
AKT3	0	0	0	0	0	0	0	0	0	0	0	0	0	0	0	0	0
KRAS	0	0	0	0	0	0	0	0	0	0	0	0	0	0	0	0	0
MALTI1	0	0	0	0	0	0	0	0	0	0	0	0	0	0	0	0	0
NFAT5	0	0	0	0	0	0	0	0	0	0	0	0	0	0	0	0	0
NFKBIA	0	0	0	0	0	0	0	0	0	0	0	0	0	0	0	0	0
NFKBIE	0	0	0	0	0	0	0	0	0	0	0	0	0	0	0	0	0
PIK3CG	0	0	0	0	0	0	0	0	0	0	0	0	0	0	0	0	0
PIK3R1	0	0	0	0	0	0	0	0	0	0	0	0	0	0	0	0	0
PLCG2	0	0	0	0	0	0	0	0	0	0	0	0	0	0	0	0	0
PPP3CB	0	0	0	0	0	0	0	0	0	0	0	0	0	0	0	0	0
PPP3R1	0	0	0	0	0	0	0	0	0	0	0	0	0	0	0	0	0
PRKCB	0	0	0	0	0	0	0	0	0	0	0	0	0	0	0	0	0
RAC1	0	0	0	0	0	0	0	0	0	0	0	0	0	0	0	0	0
RASGRP3	0	0	0	0	0	0	0	0	0	0	0	0	0	0	0	0	0
SYK	0	0	0	0	0	0	0	0	0	0	0	0	0	0	0	0	0
VAV1	0	0	0	0	0	0	0	0	0	0	0	0	0	0	0	0	0

Table 3.2 Summary of 34 genes from the BCR signalling pathway by that have previously shown regulation by EBNA3 in different cell backgrounds ranked by number of arrays showing regulation. Red cells indicate upregulation and green cells indicate down regulation. The yellow cells indicate the gene are bound by promoter proximal (within 2Kb) or are closest to top significant binding peaks EBNA2 or EBNA3 binding peaks and white cells indicate genes closest to any significant EBNA binding peak, based on ChIP-Seq data generated by the West lab using MutuIII cells. Cell line and references; 1) EBNA3A KO LCL (Hertle et al., 2009); 2) EBNA3A KO BL31 (White et al., 2010); 3) EBNA3B KO LCL (White et al., 2010); 4) EBNA3B KO BL31 (White et al., 2010); 5) EBNA3B-/3C_{low} LCL (Chen et al., 2006); 6) EBNA3C BJAB (McClellan et al., 2012); 7) EBNA3CHT LCL (Zhao et al., 2010); 8) EBNA3C KO BL31 (White et al., 2010); 9) EBNA3s KO BL31 (White et al., 2010); 10) ER/EBNA2 BL41 (Maier et al., 2006); 11) ER/EBNA2 BJAB (Maier et al., 2006); 12) EBNA2 E2HTF LCL (Zhao et al., 2006); 13) EBNA2 EREB 2.5 (Spender et al., 2006); 14) EBNA2 EREB 2.5 (Spender et al., 2006).

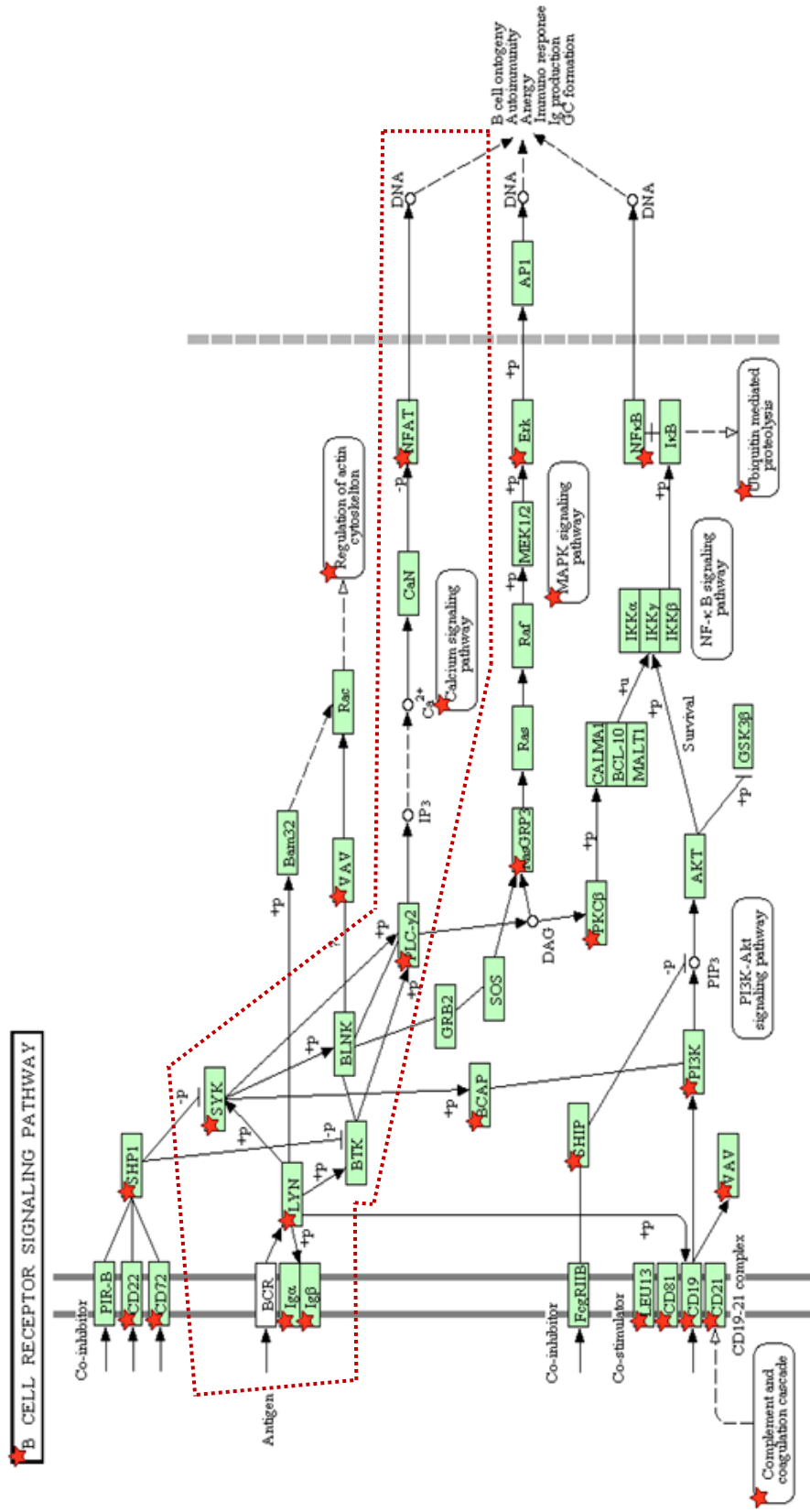


Figure 3.2. Regulation of the B-cell receptor signalling pathway. Kegg analysis of the BCR signalling pathway. Genes marked with red stars are located within 2kb of and EBNA2 or EBNA3A, 3B, 3C binding site or EBNA2 genes closest to the most significant sites. The BCR consists of a ligand binding surface immunoglobulin and the signal transducing subunits Igα (CD79A) and Igβ (CD79B). Once activated by antigen binding results in activation of protein tyrosine kinases Lyn, Syk and BTK which in turn activates a signalling pathways such as the calcium, MAPK, PI3K-Akt, and NF-κB signalling pathways. The Calcium signalling pathway is outlined by red dotted line.

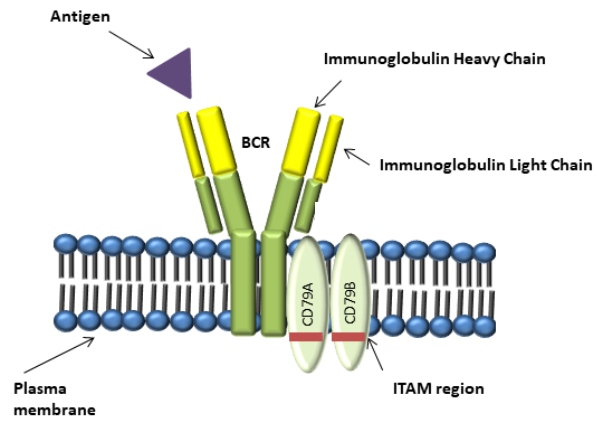


Figure 3.3 A schematic representation of the B-cell receptor. Antigen binding triggers BCR activation resulting in phosphorylation of the CD79A/B immunoreceptor tyrosine-based activation motif (ITAM) by tyrosine kinases Lyn and Syk resulting in activation of the B cell receptor signalling pathway and driving gene expression.

downregulated when EBNA2 was expressed in EBV negative BJAB B cell lymphoma cells, but not significantly altered by EBNA2 in the EBV negative BL cell line BL41. A subsequent expression screen carried out by Dr Khasnis in our laboratory using an EBV immortalised LCL (ERE2.5) expressing conditionally active EBNA2 (Kempkes et al., 1995b) found that both *CD79A* and *CD79B* were downregulated as a result of EBNA2 activation. Together, these data implicate EBNA2 in the repression of *CD79A* and *CD79B*, but in a cell background-specific manner.

In this chapter, I set out to confirm the repression of BCR signal transducing molecules *CD79A* and *CD79B* by EBNA2, and to explore the transcriptional mechanism for regulation by EBNA2.

3.2 *CD79A* and *CD79B* are repressed by EBNA2

In order to confirm *CD79A* and *CD79B* as regulatory targets of EBNA2, QPCR experiments were set up using a range of suitable cell lines sourced from a number of different research groups. We used the EBV-infected LCL (ERE2.5) expressing a conditionally active ER-EBNA2 fusion protein (Kempkes et al., 1995a) and two EBV-negative cell lines, BJABK3 and BL41K3 expressing the same ER-EBNA2 fusion protein (Kempkes et al., 1995c). The ERE2.5 cells were cultured in media containing β -estradiol before being withdrawn from β -estradiol for 4 days, allowing time for ER-EBNA2 protein to accumulate in the cytoplasm. β -estradiol was then re-added and cells were harvested after 0, 4, 8, 24 h. The BJAB and BL41 cells were harvested at a single timepoint 24hrs after β -estradiol-induced ER-EBNA2 activation. QPCR analysis was used to analyse *CD79A* and *CD79B* mRNA expression levels. The EBNA2-responsive

C promoter transcript levels were monitored to confirm EBNA2 activity in EREB2.5 cells. Levels of the EBNA2-activated cellular gene *CR2* (*CD21*) were used to confirm EBNA2 activity in BJABK3 and BL41K3 cells as they do not contain EBV genomes (Figure 3.6c and 3.7c). We detected a 9-fold down regulation of *CD79A* and a 59-fold down regulation of *CD79B* by EBNA2 24 h after β -estradiol addition in EREB 2.5 cells (Figure 3.6a and b) confirming previous microarray results (Maier et al., 2006).

In BJAB and BL41 cell backgrounds we detected a 5 fold and a 2.5 fold reduction in *CD79B* expression respectively, 24 h after EBNA2 activation (Figure 3.7b). We also observed a 2 fold reduction of *CD79A* mRNA expression in BJAB cells, but no significant repression of *CD79A* in BL41 cells (Figure 3.7a). This confirms a previously published microarray study that found *CD79B* was repressed 5-fold in BJAB cells and 2-fold in BL41 cells Whereas, *CD79A* was repressed 2.5 fold in BJAB cells 24 h after β -estradiol addition, with no repression was evident in BL41 cells. (Maier et al., 2006).

Protein analysis was carried out using the same EREB2.5 samples as described above in order to establish if the repression of mRNA impacted CD79A and CD79B protein levels in the cell. The results showed a reduction of CD79B protein expression and a total depletion of CD79A protein levels in EREB2.5 cells 24hours after ER-EBNA2 activation. (Figure 3.6d).

Taken together the data showed that *CD79A* and *CD79B* are down-regulated at the mRNA and protein level by EBNA2 in LCL and Lymphoma cell backgrounds.

3.3 Promoter-proximal EBNA2 binding overlaps with EBF-1 and RBPJk binding sites at *CD79A* and *CD79B*

To examine the mechanism of EBNA2 mediated repression of *CD79A* and *B*, we examined the chromatin landscape surrounding the EBNA2 binding sites. At *CD79A* there were two significant EBNA2 binding peaks, one (P1) overlapping the promoter and another (P2) 2kb upstream from the promoter within an active enhancer region. Both regions have high levels of H3K24Ac in the GM12878 LCL characteristic of active promoter and enhancer regions, although the H3K27Ac signal is lower around P2 (Figure 3.4). *CD79B* has one EBNA2 binding peak within its promoter region and high levels of H3K27Ac in GM12878 indicated this was an active promoter (Figure 3.5). While the H3K27Ac data are derived from a different cell line to our ChIP-seq data, both cell lines express all EBV latent genes (latency III) and EBNA2 robustly represses *CD79A* and *B* in the ER-EB2.5 LCL. Despite the presence of EBNA2 in GM12878, activation-associated marks are still present at the *CD79A* and *CD79B* promoters indicating that they retain some level of activity. The lack of repressive marks, such as H3K27Me3, in the presence of EBNA would also be indicative of active chromatin.

A genome wide study revealed that EBNA2 frequently co-localises with cellular transcription factors RBPJk and EBF-1 at many enhancer and super-enhancer regions in LCLs (Portal et al., 2013). RBPJk is a known binding partner of EBNA2 and EBF-1 is a well-established activator of *CD79A* and *CD79B* (reviewed in Lukin et al., 2008) and has recently been reported to be able to bind to EBNA2 *in vitro* (Glaser et al., 2017).

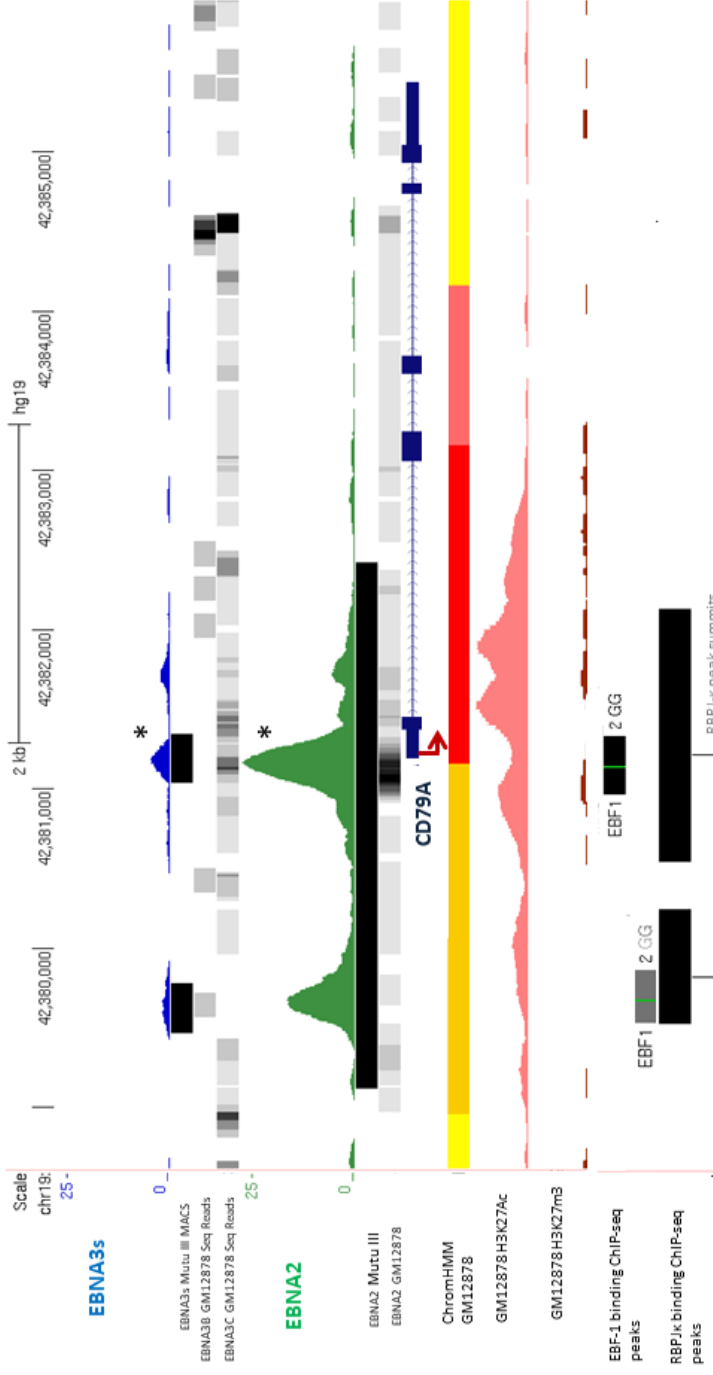


Figure 3.4 EBNA2 and EBNA3 binding sites at the CD79A locus. The number of EBNA2 and EBNA3 sequencing reads from immunoprecipitated Mutu III and GM12878 DNA are plotted per million background-subtracted total reads and aligned with the human genome. The MACS peaks indicated by the black bars represent the EBNA2 and EBNA3 binding sites. The red arrow indicates the direction of gene transcription. GM12878 H3K27Ac and H3K27me3 ChIP-seq data and chromatin segmentation by HMM from ENCODE are shown at the bottom of the panel. Chromatin segmentation by HMM colour code; Red, Strong Promoter; Pink, Weak promoter; Orange, Strong Enhancer; Yellow, Weak Enhancer. EBF-1 and RBPJk binding sites identified by ChIP-seq using GM12878 cells available through ENCODE FactorBook Motifs. *Indicates promoter proximal and top most significant EBNA2 and EBNA3 binding peaks based on ChIP-Seq data generated by the West lab using MutuIII cells. GEO GSM733771 data is publicly available from the ENCODE database (ENCODE, 2012)

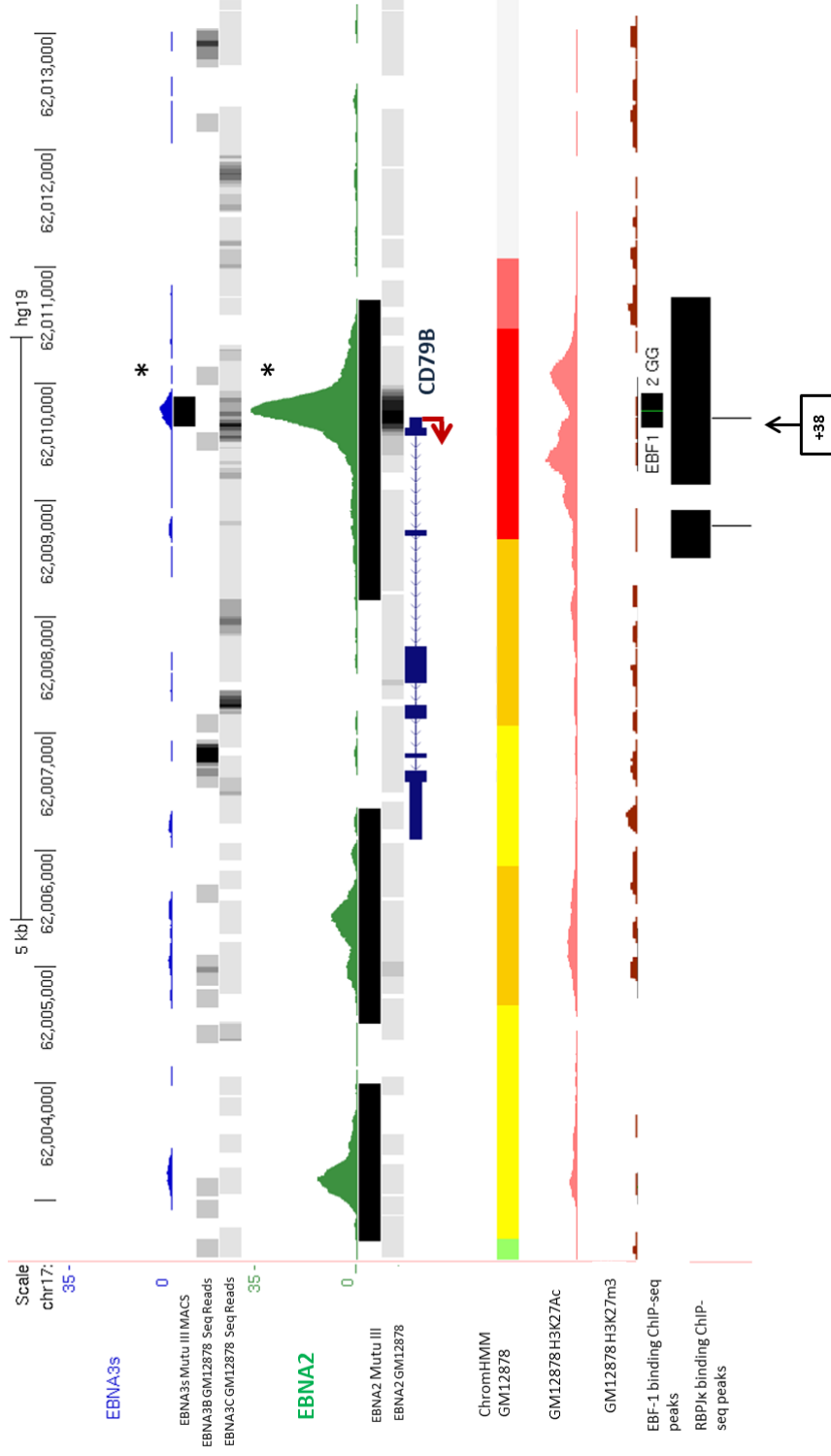


Figure 3.5 EBNA2 and EBNA3 binding sites at the *CD79B* locus. The number of EBNA2 and EBNA3 sequencing reads from immunoprecipitated Mutu III and GM12878 DNA are plotted per million background-subtracted total reads and aligned with the human genome. The MACS peaks indicated by the black bars represent the EBNA2 and EBNA3 binding sites. The red arrow indicates the direction of gene transcription. GM12878 H3K27Ac and H3K27me3 ChIP-seq data and chromatin segmentation by HMM from ENCODE are shown at the bottom of the panel. Chromatin segmentation by HMM colour code; Red, Strong Promoter; Pink, Weak promoter; Orange, Strong Enhancer; Yellow, Weak Enhancer. EBF-1 and RBPJk binding sites identified by ChIP-seq using GM12878 cells available through ENCODE FactorBook Motifs. The black arrow at the very bottom of the panel indicates ChIP-QPCR primer location. *Indicates promoter proximal and top most significant EBNA2 and EBNA3 binding peaks based on ChIP-Seq data generated by the West lab using MutuIII cells. GEO GSM733771 data is publicly available from the ENCODE database (ENCODE, 2012)

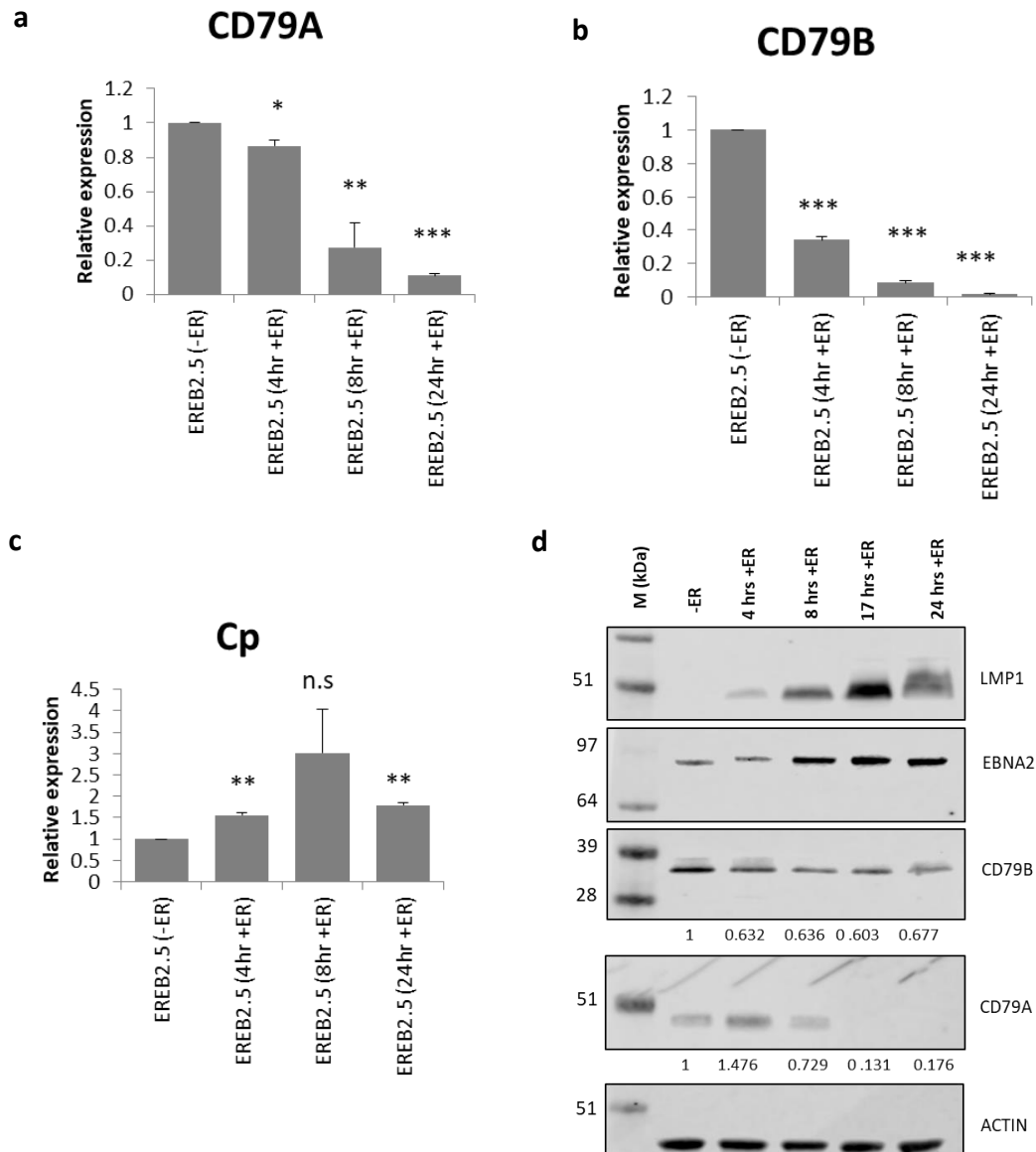


Figure 3.6. CD79A and CD79B are repressed by EBNA2 in a time dependent manner. QPCR analysis of **a) CD79A mRNA** **b) CD79B mRNA** and **c) EBV C promoter transcripts** in EREB2.5 cells treated with β -estradiol for 4, 8 and 24 h. Signals are normalised to *GAPDH* and show mean expression levels relative to no active EBNA2 (-ER) \pm standard deviation for two QPCR experiments. Results are representative of three biological repeats. p-values were calculated using the Student's T-test relative to the -ER sample and significance indicated as follows; n.s (not significant) = p-value > 0.05; * = p-value \leq 0.05; ** = p-value \leq 0.01; *** = p-value \leq 0.001. **d)** Western blot analysis of LMP1, EBNA2, CD79A and CD79B protein levels in EREB 2.5 cells treated with β -estradiol for 4, 8, and 24 h to confirm EBNA2 induction. Actin was used as a loading control. Quantification for CD79A/B antibody is shown in numbers under the Western blot; Signal strength was normalised to actin and expressed relative to EREB 2.5 (-ER).

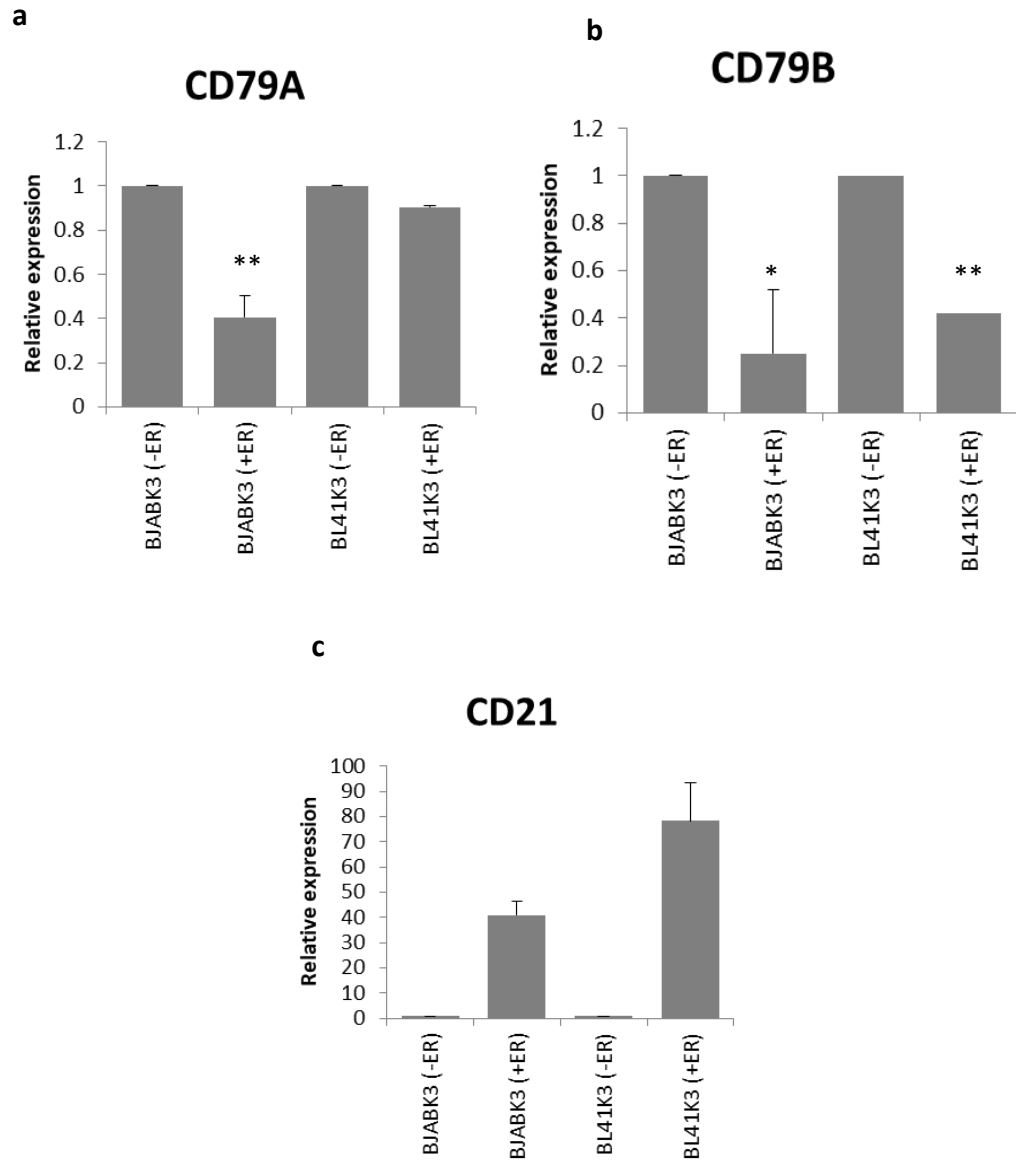


Figure 3.7. *CD79A* and *CD79B* repression by EBNA2 in BJAB and BL41 cells. QPCR analysis of **a) *CD79A***, **b) *CD79B*** and **c) *CD21*** mRNA expression in BJABK3 and BL41K3 cells treated with 1 μ M β -estradiol for 24 h. Signals are normalised to *GAPDH* and show mean expression levels relative to (-ER) \pm standard deviation of two QPCR experiments. P value were calculated the Student's T-test relative to the -ER samples and significance indicated as follows; n.s (not significant) = p-value > 0.05; * = p-value \leq 0.05; ** = p-value \leq 0.01; *** = p-value \leq 0.001.

Analysis of transcription factor binding motifs at EBNA2 binding sites at the *CD79A* and *CD79B* gene locus revealed overlapping sequences with similarity to EBF-1 and RBPJ κ binding sites (Figure 3.4 and 3.5). A simplified schematic shows the RBPJ κ consensus motif overlapping with the EBF-1 consensus motif at *CD79A* and *CD79B* promoters (Figure 3.8). Given the absence of repressive chromatin marks at the CD79 promoters, we hypothesised that *CD79A* and *CD79B* repression may be a result of competitive binding between EBNA2, EBF-1 and RBPJ κ , where EBNA2 replaces or interferes with EBF-1 function resulting in reduced transcription activation.

3.4 EBNA2 hinders EBF-1 mediated activation of *CD79B* in Luciferase reporter assays

To test our hypothesis that EBNA2 interferes with EBF-1 activation of *CD79A* and *CD79B* we set up a panel of competition based luciferase reporter assays. The *CD79Ap1p2* luciferase reporter construct contained the DNA sequences bound by EBNA2 at the *CD79A* promoter and enhancer region, the *CD79Ap1* luciferase reporter contained only the *CD79A* promoter, and the *CD79Bp* luciferase reporter construct contained the *CD79B* promoter region. The EBV-negative B-cell line DG75 was transiently transfected with the *CD79Ap1p2*, *CD79Ap1* or *CD79Bp* luciferase reporter construct, an EBF-1 expressing construct, and increasing quantities of an EBNA2 expressing construct.

Surprisingly, we found that EBNA2 was able to activate the *CD79Ap1p2* promoter and the *CD79Ap1* promoter 5-fold and 2.5-fold respectively in the presence of endogenous EBF-1 present in DG75 cells. Over expression of EBF-1 resulted in an 11-fold and a 3.5-fold activation for *CD79Ap1p2* and *CD79Ap1* construct respectively indicating the

enhancer region upstream of the *CD79A* promoter can mediate EBF-1 mediated transcriptional activation. Titration of increasing quantities of EBNA2 had no significant effect on transcriptional activation of the *CD79Ap1p2* or the *CD79Ap1* reporter constructs by EBF-1 (Figure 3.9a and b).

EBNA2 was also able to activate the *CD79Bp* reporter construct 2-fold in the presence of endogenous EBF-1. Overexpression of EBF-1, in the absence of EBNA2 resulted in a 9-fold activation of the *CD79B* promoter. The addition of increasing levels of EBNA2 reduced transcriptional activation of the *CD79Bp* promoter two fold when compared to activation by EBF-1 alone (Figure 3.9a).

As RBPJk is a known binding partner of EBNA2 and it has been reported to act as a repressor of *CD79A* and *CD79B* we examined the role of RBPJk by repeating the competition luciferase assays in a DG75 RBPJk knock-out cell line (Maier et al., 2005). The results showed that the absence of RBPJk had no effect on the ability of EBNA2 to activate the *CD79Ap1p2*, *CD79Ap1* and *CD79Bp* promoters. Again, in the presence of overexpressed EBF-1, EBNA2 did not have a significant impact on transcriptional activation of the *CD78Ap1p2* and *CD79Ap1* promoter but led to a significant reduction in transcriptional activation of the *CD79Bp* promoter (Figure 3.10). We saw an overall increase in transcription activation levels in the presence of EBF-1 in the DG75-RBPJk-knock-out cells, compared to normal DG75 cells (Figure 3.11).

Collectively, the results show that in the absence of RBPJk we see a greater activation of the *CD79A* and *CD79B* promoters. This is consistent with the repressive role of RBPJk in the absence of activated Notch at the *CD79A* and *CD79B* promoters (Smith et al., 2005).

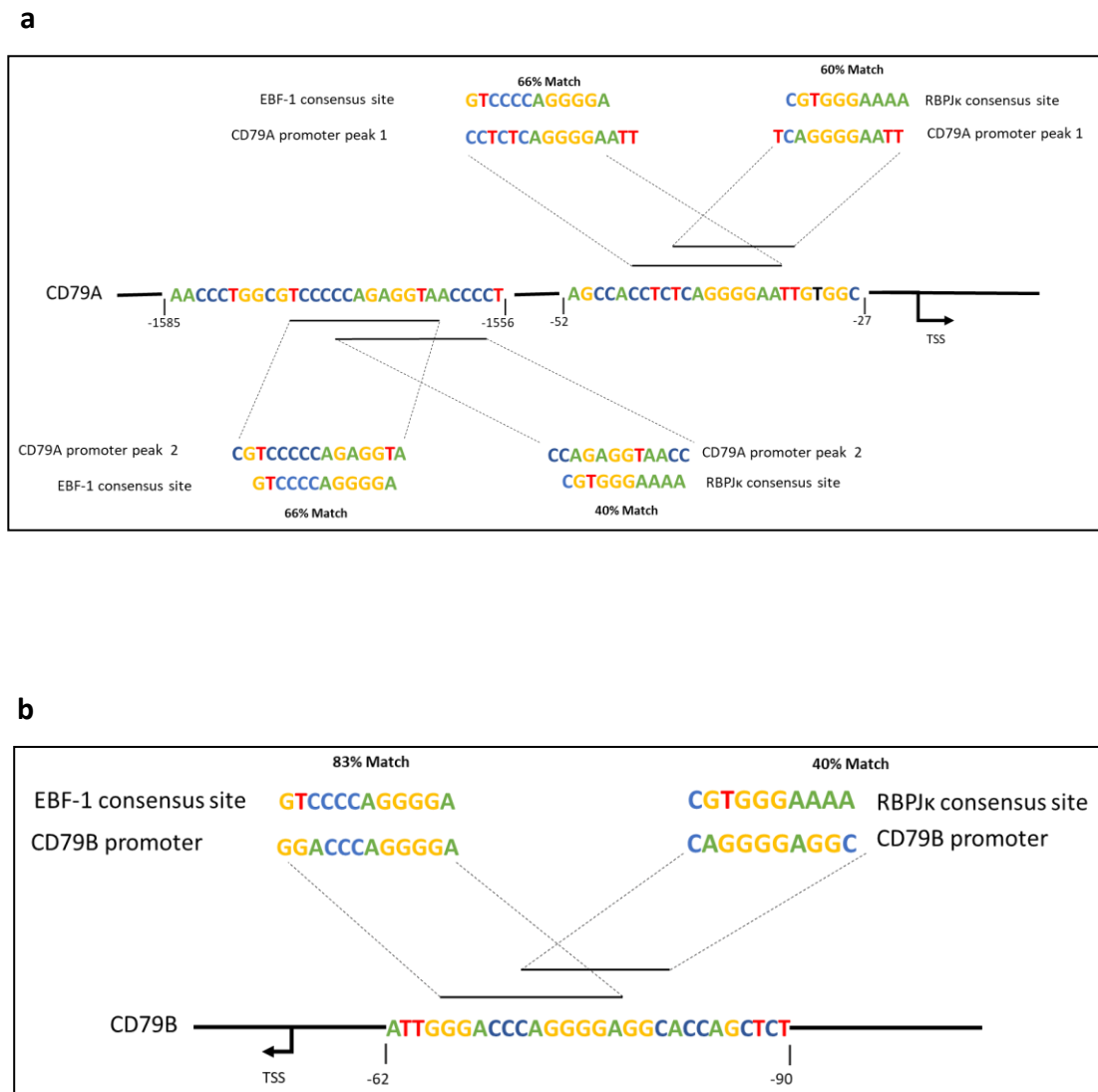


Figure 3.8. Cellular transcription factors that can mediate EBNA2 binding to the *CD79A* and *CD79B* promoter. a) The EBF-1 binding site at the *CD79A* promoter peak 1 partially overlaps with a RBPJk binding site. The EBF-1 binding site at *CD79A* promoter peak 2 is a partial match for the RBPJk binding site. **b)** Binding sites for EBF-1 and RBPJk overlap at the *CD79B* promoter.

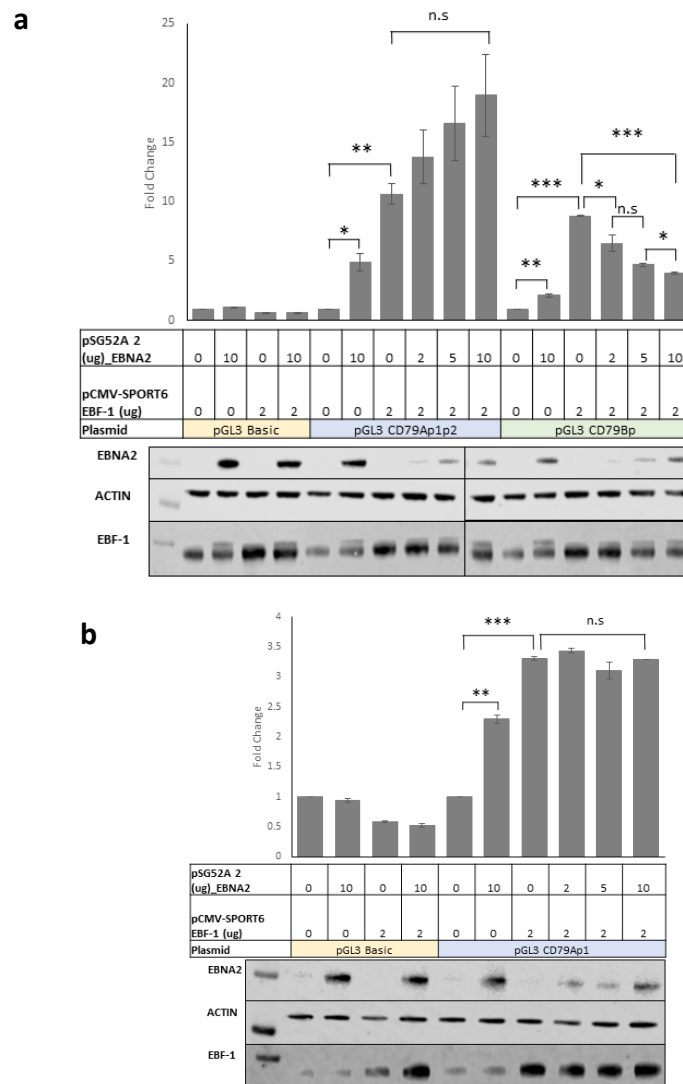


Figure 3.9. The effect of EBNA2 and EBF-1 on CD79A and CD79B promoter activity. a) DG75BK cells were transiently transfected with 2 μ g of the control vector pGL3 Basic, a pGL3_CD79Ap1p2 or pGL3_CD79Bp reporter constructs in the presence or absence of an EBNA2 expressing construct (pSG52A) and an EBF-1 expressing construct (pCMV-SPORT62-EBF-1). The cells were co-transfected with a Renilla control plasmid pRL-CMV (0.5 μ g). Firefly luciferase signals were normalised to Renilla luciferase signals. Results show the mean \pm standard deviation of two independent experiments and are expressed relative to the pGL3 luciferase reporter construct signal. Western blot analysis of EBNA2 and EBF-1 expression in transfected cells. Actin was used as a loading control. **b)** DG75BK cells were transiently transfected with 2 μ g of the control vector pGL3 Basic, a pGL3_CD79Ap1 reporter construct in the presence or absence of an EBNA2 expressing construct (pSG52A) and an EBF-1 expressing construct (pCMV-SPORT62-EBF-1). The cells were co-transfected with a Renilla control plasmid pRL-CMV (0.5 μ g). Results were processed as described above. Western blot analysis of EBNA2 and EBF-1 expression in transfected cells. Actin was used as a loading control. T-test were performed and significance indicated as follows; n.s (not significant) = p-value > 0.05; * = p-value \leq 0.05; ** = p-value \leq 0.01; *** = p-value \leq 0.001.

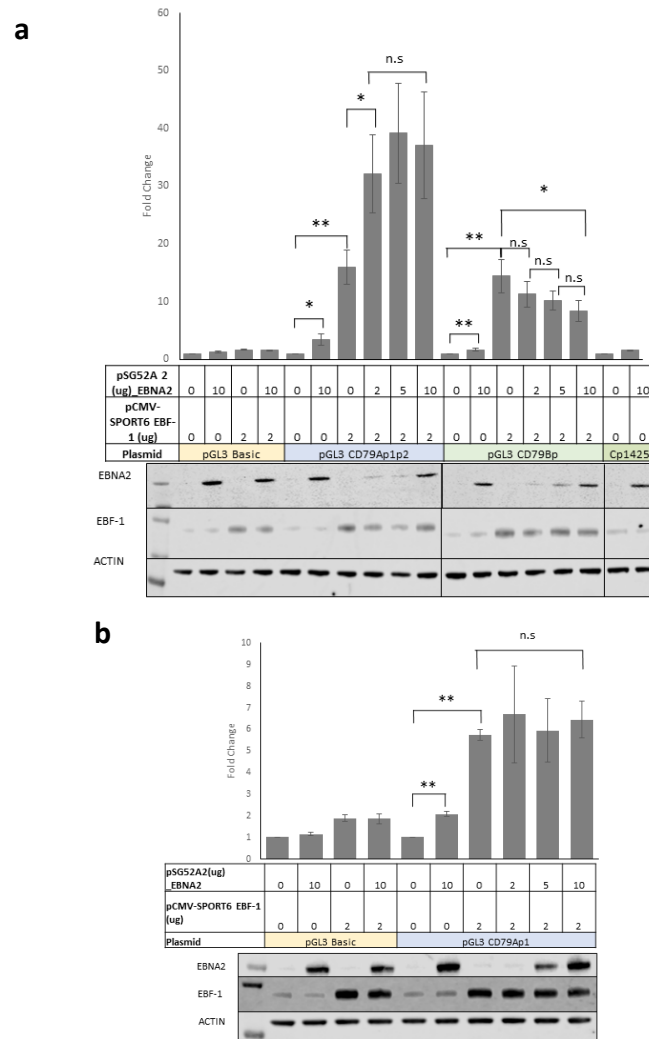


Figure 3.10. The effect of EBNA2 and EBF-1 on CD79A and CD79B promoter activity in the absence of RBPJk. a) DG75– RBPJK KO cells were transiently transfected with 2 μ g of the control vector pGL3 Basic, a pGL3_CD79Ap1p2 or pGL3_CD79Bp reporter constructs in the presence or absence of an EBNA2 expressing construct (pSG52A) and an EBF-1 expressing construct (pCMV-SPORT62-EBF-1). The cells were co-transfected with a Renilla control plasmid pRL-CMV (0.5 μ g). The EBV C promoter reporter (pCp1425GL2) was used as a RBPJk KO control. Firefly luciferase signals were normalised to Renilla luciferase signals. Results show the mean \pm standard deviation of two independent experiments and are expressed relative to the pGL3 luciferase reporter construct basic signal. Western blot analysis of EBNA2 and EBF-1 expression in transfected cells. Actin was used as a loading control. **b)** DG75 RBPJK KO cells were transiently transfected with 2 μ g of the control vector pGL3 Basic, a pGL3_CD79Ap1 reporter construct in the presence or absence of an EBNA2 expressing construct (pSG52A) and an EBF-1 expressing construct (pCMV-SPORT62-EBF-1). The cells were co-transfected with a Renilla control plasmid pRL-CMV (0.5 μ g). Results were processed as described above. Western blot analysis of EBNA2 and EBF-1 expression in transfected cells. Actin was used as a loading control. T-test were performed and significance indicated as follows; n.s (not significant) = p-value > 0.05; * = p-value \leq 0.05; ** = p-value \leq 0.01.

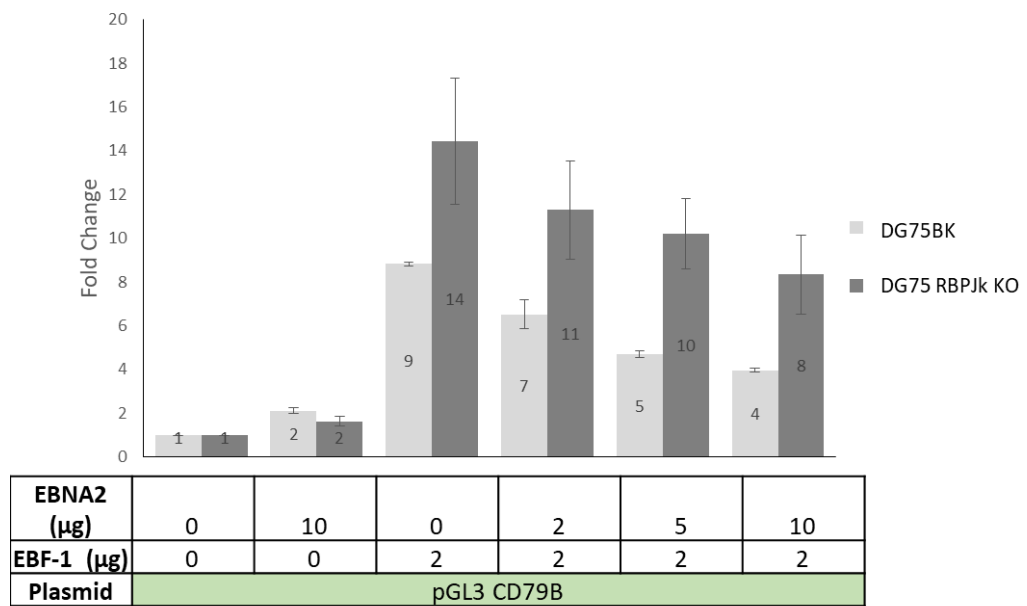
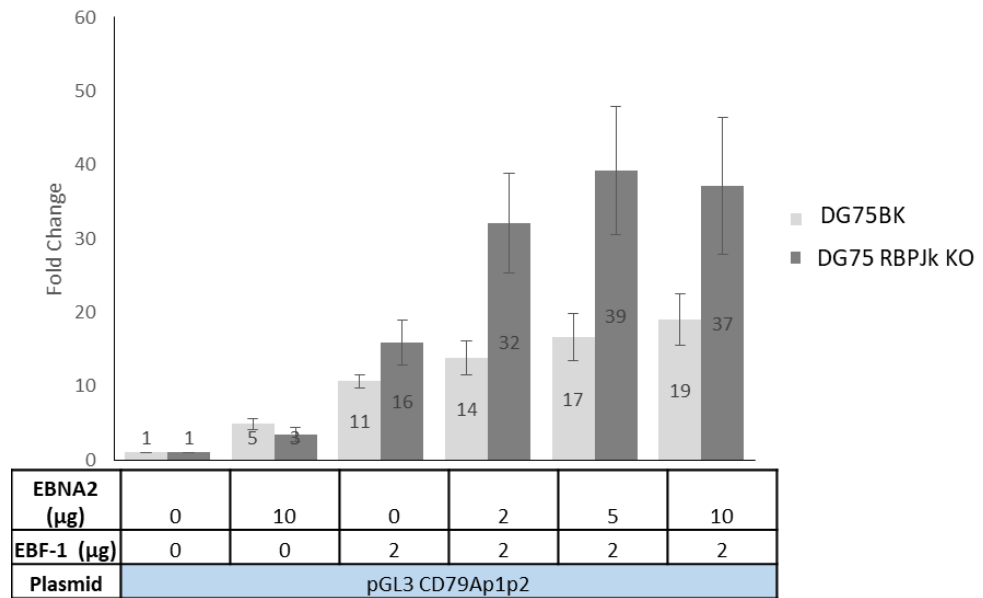


Figure 3.11. A direct comparison between promoter activity in the presence and absence of RBPJk. Luciferase assays in EBV negative DG75 and DG75 RBPJk KO cells using the control vector pGL3 basic, a CD79A promoter (P1+P2) luciferase reporter +/- an EBNA2 and EBF-1 expressing construct. Firefly luciferase signals were normalised to Renilla signals from the co-transfected control plasmid pRL-CMV (1ug). Fold change calculated relative to pGL3 basic control plasmid activation. The numbers in the bars denote fold change.

We found that EBF-1 and EBNA2 co-expression had no effect on *CD79A* promoter activation suggesting that EBNA2 alone is not sufficient to repress *CD79A* promoter activation. Interestingly, we found that co-expression of EBF-1 and EBNA2 did lead to a decrease in *CD79B* promoter activation compared to EBF-1 expression alone, independently of RBPJk, suggesting EBNA2 hinders EBF-1 mediated activation of *CD79B* in luciferase assays. Our data suggest that repression of *CD79A* and *CD79B* may occur through different mechanisms.

3.5 *CD79B* repression by EBNA2 occurs at a transcriptional level

To confirm that the down regulation of *CD79B* mRNA was a result of transcriptional regulation by EBNA2 and not post-transcriptional regulation we set out to determine the effect of EBNA2 activity on the half-life of *CD79B* mRNA. To determine the effect of EBNA2 on the half-life of *CD79B* mRNA transcripts we set up an mRNA stability assay to measure mRNA decay *in vivo* in EREB2.5 cells. We used the transcription inhibitor Actinomycin D which intercalates into DNA and prevents the helix from unwinding inhibiting the transcription process and synthesis of new mRNA (Avenidaño López and Menendez, 2008). EREB2.5 (-ER) cells and EREB2.5 (12hrs+ER) cells were treated with Actinomycin D and harvested after 2, 4, and 8 h *CD79B* mRNA levels were measured by QPCR and half-life was calculated from a non-linear regression curve using first order kinetics. The results showed the half-life of *CD79B* mRNA in the absence of active EBNA2 is 2.5hrs and in the presence of active EBNA2 is 3.4hrs (Figure 3.12). We can therefore conclude EBNA2-mediated regulation of *CD79B* occurs at a transcriptional level.

3.6 EBNA2 activation disrupts EBF-1 binding and histone acetylation at the *CD79B* promoter.

We have established that *CD79B* is repressed in response to EBNA2 activation in LCLs and BL cells and we have shown that EBNA2 hinders EBF-1 mediated *CD79B* transcription in a luciferase reporter assay. We therefore focused further experiments on *CD79B*. To examine the influence of EBNA2 on EBF-1 binding at the *CD79B* promoter *in vivo* we used CHIP-QPCR to examine EBF-1 and EBNA2 binding over a time course of induction of EBNA2 activity in EREB2.5 cells. Following withdrawal β -estradiol was re-added and cells were harvested after 0, 4, 8 and 24 h and chromatin prepared. The results showed that EBF-1 is bound at the *CD79B* promoter in the absence of EBNA2 (Figure 3.13b). EBF-1 signals increase 4 hours post EBNA2 activation. However, 8 hours post EBNA2 activation, EBF-1 binding signals fall below basal levels. This correlates with a 10-fold reduction in mRNA expression at the 8 h timepoint (Figure 3.6b). Interestingly, 24 h post EBNA2 induction EBF-1 binding signals at the *CD79B* promoter increase. This increase in EBF-1 binding does not correspond to an increase in *CD79B* transcriptional activation; *CD79B* mRNA levels are still very low (Figure 3.6b). *EBF-1* is known to be upregulated upon EBV infection, possibly through the actions of EBNA1 (Tempera et al., 2016) and we did observe an increase in EBF-1 protein levels in response to EBNA2 activation (Figure 3.13e). This increase EBF-1 binding signal 24hr post EBNA2 activation may be a result of this increase in overall EBF-1 protein levels. However, increased EBF-1 binding did not activate *CD79B* transcription in the presence of active EBNA2. EBNA2 binding follows a similar pattern to EBF-1 binding; EBNA2 binding increased 5-fold 4 h after EBNA2 activation, before EBNA2 binding reduced to below background levels 8 h after activation.

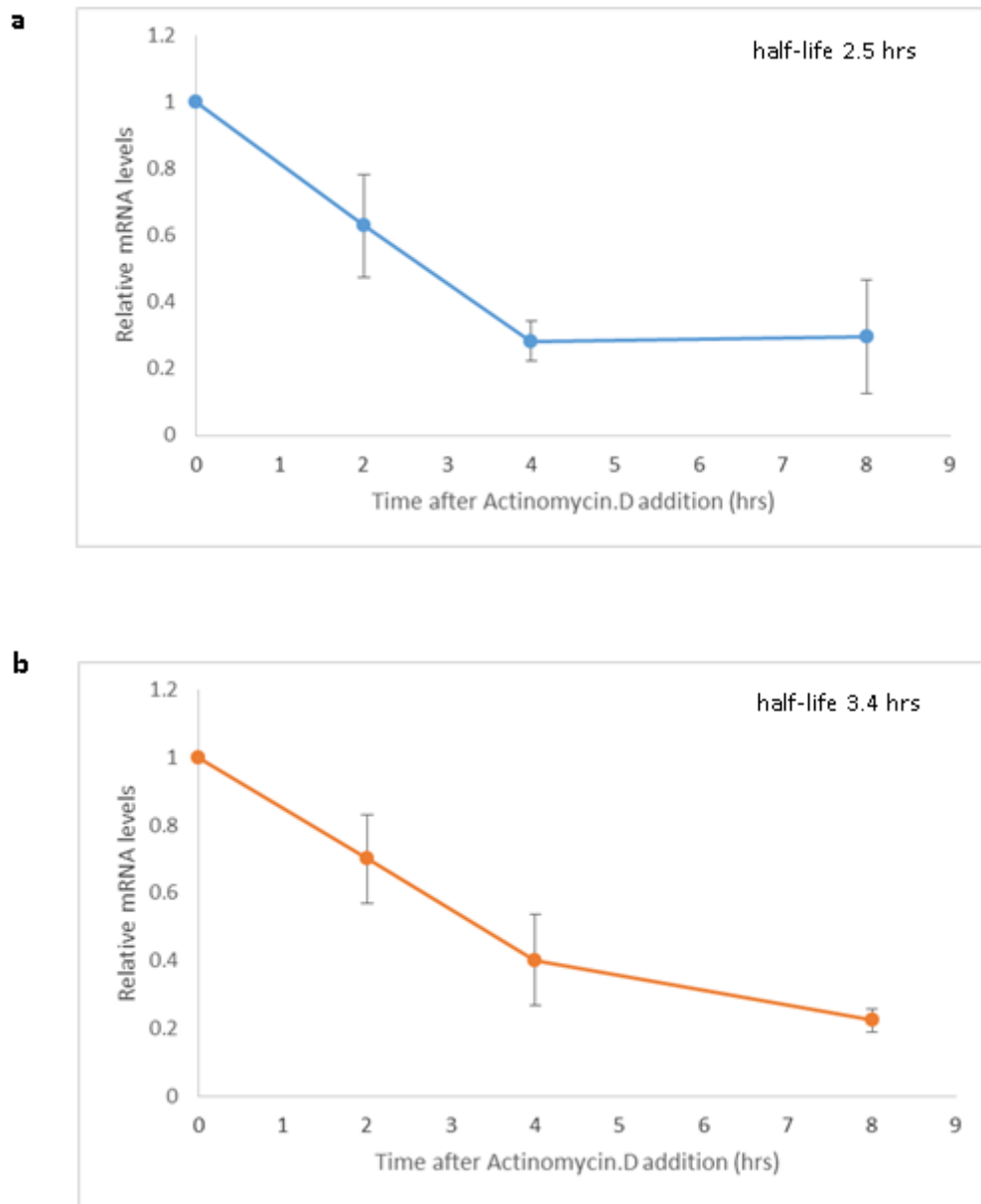


Figure 3.12. EBNA2 does not shorten *CD79B* mRNA half-life. (-ER) EREB 2.5 cells **(a)** and (+ER) EREB 2.5 cells induced for 12hr with B-estradiol **(b)** were treated with the transcription inhibitor Actinomycin D (0.5 μ M) for 2, 4 and 8 hours. *CD79B* mRNA levels were measured in duplicate by QPCR, normalized to *GAPDH* and represented relative to untreated sample. Half-life was calculated from a non-linear regression curve using first order kinetics and are displayed on the graphs which show the mean \pm standard deviation of two independent experiments.

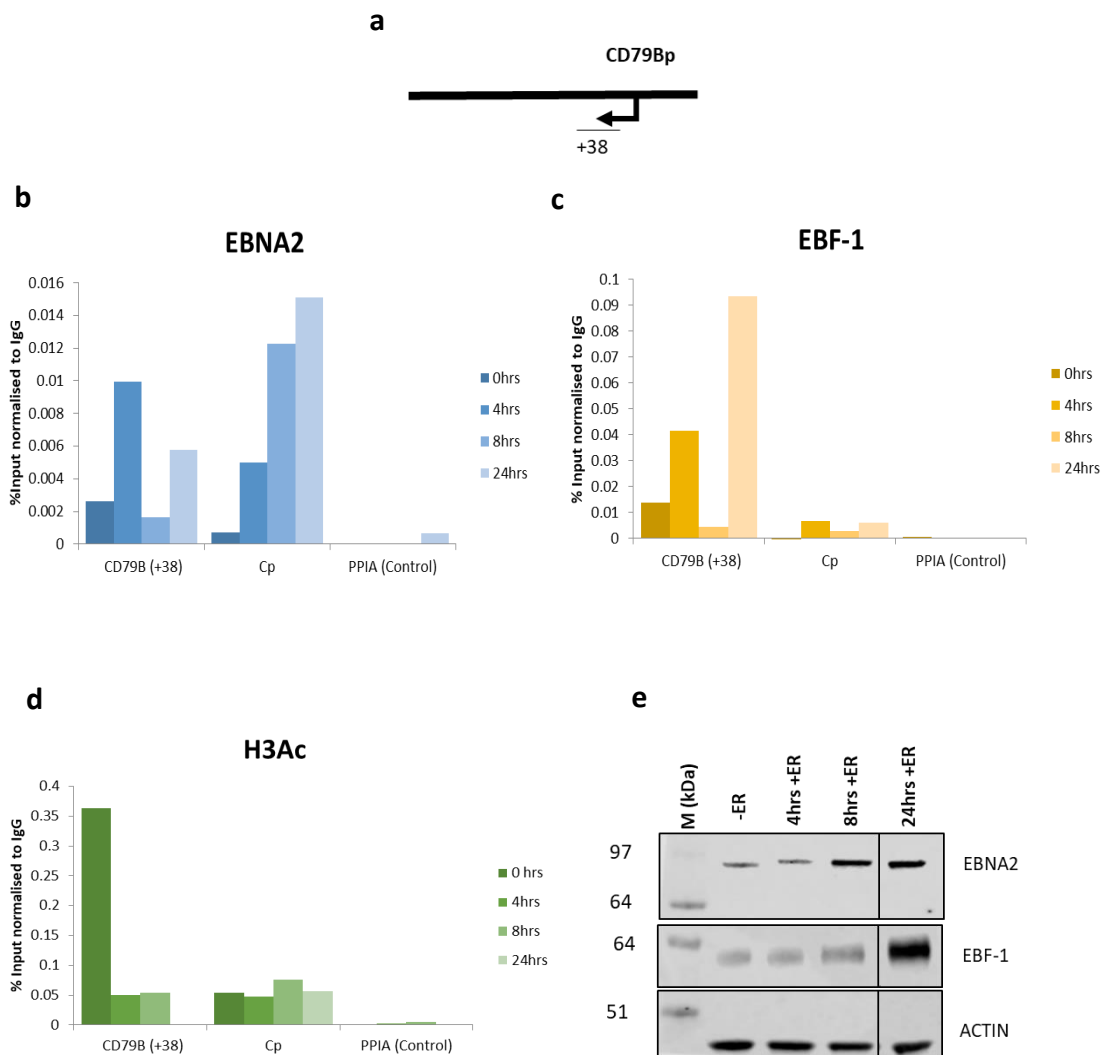


Figure 3.13 EBNA2 activation disrupts EBF-1 binding and Histone H3 Acetylation at the *CD79B* promoter. **a)** Diagram representing the location of the amplicons generated by the +38 primer set at the *CD79B* gene locus. +38 indicated the 5' end of the forward primer relative to the start of the *CD79B* mRNA sequence. **b)** Results show the mean percentage input signals after subtraction of IgG antibody controls of one representative ChIP experiment in EREB2.5 cells. Three independent experiments were carried out in total using EREB2.5 cells (\pm ER) using a monoclonal anti-EBNA2 antibody. Cp was used as a control region and PPIA was used as a negative control region. **c)** Results show the mean percentage input signals after subtraction of IgG antibody controls of one (of 3) representative ChIP experiment in EREB2.5 cells (\pm ER) using a monoclonal anti-EBF-1 antibody. **d)** Results show the mean percentage input signals after subtraction of IgG antibody controls of one (of 2) representative ChIP experiment in EREB2.5 cells (\pm ER) using a polyclonal anti-H3Ac antibody. **e)** Western blot analysis showing activation of EBNA2 and endogenous EBF-1 expression using EREB2.5 cells (\pm ER). Actin was used as a loading control.

As with EBF-1 binding, EBNA2 binding increased at the 24 h time point (Figure 3.13a). It appears that EBF-1 and EBNA2 follow a similar binding pattern at the *CD79B* promoter over a 24hr period. This experiment was repeated three times and while the kinetics of binding varied between experiments due to variation in time-courses, we always observed the same binding pattern for EBNA2 and EBF-1. When we relate this to EBNA2 and EBF-1 binding at Cp, we observed increased binding after EBNA2 activation, which is what we would expect indicating that the samples were intact and the ChIP was successful.

Next we investigated histone modifications using ChIP-QPCR with an H3Ac antibody. The *CD79B* promoter is highly acetylated in its active state and our results showed that activation of EBNA2 coincides with a fall in H3Ac signal at the *CD79B* promoter as expected when gene transcription is repressed (Figure 3.13d). To determine if the fall in H3Ac was transient we set up an extended 72 h time course, which showed that while acetylation levels recovered to an extent, they did not return to pre-EBNA2 levels and mRNA analysis showed that *CD79B* mRNA levels also remained repressed 72 h after EBNA2 activation (Figure 3.14).

Our data indicate that EBNA2 could be interfering with EBF-1 mediated transcription. EBF-1 is a pioneer transcription factor and its role is to open up the chromatin to allow the deposition of active chromatin marks (Mayran and Drouin, 2018). Our data are consistent with a model where EBNA2 interferes with the ability of EBF-1 to promote histone acetylation and thus gene activation at the *CD79B* promoter.

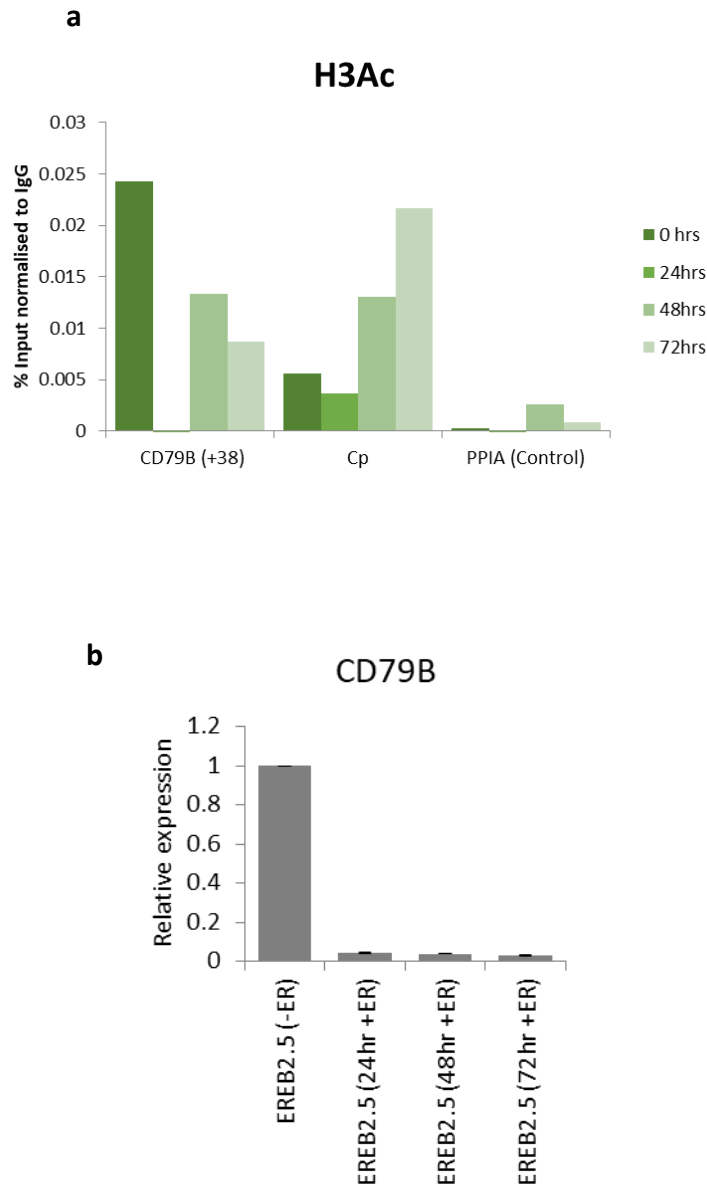


Figure 3.14. EBNA2 activation disrupts H3Ac at the *CD79B* promoter up to 72hrs. a)

Results show the mean percentage input signals after subtraction of IgG antibody controls of one representative ChIP experiment using EREB2.5 cells (\pm ER) using a polyclonal anti-H3Ac antibody. Cp was used as a positive control regions and PPIA was used as a negative control region. **b)** *CD79B* mRNA expression in EREB2.5 cells treated with β -estradiol for 0hrs, 24, 48 and 72 h. Signals are normalised to *GAPDH* and show mean expression levels relative to (-ER) \pm standard deviation of two QPCR experiments.

3.7 EBNA2 activation leads to reduced NFAT activation *in vivo*.

We next examined whether repression of CD79A and B or other BCR pathway components by EBNA2 was able to functionally regulate BCR signalling output through the Ca²⁺ signalling arm *in vivo*. To do this we transiently transfected EBV-negative BL41 cells expressing the conditionally active ER-EBNA2 fusion protein, with an NFAT luciferase reporter promoter plasmid containing 3 NFAT binding motifs upstream of a luciferase promoter (Clipstone and Crabtree, 1992). The ER-EBNA2 fusion protein was activated 5 h post transfection by the addition of β -estradiol and 24 h later the cells were treated with anti-IgM to cross-link the BCR and initiate downstream signalling. The cells were harvested 18 h after BCR stimulation and the impact of EBNA2 on the activation levels of the NFAT reporter were measured. *CR2 (CD21)* gene expression was used as a positive control to confirm EBNA2 activity. Interestingly, expression of CR2/CD21, in cells containing the NFAT reporter with active EBNA2, fell 3-fold in IgM treated cells compared to mock treated cells. As CR2/CD21 is involved in the BCR pathway this downregulation could be a result of EBNA2 mediated repression of the BCR pathway. We did observe an upregulation of CR2/CD21 in the presence of EBNA2 confirming its activity. *CD79B* gene expression in anti-IgM treated cells was compared to mock treated cells to confirm the addition anti-IgM did not affect *CD79B* repression by EBNA2 (Figure 3.16). We found that activation of EBNA2 did not significantly alter NFAT activity in mock treated cells. However, in anti-IgM treated cells, EBNA2 activation resulted in a ~ 5-fold decrease in NFAT activity (Figure 3.15). These results demonstrate that EBNA2 activation repressed BCR signalling that led to a reduction in calcium flux resulting in lower NFAT luciferase reporter activity.

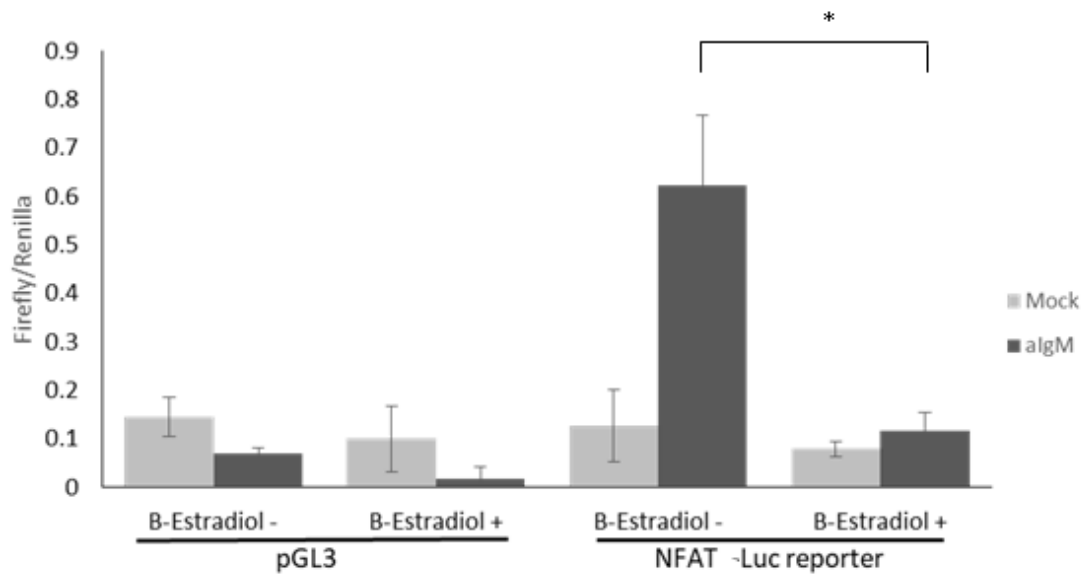


Figure 3.15. EBNA2 blocks NFAT activity. 1×10^6 EBV-negative BL cells expressing a conditionally active ER-EBNA2 fusion protein (BL41K3) were transfected with an empty plasmid (pGL3 basic) or an pGL3_NFAT luciferase reporter. The cells were incubated for 24 hours in the +/- β -estradiol (EBNA2) followed by an 18hrs incubation +/- anti-IgM and analysed for luciferase activity. For the mock experiment no anti-IgM was added to confirm NFAT activation was a result of BCR crosslinking. Values were normalised to Renilla signals from the co-transfected control plasmid pRL-TK (2.5 μ g) and show the mean \pm standard deviation from two independent experiments carried out in duplicate. T-test was performed and significance indicated as follows; n.s (not significant) = p-value > 0.05; * = p-value \leq 0.05; ** = p-value \leq 0.01; *** = p-value \leq 0.001.

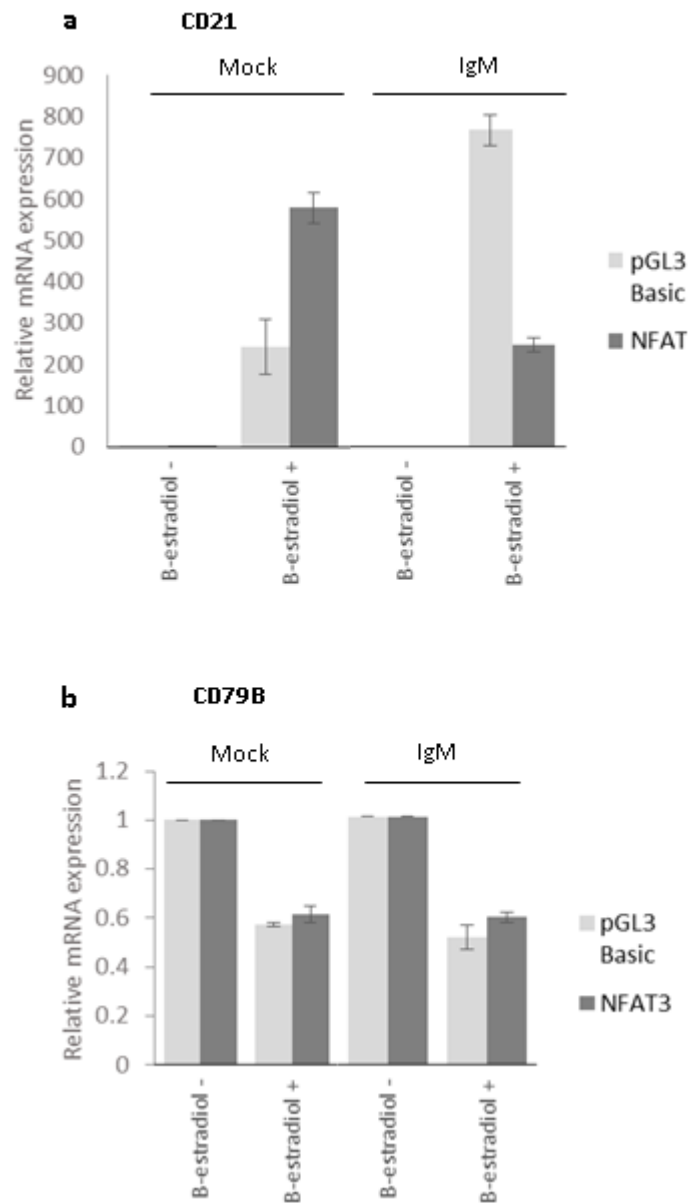


Figure 3.16. EBNA2 activation induced *CD21* mRNA expression and represses *CD79B* mRNA expression in IgM treated cells. A cells to CT kit was used to extract RNA from 1×10^5 BL41K3 cells that had been transfected with an empty plasmid (pGL3 basic) or an pGL3_NFAT₃ luciferase reporter. The cells were incubated for 24 hours in the +/- β -estradiol (EBNA2) followed by an 18hrs incubation +/- anti-IgM to initiate BCR signalling. **a)** The EBNA2 responsive gene *CD21* was used as a control for EBNA2 induction. Signals were normalised to *GAPDH* and $\Delta\Delta CT$ values are shown relative to - β -estradiol samples \pm standard deviation of duplicate QPCR reactions. **b)** *CD79B* signals were normalised to *GAPDH* and $\Delta\Delta CT$ values are shown relative to - β -estradiol samples \pm standard deviation of duplicate QPCR reactions.

3.8 Conclusion.

In this chapter we confirmed the repression of BCR signal transducing molecules *CD79A* and *CD79B* by EBNA2 in LCLs and lymphoma cell lines. We explored the mechanism of their repression by EBNA2 using *in vitro* and *in vivo* techniques. A competition based luciferase assay revealed that EBNA2 alone can activate both the *CD79A* and *CD79B* promoters independent of RBPJk. We also found that co-expression of EBNA2 and EBF-1 led to a decrease in activation of the *CD79B* promoter, also independently of RBPJk. EBF-1 and EBNA2 co-expression had no effect on *CD79A* promoter activation. Having established EBNA2 was able to repress *CD79B* at the transcriptional level we used ChIP-QPCR to investigate EBF-1 and EBNA2 binding patterns at the *CD79B* promoter. We found that EBNA2 and EBF-1 bound at the same time and followed similar kinetics. We used the same method to investigate H3Ac levels over the same length of time and found that H3Ac levels fall after EBNA2 activation and do not recover to pre-EBNA2 levels. We propose that EBNA2 interferes with the ability of EBF-1 to promote histone acetylation and gene activation at the *CD79B* promoter.

We have identified a potential transcription mechanism used by EBNA2 to repress *CD79B* and we have also shown that activation of EBNA2 leads to a reduction of NFAT activity *in vivo*.

4. Regulation of the B-cell receptor signalling molecules *NFATC1*, *NFATC2* and *PLC γ 2* by EBV transcription factors.

4.1 Introduction

DAVID pathway analysis, (see Chapter 3, section 3.1) found that the BCR signalling pathway was the only significantly enriched pathway for EBNA-bound genes (Table 3.1). In this chapter, we investigated the role of these proteins in direct regulation of additional components of the calcium signalling pathway downstream of CD79A and CD79B. These included the membrane-associated enzyme PLC γ 2 and the transcription factors NFATC1 and NFATC2 (Figure 4.1). Deregulation of this signalling pathway, or abnormal expression of its components, such as the NFAT protein family, have been linked to solid epithelial tumours, lymphoma and lymphoid leukaemia (Jauliac et al., 2002, Medyouf et al., 2007).

Analysis of ChIP-seq studies carried out in our laboratory identified *NFATC1* as a potential direct target of EBNA2 and EBNA3 proteins based on it being the closest gene to one of the most significant EBNA2 binding sites and the closest gene to a significant EBNA3 binding site. Our ChIP-seq data mapped eight intragenic EBNA2 binding sites located in *NFATC1*; with the most significant EBNA2 binding site located 73 kb downstream from the *NFATC1* TSS (Figure 4.2). There were two significant intragenic EBNA3 binding sites identified in *NFATC1* by peak calling (MACs), but these were both very small and hard to distinguish over background, however *NFATC1* has been reported as an EBNA3B and EBNA3C regulated gene in published microarrays (White et al., 2010, Zhao et al., 2011b) (Figure 4.2 and Table 3.2). *NFATC2* was identified as an EBNA2 target gene because it was the closest gene to a significant EBNA2 site (Figure

4.3). While the BCR pathway was not found to be enriched for genes closest to top significant EBNA3 binding sites, CHIP-seq mapped three EBNA3 binding sites at the *NFATC2* locus that overlapped with some of the EBNA2 binding sites (Figure 4.3). *NFATC2* has also been reported as an EBNA3B and EBNA3C regulated gene in published microarrays (White et al., 2010, Zhao et al., 2011b) (Figure 4.3 and Table 3.2). *PLC γ 2* was identified as an EBNA2 binding target because it was the closest gene to one of the most significant EBNA2 binding sites. This EBNA2 peak is located 21 kb downstream of the *PLC γ 2* TSS (Figure 4.4). There also are a number of small EBNA3 peaks downstream of the *PLC γ 2* TSS, however these were not identified as significant. *PLC γ 2* has been identified as an EBNA2 regulated gene in a previously published microarray (Maier et al., 2006) (Figure 4.4 and Table 3.2). All three genes had been identified as potential EBNA binding targets and various published microarray studies have implicated the EBNA proteins in their downregulation (Table 3.1 and 3.2). Other signalling molecules involved in the calcium signalling pathway including LYN, SYK, PI3K and CD19 are also involved in the PIK3-AKT pathway and were studied by Dr Sarika Khasnis for her PhD thesis.

In this chapter, I set out to investigate whether *NFATC1*, *NFATC2* and *PLC γ 2* show consistent regulation by EBNA2 and EBNA3 proteins at the mRNA and protein level, and to explore the transcription regulation mechanisms involved in their regulation.

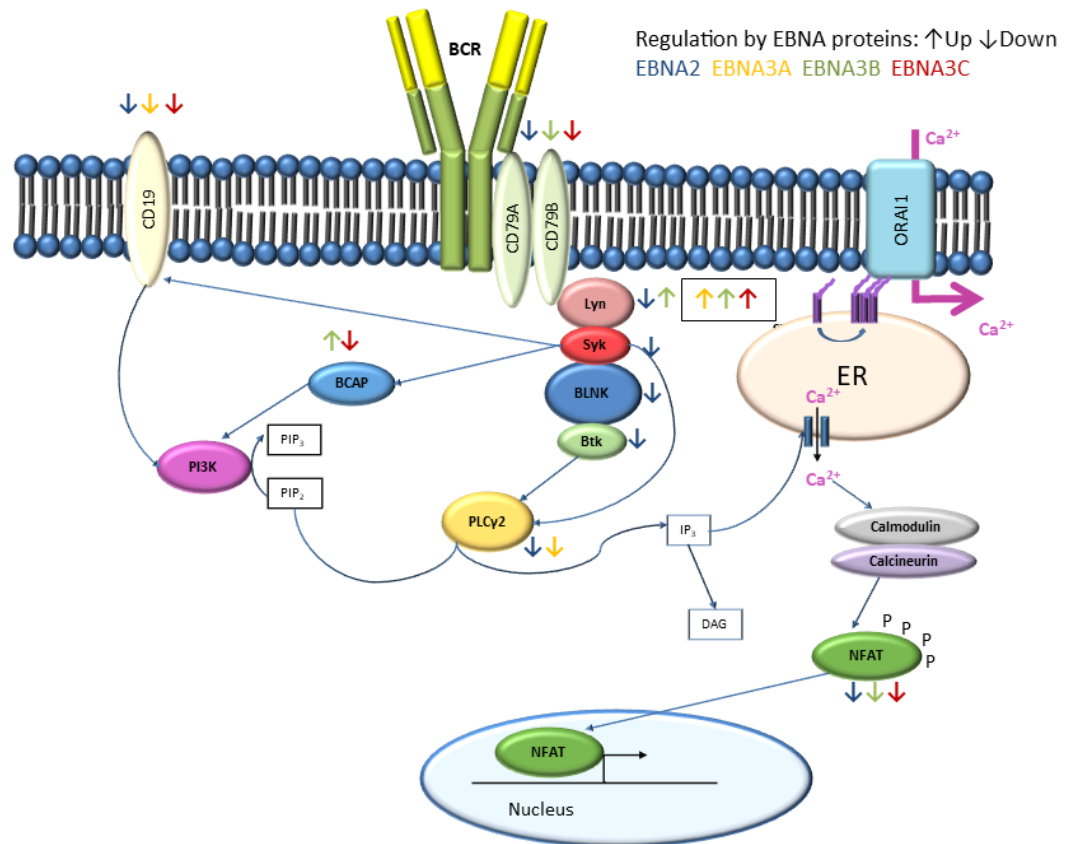


Figure 4.1 A schematic representation of the regulation of the calcium signalling pathway by EBNA2 and EBNA3 proteins. Antigen binding triggers BCR activation resulting in phosphorylation of the CD79A/B immunoreceptor tyrosine-based activation motif (ITAM) by tyrosine kinases Lyn and Syk. Next BLNK is recruited with PLCG2 and its co-activator Btk induces PIP₂ cleavage into DAG and IP₃. Activation of the IP₃R by IP₃ allows the release of Ca²⁺ from the endoplasmic Reticulum (ER). The low Ca²⁺ concentration in the ER triggers Stromal Interaction Molecule 1 (STIM1) oligomerisation leading to activation of Ca²⁺ release –activated channels (CRAC), encoded by ORAI1 multimers, responsible for Store Operated Ca²⁺ Entry (SOCE). The resulting increase of cytoplasmic Ca²⁺ concentration activates Calmodulin and Calcineurin which in turn dephosphorylate NFATs exposing their nuclear localisation signal allowing NFAT translocation to the nucleus. Once in the nucleus NFATs drive gene expression. EBNA2 and EBNA3 regulation is indicated by colour coded, upward or downward arrows and is based on the Taqman array card experiment carried out by Dr Sarika Khasnis.

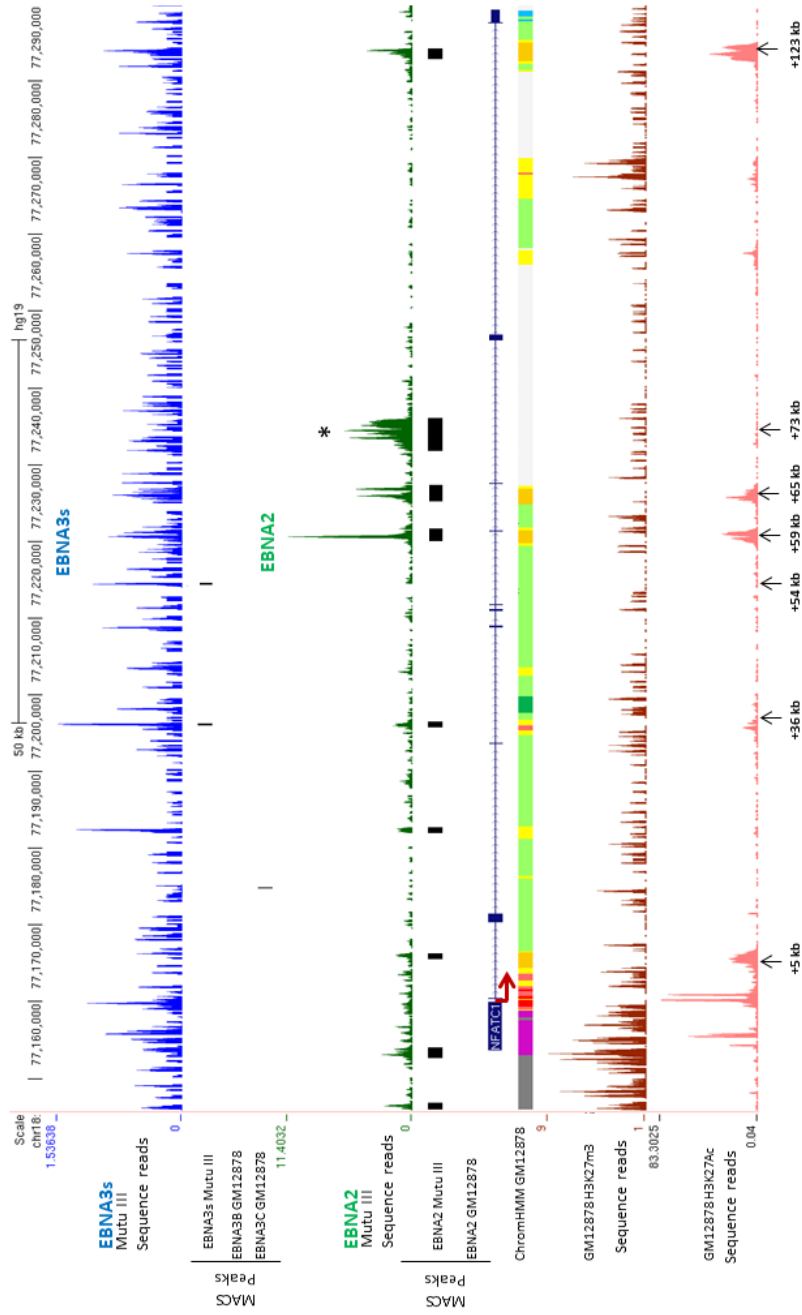


Figure 4.2 EBNA2 and EBNA3 binding sites at the *NFATC1* locus. The number of EBNA2 and EBNA3 sequencing reads from immunoprecipitated Mutu III and GM12878 DNA are plotted per million background-subtracted total reads and aligned with the human genome. The Model-based Analysis for ChIP-Seq (MACS) peaks indicated by the black bars represent the EBNA2 and EBNA3 binding sites. The red arrow indicates the direction of gene transcription. GM12878 H3K27Ac and H3K27me3 ChIP-seq data and chromatin segmentation by HMM from ENCODE are shown at the bottom of the panel. Chromatin segmentation by HMM colour code; Red, Strong Promoter; Pink, Weak promoter; Orange, Strong Enhancer; Yellow, Weak Enhancer. * Indicates promoter-proximal and top most significant EBNA2 and EBNA3 binding peaks based on ChIP-Seq data generated by the West lab using MutuIII cells. Black arrows indicate ChIP-QPCR primer locations and kb is used to define the distance from the transcription start site; 1 kb = 1000 base pairs

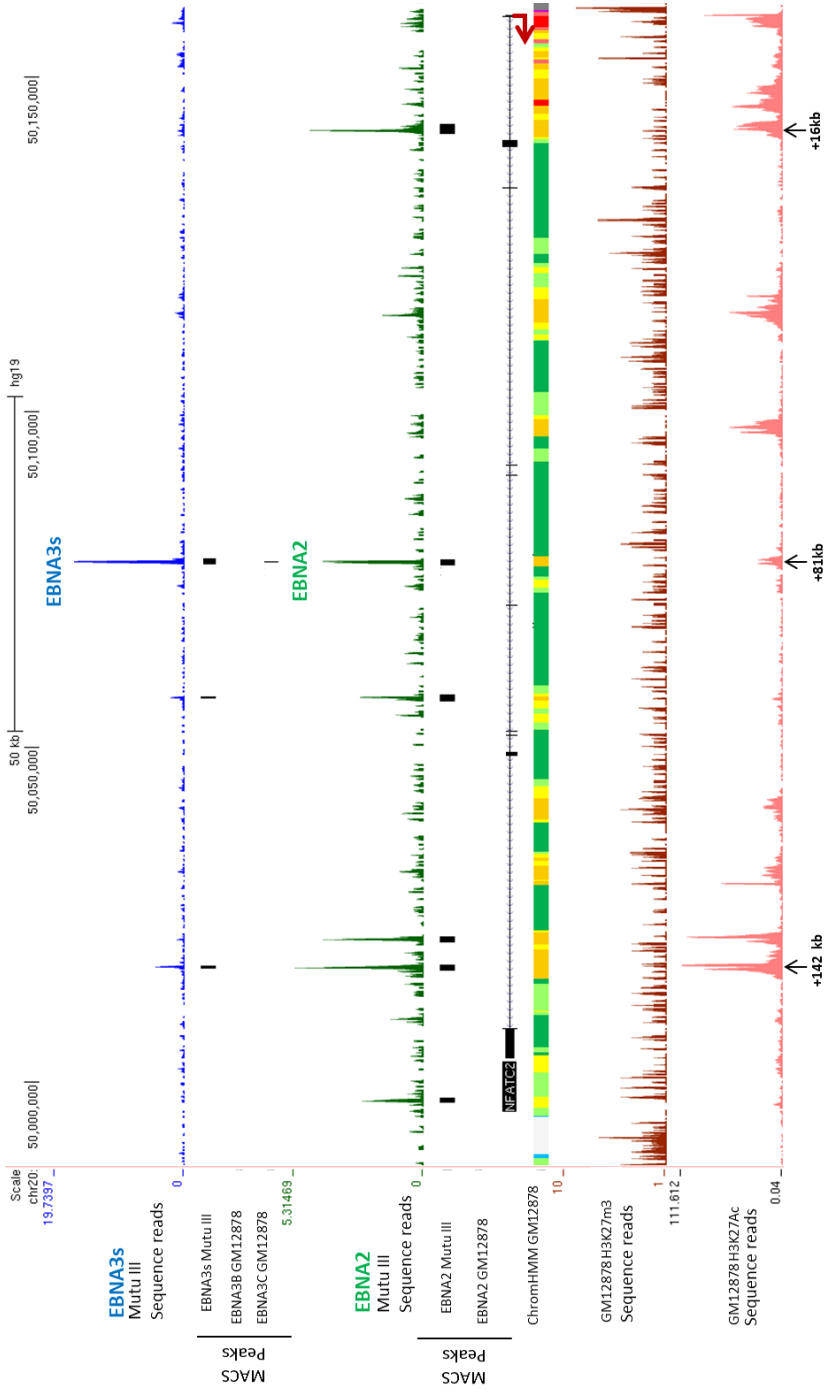


Figure 4.3 EBNA2 and EBNA3 binding sites at the *NFATC2* locus. The number of EBNA2 and EBNA3 sequencing reads from immunoprecipitated Mutu III and GM12878 DNA are plotted per million background-subtracted total reads and aligned with the human genome. The Model-based Analysis for ChIP-Seq (MACS) peaks indicated by the black bars represent the EBNA2 and EBNA3 binding sites. The red arrow indicates the direction of gene transcription. GM12878 H3K27Ac and H3K27me3 ChIP-seq data and chromatin segmentation by HMM from ENCODE are shown at the bottom of the panel. Chromatin segmentation by HMM colour code; Red, Strong Promoter; Pink, Weak promoter; Orange, Strong Enhancer; Yellow, Weak Enhancer. EBNA2 and EBNA3 binding peaks based on ChIP-Seq data generated by the West lab using MutuIII cells. Black arrows indicate ChIP-QPCR primer locations and kb is used to define the distance from the transcription start site; 1 kb = 1000 base pairs.

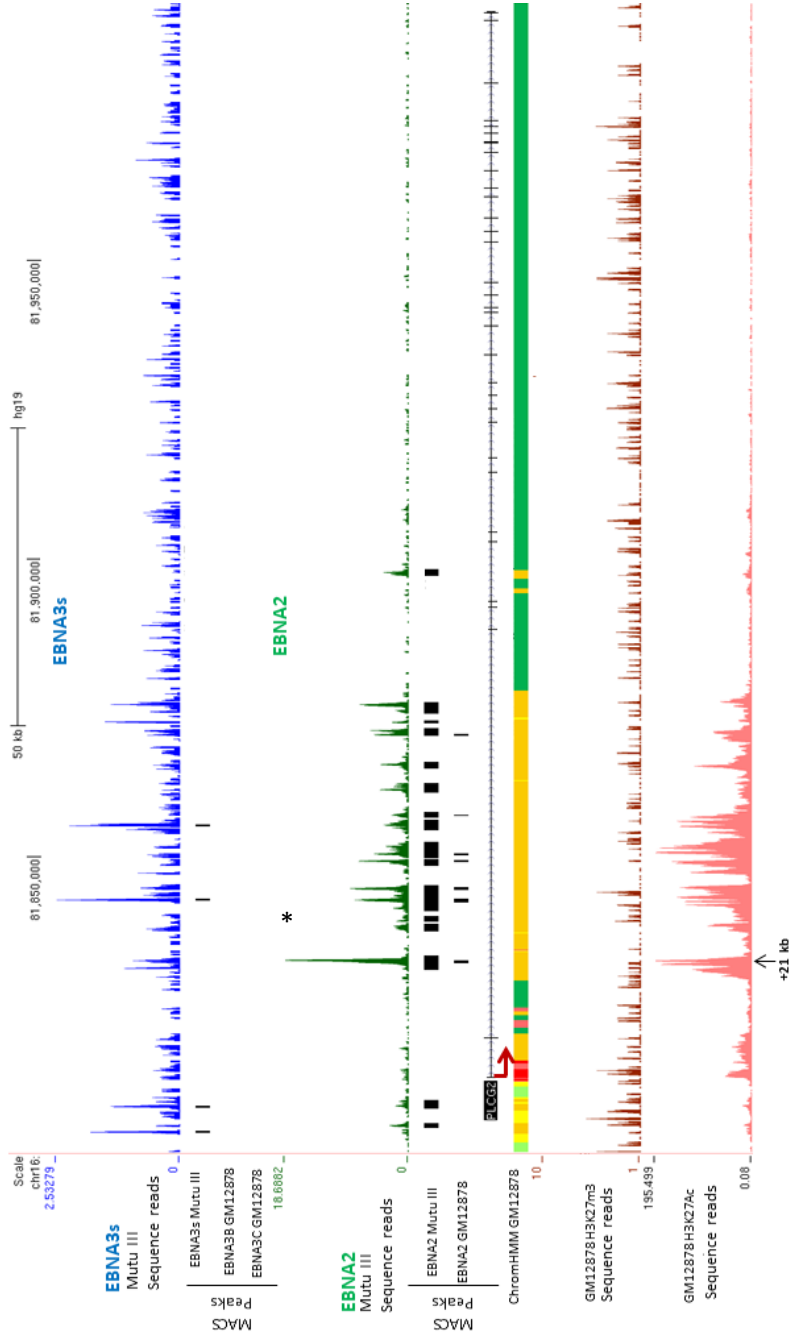


Figure 4.4 EBNA2 and EBNA3 binding sites at the *PLCy2* locus. The number of EBNA2 and EBNA3 sequencing reads from immunoprecipitated Mutu III and GM12878 DNA are plotted per million background-subtracted total reads and aligned with the human genome. The Model-based Analysis for ChIP-Seq (MACS) peaks indicated by the black bars represent the EBNA2 and EBNA3 binding sites. The red arrow indicates the direction of gene transcription. GM12878 H3K27Ac and H3K27me3 ChIP-seq data and chromatin segmentation by HMM from ENCODE are shown at the bottom of the panel. Chromatin segmentation by HMM colour code; Red, Strong Promoter; Pink, Weak promoter; Orange, Strong Enhancer; Yellow, Weak Enhancer. *Indicates promoter-proximal and top most significant EBNA2 and EBNA3 binding peaks based on ChIP-Seq data generated by the West lab using MutuIII cells. Black arrows indicate ChIP-QPCR primer locations and kb is used to define the distance from the transcription start site; 1 kb = 1000 base pairs

4.2 *NFATC1* is repressed by EBNA2 at the mRNA level

A previously published microarray study identified *NFATC1* as a gene downregulated by EBNA2 in an EBV-negative B cell lymphoma cell line that expresses a conditionally active oestrogen receptor (ER)-EBNA2 fusion protein (BJABK3). Array analysis detected a 1.5-fold reduction in *NFATC1* mRNA levels 24 h after EBNA2 activation (Maier et al., 2006), but this has not been followed up or confirmed in other studies or cell lines. A high throughput gene expression analysis using microfluidics cards carried out in our laboratory by Dr Sarika Khasnis used an EBV-infected LCL (EREB 2.5) expressing the same conditionally active oestrogen receptor-EBNA2 (ER-EBNA2) fusion protein (Kempkes et al., 1995a). The results showed that *NFATC1* was downregulated two-fold by EBNA2 in this cell background (Figure 4.5a). Subsequent QPCR analysis was carried out to examine *NFATC1* regulation over an EBNA2 activation timecourse in EREB 2.5 cells, BJAB and BL41 cells, to confirm the previous microarray data in the BJAB cell background and examine EBNA2 regulation in another cell background (the BL41 BL cell line). These results showed that *NFATC1* was downregulated 10-fold by EBNA2 over a 24 h period in EREB2.5 cells (Figure 4.5b). Protein analysis was carried out using the same EREB2.5 samples as described above in order to establish if the repression of mRNA impacted *NFATC1* protein levels in the cell. A *NFATC1* specific antibody was used that should recognise all known isoforms and *NFATC1* typically runs as a doublet around 101 kDa. The results showed that mRNA repression by EBNA2 was not accompanied by reduced protein expression in the EREB2.5 cells after EBNA2 activation. Next we used the EBV-negative B cell lines BJAB and BL41 cell lines expressing a conditionally active oestrogen receptor (ER)-EBNA2 fusion protein. Levels of the EBNA2-activated cellular gene *CR2* (*CD21*) were used to confirm EBNA2 activity

in BJAB and BL41 cells (Figure 3.7c). As these cell lines do not express any other EBV proteins they are useful to determine whether EBNA2 alone is able to downregulate *NFATC1*. Our QPCR analysis showed that *NFATC1* was not significantly repressed by the activation of EBNA2 in BJAB or BL41 cells 24 h after ER-EBNA2 activation (Figure 4.6a). Therefore we were unable to confirm the result from the microarray study by Maier et al. (2006). Collectively the results from our laboratory show that *NFATC1* mRNA expression is repressed by EBNA2 in an LCL, but not in a lymphoma cell background.

QPCR analysis of *NFATC2* mRNA and protein analysis found no evidence of regulation by EBNA2 in EREB2.5 cells (Figure 4.20). We found no evidence of regulation in BL41 cells, but we did some repression of *NFATC2* in BJAB cells although it was not very robust (Figure 4.6b) leading to the conclusion that *NFATC2* is not robustly regulated by EBNA2 and that regulation is cell line specific.

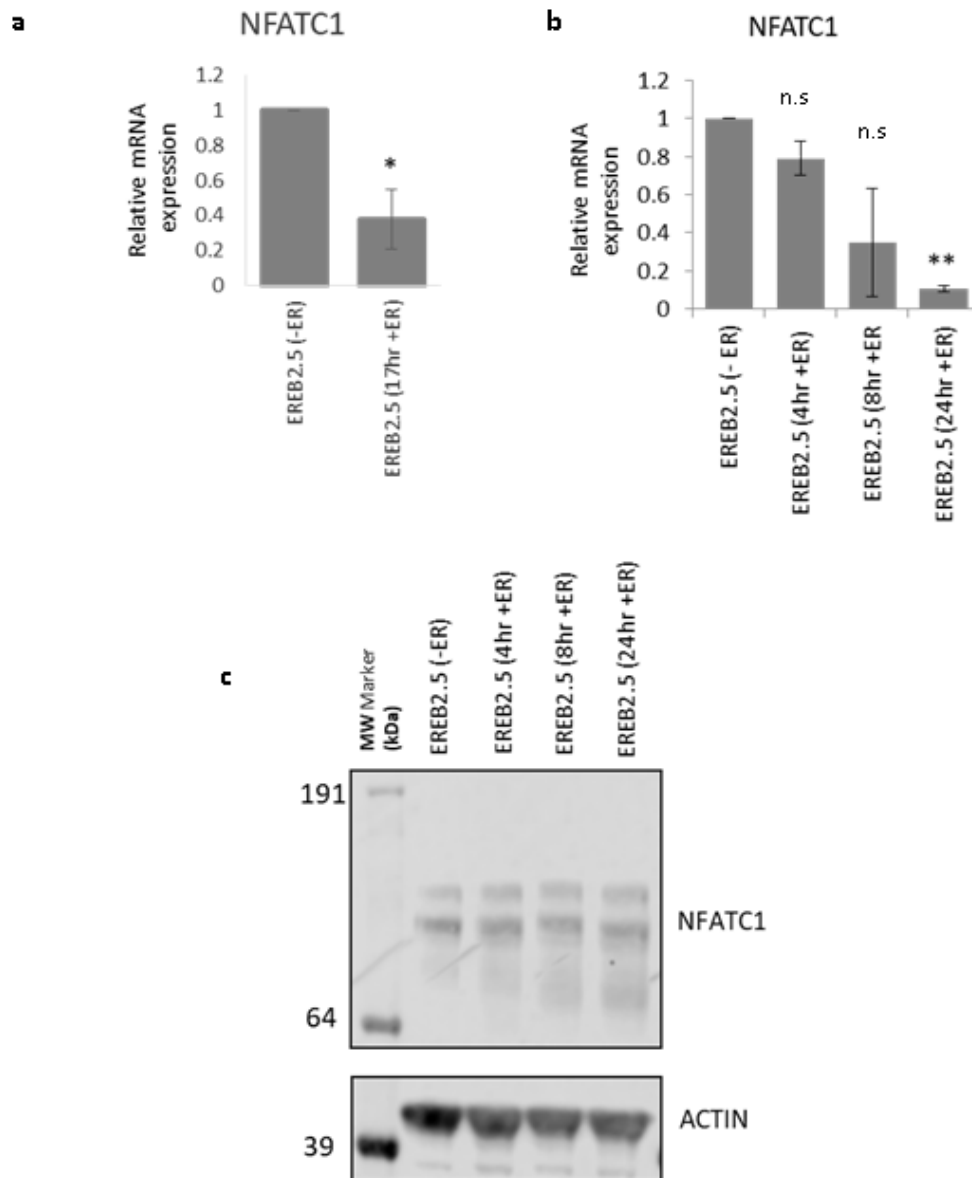
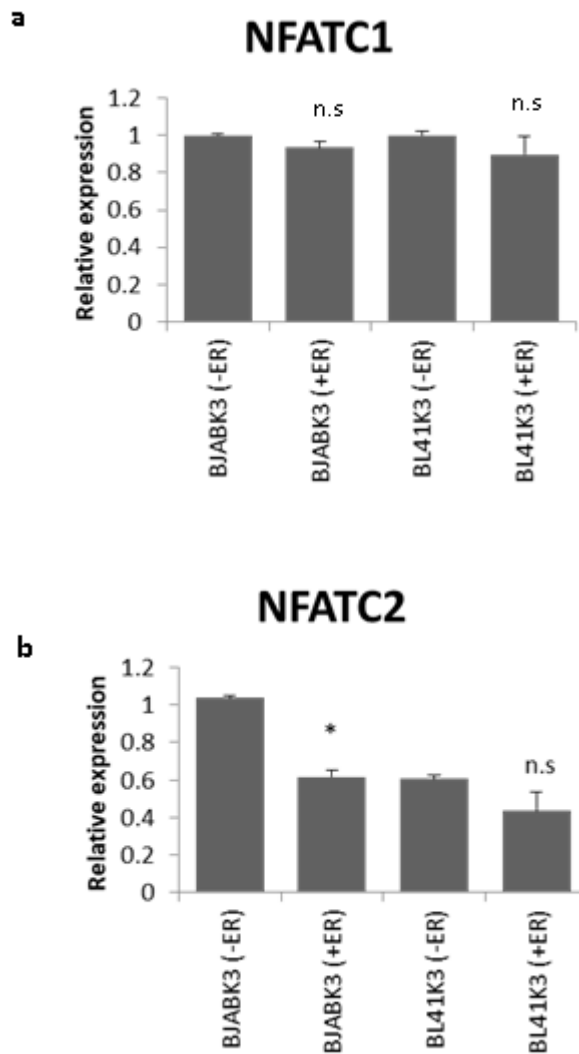


Figure 4.5. Regulation of NFATC1 by EBNA2 in EREB2.5 cell line **a)** QPCR analysis of NFATC1 mRNA expression in EREB2.5 cells by Dr Sarika Khasnis. Signals normalised to *GUSB* mRNA. Results show mean mRNA levels relative to EREB2.5 (ER-) \pm standard deviation of two independent experiments. **b)** QPCR analysis of NFATC1 mRNA expression in EREB2.5 cells. Signals normalised to GAPDH. Results show mean mRNA levels relative to EREB2.5 (-ER) \pm standard deviation of two QPCR experiments. Student T-test P values were calculated relative to the -ER sample and significance indicated as follows; n.s (not significant) = p-value > 0.05; * = p-value \leq 0.05; ** = p-value \leq 0.01; *** = p-value \leq 0.001. **c)** Western blot analysis of NFATC1 protein expression in EREB2.5 cells. Actin was used as a loading control.



4.6 Regulation of NFATC1 and NFATC2 in BJABkK3 and BL41K3 cell lines by EBNA2.

QPCR analysis of (a) NFATC1 and (b) NFATC2 mRNA expression in BJABK3 and BL41K3 cells conditionally expressing EBNA2. β -estradiol was added to cells (+ER) to activate EBNA2 and samples were harvested after 24 h. The figure above shows mean expression levels relative to BJABK3 (ER-) \pm standard deviation of two QPCR experiments and mean expression levels relative to BL41K3 (ER-) \pm standard deviation of two QPCR experiments. Student T-test P values were calculated relative to the -ER sample and significance indicated as follows; n.s (not significant) = p-value > 0.05; * = p-value \leq 0.05; ** = p-value \leq 0.01; *** = p-value \leq 0.001.

4.3 *NFATC1* and *NFATC2* are repressed by EBNA3B and EBNA3C at the mRNA and the protein level

Our ChIP-seq data also identified *NFATC1* and *NFATC2* as potential EBNA3 target genes (Figure 4.2 and 4.3) and *NFATC1* and *NFATC2* were detected as EBNA3B and EBNA3C regulated genes in a previously published microarray analysis White et al. (2010) (Table 3.2). This microarray study used an EBV-negative Burkitt's Lymphoma cell line (BL31) infected with either recombinant wild-type EBV (wtBac) or knock-out viruses to study the impact of loss of EBNA3A, 3B and 3C individually and in combination on cellular gene expression. BL31 cell lines infected with the respective revertant virus were also studied as a control for unexpected additional genetic changes in knock-out viruses. This study reported down regulation of *NFATC1* and *NFATC2* by EBNA3B and EBNA3C proteins since the expression of *NFATC1* and *NFATC2* increased on loss of either protein. EBNA3A did not appear to regulate either gene (Figure 4.7). In fact, examining the data from each cell line clone indicated that two EBNA3A KO cell lines showed upregulation of *NFATC1* and *NFATC2* in the absence of EBNA3A and two clones did not (White et al., 2010) (Figure 4.7). Consistent regulation of *NFATC1* and *NFATC2* by EBNA3A was therefore not apparent.

We next looked for evidence of regulation of *NFATC1* and *NFATC2* by EBNA3s in a lymphoblastoid cell line background. We collated published microarray data generated from a number of lymphoblastoid cell line systems studying EBNA3 gene regulation (Table 3.2). These included an EBNA3A knock-out LCL generated by infecting primary B cells from two different donors (D1 and D3) with a wild-type EBV (LCL wtBAC), a recombinant EBV virus carrying a deletion of the second exon of EBNA3A (LCL3A mtA), or with a recombinant EBV virus lacking the entire coding region of EBNA3A

(LCL3AmtB) (Hertle et al., 2009). To study the impact of EBNA3B on gene expression an EBNA3B Knock-out LCL derived from EBV-negative peripheral blood leukocytes from three donors infected with wild-type EBV, or with EBNA3BKO producer lines carrying the EBNA3B KO BAC was used (White et al., 2010). EBNA3C is essential for LCL outgrowth, so in order to study the effects of EBNA3C on gene expression a stable cell line expressing conditionally active EBNA3C (EBNA3CHT) was generated by the Allday laboratory (Skalska et al., 2013). This cell line was generated by infecting peripheral B cells with a recombinant EBNA3C that is fused at the C terminus to a 4-hydroxytamoxifen (HT)-sensitive murine oestrogen receptor (LCL 3CHT). Activation of EBNA3C is achieved by culturing the cells in media supplemented with 4-hydroxytamoxifen (HT) which interacts with and activates the oestrogen receptor leading to translocation of EBNA3C to the nucleus. To deactivate EBNA3C cells are withdrawn from HT. These microarray studies showed that *NFATC1* was not regulated by EBNA3A, EBNA3B or EBNA3C proteins in an LCL cell background (Figure 4.8) (Hertle et al., 2009), (White et al., 2010), (Skalska et al., 2013). The microarray study by White et al. (2010) showed that *NFATC2* was not regulated by EBNA3B in LCLs. There is some evidence of *NFATC2* downregulation by EBNA3C in an LCL 3CHT cell line (Chen et al., 2006). However, a subsequent microarray also using a LCL 3CHT cell line showed that clone LCL-A13-C2 shows upregulation of *NFATC2* by EBNA3C, while clones LCL-C19-C1 and LCL-C19-C2 both show some downregulation of *NFATC2* (Skalska et al., 2013) (Figure 4.9). Overall, these results suggest *NFATC2* is not robustly regulated by EBNA3C in an LCL background.

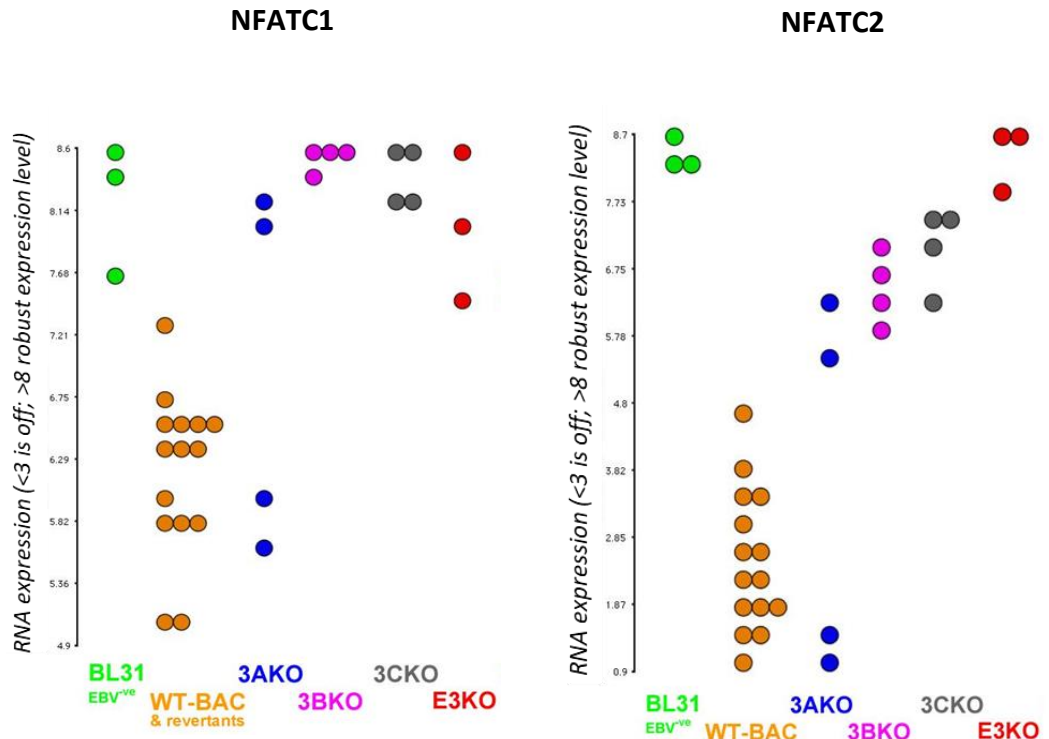


Figure 4.7. Regulation of NFATC1 and NFATC2 by EBNA3. Published gene expression analysis by White et al. (2010) using the EBV-negative Burkitt's Lymphoma cell line BL31 infected with a wild-type EBV virus or EBNA 3A, 3B or 3C knock-out bacmids. The dot plots are used to visualise the raw data at gene and transcript levels from the microarray. The EBV-wild-type & revertants data was combined into a single group to make the data easier to visualise. Y axis is log₂ values; <3 is off; >8 is robust expression level. The dot plots available from <http://www.epstein-barrvirus.org.uk/arrays2.php> courtesy of Dr Robert White.

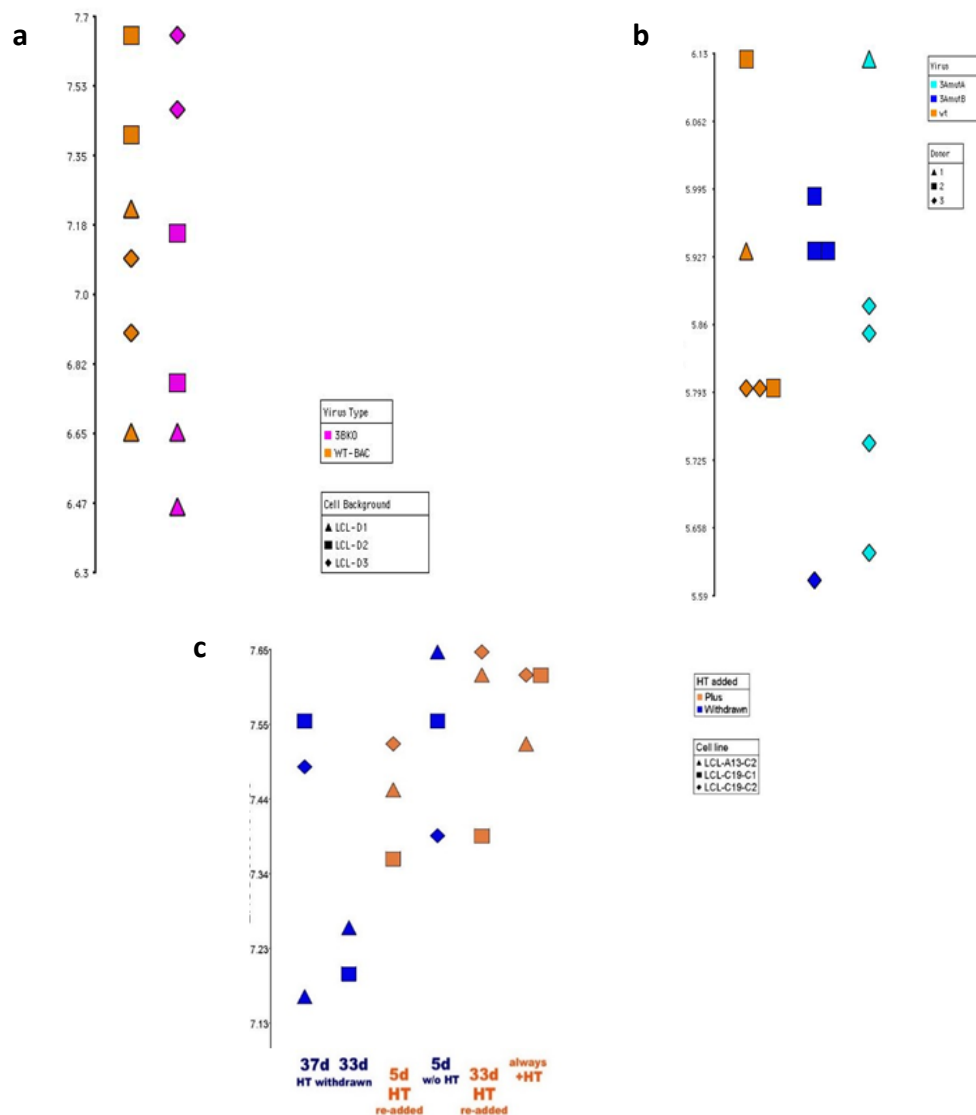


Figure 4.8. Regulation of NFATC1 by EBNA3 in LCLs. Microarray gene expression analysis of NFATC1 mRNA expression in using **a**) an EBNA3B Knock-out LCL derived from EBV negative peripheral blood leukocytes from three donors infected with wild-type EBV, or with EBNA3BKO producer lines carrying the EBNA3B KO Bac (White *et al.*, 2010) **b**) an EBNA3A knock-out LCL generated by infecting primary B cells from three different donors (D1, D2, D3) with a wild-type EBV (LCL wtBAC), with a recombinant EBV virus carrying a deletion of the second exon of EBNA3A (LCL3A mtA), or with a recombinant EBV virus lacking the entire coding region of EBNA3A (LCL3AmtB)(Hertle *et al.*, 2009) **c**) an LCL conditionally expressing EBNA3C generated by infecting peripheral B cells with a recombinant EBNA3C that is fused at the C terminus to a 4-hydroxytamoxifen (HT)-sensitive murine oestrogen receptor (LCL 3CHT). Activation of EBNA3C is achieved by culturing the cells media supplemented with 4-hydroxytamoxifen (HT). To deactivate EBNA3C cells are withdrawn from HT. (Skalska *et al.*, 2013). The dot plot shows samples that have been cultured in HT, withdrawn from HT for 5, 33 and 37 days, and have had HT re-added for 5 and 33 days to study the impact of EBNA3C expression of NFATC1 mRNA levels. The dot plots are used to visualise the raw data at gene and transcript level from the microarray and are available from <http://www.epstein-barrvirus.org.uk/arrays2.php>

A high throughput gene expression analysis using microfluidics cards (Taqman) was carried out in our laboratory by Dr Sarika Khasnis using an EBV-negative Burkitt's Lymphoma cell line (BL31) infected with either a recombinant wild-type EBV (wtBac), an EBNA3A knock-out EBV (BL31 E3AKO), an EBNA3B Knock-out EBV (BL31 E3BKO), EBNA3C Knock-out EBV (BL31E3CKO), EBNA3A, 3B, 3C Knock-out EBV (BL31 E3KO), or by their respective revertant virus to restore the deleted gene (BL31 3A rev2, BL31 3B rev2.2, BL31 3C rev2, BL31 E3 rev) (Anderton et al., 2008) to confirm the previous microarray data. The identity of the cells lines was confirmed by Western blot upon arrival at our laboratory (Figure 4.10). The gene expression analysis indicated that *NFATC1* is downregulated by the EBNA3A, EBNA3B and EBNA3C proteins (Figure 4.11). In the cells infected with the wild-type EBV bacmid and the EBNA3 revertant viruses mRNA levels were more than five-fold lower, whereas mRNA levels in the BL31 cells infected with the EBNA3A, 3B and 3C KO EBV virus were similar to that of the uninfected BL31 cells. The EBNA3A regulation we detected is likely because the cell lines we have used (3AKO-3 and 3AKO-1.1) are the two where regulation was detected (Figure 4.7)(White et al., 2010). We cannot confirm this because cell line clone specific data and identities were not provided in the study or on the website. Our data therefore confirm that *NFATC1* is robustly regulated by EBNA3B and EBNA3C in a BL cell background.

Our gene expression analysis also indicated that *NFATC2* is downregulated by the EBNA3B and EBNA3C proteins (Figure 4.11). In the cells infected with the wild-type EBV bacmid and the EBNA3s revertant cell lines mRNA levels are more than 10-fold lower, whereas mRNA levels in the BL31 cells infected with the EBNA3B and 3C KO EBV virus were similar to that of the uninfected BL31 cells. Our data showed that *NFATC2* is

not significantly regulated by EBNA3A (Figure 4.11). The cell lines we used (3AKO-3 and 3AKO-1.1) are two where regulation by EBNA3A was detected in one and not the other (Figure 4.7) (White et al., 2010). However, as explained above, we cannot confirm this as cell line clone specific data and identities were not provided in the study or on the website. Therefore, our data confirms *NFATC2* is robustly regulated by EBNA3B and EBNA3C.

Protein analysis was next carried out using the same cell lines to establish if mRNA downregulation by EBNA3B and EBNA3C impacted the overall levels of protein in the cell. The results showed that repression by EBNA3B and EBNA3C resulted in an almost complete loss of NFATC1 protein expression in the BL31 cells infected with the EBV wtBac. Protein expression in the EBNA3B KO and EBNA3C KO cells remained at a similar level to the uninfected BL31 cells, while the cells infected with the respective 3B and 3C revertant EBV viruses lost NFATC1 protein expression (Figure 4.12). The results for NFATC2 were similar where EBNA3B and EBNA3C resulted in a loss of NFATC2 protein expression in the BL31 cells infected with the EBV wtBac. Protein expression in the EBNA3B KO and EBNA3C KO cells remained at a similar level to the uninfected BL31 cells, while the cells infected with the respective 3B and 3C revertant EBV viruses lost NFATC2 protein expression (Figure 4.12).

To determine whether this regulation could be observed in other cell backgrounds we repeated the experiment in another Burkitt's Lymphoma cell line. The QPCR and protein analysis was repeated in the EBV-negative Burkitt's Lymphoma cell line (BL2) infected with either a recombinant wild-type EBV (wtBac), EBNA3C Knock-out EBV (BL31E3CKO1) or EBNA3C Knock-out 2 EBV (BL31E3CKO2). The results showed a four-

fold decrease in *NFATC1* mRNA levels in the BL2 cells infected with the wt-EBV virus relative to the uninfected BL2 cells. BL2 cells infected with the EBNA3C knock-out EBV virus showed higher levels of *NFATC1* expression than their WT-EBV infected counterpart which indicated that *NFATC1* is repressed by EBNA3C, although the repression does not appear to be very robust (Figure 4.13a). The repression was more convincing at the protein level where BL2 cell infected with a wt-EBV resulted in loss of *NFATC1* protein expression and infection with an EBNA3C KO EBV retained *NFATC1* protein expression levels. *NFATC2* was also repressed in the BL2 cells infected with the wild-type EBV virus. There was a seven-fold decrease in *NFATC2* mRNA expression relative to the uninfected BL2 cells. BL2 cells infected with the EBNA3C knock-out EBV virus showed significantly higher levels of *NFATC2* expression than their WT-EBV infected counterpart indicating that *NFATC2* is repressed by EBNA3C (Figure 4.13a). This repression was also evident at the protein level where BL2 cell infected with a wt-EBV virus resulted in loss of *NFATC2* protein expression and infection with a EBNA3C KO EBV retained *NFATC2* protein expression levels (Figure 4.13b).

Collectively, these results suggest that *NFATC1* and *NFATC2* are repressed by EBNA3B and EBNA3C at the mRNA and the protein level in a Burkitt's Lymphoma cell background. While *NFATC1* and *NFATC2* regulation appears to be cell line specific, we see evidence of EBNA3 binding close to the *NFATC1* and *NFATC2* genes in Mutu III cells suggesting EBNA3 may still play a role in NFAT regulation. The next step was to confirm EBNA2 and EBNA3 binding sites along the *NFATC1* and *NFATC2* gene locus identified from our original ChIP-Seq data, and to determine if binding of EBNA2 and EBNA3 was present in LCLs and in BL31 cells and whether this correlated with our regulation data.

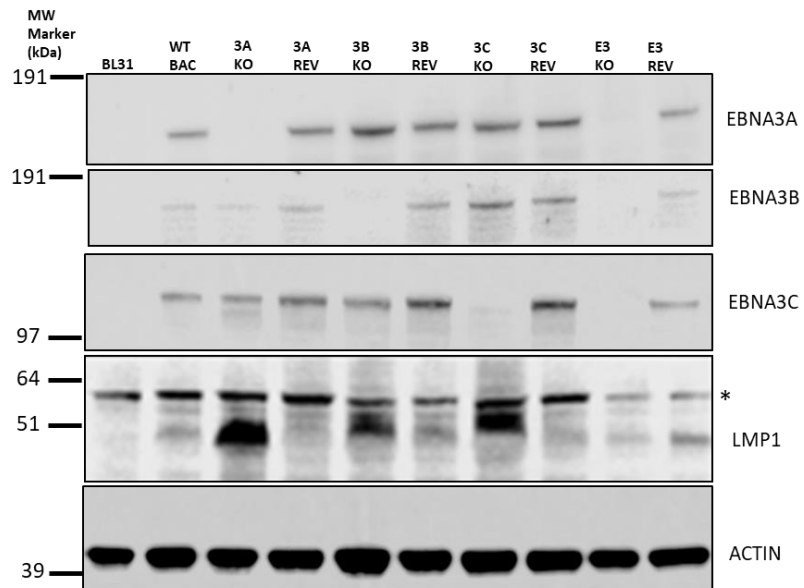


Figure 4.10 The identity of the BL31 cell series was confirmed by western blot on arrival in the laboratory. Clones used; BL31; wtBAC3; BL31 3AKO-1.1; BL31 3Arev-2; BL31 3BKO-1; BL31 3Brev-2.2; BL31 3CKO-6; BL31 3Crev-2; BL31 E3KO; BL31 E3rev.

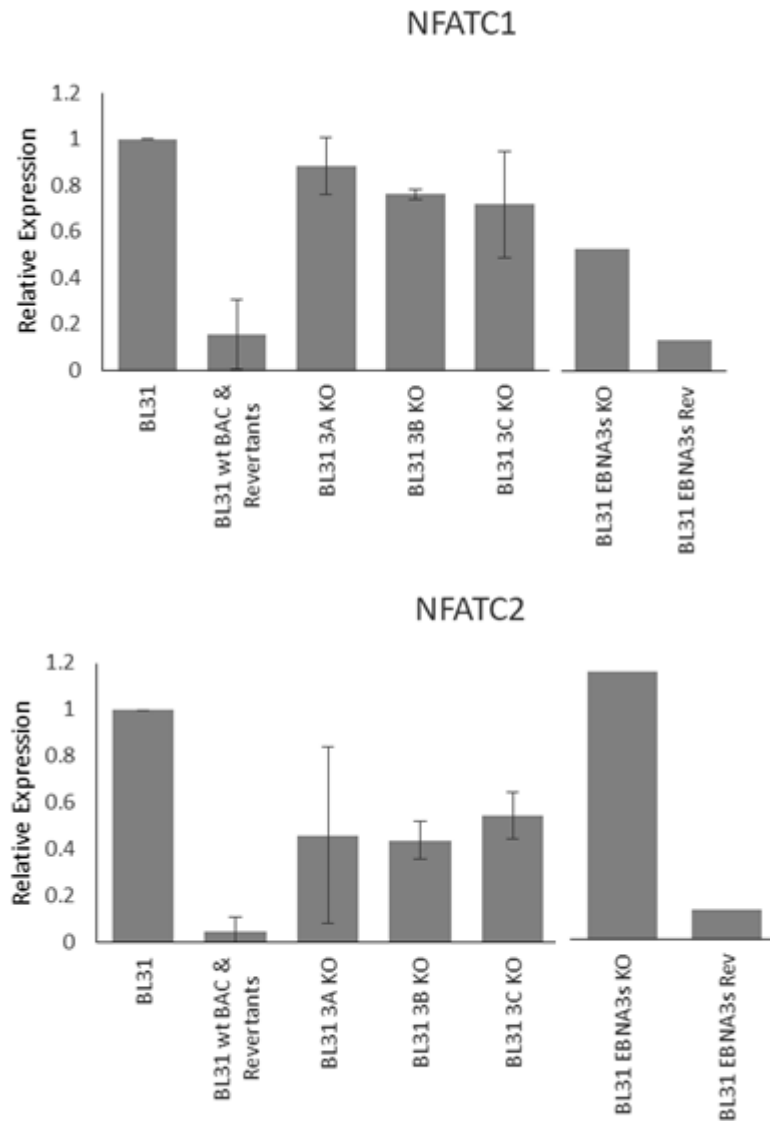


Figure 4.11 Regulation of *NFATC1* and *NFATC2* by EBNA3. QPCR analysis of *NFATC1* and *NFATC2* gene expression carried out by Dr. Sarika Khansis using the BL31 cell line derived from the EBV-negative Burkitt's lymphoma BL31 cell line series infected with wild-type recombinant EBV bacmids or EBNA 3A, 3B and 3C knock-out and revertant bacmids (kindly provided by Prof M. Allday) (Anderton *et al.*, 2008). Signals were normalised to *GUSB* mRNA levels. Results show mean mRNA levels relative to the EBV-negative BL31 cell line \pm standard deviation from two different clones. Clones used: BL31wtBAC2 +wtBAC3; BL31 3AKO-3 and 3AKO-1.1; BL31 3Arev-2; BL31 3BKO-1 and 3BKO-8.2; BL31 3Brev-2.2; BL31 3CKO-6 and 3CKO-3; BL31 3Crev-2; BL31 E3KO; BL31 E3rev.

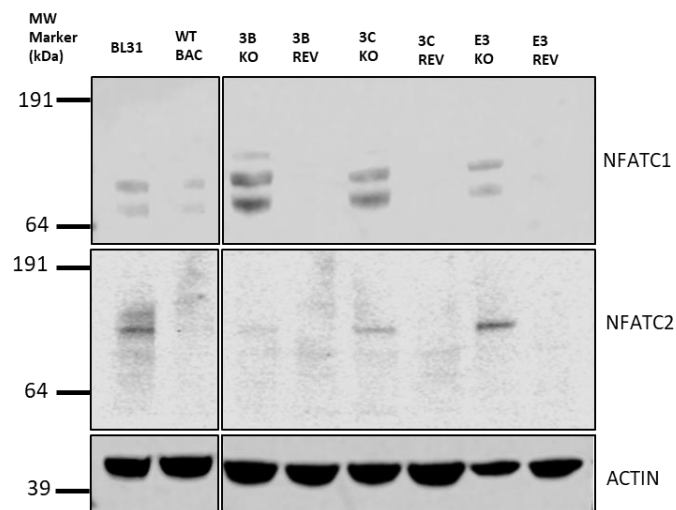


Figure 4.12 Regulation of NFATC1 and NFATC2 by EBNA3B and EBNA3C. a) Western blot analysis of NFATC1 and NFATC2 protein expression using the BL31 cell line derived from the EBV-negative Burkitt's lymphoma BL31 cell line series infected with wild-type recombinant EBV bacmids or 3B and 3C knock-out and revertant bacmids (kindly provided by Prof M. Allday) (Anderton *et al.*, 2008). Actin was used as a loading control. Clones used; BL31; wtBAC3; BL31 3AKO-1.1; BL31 3Arev-2; BL31 3BKO-1; BL31 3Brev-2.2; BL31 3CKO-6; BL31 3Crev-2; BL31 E3KO; BL31 E3rev.

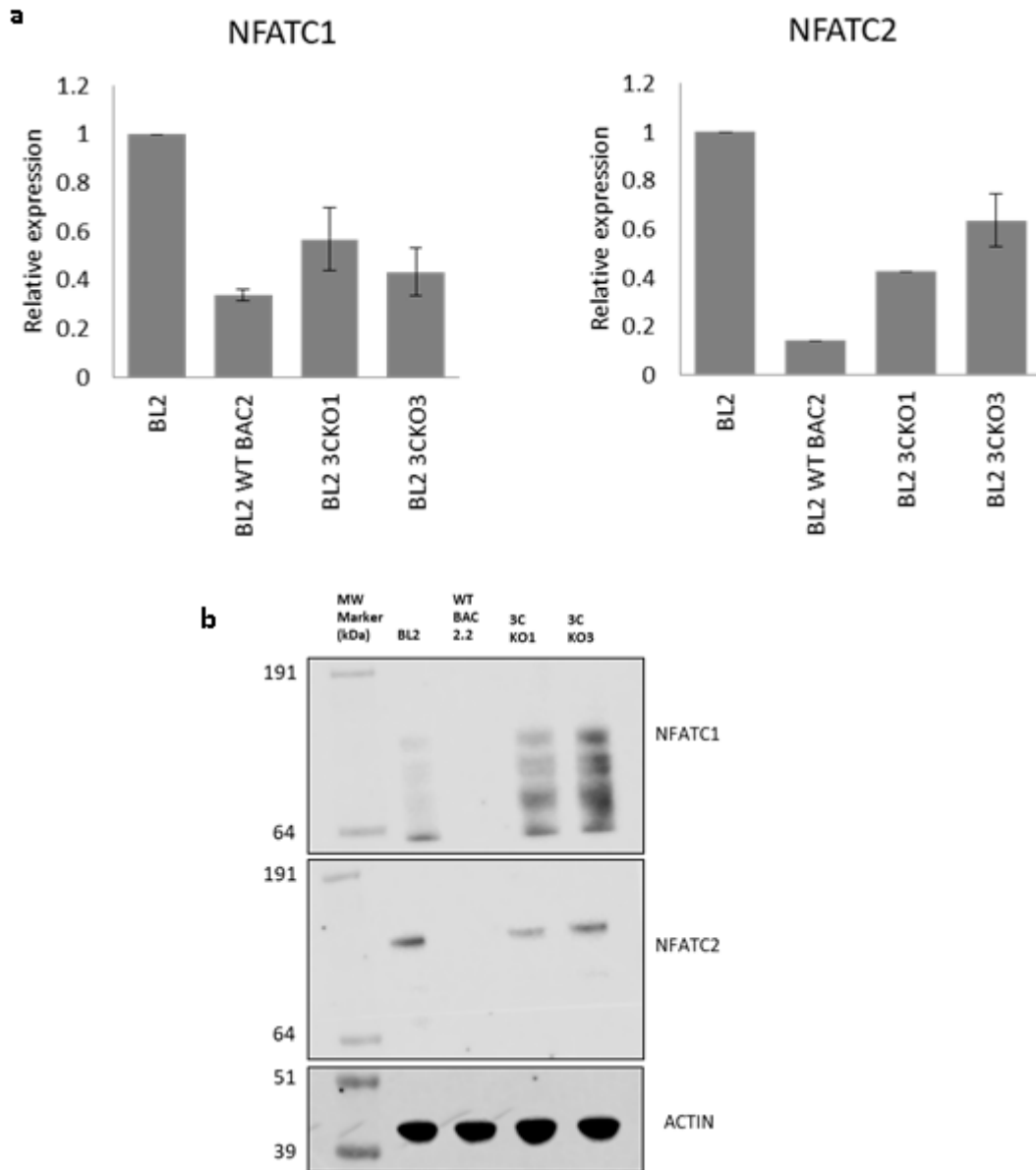


Figure 4.13. Regulation of NFATC1 and NFATC2 by EBNA3C in the BL2 cell line. a) QPCR analysis of *NFATC1* and *NFATC2* mRNA expression in using the EBV-negative Burkitt's lymphoma BL2 cell line series infected with wild-type recombinant EBV bacmids, an EBNA3C KO1 EBV virus, or an EBNA3C KO2 EBV virus (kindly provided by Prof M. Allday) (Anderton *et al.*, 2008). Signals were normalised to *GAPDH* mRNA levels. Results show mean mRNA levels relative to the EBV-negative BL2cell line \pm standard deviation from two QPCR experiments. **b)** Western blot analysis of NFATC1 and NFATC2 protein expression levels using the BL2 cell line cell line series described above. Actin was used as a loading control.

4.4 EBNA2 and EBNA3 binding is not detected at *NFAT* regulatory sites.

NFATC1 was identified as a gene closest to one of the most significant EBNA2 peaks and closest to any significant EBNA2 and EBNA3 peak irrespective of distance by the initial binding site analysis (Table 3.1). The CHIP-seq data showed there were two significant intragenic EBNA3 peaks and eight intragenic EBNA2 binding peaks in Mutu III cells, of which only one EBNA2 and EBNA3 binding site overlapped suggesting that EBNA2 and EBNA3 may be working independently to repress *NFATC1* transcription (Figure 4.2). However, we did not find evidence of consistent regulation of *NFATC1* by EBNA2, but we saw significant down regulation of *NFATC1* at the mRNA and the protein level (Figures 4.11, 4.12) in the presence of EBNA3B and EBNA3C in BL cells confirming a role for EBNA3B and EBNA3C in *NFATC1* gene expression control, although whether these effects are the result of direct binding to gene regulatory elements or indirect effects of other factors cannot be determined from these data.

NFATC2 was identified as a gene closest to any significant EBNA2 binding peak irrespective of distance by the initial binding site analysis (Table 3.1) and while CHIP-seq data showed there were 6 significant intragenic EBNA2 binding peaks *NFATC2* did not show consistent regulation by EBNA2 at the mRNA or protein level. Our CHIP-seq data showed that three EBNA2 binding site overlapped with EBNA3 binding sites (Figure 4.3) in Mutu III cells. We also saw significant down regulation of *NFATC2* at the mRNA and the protein level (Figures 4.11, 4.12, 4.13) in the presence of EBNA3B and EBNA3C in BL cells. This implicated EBNA3B and EBNA3C in *NFATC2* transcriptional regulation.

To explore whether *NFATC1/2* regulation correlated with direct binding of the EBNA proteins we used CHIP-QPCR to measure EBNA binding at previously identified EBNA binding sites. We carried out initial analysis in the Mutu III cells used for CHIP-seq analysis using EBNA3B, EBNA3C and EBNA2 specific antibodies. At *NFATC1* the original CHIP-seq data identified two EBNA3 binding peaks +36 kb and +54 kb upstream from the TSS, but we could not confirm EBNA3B or EBNA3C binding at these sites. We were able to confirm binding at EBNA3C binding sites at +59 kb and +65 kb locations (Figure 4.14). Both of these sites correspond with elevated levels of H3K27Ac indicating they could be active regulatory elements (Figure 4.2). The +54 kb site did not correspond with areas of H3K27Ac. We were unable to detect significant binding of EBNA2 at any of the previously identified EBNA2 binding sites across the *NFATC1* locus in Mutu III cells (Figure 4.15a).

At *NFATC2* we were able to confirm EBNA3C binding at the +142 kb peak and EBNA3B and EBNA3C binding at the +81 kb site and both sites corresponded with regions of H3K27Ac (Figure 4.14 and 4.3). We were unable to detect significant enrichment for EBNA2 at any of the previously identified EBNA2 binding sites across the *NFATC2* locus in Mutu III cells (Figure 4.15b).

Our results correlate with our earlier findings that EBNA2 was not a consistent regulator of *NFATC1* or *NFATC2*. We were only able to confirm some of the original CHIP-Seq data in Mutu III cells.

When we repeated this experiment in the BL31 wtBAC cell line we found that there was no significant binding of EBNA3B or EBNA3C at any of the previously identified EBNA3 binding sites at the *NFATC1* or *NFATC2* gene locus (Figure 4.16). Similarly, there was no

significant binding detected for EBNA2 at the *NFATC1* or *NFATC2* gene locus when we repeated the experiment in EREB2.5 LCLs (Figure 4.17). Most likely that the effects on mRNA expression detected in the specific cell lines is the result of indirect effects of the EBNA2s and not direct gene binding.

A subsequent CHIP-seq experiment carried out by our laboratory using GM12878 LCLs and antibodies specific for EBNA3B, EBNA3C and EBNA2 proteins also did not find EBNA2 binding at either the *NFATC1* or *NFATC2* gene locus. Similarly there was no EBNA3B or EBNA3C binding observed, with the exception of an EBNA3C peak matching the location of the +81kb peak at the *NFATC2* locus (Figures 4.2 and 4.3) (Gunnell et al., 2016). However, it should be noted that the data generated from this study is of low quality due to the low number of background subtracted reads per million.

Taken together these findings point to the conclusion that *NFATC1* and *NFATC2* are not directly regulated by the EBNA proteins and that although some binding is observed at some sites in Mutu III cells, binding appears to be very cell line specific. Repression of *NFATC1* and *NFATC2* by EBNA 3B and 3C are therefore most likely to be the result of repression of upstream components of the BCR signalling pathway.

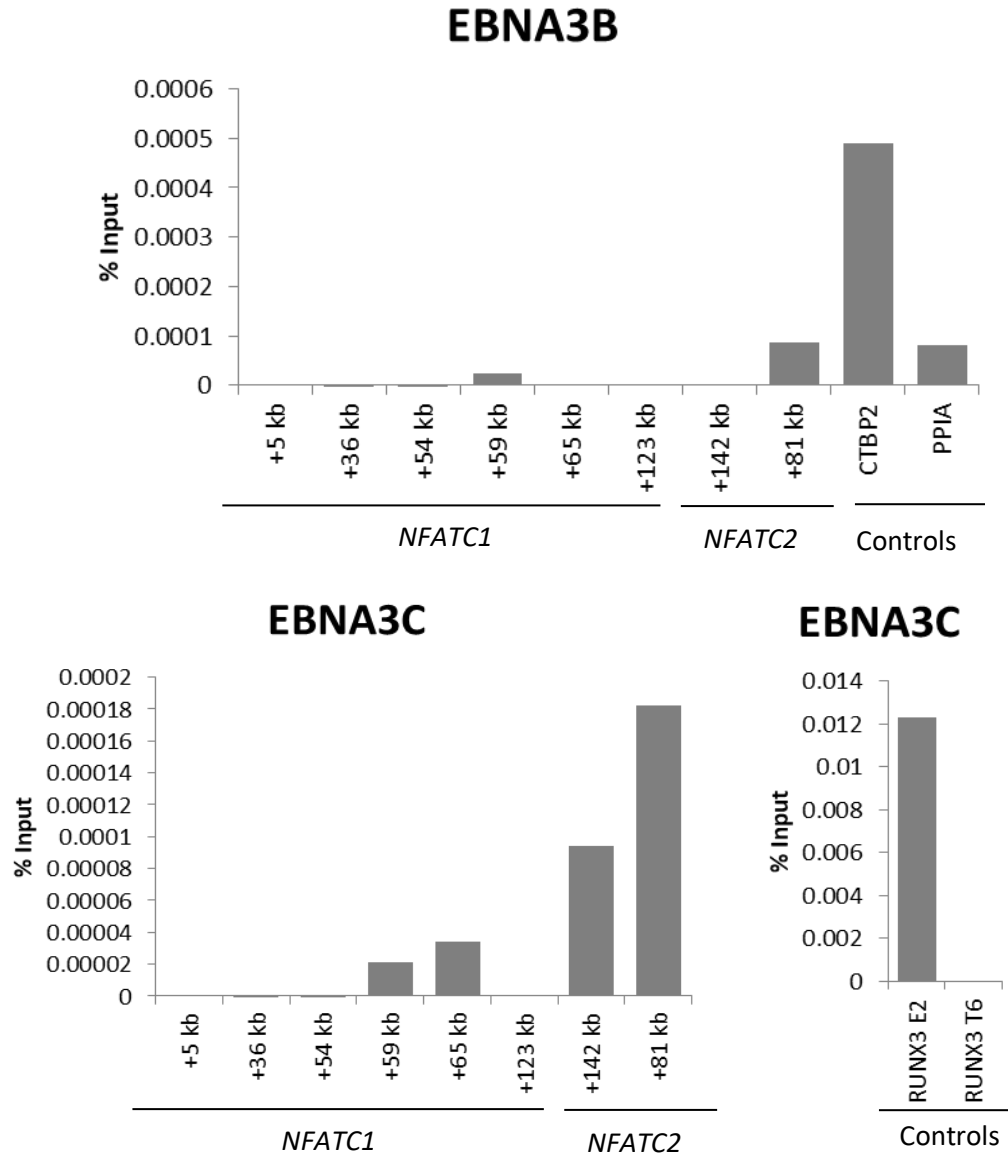
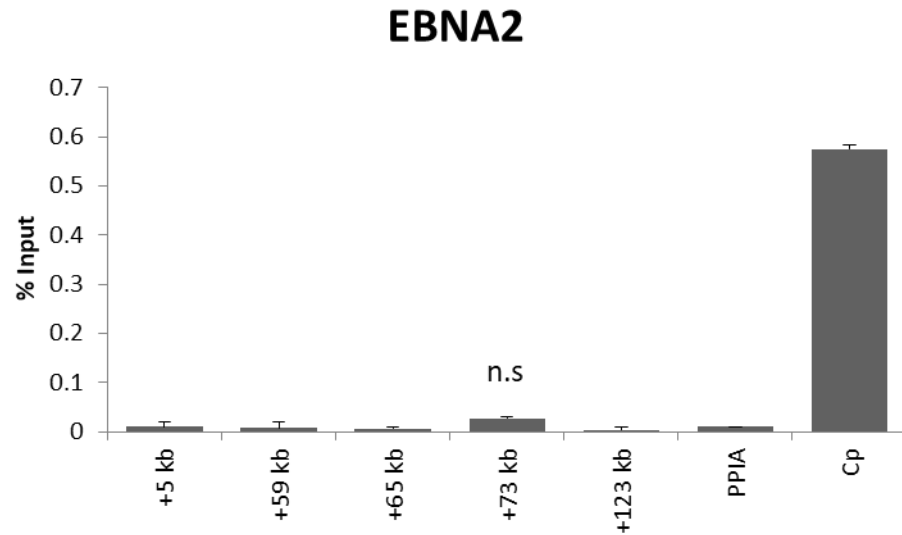


Figure 4.14 EBNA3B and EBNA3C binding was confirmed at the *NFATC1* and *NFACT2* gene locus in Mutu III cells. Results show the mean percentage input signals after subtraction of IgG antibody controls from one ChIP experiment using Mutu III cells using anti-EBNA3B and anti-EBNA3C antibodies. CTBP2 and RUNX3 E2 were used as a positive control regions for EBNA3B and EBNA3C antibodies respectively.

a



b

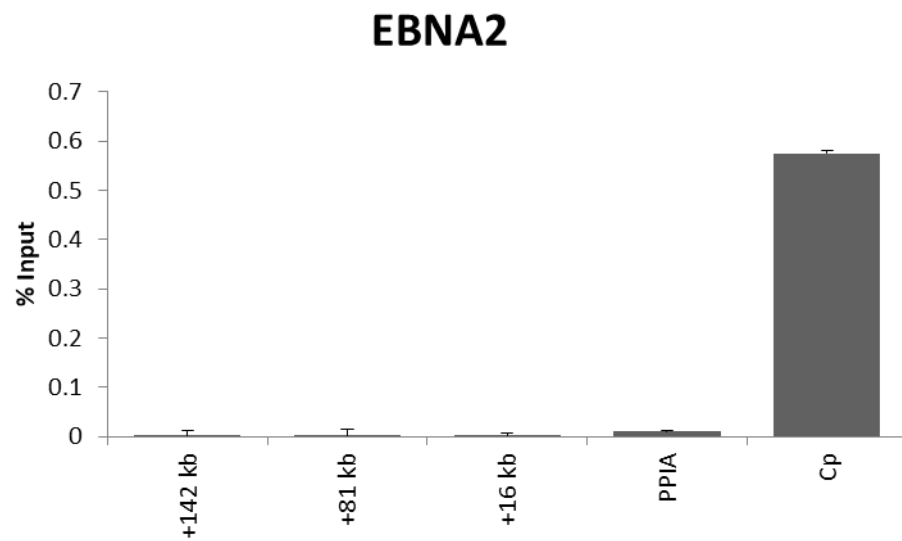


Figure 4.15 EBNA2 binding could not be confirmed at the *NFATC1* and *NFACT2* gene locus in Mutu III cells. a) EBNA2 binding at the *NFATC1* gene locus. b) EBNA2 binding at the *NFACT2* gene locus. Results show the mean percentage input signals after subtraction of IgG antibody controls \pm standard deviation of two independent ChIP experiments using Mutu III cells using an anti-EBNA2 antibody. EBV C promoter was used as a positive control regions for EBNA2 binding.

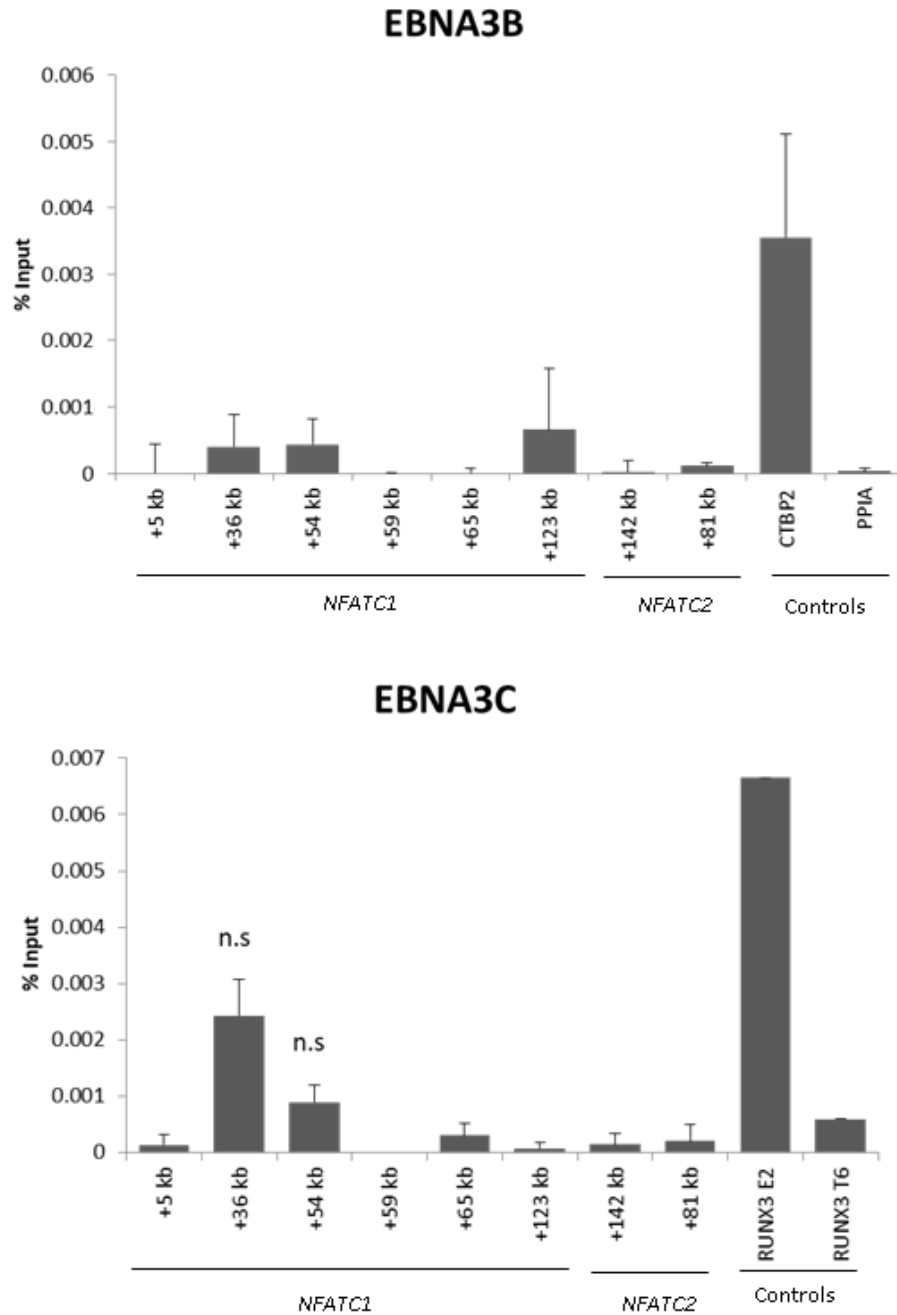


Figure 4.16 EBNA3B and EBNA3C do not bind at the *NFATC1* and *NFACT2* gene locus in BL31 cells. Results show the mean percentage input signals after subtraction of IgG antibody controls \pm standard deviation of two independent ChIP experiments using two different chromatin batches from BL31 EBV-WT bac cells using anti-EBNA3B and anti-EBNA3C antibodies. CTBP2 and RUNX3 E2 were used as a positive control regions for EBNA3B and EBNA3C antibodies respectively. Student T-test P values were calculated relative to the negative control (RUNx3 T6) and significance indicated as follows; n.s (not significant) = p-value > 0.05; * = p-value \leq 0.05; ** = p-value \leq 0.01; *** = p-value \leq 0.001.

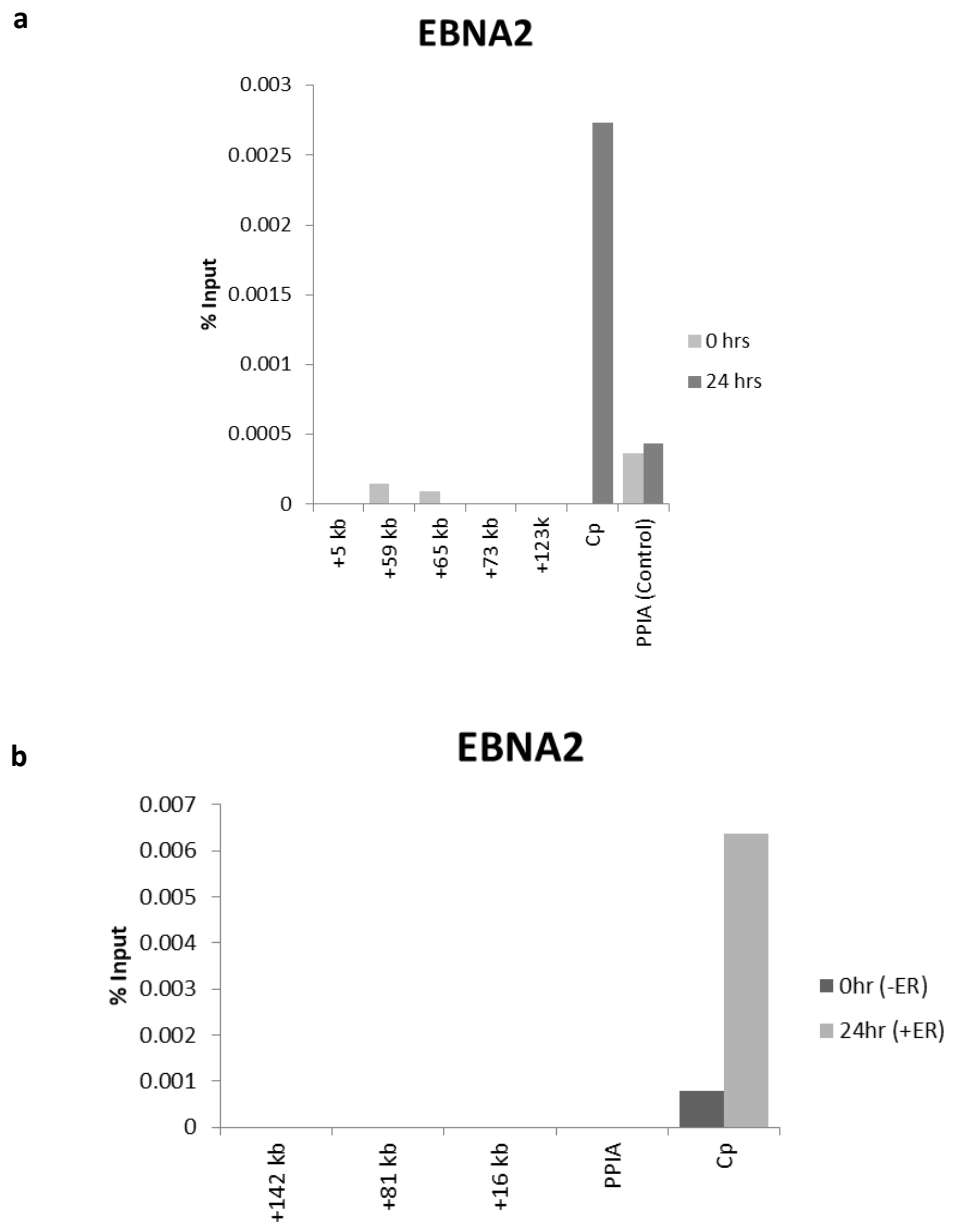


Figure 4.17 EBNA2 is not enriched at *NFATC1* and *NFATC2* gene locus. a) EBNA2 binding at the *NFATC1* gene locus. **b)** EBNA2 binding at the *NFATC2* gene locus. Results show the mean percentage input signals after subtraction of IgG antibody controls of a ChIP experiment in EREB2.5 cells (-ER and 24hrs +ER) using a monoclonal anti-EBNA2 antibody. Cp was used as a positive control regions and PPIA was used as a negative control region.

4.5 EBNA2 regulation of *PLCγ2* is cell line specific.

PLCγ2 is an important signalling molecule in the BCR signalling pathway and is an upstream effector of *NFATC1* and *NFATC2*. *PLCγ2* was identified as an EBNA2 target gene and has a top significant EBNA2 peak located 21 kb downstream of its TSS (Figure 4.4). A previous microarray using BJAB cells expressing conditionally active EBNA2, detected mRNA downregulation by EBNA2 (Maier et al., 2006). We confirmed *PLCγ2* mRNA levels were significantly repressed by the activation of EBNA2 in BJAB cells (Figure 4.18b). However, we found that repression of *PLCγ2* was not significant (p-value 0.0511) in EREB2.5 24 h after EBNA2 activation and that *PLCγ2* mRNA levels were not affected by EBNA2 activation in EBV-negative BL41 cells (Figure 4.18a and c).

To confirm the EBNA2 binding peaks identified from the original ChIP-seq binding data in Mutu III cells. We carried out a ChIP-QPCR experiment using primers located at the centre the +21 kb EBNA2 binding peak originally identified by the ChIP-Seq. This experiment was carried out in Mutu III cells using EBNA2 specific antibodies. We were able to confirm the +21 kb EBNA2 binding peak in Mutu III cells (Figure 4.19a), however when we repeated the ChIP-QPCR in EREB2.5 LCL we did not observe EBNA2 binding (Figure 4.19b). A ChIP-seq experiment carried out by our laboratory using GM12878 LCLs and antibodies specific for EBNA2 proteins did show an EBNA2 binding peak matching the location of the +21 kb peak at the *PLCγ2* gene locus (Figure 4.4) (Gunnell et al., 2016). However, as mentioned previously it should be noted that the data generated from this study is of low quality due the low number of background subtracted reads per million.

Together, these data suggest that *PLC γ 2* regulation by EBNA2 is cell line specific and we cannot be confident that EBNA2 is directly involved in its repression.

4.6 Conclusion

Overall, this chapter confirms that *NFATC1* and *NFATC2* are repressed at the mRNA level by EBNA2 and at the mRNA and protein level by EBNA3B and EBNA3C in a cell line specific manner. However, we were unable to confirm direct binding of EBNA proteins indicating that this repression is not a result of direct transcriptional regulation. NFATs are positioned at the end of the calcium signalling cascade and upstream components have also been identified as EBNA regulated binding targets (Figure 4.2). It is likely that repression of *NFATC1/2* is a result of EBV-mediated reduced signal transduction along the calcium signalling pathway. Similarly, regulation of *PLC γ 2* by EBNA2 is cell line specific and we cannot confirm direct involvement of EBNA2 in its repression.

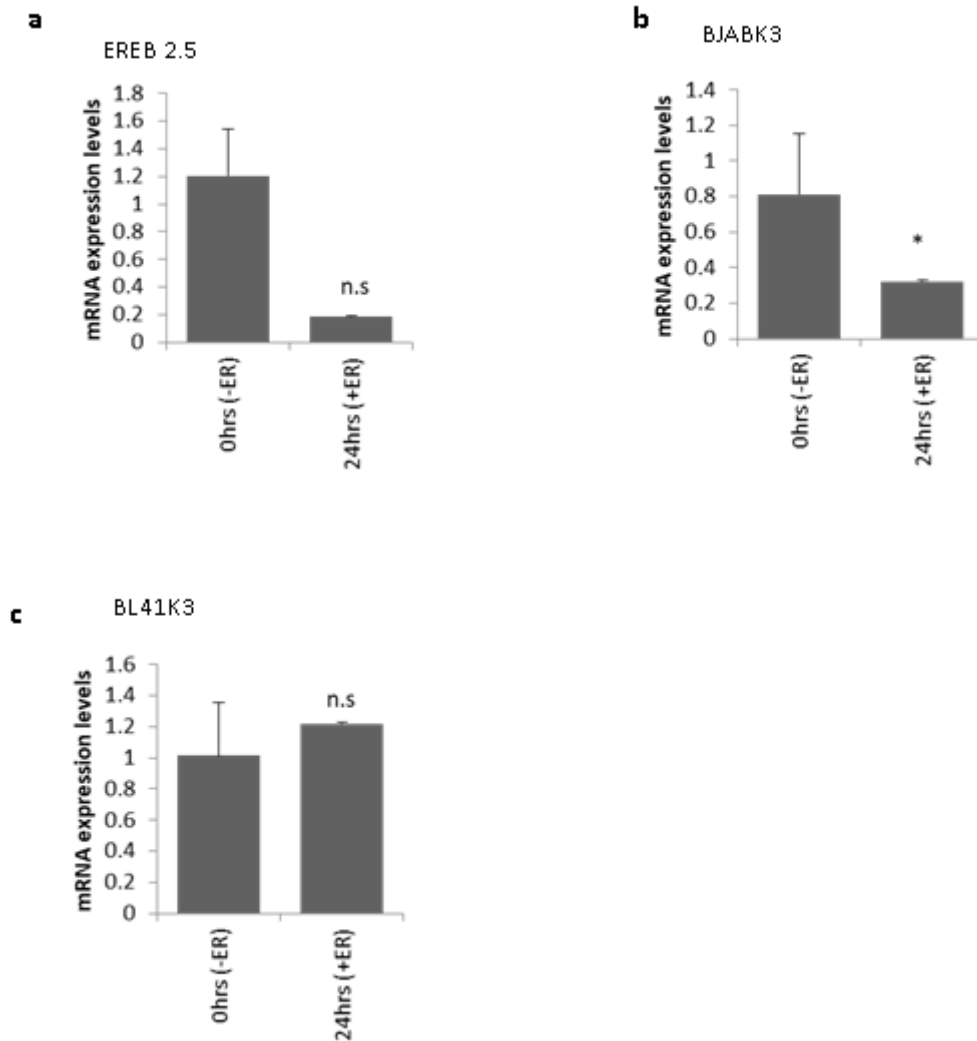


Figure 4.18. *PLCy2* mRNA analysis. a) QPCR analysis of *PLCy2* mRNA expression in EREB2.5 cells. Signals normalised to GAPDH. Results show mean mRNA levels relative to EREB2.5 (-ER) \pm standard deviation of two QPCR experiments. QPCR analysis of *PLCy2* mRNA expression in b) BJABK3 and c) BL41K3 cells conditionally expressing EBNA2. β -estradiol was added to cells (+ER) to activate EBNA2 and samples were harvested after 24 h. The figure above shows mean expression levels relative to BJABK3 (ER-) \pm standard deviation of two QPCR experiments and mean expression levels relative to BL41K3 (ER-) \pm standard deviation of two QPCR experiments. Student T-test p-values were calculated relative to the -ER sample and significance indicated as follows; n.s (not significant) = p-value > 0.05; * = p-value \leq 0.05; ** = p-value \leq 0.01; *** = p-value \leq 0.001.

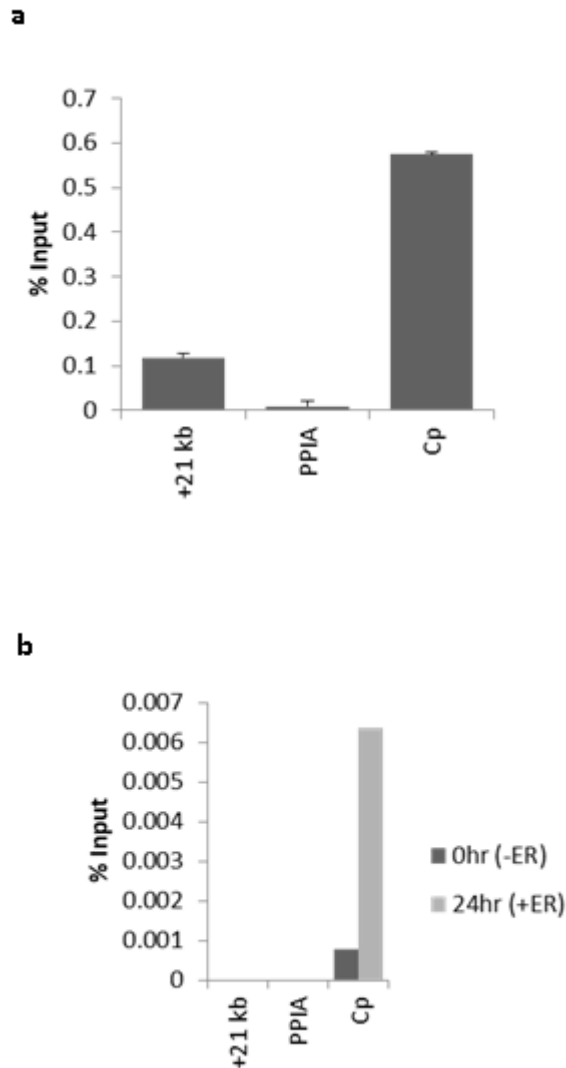


Figure 4.19 EBNA2 binding at the *PLCγ2* gene locus. a) EBNA2 binding at the *PLCγ2* gene locus in Mutu III cells. Results show the mean percentage input signals after subtraction of IgG antibody controls \pm standard deviation of two independent CHIP experiments in Mutu III cells using an anti-EBNA2 antibody. **b)** EBNA2 binding at the *PLCγ22* gene locus in EREB2.5 cells. Results show the percentage input signals after subtraction of IgG antibody controls of a CHIP experiment in EREB2.5 cells (-ER and 24hrs +ER) using a monoclonal anti-EBNA2 antibody. Cp was used as a positive control regions and PPIA was used as a negative control region.

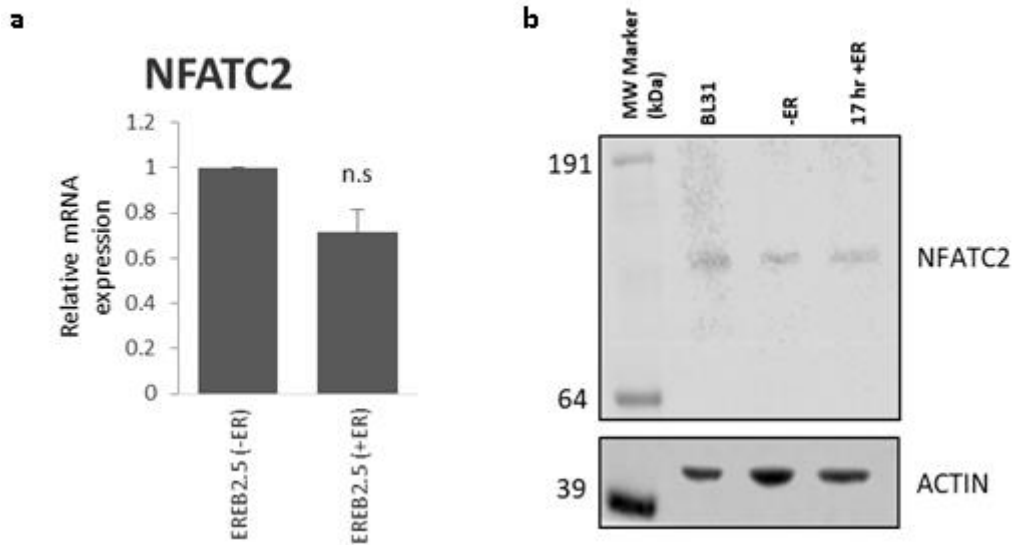


Figure 4.20. Regulation of NFATC2 by EBNA2 in EREB2.5 cell line a) QPCR analysis of NFATC2 mRNA expression in EREB2.5 cells by Dr. Sarika Khasnis. Signals normalised to *GUSB* mRNA. Results show mean mRNA levels relative to EREB2.5 (ER-) \pm standard deviation of two independent experiments. Student T-test P values were calculated relative to the -ER sample and significance indicated as follows; n.s (not significant) = p-value > 0.05; * = p-value \leq 0.05; ** = p-value \leq 0.01; *** = p-value \leq 0.001. **b)** Western blot analysis of NFATC2 protein expression in EREB2.5 cells. Actin was used as a loading control.

5. EBV latent proteins regulate cellular genes *MYC* and *BCL2L11* through large scale reorganisation of enhancer-promoter interactions.

5.1 Introduction

The EBNA2 and the EBNA3 family of transcription factors (EBNA3A, 3B and 3C) play an important role in the transcriptional reprogramming of host B cells that leads to deregulation of cellular genes involved in growth control and survival (Zhao et al., 2011b, Spender et al., 2002, Maier et al., 2006, McClellan et al., 2012, Hertle et al., 2009, White et al., 2010). EBNA2 and EBNA3 frequently target cellular and viral genes that drive proliferation.

In this chapter, we set out to investigate how EBV transcription factors regulate two key cellular genes, *MYC* and *BCL2L11*, involved in lymphomagenesis. *MYC* is an oncogene involved in cell cycle progression, differentiation and apoptosis (Hoffman and Liebermann, 2008) and EBNA2 is a known positive regulator of *MYC* (Kaiser et al., 1999). *BCL2L11*, is a gene that encodes pro-apoptotic protein Bim, a member of the BCL-2 protein family. Bim is a key regulator of B cell survival and its repression leads to uncontrolled B cell proliferation and lymphomagenesis. EBNA3A and EBNA3C have been shown to work together to direct polycomb-mediated silencing of *BCL2L11* (Anderton et al., 2008).

The mechanisms of deregulation of *MYC* and *BCL2L11* by EBNA proteins are not fully understood (Thorley-Lawson and Allday, 2008). Previously published genome-wide binding site analyses indicate that EBNA2 and EBNA3s are able to deregulate cellular gene targets by preferentially binding to long-range regulatory elements that can act on gene promoters (McClellan et al., 2013, McClellan et al., 2012, Zhao et al., 2011b,

Zhou et al., 2015). An EBNA2 bound enhancer region was identified -425 kb upstream of *MYC* by Zhao et al (2011). The *BCL2L11* promoter is thought to be the target of EBNA3 proteins (McClellan et al., 2012, McClellan et al., 2013, Paschos et al., 2009) and EBNA3A and EBNA3C mediated gene silencing is associated with recruitment of polycomb repressor complex 1 and 2 (PRC1, 2) and the deposition of the gene silencing mark H3K27Me3.

EBNA2 ChIP-sequencing data from our laboratory mapped EBNA2 binding sites both upstream (-556, -428, and -186/168 kb) and downstream (+450, +570, +900 kb, and 1.8 Mb) from *MYC* (Figure 5.1a and b). The upstream regions showed a high level of H3K27Ac characteristic of active enhancers (Figure 5.1c) and all EBNA2 bound regions with the exception of +900kb enhancer are classed as super-enhancers (Khan and Zhang, 2016). To study the role of these EBNA2-bound enhancers and super-enhancers in *MYC* activation, initial studies were carried out in our group by Dr David Wood using circular chromosome conformation capture-sequencing (4C-seq) (Wood et al., 2016). Using this technique he analysed the effect of EBNA2 binding on *MYC* promoter-enhancer interactions by using a *MYC* promoter fragment as bait to capture interacting regions that were then sequenced and mapped to the human genome. This analysis was carried out using the EREB 2.5 cell line conditionally expressing an ER-EBNA2 fusion protein. These results demonstrated that EBNA2 induced substantial directional reorganisation of interactions across the *MYC* regulatory domain by increasing *MYC* promoter interactions with upstream EBNA2-bound elements (-556, 428, and -186/168

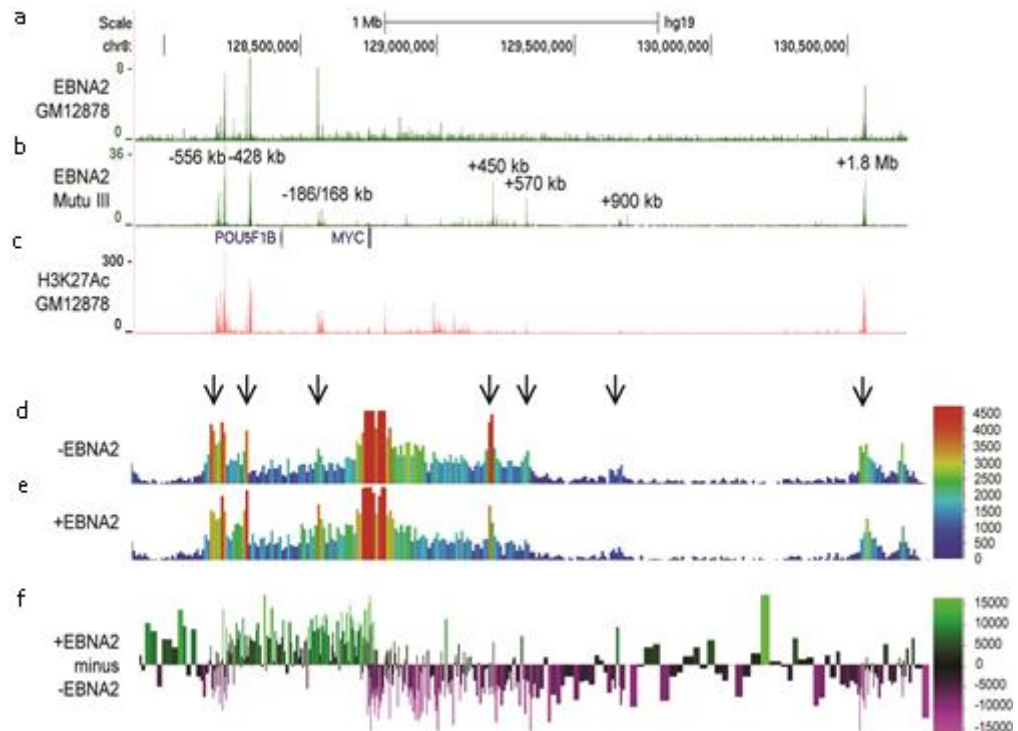


Figure 5.1. EBNA2 binding induces directional reorganisation of MYC promoter-enhancer interactions a) EBNA2 ChIP-seq reads in EBV-infected GM12878 cells b) in EBV positive Mutu III BL cells that express full latency III panel of EBV proteins c) H3K27Ac signals in GM12878 cells from ENCODE. Numbering indicates the position of the enhancers clusters relative to the MYC transcription start site. d) Sequencing reads from 4C-Seq using the MYC promoter as bait in EREB2.5 cells expressing a conditionally active ER-EBNA2 fusion protein cultured in the absence of β -estradiol (-EBNA2). Reads shown are from one of two replicates. Scale bar shows reads per 10kb window per million reads of sequencing library. e) 4C-Seq reads from EREB2.5 cells cultured in the presence of β -estradiol (+EBNA2). f) Subtraction of -EBNA2 4C-seq reads from +EBNA2 4C-seq reads. The scale bar shows the normalised interaction read count difference.

kb) and reducing interactions with downstream regions including the +450, +570, +900 kb, and 1.8 Mb EBNA2-bound elements (Figure 5.1d-f) (Wood et al., 2016).

Working alongside Dr Wood, I set out to determine if the same changes in enhancer-promoter interactions at *MYC* were evident in the more physiological setting of EBV infection of naïve B cells. Alongside EBV infection, we also examined *MYC* promoter-enhancer interactions when B cells were activated by treatment with CD40 ligand (CD40L) and IL-4 which mimics short-term B cell activation.

I also investigated the mechanisms of *MYC* activation by EBNA2 and *BCL2L11* silencing by EBNA3 proteins.

5.2 EBV infection leads to *MYC* upregulation in primary B-cells.

Stimulation with CD40L and IL-4 activates naïve B-cells by switching on downstream signalling pathways leading to short term proliferation, whereas EBV infected B cells grow out into immortal cell lines. We used uninfected, EBV infected (+EBV) and CD40L/IL-4 stimulated naïve B cells provided by Dr Shannon-Lowe (University of Birmingham). The isolated naïve B cells were harvested untreated or infected with EBV or stimulated with CD40L/IL-4 and harvested after 48 h. It has been previously established that *MYC* is upregulated in response to EBNA2 in LCLs (Kaiser et al., 1999). We used QPCR analysis to confirm *MYC* was also upregulated on EBV infection in naïve B cells. We found that *MYC* levels showed a 3 fold upregulation 48 h post EBV infection compared to the uninfected B-cells and the CD40/IL-4 stimulated B-cells (Figure 5.2).

Next, we set out to investigate whether EBV infection of naïve B-cells induced different patterns of enhancer and promoter interactions compared to CD40L/IL-4 B-cells.

5.3 EBV infection of naïve B-cells results in a different pattern of chromatin reorganisation to that induced by physiological B-cell activation.

To investigate whether EBV infection of naïve B-cells induced different patterns of enhancer and promoter interactions than CD40L/IL-4 stimulated B-cells we carried out 4C-seq strategy using the *MYC* promoter as bait in uninfected naïve B cells, EBV infected B-cells, and CD40L/IL-4 stimulated B cells. We found that in naïve B cells the *MYC* promoter region interacted with the -556, -428, +450 and +570 kb upstream and downstream enhancer regions (Figure 5.3b) which is consistent with some pre-existing enhancer-promoter interactions in resting B-cells, and the classification of the -556 kb region as a super enhancer in CD19+ B-cells (Khan and Zhang, 2016). Comparing the promoter interactions in EBV infected naïve B-cells with those in naïve B cells identified a number of changes on EBV infection that were similar to those in EREB2.5 cells on EBNA2 activation. We observed a reduction in downstream interactions with the +450 kb and +1.8 Mb elements and an increase in upstream interactions that included the -556kb and -428kb elements (Figure 5.3b, c and e). However, the interactions at the upstream -186/168 kb region were not seen in EBV-infected naïve B cells. However, recent capture Hi-C data generated by Dr David Wood using EBV-infected B cells harvested 5 days post infection did show interactions between the 186/168 kb region, so it is possible that these interaction are initiated during a later stage of infection.

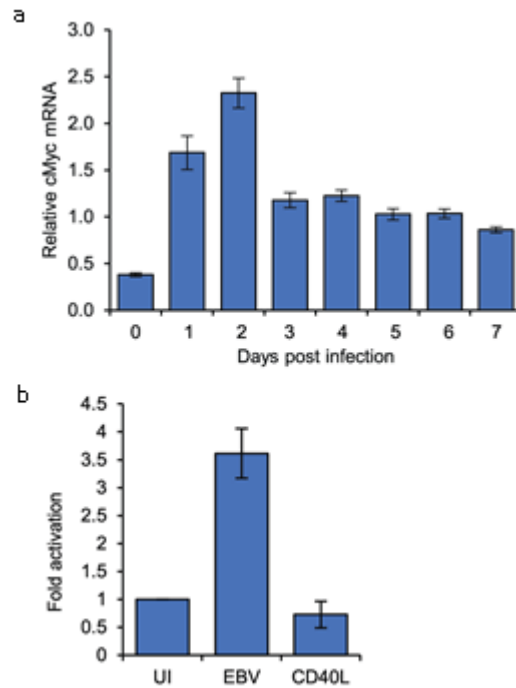


Figure 5.2 MYC mRNA induction on EBV infection. a) QPCR analysis of MYC mRNA expression over a B-cell infection time course to determine the optimum time for MYC induction. b) QPCR analysis of MYC mRNA expression in the naïve, EBV-infected and CD40/IL-4 stimulated B cell samples used for 4C-seq. Samples used in this experiment were harvested 48hrs after EBV-infection or CD40/IL-4 stimulation. Signals were normalised to β 2-microglobulin. Results show the mean \pm standard deviation of QPCR duplicates. (Wood et al., 2016)

We found that *MYC* enhancer-promoter interactions in CD40/IL-4 stimulated cells were reorganised in an inverse manner compared to EBV infected cells. We detected an increase in downstream promoter interactions and a reduction in upstream interactions. The downstream regions +235 to +432 interacted with the *MYC* promoter at a high level in CD40/IL-4 stimulated cells (Figure 5.3b, d and f). These regions are not bound by EBNA2 and do not show significant interaction with the *MYC* promoter in EBV-infected cells. However, these regions do interact with the *MYC* promoter in CD34+ haemopoietic progenitor cells (Mifsud et al., 2015). We also found increased interactions between the +450 kb downstream region and the *MYC* promoter in CD40/IL-4 stimulated cells compared to uninfected cells. Whereas, in EBV infected cells we saw a reduction in interactions between the +450 kb region and the *MYC* promoter. This region is bound by EBNA2 and also contains two binding sites for chromatin boundary and looping factor CTCF. Interactions between CTCF sites can lead to chromatin loops that can prevent long-range enhancer-promoter interactions by isolating them on separate loops, or establishing loop formation that can bring enhancers and promoters in closer proximity to each other. Our laboratory has previously shown that EBNA2 promotes CTCF interactions at the *MYC* -556 SE by looping out a specific region from the enhancer-promoter hub (Wood et al., 2016). It is possible that EBNA2 promotes similar CTCF interactions at the +450 region excluding it from interacting with the *MYC* promoter. However, further investigation would be needed to confirm such interactions.

In conclusion, the difference between the *MYC* promoter interactions in the EBV infected and CD40L/IL-4 stimulated naïve B-cells suggests that viral and physiological activation of *MYC* proceed via different mechanisms leading to distinct patterns of

chromatin reconfiguration. EBV infection resulted in similar enhancement of upstream *MYC* promoter-enhancer interactions shown on EBNA2 activation in LCLs indicating that EBNA2 is a key driver of these changes.

5.4 The SWI/SNF ATPase BRG1 is required for *MYC* upstream enhancer-promoter interactions.

BRG1, the ATPase subunits of the chromatin remodeller SWI/SNF, is required for the interaction of the +1.8/1.9 Mb *MYC* enhancer with the *MYC* promoter in leukaemic cells (Shi et al., 2013) and EBNA2 has been shown to be able to interact with BRG1 through the Snf5 subunit of SWI/SNF (Wu et al., 1996). We therefore examined the binding and potential role of BRG1 in EBNA2-directed enhancer promoter interactions. ChIP-QPCR data from our laboratory using EREB2.5 cells detected increased levels of H3Ac and BRG1 binding across EBNA2-bound enhancer regions in the presence of EBNA2 (Wood et al., 2016). The increased binding of BRG1 at the -556, -428 and -186-168 kb regions in the presence of EBNA2 is consistent with the ability of EBNA2 to interact with BRG1 via the snf5 subunit of SWI/SNF (Wu et al., 1996). To determine if BRG1 was required for the interaction of EBNA2-bound enhancers to the *MYC* promoter we knocked-down BRG1 expression and examined the effects of this on enhancer-promoter interactions in EBV-infected GM12878 cells using standard low throughput PCR-based chromatin conformation capture (3C) (Naumova et al., 2012). The siRNA mediated BRG1 knock-down was carried out by Dr David Wood and I carried out the 3C experiment.

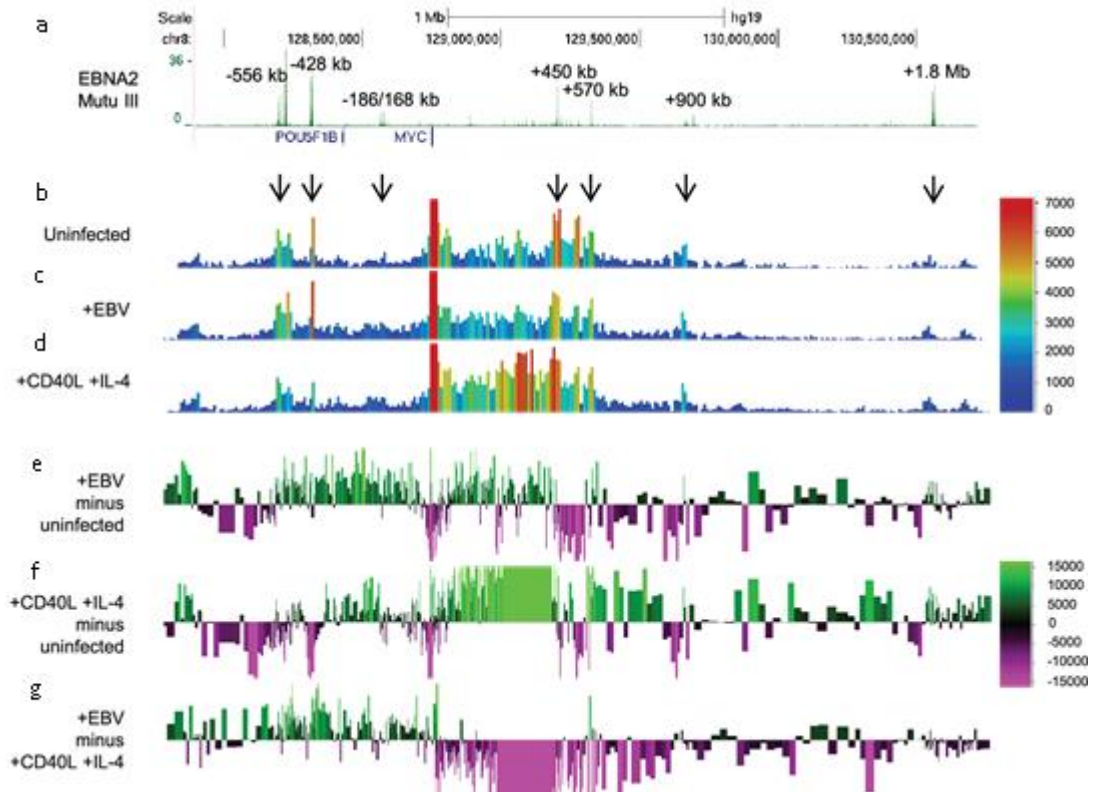


Figure 5.3 EBV infection of naïve B cells induces directional reorganisation of MYC promoter-enhancer interactions. **a)** EBNA2 ChIP-seq reads in MUTU III BL cells as explained in **figure 1**. Sequencing reads from 4C-Seq using the MYC promoter as bait as explained in **figure 1** in uninfected naïve B-cells (**b**), B-cells 48hrs after EBV infection (**c**), and B-cells 48hrs after stimulation with CD40/IL-4 (**d**). Subtraction of uninfected B cells 4C-seq reads from EBV-infected B cells 4C-Seq reads (**e**), or CD40/IL-4 treated cells (**f**). Reads shown are from both replicates combined. The scale bar shows the normalised interaction read count difference. **g)** Subtraction of 4C-seq reads from CD40/IL-4 treated cells from those obtained from EBV-infected cells. Reads shown are from both replicates combined. The scale bar shows the normalised interaction read count difference. (Wood et al., 2016)

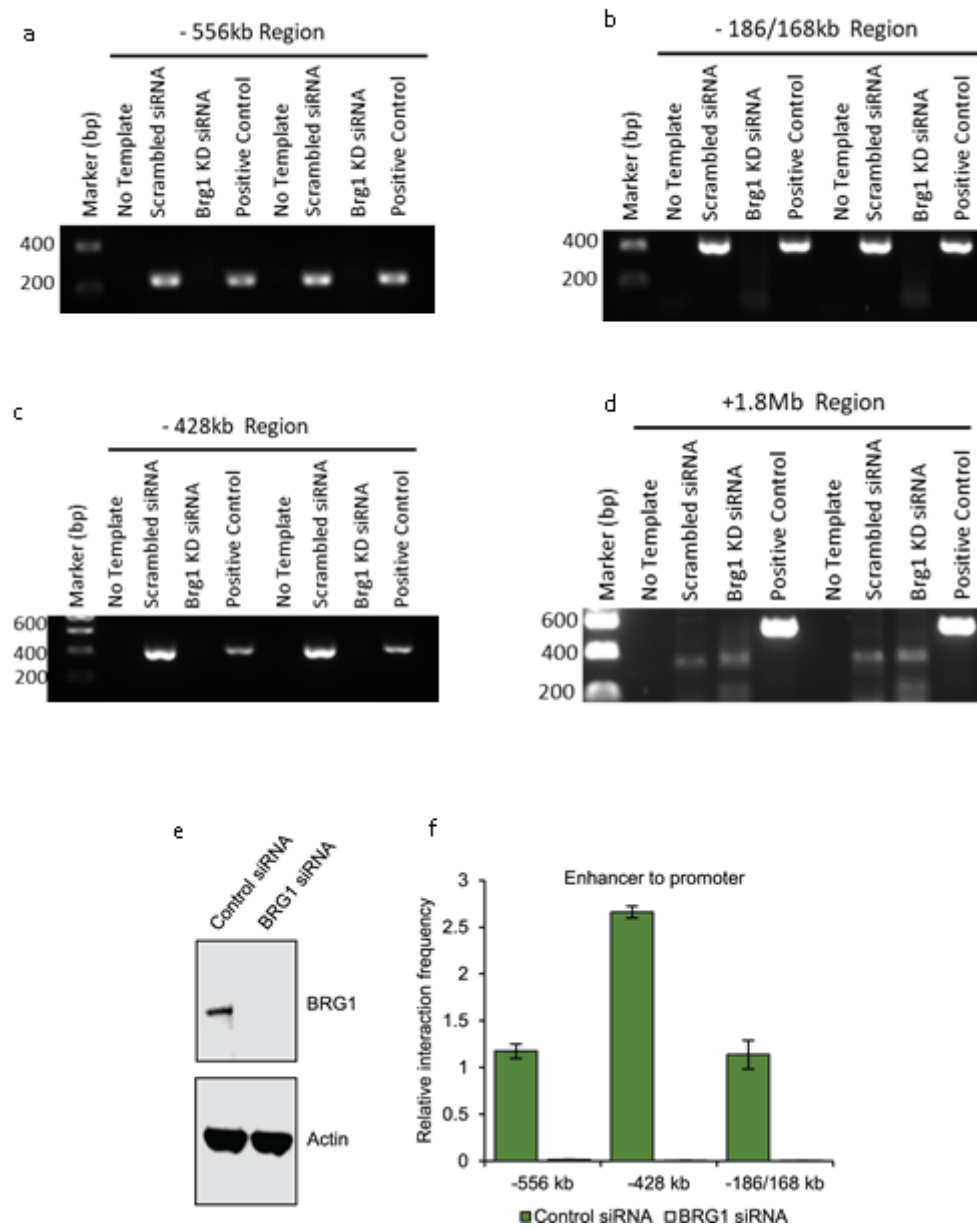


Figure 5.4 BRG1 is required for upstream MYC enhancer-promoter interactions in EBV-infected cells. Chromosome conformation capture (3C) analysis of MYC promoter interactions between **a**) -556 kb **b**) -186/168 kb, **c**) -428 kb, and **d**) +1.8 Mb EBNA2-bound enhancer regions in GM12878 cells transiently transfected with control (scrambled siRNA) or BRG1-specific siRNAs. Location of primers indicated in **figure 3.3**. Positive controls show amplification of GeneArt Strings DNA fragments designed to represent each of the four anticipated ligation products. **e**) Western blot analysis of BRG1 expression on GM12878 cells transiently transfected with control or BRG1-specific siRNA. Actin was used as a loading control. **f**) Quantification of the 3C analysis detailed above (**a-c**) Results show the mean \pm standard deviation of signals from duplicate PCRs. Data for +1.8 Mb enhancer not plotted as we did not observe enhancer–promoter interactions. (Wood et al., 2016)

Our 3C analysis found that that siRNA-mediated BRG1 knockdown in GM12878 cells (Figure 5.4e) led to a loss of *MYC* promoter interactions with the -556, -428 and -186/168 enhancer regions (Figure 5.4a-c and f). We were unable to detect any interactions between the +1.8 Mb enhancer and the *MYC* promoter in the presence or absence of BRG1 (Figure 5.4d). This is consistent with our 4C data where we observed low-level interaction frequency in both uninfected and EBV-infected cells in this region in EBV-infected cells (Figure 5.1 and 5.3). Taken together these results indicate that BRG1 is required for EBNA2 to maintain active upstream enhancer-promoter interactions.

5.5 Inhibition of EZH2 by UNC1999 results in de-repression of the *BCL2L11* enhancer hub

BCL2L11 encodes the pro-apoptotic protein Bim, a key regulator of B cell survival. EBNA3A and EBNA3C have been shown to work together to direct polycomb-mediated silencing of *BCL2L11* (Anderton et al., 2008).

Our laboratory has previously demonstrated the repression of *BCL2L11* was associated with EBNA3A and EBNA3C binding at the *BCL2L11* promoter but our EBNA3 protein ChIP-seq analysis also detected EBNA3 binding sites at distal regions across the *BCL2L11* locus. These included three sites upstream of *BCL2L11* in the intragenic region of the neighbouring acyl-CoA oxidase-like gene *ACOXL* and three sites downstream of *BCL2L11* (Figure 5.5a) (McClellan et al., 2013, McClellan et al., 2012). These new putative *BCL2L11* enhancer sites were designated enhancers 1-6. ChIP-QPCR carried

out by Dr Wood in our laboratory confirmed that EBNA3A and EBNA3C bind to these *BCL2L11* long-range elements (Wood et al., 2016). A subsequent 3C analysis was carried out by Dr Wood in the EBV-negative BL31 cell line series infected with recombinant wild-type, EBNA3A KO or EBNA3C KO EBVs (Anderton et al., 2008). The results showed that in uninfected BL31 cells, or those infected with and EBNA3A or EBNA3C KO EBV all long-range enhancers regions, with the exception of enhancer 1, interacted with the *BCL2L11* promoter and *BCL2L11* mRNA was expressed. However, all these interactions were lost in cells infected with wild-type EBV and *BCL2L11* mRNA expression was also lost, indicating that *BCL2L11* silencing by EBNA3A and EBNA3C was associated with inactivation of an active enhancer-promoter hub (Wood et al., 2016). Further CHIP-QPCR studies also found that H3K27 methyltransferase EZH2, a subunit of PRC2, bound to all EBNA3A and EBNA3C targeted enhancers in wild-type EBV-infected BL31 cells (Wood et al., 2016), which is consistent with previously published studies that have shown EBNA3A and EBNA3C induced deposition of the PRC silencing mark H3K27me3 across the *BCL2L11* promoter (Paschos et al., 2009).

Deregulation of EZH2 has been observed in many malignancies and the inhibition of EZH2 catalytic activity is emerging as a therapeutic approach to treating cancers. The potent selective EZH2 inhibitor tazemetostat, currently undergoing phase I clinical trials, has demonstrated anti-cancer activity in multiple B cell malignancies including, non-Hodgkin Lymphoma and Diffuse Large B cell Lymphoma (Lue and Amengual, 2018). To determine if EBV mediated silencing of *BCL2L11* could be reversed through

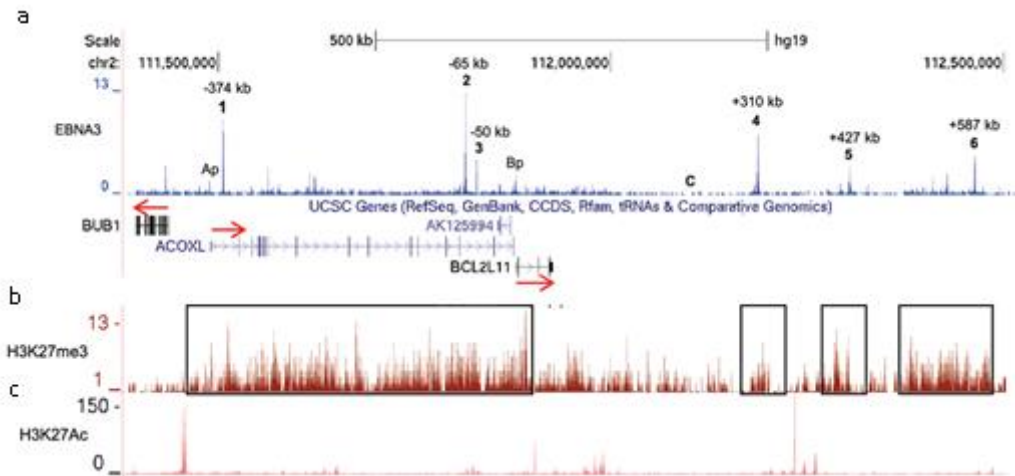


Figure 5.5 EBNA3 bound enhancers at the *BCL2L11/ACOXL* locus are within H3K27me3 repressed domains **a)** ChIP-seq results showing EBNA3A/3B/3C binding in Mutu III BL cells (McClellan et al., 2013). The major EBNA3-bound sites are numbered 1-6 and their location relative to the *BCL2L11* transcription start site is indicated. The *ACOXL* gene promoter (Ap) and the *BCL2L11* gene promoter (Bp) are also labelled. **b)** H3K27me3 signals in GM12878 cells (ENCODE) **c)** H3K27Ac signals in GM12878 cells (ENCODE). Black boxes show the H3K27me3 domain encompassing the entire *ACOXL* gene, the *BCL2L11* promoter, and enhancers 1-3 and the domains that encompass enhancers 4,5 and 6. (Wood et al., 2016)

the loss of EZH2 activity, EBV-negative BL31 cells and wild-type EBV-infected BL31 (wt BAC2) cells were treated with EZH1/2 inhibitor UNC1999. We found that in EBV-infected BL31 cells, *BCL2L11* mRNA expression increased 3.6 and 5.4-fold after 8 h and 18 h of UNC1999 treatment. This is consistent with the reversal of PRC2-mediated gene repression. In contrast, treatment of EBV-negative BL31 cells with UNC1999 resulted in only small increases (1.8 and 2.7 fold) in *BCL2L11* mRNA expression after 8 h and 18 h respectively (Figure 5.6a and b). To assess the effect of increased expression of *BCL2L11* on apoptosis, Caspase 3/7 activity was measured after UNC1999 treatment. Treatment of EBV-infected with UNC1999 cells led to large increases in Caspase 3/7 activity, whereas Caspase 3/7 activity in EBV-negative BL31 was low and only increased slightly after UNC1999 treatment, consistent with the small increase in *BCL2L11* expression (Figure 5.6c and d). Together, these two experiments show that PRC-mediated silencing of *BCL2L11* by EBNA3A and EBNA3C could be reversed by EZH1/2 inhibition and resulted in the induction of apoptosis. 3C analysis of the *BCL2L11* locus on the UNC1999 treated EBV-infected BL31 cells by Dr Wood showed that inhibition of EZH1/2 activity led to increased interactions between the *BCL2L11* promoter and all enhancers, and the *ACOXL* promoter (Figure 5.7), indicating that EZH1/2 activity is required for inactivation of the *BCL2L11* enhancer hub and *BCL2L11* silencing in EBV-infected cells (Wood et al., 2016).

5.6 Conclusion

Overall, this chapter has demonstrated that the difference between the *MYC* promoter interactions in the EBV infected and CD40L/IL-4 stimulated naïve B-cells suggests that

EBV and CD40 effects on MYC occur through different mechanisms leading to distinct patterns of chromatin reconfiguration. We have also shown that EBV manipulates *MYC* enhancers function in a distinct manner to drive tumorigenesis by inducing directional BRG1 dependent reorganisation of long range enhancer-promoter interactions. We demonstrated that EBV-mediated repression of tumour suppressor *BCL2L11* can be reversed through PRC2 methyltransferase EZH2 inhibition. Together these data show that EBV is able to manipulate *MYC* and *BCL2L11* expression to provide a survival advantage for EBV infected B cells.

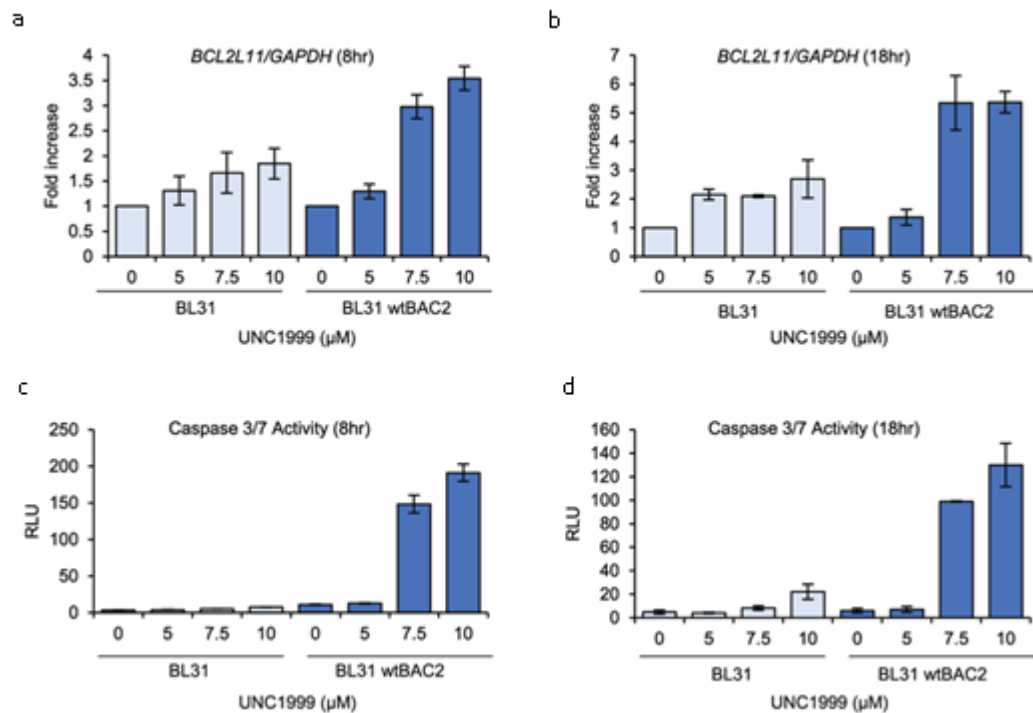


Figure 5.6 EZH1/2 activity is required for EBV mediated silencing of BCL2L11. **a)** QPCR analysis of BCL2L11 mRNA expression in EBV-negative BL31 cells or BL31 cells infected with wild-type recombinant EBV (BL31 wtBAC2) treated with the EZH1/2 inhibitor UNC1999 for 8 h. Signals were normalised to GAPDH mRNA levels and expressed as fold increase relative to untreated cells. Results show the mean \pm standard deviation of duplicate QPCR experiments. **b)** QPCR analysis of BCL2L11 mRNA expression in EBV-negative BL31 cells or BL31 cells infected with wild-type recombinant EBV (BL31 wtBAC2) treated with the EZH1/2 inhibitor UNC1999 for 18 h. Signals were normalised to GAPDH mRNA levels and expressed as fold increase relative to untreated cells. Results show the mean \pm standard deviation of duplicate QPCR experiments. **c)** Caspase 3/7 activity in BL31 or BL31 wtBAC2 cells treated with UNC1999 for 8 h. Caspase signals are shown corrected for the number of live cells. **d)** Caspase 3/7 activity in BL31 or BL31 wtBAC2 cells treated with UNC1999 for 18 h. Caspase signals are shown corrected for the number of live cells. (Wood et al., 2016)

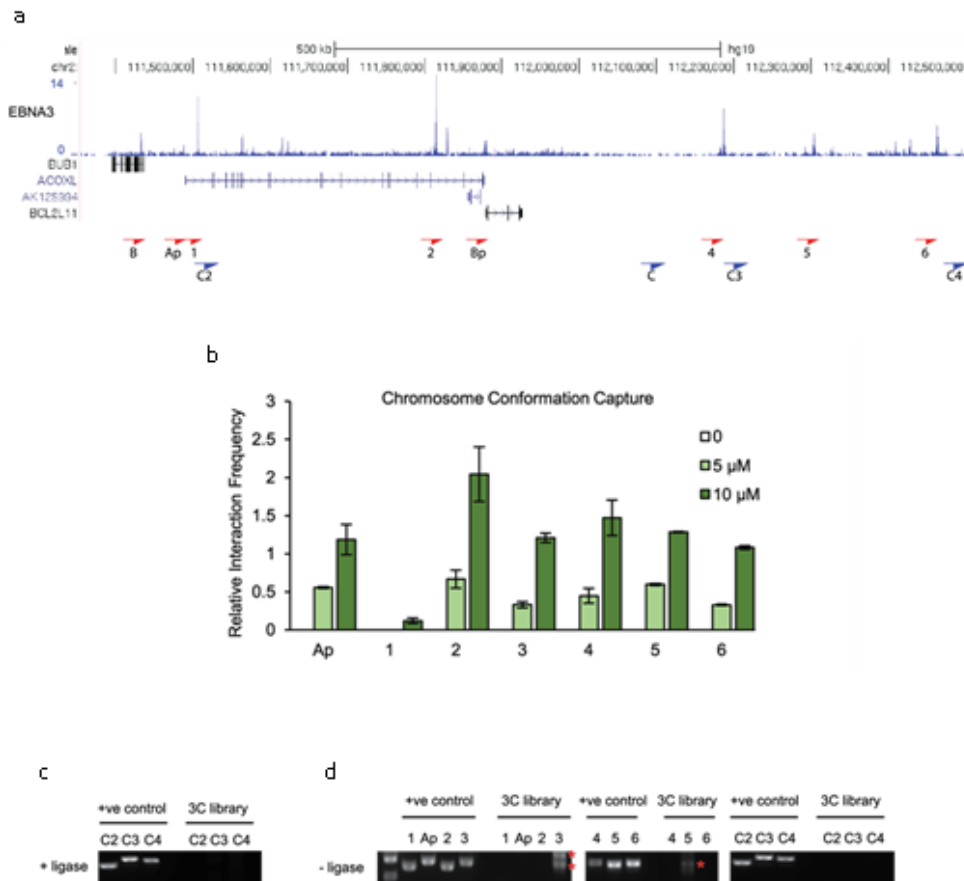


Figure 5.7 EZH1/2 activity is required for disruption of the BCL2L11 and ACOXL enhancer hub. a) EBNA3 binding at the *BCL2L11* locus as in figure 3.6 showing the locations of the primers used for 3C analysis. Red arrows indicate the position of the 1-6 enhancer primers used for promoter interaction analysis. Primer design is unidirectional (Naumova et al., 2012). A control region (C) not bound by EBNA3s was included in the analysis. **b)** Chromosome conformation capture (3C) analysis of the *BCL2L11* promoter interactions between enhancers 1-6 and the ACOXL promoter in BL31 wtBAC2 cells treated with UNC1999 for 24 h **c)** 3C analysis in BL31 cells to examine *BCL2L11* promoter interactions with additional intervening control regions where there is no EBNA3A or EBNA3C binding (C2, C3, C4). Positive controls show amplification of a digested and ligated genomic PCR fragment library containing all ligation junctions. **d)** Control 3C analysis using BL31 cell chromatin that was digested but incubated in the absence of ligase (-ligase). Analysis was performed using primers to detect enhancer-promoter and promoter-promoter interactions as described above and using the additional control primers. Red asterisks indicate the position of non-specific PCR products of the incorrect sizes (verified by sequencing) (Wood et al, 2016)

6. Discussion

Epstein-Barr virus preferentially infects B lymphocytes and is associated with the development of Burkitt's, Hodgkin's and post-transplant lymphoma. The EBV transcription factors, EBNA2, 3A, 3B and 3C drive immortalisation through the epigenetic reprogramming of cellular genes. Pathway analysis showed that the B-cell receptor (BCR) signalling pathway was significantly enriched for EBNA-bound genes, implicating EBNA in its regulation. Deregulation of the B-cell receptor signalling pathway affects cell growth and survival. We have identified EBNA binding sites at promoter-proximal elements near the BCR genes *CD79A* and *CD79B*. We have also identified significant EBNA binding site close to downstream effectors of the BCR signalling pathway, *NFATC1*, *NFATC2* and *PLCγ2*. In this study, we explored the transcriptional repression of the BCR signalling pathway components by EBNA2 and EBNA3 and its functional implications.

We also investigated EBNA2 activation of oncogene *MYC* and EBNA3A and EBNA3C silencing of the pro-apoptotic gene *BCL2L11*; both key genes involved in growth regulation and lymphoma development.

6.1 Deregulation of the BCR signalling pathway by the EBNA2 and EBNA3 proteins

The BCR plays an essential role in B cell development and function (Geisberger et al., 2006, Reth, 1992). The BCR comprises of the ligand binding subunit, IgM, and two signal transducing subunits, Igα and Igβ (also known as *CD79A* and *CD79B*). *CD79A* and

CD79B are expressed in virtually all immature and mature B cells, as both proteins are required for BCR surface expression and B cell activation (Clark et al., 1992). Activation of the BCR through antigen binding results in signal transduction through various signalling pathways including the Ca^{2+} signalling pathway leading to activation of the NFAT family of transcription factors.

Previous ChIP-seq studies carried out in our laboratory had identified promoter-proximal EBNA2 binding sites at *CD79A* and *CD79B*, implicating EBNA2 in their regulation. Published microarray studies have also shown *CD79A* and *CD79B* to be regulated by EBNA2. In this study we confirmed that EBNA2 was a negative regulator of *CD79A* and *CD79B* in both LCL and lymphoma cell backgrounds and we also showed reduced *CD79A* and *CD79B* protein levels in response to EBNA2 activation in LCLs. The chromatin landscape surrounding the promoter proximal EBNA2 binding sites at *CD79A* and *CD79B* corresponded with regions of H3K27Ac in an LCL indicating that the EBNA2 bound promoter regions were still active in cells that express EBNA2. A genome-wide study by Portal et al. (2013) revealed that EBNA2 frequently co-localises with RBPJk (a known EBNA2 binding partner), and EBF-1 at enhancer and super-enhancer regions. A recent study has also shown that EBNA2 is still recruited to chromatin in RBPJk deficient B cells and found that RBPJk independent EBNA2 peaks are enriched for EBF-1 binding in LCLs (Glaser et al., 2017).

The co-localisation of EBF-1 with EBNA2 is interesting, because EBF-1 is a known activator of *CD79A* and *CD79B* and its activity is essential for driving B cell specification, lineage commitment and formation of the pre-BCR and Ig rearrangement (Gao et al., 2009, Hagman, 2015). EBF-1 regulates gene expression in co-operation with other DNA

binding proteins such as E2A, PAX5 and Runx1 (Hagman, 2015). Binding site analysis of the *CD79A* and *CD79B* promoter-proximal EBNA2 bound chromatin regions revealed overlapping binding sites for EBF-1 and RBPJ κ , although the EBF-1 binding sites were a better match than the RBPJ κ sites (Figure 3.4 and 3.5). This led us to hypothesise that *CD79A* and *CD79B* repression may be a result of competitive binding between EBNA2, EBF-1 and RBPJ κ , where EBNA2 replaces EBF-1 at the gene promoter resulting in a reduced ability of EBF-1 to activate transcription.

To test this hypothesis we carried out a panel of competition based luciferase reporter assays. When we transfected luciferase reporter constructs that contained the EBNA2 bound-promoter and enhancer regions of *CD79A*, or the EBNA2-bound promoter region of *CD79B*, into EBV-negative DG75 cells and DG75-RBPJ κ -KO cells we found that EBNA2 alone was able to activate the *CD79A* and *CD79B* promoters, independent of RBPJ κ . This is interesting as we do not see activation of *CD79A* and *CD79B* after EBNA2 activation *in vivo* (Figure 3.6a&b). It is likely that there are other factors present at the *CD79A* and *CD79B* gene loci that prevent EBNA2 mediated activation of these genes *in vivo*. The co-expression of EBNA2 and EBF-1 led to a decrease in activation of the *CD79B* promoter by EBF-1, but had no effect on activation of the *CD79A* promoter, both again independent of RBPJ κ .

It is interesting that the regulation of *CD79B* in the presence of EBNA2 is independent of RBPJ κ , because gene regulation by EBNA2 is often in co-operation with RBPJ κ . However, here EBNA2 is not acting with its usual binding partner and repression must be occurring through an RBPJ κ independent mechanism (Figure 6.1). Interestingly, work by the Kempkes laboratory found that RBPJ κ independent EBNA2 repressed

genes are enriched for genes involved in B cell signalling. Consistent with our own work, they identified *CD79B* as an RBPJK independent EBNA2 repressed gene (Glaser et al., 2017). They also found EBNA2 and EBF-1 are able to bind *in vitro* (Glaser et al., 2017). Based on our data, and the possibility that EBF-1 can act as an EBNA2 binding partner we hypothesised that rather than compete, EBNA2 binds EBF-1 and hinders its ability to activate transcription of *CD79B* (Figure 6.1).

We were not able to confirm *CD79A* repression by EBNA2 alone. However a limitation of luciferase assays is that the luciferase reporter construct does not necessarily represent the true control element of the gene, as it has been taken out of its usual chromatin context. We therefore cannot categorically state that *CD79A* is not regulated by EBNA2. Another factor to consider is that our luciferase assays were carried out in EBV-negative lymphoma cells in order to investigate the role of EBNA2 specifically, but other EBV proteins have been implicated in the repression of *CD79A*. For example, induction of LMP1 results in the repression of *CD79A*, although the mechanism of this repression remains unknown (Vockerodt et al., 2008). Also, regulation of *CD79A* by EBF-1 has been well characterised and its expression in B cells by EBF-1 relies on the presence of Runx1 (Maier et al., 2004). The EBV-negative DG75 cells used in our luciferase assay express Runx1 (Spender et al., 2005), it is possible that EBF-1 and Runx1 are driving *CD79A* promoter activation. Interestingly, *in vivo* we see robust 10-fold repression of *CD79A* in LCLs where Runx1 is not expressed, but in lymphoma cell lines (BJAB and BL41), where Runx1 is expressed (Schlick et al., 2011, Spender et al., 2005), we do not see robust repression in BJAB cells and we see no repression at all in BL41 cells. It would be interesting to see if overexpression of RUNX1 in LCLs could relieve *CD79A* repression.

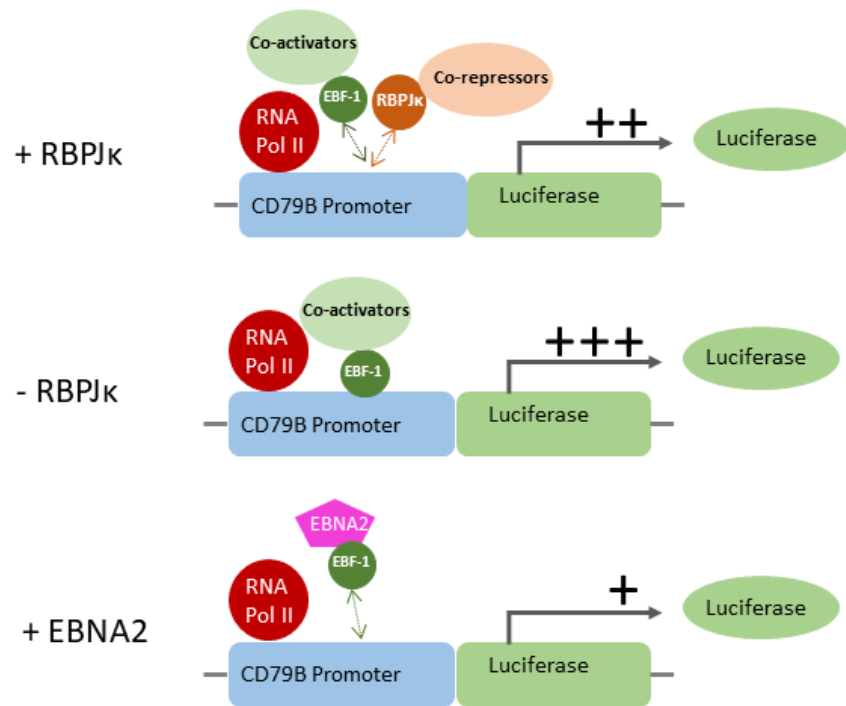


Figure 6.1. Model of suggested mechanism of EBNA2 induced, RBPJk independent, repression of *CD79B* expression. a) RBPJk and EBF-1 compete to bind overlapping binding sites. RBPJk represses *CD79B* transcription. b) Loss of RBPJk relieves repression and increases *CD79B* transcription. c) EBNA2 binds EBF-1 and destabilises EBF-1 binding interfering with activation (RBPJk independent).

Having established that *CD79B* mRNA expression was repressed in response to EBNA2 activation in LCLs and lymphoma cells and that EBNA2 hinders EBF-1 mediated activation of *CD79B* promoter constructs in luciferase reporter assays, we further explored the interplay between EBF-1 and EBNA2 at the *CD79B* promoter *in vivo*. To do this we set up a ChIP-QPCR assay to observe EBF-1 and EBNA2 binding over a 24hr time course of EBNA2 induction in EREB2.5 cells. We found that EBNA2 and EBF-1 are bound at the *CD79B* promoter at the same time and their binding patterns follow similar kinetics. We also found that H3Ac levels fell after EBNA2 activation and did not recover. *CD79B* mRNA transcript levels also remained repressed. We have shown that EBNA2 could be interfering with EBF-1 mediated transcriptional activation of *CD79B*. The role of EBF-1 as a pioneer transcription factor is to open up the chromatin to allow the deposition of active chromatin markers (Mayran and Drouin, 2018). We propose a model where interference from EBNA2 could disrupt the ability of EBF-1 to promote histone acetylation and leave the promoter vulnerable to histone deacetylases leading to reduced gene activation at the *CD79B* promoter (Figure 6.2).

Normal BCR activation leads to an influx of Ca^{2+} ions, from intra and extra cellular sources, and a sustained increase in cytoplasmic calcium levels resulting in activation of the NFAT family of transcription factors via the Ca^{2+} signalling pathway. To determine if EBNA2 was able to functionally regulate Ca^{2+} signalling through the BCR *in vivo*, we transiently transfected EBV-negative BL cells expressing a conditionally active ER-EBNA2 fusion protein, with a plasmid containing three NFAT binding sites located upstream of a luciferase reporter. This plasmid can be used to assay signal

transduction through Ca^{2+} , Calcineurin, and NFAT activity (Clipstone and Crabtree, 1992). We crosslinked the BCR using anti-IgM to stimulate BCR signalling and we found that signal transduction in IgM treated cells expressing active EBNA2 was reduced to background levels similar to unstimulated cells. Our results demonstrate that EBNA2 has a measurable impact on BCR signalling leading to reduced NFAT activity. In literature, reduced NFAT activity has been shown to potentially result in deregulation of cell cycle progression, apoptosis, growth and proliferation (Mognol et al., 2016).

To further investigate the involvement of EBV in deregulation of downstream BCR signalling genes we selected potential EBNA regulatory targets *NFATC1*, *NFATC2* and *PLC γ 2* for further study. *NFATC1* and *NFATC2* have been identified as EBNA3B and EBNA3C regulatory targets by existing published microarrays (White et al., 2010) and by a gene expression study carried out in our laboratory in a BL31 cells background. We confirmed mRNA repression of *NFATC1* and *NFATC2* by EBNA3C in a BL cell background and using Western blot analysis we showed that *NFATC1* and *NFATC2* are also repressed at the protein level by both EBNA3B and EBNA3C.

ChIP-seq data from our laboratory obtained from Mutu III cells showed multiple EBNA3 binding peaks at the *NFATC1* and *NFATC2* locus, all correlating with high levels of H3K27Ac, indicative of an active regulatory region, and an absence of H3K27Me3 in GM12878 cells (ENCODE, 2012). The lack of H3K27Me3 could rule out EBNA3 mediated repression by PRC2/EZH as a regulatory mechanism. However, we were unable to confirm any significant binding of EBNA3B and EBNA3C within the active regulatory regions of *NFATC1* and *NFATC2* in BL cells. A subsequent ChIP-seq experiment carried out by our lab using GM12878 cells also did not show enrichment for EBNA3B or EBNA3C at the

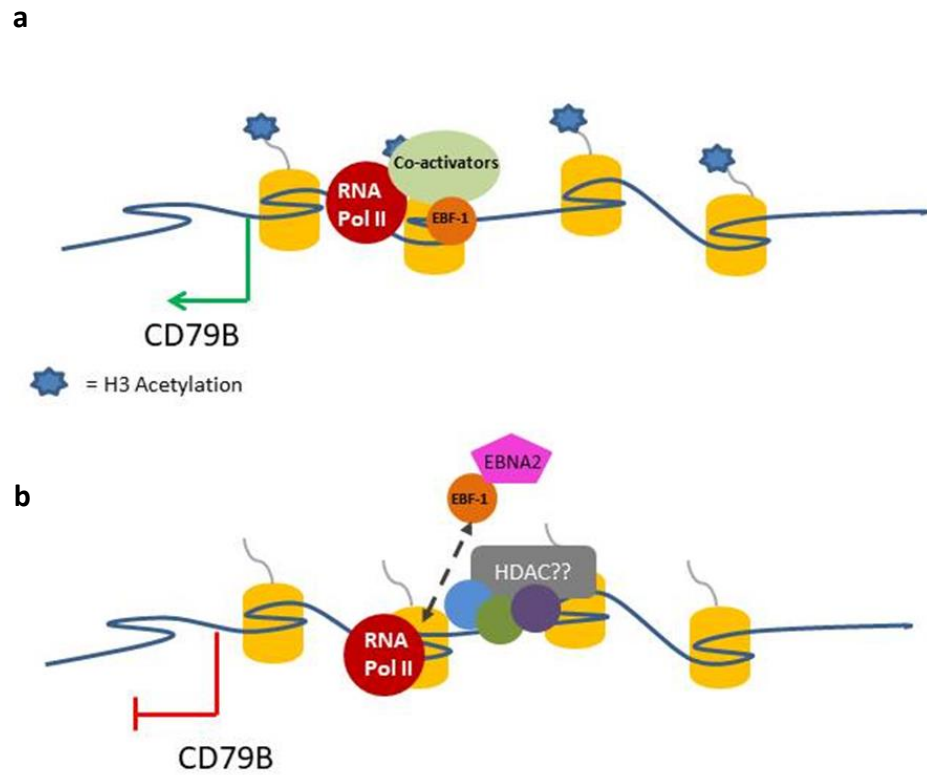


Figure 6.2. Proposed model for EBNA2 inference with the ability of EBF-1 to activate transcription. a) High levels of H3Ac and EBF-1 binding along with other co-activators results in active transcription. **b)** EBNA2 binds to EBF-1 and destabilises EBF-1 binding to the promoter interfering with activation. Histone deacetylases may bind and silence the promoter resulting in repression of transcription.

NFATC1 and *NFATC2* locus. While we have clear evidence that *NFATC1* and *NFATC2* are repressed both at the mRNA and the protein levels by EBNA3 proteins, we have not been able to confirm EBNA3 binding at all sites, even in cell lines where mRNA regulation is apparent. This suggests that EBNA3 proteins may not be directly involved in the regulation of *NFATC1* and *NFATC2*. This also shows it is important to confirm ChIP-seq data, as this technique is sensitive and may result in false positive peak calls.

NFATC1 had also been identified as an EBNA2 target and a published microarray study has shown it to be repressed by EBNA2 in a lymphoma cell background (Maier et al., 2006). We confirmed *NFATC1* was repressed by EBNA2 in an LCL cell background, however we were not able to prove repression by EBNA2 in a lymphoma cell background. The key difference between the LCL (ERE2.5) and the lymphoma cell lines, BL41K3 and BJABk3, is that while they all express conditionally active EBNA2, the ERE2.5 cells are EBV-positive and express the full latency III panel of EBV genes, whereas the BL cells are EBV negative and the only express EBNA2. It is therefore possible that the cell type specific repression we observed is because EBNA2 alone is not sufficient to significantly repress *NFATC1*. Western blot analysis of *NFATC1* protein levels in ERE2.5 cells revealed that protein levels did not fall after EBNA2 activation and therefore did not correlate with mRNA levels. In fact, an additional protein band appeared (approx. 75kDa) 24 h post EBNA2 activation. It is possible this band represents a truncated isoform, *NFATC1* α A, with a mass of approximately 77kDa (Consortium, 2018). *NFATC1* α A expression is induced in proliferating B cells to protect them from apoptosis (Serfling et al., 2012). The primers used for our mRNA analysis did not detect all *NFATC1* isoforms. In particular they could not detect *NFATC1* α A, whereas the antibody used to detect *NFATC1* protein could detect all known isoforms.

It is possible the discrepancy between our NFATC1 mRNA and protein analysis was because NFATC1 α A transcripts were missed. This would mean EBNA2 may not be a regulator of *NFATC1*. Our protein and mRNA analysis of *NFATC2* confirmed it was not robustly regulated by EBNA2 in LCLs or lymphoma cell lines.

ChIP-seq analysis carried out by our laboratory in MutuIII cells had identified significant EBNA2 binding peaks at the *NFATC1* gene locus that correlated with highly acetylated regions indicative of active regulatory sites, or enhancers. We used ChIP-QPCR in EREB2.5 cells to further investigate the role of EBNA2 in the repression of *NFATC1*. However, we did not observe any significant binding of EBNA2 within the active regulatory regions of *NFATC1* and can therefore not implicate EBNA2 in the direct regulation of *NFATC1*.

When we investigated *PLC γ 2*, an upstream signalling component of the Ca²⁺ signalling pathway we confirmed that it was repressed by EBNA2 in a BJAB cells, and we also confirmed the EBNA2 binding peak in MutuIII cells using ChIP-QPCR. However, mRNA analysis of *PLC γ 2* in LCL and BL cells did not show significant regulation by EBNA2 and we did not observe EBNA2 binding in EREB2.5 cells using ChIP-QPCR. Together, these data suggest *PLC γ 2* regulation by EBNA2 is cell line specific and we cannot implicate EBNA2 in its regulation.

6.2 Survival implications for EBV.

EBV manipulates various aspects of B cell activation, such as the BCR signalling pathway, to induce cell proliferation, differentiation and drive EBV-infected B cells through GC reactions to become latently infected memory B cells (Thorley-Lawson,

2015, Roughan and Thorley-Lawson, 2009). We have shown that EBNA2 is responsible for the repression of BCR component *CD79B*. We implicated EBF-1 as a partner in EBNA2 mediated repression and proposed a mechanism where EBNA2 disrupts the ability of EBF-1 to promote histone acetylation and activation at the *CD79B* promoter. We also showed that activation of EBNA2 leads to reduced signal transduction along the calcium signalling pathway. EBV is already known to exploit BCR signalling through its membrane protein LMP2A, which functions as a constitutively active BCR. The ability of LMP2A to mimic the BCR in cells lacking functional BCR allows EBV to promote cell survival (Mancao and Hammerschmidt, 2007), or it can block active BCR signalling, by blocking calcium mobilisation in favour of its own signalling outcomes (Miller et al., 1993). Here, we have shown that EBNA2 is also capable of repressing of BCR signal propagation and calcium mobilisation in BL cells, which may contribute to EBV regulation of B cell growth and survival. In EBV infected B cells, activation of the BCR can trigger plasma cell differentiation leading to a switch from latency to lytic replication (Thorley-Lawson, 2015). By suppressing activated BCR signal transduction EBNA2 could be protecting latent cells from aberrant reactivation.

There is relatively little known about factors that directly regulate NFAT expression. There is some evidence that there is an element of self-regulation by the NFAT family and of AP-1/NFAT co-operation to regulate NFAT transcription (Zhou et al., 2002). There is no evidence of known EBNA2 or EBNA3 DNA binding partners RBPJk or PU.1 binding at active regulatory regions along the *NFATC1* or *NFATC2* gene locus (ENCODE, 2012). Although, we have evidence of robust down regulation of *NFATC1* and *NFATC2* in response to the EBNA3 proteins, we do not have significant evidence of direct regulation. Given the element of self-regulation by the NFATs, it is possible that

modulation by upstream tyrosine kinases LYN and SYK by the EBNA3 proteins (Khasnis, 2018) might lead to a fall in NFAT activation and transcription. We only see consistent NFAT regulation by EBNA3B and EBNA3C in BL cells and not in LCLs. This could be because in Burkitt's lymphoma cell lines various signalling pathways are distorted during outgrowth, in particular the constitutive activation of MYC as a result of translocation, whereas LCLs are established through EBV-infection of resting B cells *in vitro* and provide more physiological relevance to EBV-infected B cells. Nevertheless, we have observed robust repression of *NFATC1* and *NFATC2* by the EBNA3 proteins in EBV-positive BL cells and this repression of NFAT activity could still provide EBV with a survival advantage through regulation of growth control and cell cycle progression. As outlined in section 1.2.3, *NFATC1* and *NFATC2* differentially regulate the cell cycle; *NFATC1* activates genes involved in cell cycle progression, such as cyclin A2, whereas *NFATC2* acts as an inhibitor of cyclin A2 (Carvalho et al., 2007, Karpurapu et al., 2008). Oncogene *NFATC1* has also been implicated in the upregulation of anti-apoptotic genes and tumour suppressor *NFATC2* is involved in the upregulation of pro-apoptotic genes (Mognol et al., 2016). The indirect repression of *NFATC1* and *NFATC2* by EBNA proteins may be a strategy used by EBV to balance out the expression of oncogenes and tumour suppressor genes to drive cell survival by manipulating survival pathways, complementing the activities of LMP2A.

6.3 Regulation of cellular genes by EBNA2 and EBNA3 proteins through reorganisation of long distance enhancer-promoter interactions.

Our laboratory showed that EBNA2 induced large-scale directional chromatin restructuring of the 3 Mb *MYC* locus in LCLs (Wood et al., 2016). In my work I examined whether activation of naïve B cell via EBV infection, or 'normal' CD40 ligand activation also resulted in such large scale chromatin restructuring and we explored the mechanisms of *MYC* activation by EBNA2 and *BCL2L11* silencing by EBNA3.

To study the *MYC* chromatin reorganisation upon EBV infection we used uninfected, EBV-infected and CD40L/IL-4 stimulated resting B cells. These samples provided us with a comparison between physiological and EBV mediated B cell activation. In a normal immune response T cells will activate CD40 signal transduction in B cells using its CD40 ligand located on the cell surface. Activation of the CD40 receptor leads to activation of different signalling pathways including NF- κ B, MAPK, PI3K-AKT to protect GC B cells from apoptosis and drive proliferation (Aggarwal, 2004). Studies have shown that CD40-mediated activation of the NF- κ B signalling pathway is strictly controlled and is only active in pre- and post- GC B cells (Basso et al., 2004). In contrast, in EBV infected cells the NF- κ B signalling pathway is activated by viral EBV membrane protein LMP1, which mimics the CD40 receptor by acting as a constitutively active CD40 leading to aberrant activation of NF- κ B signalling resulting in activation target genes, such as *MYC* and *Bcl2*, resulting in uncontrolled proliferation and evasion of apoptosis (Kieser and Sterz, 2015).

We found that *MYC* was upregulated in response to EBV infection after 24 h and remained upregulated for at least 7 days post infection, whereas *MYC* was not

upregulated in CD40L stimulated B cells after 24 h. In fact, *MYC* expression levels were the same in uninfected resting B cells and CD40L/IL-4 stimulated B cells. These findings are consistent with the fact that CD40 ligand activation leads to short-term proliferation and EBV infected B cells grow out into immortal cell lines. This low *MYC* expression in response to CD40 receptor activation is also consistent with *MYC* expression in centroblasts undergoing the GC reaction after antigen binding, where studies by Klein et al (2003) found *MYC* to be actively repressed.

Our 4C-Seq experiment found that EBV infection of resting B cells induced similar directional changes in enhancer-promoter interactions across the *MYC* locus as seen in EBV-infected cell lines with a reduction in downstream interactions and an increase in upstream interactions. In contrast, 'normal' stimulation of B cells led to an increase in downstream enhancer-promoter interactions and a decrease in upstream enhancer-promoter interactions. These data together suggest that remodelling of *MYC* promoter-enhancer interactions is highly specific depending on the stimuli it is exposed to. One of the downstream regions where we found increased enhancer-promoter interactions in CD40 ligand activated B cells and a decrease in interaction in EBV-infected B cells compared to uninfected was the +450 kb region. This region is bound by EBNA2 and ChIP-seq data from ENCODE shows it contains two CTCF binding sites. Interactions between CTCF sites can form chromatin loops that could either prevent long-range enhancer-promoter interactions by isolating them on separate loops, or bring enhancers and promoters in closer proximity to each other. Our laboratory has previously shown that EBNA2 promotes CTCF interactions at the *MYC* -556 SE by looping out a specific region from the enhancer-promoter hub (Wood et al., 2016). It is possible that EBNA2 promotes similar CTCF interactions at the +450 region

excluding it from interacting with the *MYC* promoter. However, further investigation would be needed to confirm such interactions. A targeted 3C approach could be used to compare interactions between the two CTCF site in the presence and absence of EBNA2.

EBNA2 is essential for B cell immortalisation and the continuous growth of EBV-infected B cells (Cohen et al., 1989, Kempkes et al., 1995b). The upregulation of *MYC* by EBNA2 is key to driving B cell proliferation after initial infection and promoting immortalisation (Kaiser et al., 1999). Our data shows that EBV manipulates *MYC* enhancer-promoter interactions to drive lymphomagenesis. We have shown that EBV infection induces directional re-organisation of enhancer-promoter interactions over 3 Mbs, with increased upstream and decreased downstream enhancer-promoter interactions. The resulting *MYC* enhancer interaction landscape in EBV-infected cells is distinct from leukemia cells, where downstream enhancers predominantly control *MYC* activation (Shi et al., 2013). Our data therefore shows that *MYC* activation in EBV-infected B cells occurs through a mechanism distinct from other B cell lymphomas.

Our investigation of the mechanism of *MYC* activation by EBNA2 demonstrated that EBNA2 mediated *MYC* activation through upstream enhancer interactions was dependent on the recruitment of SWI/SNF subunit BRG1. This is consistent with previous studies that have shown that EBNA2 is able to interact with BRG1 through the Snf5 subunit of SWI/SNF, and that BRG1 is required for interaction of the +1.8/1.9 Mb *MYC* enhancer with the *MYC* promoter in AML cells (Wu et al., 1996, Shi et al., 2013). In AML cells, BRG1 knock-down resulted in decreased downstream and increased upstream enhancer-promoter interactions, indicative of directionality in the effects of

BRG1 on enhancer looping. We found that, in EBV-infected cells, BRG1 is required to maintain upstream enhancer-promoter interactions. Therefore, our data are consistent with a model where BRG1-dependent chromatin remodelling is required for MYC enhancer-promoter interactions. Together, these data show that EBV manipulates *MYC* enhancer function in a distinct manner by inducing directional BRG1 dependent reorganisation of long range enhancer-promoter interactions.

Another strategy employed by EBV to avoid apoptosis and promote survival is the repression of *BCL2L11* (Thorley-Lawson and Allday, 2008). Deregulation of *BCL2L11* has been implicated in tumourigenesis of multiple B cell malignancies. For example, inactivation of a single *BCL2L11* allele in E μ -*MYC* transgenic mice accelerated *MYC*-induced lymphoma development, suggesting *BCL2L11* acts as a tumour suppressor (Egle et al., 2004). Further evidence of the tumour suppressing role of *BCL2L11* is its deletion in 40% of mantle cell lymphomas, its silencing in natural killer cell lymphomas through CpG methylation, and the fact that it is targeted by oncogenic miRNAs, miR-32 and miR-17-92 (Katz et al., 2014, Tagawa et al., 2005, Küçük et al., 2015, Ambs et al., 2008, Ventura et al., 2008). We were the first to show that *BCL2L11* is controlled through a long-range enhancer-promoter interaction and that inactivation of this enhancer-promoter hub by EBNA3A and EBNA3C leads to the recruitment of PRC2 methyltransferase EZH2 resulting in *BCL2L11* repression (Wood et al., 2016). While no direct contact between PRC1 and PRC2 complexes and EBNA3A and EBNA3C has been reported, PRC-dependent and H3K27Me3-associated gene silencing by EBNA3A and EBNA3C has been demonstrated (Skalska et al., 2010, McClellan et al., 2012, McClellan et al., 2013, Harth-Hertle et al., 2013, Kalchschmidt et al., 2016). While, the exact mechanism of PCR recruitment and repression by EBNA3A and EBNA3C remains

unclear, time-course studies have shown that activating marks from promoters and enhancers of genes repressed by EBNA3A and EBNA3C are lost prior to the binding of PRCs and the deposition of H3K27me3 (Harth-Hertle et al., 2013, Kalchschmidt et al., 2016). Therefore, PRC recruitment and H3K27Me3 deposition may be a consequence of a repressive event. This model of PRC recruitment is consistent with a recent discovery that conclusively showed knock-down of PRC2 subunit SUZ12 had no effect on EBNA3C mediated repression (Paschos et al., 2019). However, PRC2 may still be important for EBNA3A-mediated regulation. We have shown in this study, that EBV-induced repression of *BCL2L11* can be reversed through inhibition of the PRC2 methyltransferase EZH2. The inhibition of EZH2 catalytic activity is emerging as a therapeutic approach to treating cancers, with selective EZH2 inhibitor tazemetostat currently undergoing phase I clinical trials (Lue and Amengual, 2018). The reversal of *BCL2L11* repression by EZH2 inhibition in EBV-infected cells provides a therapeutic rationale for the use of selective EZH2 inhibitors as a treatment for EBV-positive lymphomas.

6.4 Future work

- 1) Examination of the EBNA2-EBF-1 mediated repression of *CD79B* to further elucidate the regulatory mechanism.
- 2) Further investigation of EBNA2 mediated reduction in Ca^{2+} in response to BCR stimulation.
- 3) Investigation of the role of Runx1 on *CD79A* expression in EBV-infected cells.
- 4) Further examination of the indirect regulation of *NFATC1* and *NFATC2* by EBNA3 proteins by investigating the impact EBNA3-mediated modulation of upstream BCR components *LYN* and *SYK* on *NFATC1* and *NFATC2* expression.
- 5) Further investigation of the possibility that EBNA2 promotes CTCF interactions at the +450 region excluding it from interacting with the *MYC* promoter through loop formation. A targeted 3C approach could be used to compare interactions between the two CTCF sites in the presence and absence of EBNA2.

7. Bibliography

- ADAMS, A. & LINDAHL, T. 1975. Epstein-Barr virus genomes with properties of circular DNA molecules in carrier cells. *Proceedings of the National Academy of Sciences of the United States of America*, 72, 1477-1481.
- AGGARWAL, B. B. 2004. Nuclear factor- κ B: The enemy within. *Cancer Cell*, 6, 203-208.
- ALLAN, G. J., INMAN, G., PARKER, B. D., ROWE, D. T. & FARRELL, P. J. 1992. *Cell growth effects of Epstein-Barr virus leader protein*.
- ALLDAY, M. J., BAZOT, Q. & WHITE, R. E. 2015. The EBNA3 Family: Two Oncoproteins and a Tumour Suppressor that Are Central to the Biology of EBV in B Cells. *Curr Top Microbiol Immunol*, 391, 61-117.
- ALLEN, B. L. & TAATJES, D. J. 2015. The Mediator complex: a central integrator of transcription. *Nat Rev Mol Cell Biol*, 16, 155-66.
- ALLFREY, V. G., FAULKNER, R. & MIRSKY, A. E. 1964. ACETYLATION AND METHYLATION OF HISTONES AND THEIR POSSIBLE ROLE IN THE REGULATION OF RNA SYNTHESIS. *Proc Natl Acad Sci U S A*, 51, 786-94.
- AMBS, S., PRUEITT, R. L., YI, M., HUDSON, R. S., HOWE, T. M., PETROCCA, F., WALLACE, T. A., LIU, C. G., VOLINIA, S., CALIN, G. A., YFANTIS, H. G., STEPHENS, R. M. & CROCE, C. M. 2008. Genomic profiling of microRNA and messenger RNA reveals deregulated microRNA expression in prostate cancer. *Cancer Res*, 68, 6162-70.
- ANDERTON, E., YEE, J., SMITH, P., CROOK, T., WHITE, R. E. & ALLDAY, M. J. 2008. Two Epstein-Barr virus (EBV) oncoproteins cooperate to repress expression of the proapoptotic tumour-suppressor Bim: clues to the pathogenesis of Burkitt's lymphoma. *Oncogene*, 27, 421-33.
- ANSARI, S. A., PAUL, E., SOMMER, S., LIELEG, C., HE, Q., DALY, A. Z., RODE, K. A., BARBER, W. T., ELLIS, L. C., LAPORTA, E., ORZECZOWSKI, A. M., TAYLOR, E., REEB, T., WONG, J., KORBER, P. & MORSE, R. H. 2014. Mediator, TATA-binding protein, and RNA polymerase II contribute to low histone occupancy at active gene promoters in yeast. *J Biol Chem*, 289, 14981-95.
- AVENDAÑO LÓPEZ, C. & MENENDEZ, J. C. 2008. DNA Intercalators and Topoisomerase Inhibitors.
- BABCOCK, G. J., DECKER, L. L., VOLK, M. & THORLEY-LAWSON, D. A. 1998. EBV persistence in memory B cells in vivo. *Immunity*, 9, 395-404.
- BAKSH, S., DECAPRIO, J. A. & BURAKOFF, S. J. 2000. Calcineurin regulation of the mammalian G0/G1 checkpoint element, cyclin dependent kinase 4. *Oncogene*, 19, 2820-7.
- BANERJI, J., OLSON, L. & SCHAFFNER, W. 1983. A lymphocyte-specific cellular enhancer is located downstream of the joining region in immunoglobulin heavy chain genes. *Cell*, 33, 729-40.
- BANERJI, J., RUSCONI, S. & SCHAFFNER, W. 1981. Expression of a beta-globin gene is enhanced by remote SV40 DNA sequences. *Cell*, 27, 299-308.
- BANNISTER, A. J. & KOUZARIDES, T. 2005. Reversing histone methylation. *Nature*, 436, 1103-6.
- BANNISTER, A. J. & KOUZARIDES, T. 2011. Regulation of chromatin by histone modifications. *Cell Res*, 21, 381-95.
- BASSO, K., KLEIN, U., NIU, H., STOLOVITZKY, G. A., TU, Y., CALIFANO, A., CATTORETTI, G. & DALLA-FAVERA, R. 2004. Tracking CD40 signaling during germinal center development. *Blood*, 104, 4088-96.
- BECKER, P. B. & HÖRZ, W. 2002. ATP-Dependent Nucleosome Remodeling. *Annual Review of Biochemistry*, 71, 247-273.
- BELL, A., SKINNER, J., KIRBY, H. & RICKINSON, A. 1998. Characterisation of regulatory sequences at the Epstein-Barr virus BamHI W promoter. *Virology*, 252, 149-61.

- BELL, A. C., WEST, A. G. & FELSENFELD, G. 1999. The protein CTCF is required for the enhancer blocking activity of vertebrate insulators. *Cell*, 98, 387-96.
- BEN-BASSAT, H., GOLDBLUM, N., MITRANI, S., GOLDBLUM, T., YOFFEY, J. M., COHEN, M. M., BENTWICH, Z., RAMOT, B., KLEIN, E. & KLEIN, G. 1977. Establishment in continuous culture of a new type of lymphocyte from a "Burkitt like" malignant lymphoma (line D.G.-75). *Int J Cancer*, 19, 27-33.
- BENATAR, T., CARSETTI, R., FURLONGER, C., KAMALIA, N., MAK, T. & PAIGE, C. J. 1996. Immunoglobulin-mediated signal transduction in B cells from CD45-deficient mice. *The Journal of Experimental Medicine*, 183, 329.
- BLAIR, R. H., GOODRICH, J. A. & KUGEL, J. F. 2012. Single-molecule fluorescence resonance energy transfer shows uniformity in TATA binding protein-induced DNA bending and heterogeneity in bending kinetics. *Biochemistry*, 51, 7444-55.
- BOERMA, E. G., SIEBERT, R., KLUIN, P. M. & BAUDIS, M. 2009. Translocations involving 8q24 in Burkitt lymphoma and other malignant lymphomas: a historical review of cytogenetics in the light of today's knowledge. *Leukemia*, 23, 225-34.
- BOLLER, S., RAMAMOORTHY, S., AKBAS, D., NECHANITZKY, R., BURGER, L., MURR, R., SCHUBELER, D. & GROSSCHEDL, R. 2016. Pioneering Activity of the C-Terminal Domain of EBF1 Shapes the Chromatin Landscape for B Cell Programming. *Immunity*, 44, 527-541.
- BORGHESI, L., AITES, J., NELSON, S., LEFTEROV, P., JAMES, P. & GERSTEIN, R. 2005. E47 is required for V(D)J recombinase activity in common lymphoid progenitors. *J Exp Med*, 202, 1669-77.
- BRAY, S. J. 2016. Notch signalling in context. *Nature Reviews Molecular Cell Biology*, 17, 722.
- CAHIR-MCFARLAND, E. D., CARTER, K., ROSENWALD, A., GILTANNE, J. M., HENRICKSON, S. E., STAUDT, L. M. & KIEFF, E. 2004. Role of NF- κ B in Cell Survival and Transcription of Latent Membrane Protein 1-Expressing or Epstein-Barr Virus Latency III-Infected Cells. *Journal of Virology*, 78, 4108-4119.
- CAPELLO, D., CERRI, M., MUTI, G., BERRA, E., ORESTE, P., DEAMBROGI, C., ROSSI, D., DOTTI, G., CONCONI, A., VIGANO, M., MAGRINI, U., IPPOLITI, G., MORRA, E., GLOGHINI, A., RAMBALDI, A., PAULLI, M., CARBONE, A. & GAIDANO, G. 2003. Molecular histogenesis of posttransplantation lymphoproliferative disorders. *Blood*, 102, 3775-85.
- CARVALHO, L. D. S., TEIXEIRA, L. K., CARROSSINI, N., CALDEIRA, A. T. N., ANSEL, K. M., RAO, A. & VIOLA, J. P. B. 2007. The NFAT1 Transcription Factor is a Repressor of Cyclin A2 Gene Expression. *Cell Cycle*, 6, 1789-1795.
- CHEN, A., DIVISCONTE, M., JIANG, X., QUINK, C. & WANG, F. 2005. Epstein-Barr virus with the latent infection nuclear antigen 3B completely deleted is still competent for B-cell growth transformation in vitro. *J Virol*, 79, 4506-9.
- CHEN, A., ZHAO, B., KIEFF, E., ASTER, J. C. & WANG, F. 2006. EBNA-3B- and EBNA-3C-regulated cellular genes in Epstein-Barr virus-immortalized lymphoblastoid cell lines. *J Virol*, 80, 10139-50.
- CLAPIER, C. R., IWASA, J., CAIRNS, B. R. & PETERSON, C. L. 2017. Mechanisms of action and regulation of ATP-dependent chromatin-remodelling complexes. *Nature Reviews Molecular Cell Biology*, 18, 407.
- CLARK, M. R., CAMPBELL, K. S., KAZLAUSKAS, A., JOHNSON, S. A., HERTZ, M., POTTER, T. A., PLEIMAN, C. & CAMBIER, J. C. 1992. The B cell antigen receptor complex: Association of Ig γ - and Ig β with distinct cytoplasmic effectors. *Science*, 258, 123-126.
- CLIPSTONE, N. A. & CRABTREE, G. R. 1992. Identification of calcineurin as a key signalling enzyme in T-lymphocyte activation. *Nature*, 357, 695-7.
- COHEN, J. I., WANG, F., MANNICK, J. & KIEFF, E. 1989. Epstein-Barr virus nuclear protein 2 is a key determinant of lymphocyte transformation. *Proc Natl Acad Sci U S A*, 86, 9558-62.
- CONSORTIUM, T. U. 2018. UniProt: a worldwide hub of protein knowledge. *Nucleic Acids Research*, 47, D506-D515.

- CORONA, D. F. & TAMKUN, J. W. 2004. Multiple roles for ISWI in transcription, chromosome organization and DNA replication. *Biochim Biophys Acta*, 1677, 113-9.
- CUTHBERT, G. L., DAUJAT, S., SNOWDEN, A. W., ERDJUMENT-BROMAGE, H., HAGIWARA, T., YAMADA, M., SCHNEIDER, R., GREGORY, P. D., TEMPST, P., BANNISTER, A. J. & KOUZARIDES, T. 2004. Histone deimination antagonizes arginine methylation. *Cell*, 118, 545-53.
- DABAN, J. R. 2000. Physical constraints in the condensation of eukaryotic chromosomes. Local concentration of DNA versus linear packing ratio in higher order chromatin structures. *Biochemistry*, 39, 3861-6.
- DAL PORTO, J. M., GAULD, S. B., MERRELL, K. T., MILLS, D., PUGH-BERNARD, A. E. & CAMBIER, J. 2004. B cell antigen receptor signaling 101. *Mol Immunol*, 41, 599-613.
- DANG, C. V., O'DONNELL, K. A., ZELLER, K. I., NGUYEN, T., OSTHUS, R. C. & LI, F. 2006. The c-Myc target gene network. *Semin Cancer Biol*, 16, 253-64.
- DEKOTER, R. P. & SINGH, H. 2000. Regulation of B Lymphocyte and Macrophage Development by Graded Expression of PU.1. *Science*, 288, 1439.
- DENSLOW, S. A. & WADE, P. A. 2007. The human Mi-2/NuRD complex and gene regulation. *Oncogene*, 26, 5433-8.
- DEVERGNE, O., HATZIVASSILIOU, E., IZUMI, K. M., KAYE, K. M., KLEIJNEN, M. F., KIEFF, E. & MOSIALOS, G. 1996. Association of TRAF1, TRAF2, and TRAF3 with an Epstein-Barr virus LMP1 domain important for B-lymphocyte transformation: role in NF-kappaB activation. *Mol Cell Biol*, 16, 7098-108.
- DIXON, J. R., SELVARAJ, S., YUE, F., KIM, A., LI, Y., SHEN, Y., HU, M., LIU, J. S. & REN, B. 2012. Topological domains in mammalian genomes identified by analysis of chromatin interactions. *Nature*, 485, 376.
- EGLE, A., HARRIS, A. W., BOUILLET, P. & CORY, S. 2004. Bim is a suppressor of Myc-induced mouse B cell leukemia. *Proceedings of the National Academy of Sciences of the United States of America*, 101, 6164.
- ELIOPOULOS, A. G., BLAKE, S. M., FLOETTMANN, J. E., ROWE, M. & YOUNG, L. S. 1999a. Epstein-Barr virus-encoded latent membrane protein 1 activates the JNK pathway through its extreme C terminus via a mechanism involving TRADD and TRAF2. *J Virol*, 73, 1023-35.
- ELIOPOULOS, A. G., GALLAGHER, N. J., BLAKE, S. M., DAWSON, C. W. & YOUNG, L. S. 1999b. Activation of the p38 mitogen-activated protein kinase pathway by Epstein-Barr virus-encoded latent membrane protein 1 coregulates interleukin-6 and interleukin-8 production. *J Biol Chem*, 274, 16085-96.
- ENCODE 2012. An integrated encyclopedia of DNA elements in the human genome. *Nature*, 489, 57-74.
- EPSTEIN, M. A., ACHONG, B. G. & BARR, Y. M. 1964. VIRUS PARTICLES IN CULTURED LYMPHOBLASTS FROM BURKITT'S LYMPHOMA. *Lancet*, 1, 702-3.
- FARRELL, P. J. 2019. Epstein-Barr Virus and Cancer. *Annu Rev Pathol*, 14, 29-53.
- FINGEROTH, J. D., WEIS, J. J., TEDDER, T. F., STROMINGER, J. L., BIRO, P. A. & FEARON, D. T. 1984. Epstein-Barr virus receptor of human B lymphocytes is the C3d receptor CR2. *Proc Natl Acad Sci U S A*, 81, 4510-4.
- FRAPPIER, L. 2012. Contributions of Epstein-Barr nuclear antigen 1 (EBNA1) to cell immortalization and survival. *Viruses*, 4, 1537-47.
- FRUEHLING, S. & LONGNECKER, R. 1997. The immunoreceptor tyrosine-based activation motif of Epstein-Barr virus LMP2A is essential for blocking BCR-mediated signal transduction. *Virology*, 235, 241-51.
- FU, C., TURCK, C. W., KUROSAKI, T. & CHAN, A. C. 1998. BLNK: a central linker protein in B cell activation. *Immunity*, 9, 93-103.
- GAO, H., LUKIN, K., RAMÍREZ, J., FIELDS, S., LOPEZ, D. & HAGMAN, J. 2009. Opposing effects of SWI/SNF and Mi-2/NuRD chromatin remodeling complexes on epigenetic

- reprogramming by EBF and Pax5. *Proceedings of the National Academy of Sciences*, 106, 11258.
- GASZNER, M. & FELSENFELD, G. 2006. Insulators: exploiting transcriptional and epigenetic mechanisms. *Nat Rev Genet*, 7, 703-13.
- GEISBERGER, R., LAMERS, M. & ACHATZ, G. 2006. The riddle of the dual expression of IgM and IgD. *Immunology*, 118, 429-437.
- GHIRLANDO, R., GILES, K., GOWHER, H., XIAO, T., XU, Z., YAO, H. & FELSENFELD, G. 2012. Chromatin domains, insulators, and the regulation of gene expression. *Biochimica et biophysica acta*, 1819, 644-651.
- GILLIES, S. D., MORRISON, S. L., OI, V. T. & TONEGAWA, S. 1983. A tissue-specific transcription enhancer element is located in the major intron of a rearranged immunoglobulin heavy chain gene. *Cell*, 33, 717-28.
- GIRES, O., KOHLHUBER, F., KILGER, E., BAUMANN, M., KIESER, A., KAISER, C., ZEIDLER, R., SCHEFFER, B., UEFFING, M. & HAMMERSCHMIDT, W. 1999. Latent membrane protein 1 of Epstein-Barr virus interacts with JAK3 and activates STAT proteins. *The EMBO journal*, 18, 3064-3073.
- GLASER, L. V., RIEGER, S., THUMANN, S., BEER, S., KUKLIK-ROOS, C., MARTIN, D. E., MAIER, K. C., HARTH-HERTLE, M. L., GRÜNING, B., BACKOFEN, R., KREBS, S., BLUM, H., ZIMMER, R., ERHARD, F. & KEMPKES, B. 2017. EBF1 binds to EBNA2 and promotes the assembly of EBNA2 chromatin complexes in B cells. *PLoS Pathogens*, 13, e1006664.
- GNANASUNDRAM, S. V., PYNDIAH, S., DASKALOGIANNI, C., ARMFIELD, K., NYLANDER, K., WILSON, J. B. & FÅHRAEUS, R. 2017. PI3K δ activates E2F1 synthesis in response to mRNA translation stress. *Nature Communications*, 8, 2103.
- GOTTSCHALK, S., NG, C. Y., PEREZ, M., SMITH, C. A., SAMPLE, C., BRENNER, M. K., HESLOP, H. E. & ROONEY, C. M. 2001. An Epstein-Barr virus deletion mutant associated with fatal lymphoproliferative disease unresponsive to therapy with virus-specific CTLs. *Blood*, 97, 835-43.
- GROSSMAN, S. R., JOHANNSEN, E., TONG, X., YALAMANCHILI, R. & KIEFF, E. 1994. The Epstein-Barr virus nuclear antigen 2 transactivator is directed to response elements by the J kappa recombination signal binding protein. *Proc Natl Acad Sci U S A*, 91, 7568-72.
- GROZINGER, C. M. & SCHREIBER, S. L. 2002. Deacetylase enzymes: biological functions and the use of small-molecule inhibitors. *Chem Biol*, 9, 3-16.
- GRUHNE, B., SOMPALLAE, R., MARESCOTTI, D., KAMRANVAR, S. A., GASTALDELLO, S. & MASUCCI, M. G. 2009. The Epstein-Barr virus nuclear antigen-1 promotes genomic instability via induction of reactive oxygen species. *Proc Natl Acad Sci U S A*, 106, 2313-8.
- GUNNELL, A., WEBB, H. M., WOOD, C. D., MCCLELLAN, M. J., WICHAIDIT, B., KEMPKES, B., JENNER, R. G., OSBORNE, C., FARRELL, P. J. & WEST, M. J. 2016. RUNX super-enhancer control through the Notch pathway by Epstein-Barr virus transcription factors regulates B cell growth. *Nucleic Acids Res*, 44, 4636-50.
- HABERLE, V. & STARK, A. 2018. Eukaryotic core promoters and the functional basis of transcription initiation. *Nature Reviews Molecular Cell Biology*, 19, 621-637.
- HAGMAN, J. 2015. Chapter 3. Transcriptional Regulation of Early B Cell Development.
- HARRIS, W. J., HUANG, X., LYNCH, J. T., SPENCER, G. J., HITCHIN, J. R., LI, Y., CICERI, F., BLASER, J. G., GREYSTOKE, B. F., JORDAN, A. M., MILLER, C. J., OGILVIE, D. J. & SOMERVILLE, T. C. 2012. The histone demethylase KDM1A sustains the oncogenic potential of MLL-AF9 leukemia stem cells. *Cancer Cell*, 21, 473-87.
- HARTH-HERTLE, M. L., SCHOLZ, B. A., ERHARD, F., GLASER, L. V., DOLKEN, L., ZIMMER, R. & KEMPKES, B. 2013. Inactivation of intergenic enhancers by EBNA3A initiates and maintains polycomb signatures across a chromatin domain encoding CXCL10 and CXCL9. *PLoS Pathog*, 9, e1003638.

- HATA, A., SABE, H., KUROSAKI, T., TAKATA, M. & HANAFUSA, H. 1994. Functional analysis of Csk in signal transduction through the B-cell antigen receptor. *Molecular and cellular biology*, 14, 7306-7313.
- HAYAMI, S., KELLY, J. D., CHO, H. S., YOSHIMATSU, M., UNOKI, M., TSUNODA, T., FIELD, H. I., NEAL, D. E., YAMAUE, H., PONDER, B. A., NAKAMURA, Y. & HAMAMOTO, R. 2011. Overexpression of LSD1 contributes to human carcinogenesis through chromatin regulation in various cancers. *Int J Cancer*, 128, 574-86.
- HAYNES, S. R., DOLLARD, C., WINSTON, F., BECK, S., TROWSDALE, J. & DAWID, I. B. 1992. The bromodomain: a conserved sequence found in human, Drosophila and yeast proteins. *Nucleic Acids Res*, 20, 2603.
- HEINZ, S., BENNER, C., SPANN, N., BERTOLINO, E., LIN, Y. C., LASLO, P., CHENG, J. X., MURRE, C., SINGH, H. & GLASS, C. K. 2010. Simple Combinations of Lineage-Determining Transcription Factors Prime cis-Regulatory Elements Required for Macrophage and B Cell Identities. *Molecular Cell*, 38, 576-589.
- HENLE, W., DIEHL, V., KOHN, G., ZUR HAUSEN, H. & HENLE, G. 1967. Herpes-type virus and chromosome marker in normal leukocytes after growth with irradiated Burkitt cells. *Science*, 157, 1064-5.
- HERMANSON, G. G., BRISKIN, M., SIGMAN, D. & WALL, R. 1989. Immunoglobulin enhancer and promoter motifs 5' of the B29 B-cell-specific gene. *Proceedings of the National Academy of Sciences of the United States of America*, 86, 7341-7345.
- HERMANSON, G. G., EISENBERG, D., KINCADE, P. W. & WALL, R. 1988. B29: a member of the immunoglobulin gene superfamily exclusively expressed on beta-lineage cells. *Proc Natl Acad Sci U S A*, 85, 6890-4.
- HERTLE, M. L., POPP, C., PETERMANN, S., MAIER, S., KREMMER, E., LANG, R., MAGES, J. & KEMPKES, B. 2009. Differential Gene Expression Patterns of EBV Infected EBNA-3A Positive and Negative Human B Lymphocytes. *PLoS Pathog*, 5, e1000506.
- HOFFMAN, B. & LIEBERMANN, D. A. 2008. Apoptotic signaling by c-MYC. *Oncogene*, 27, 6462-6472.
- HOFFMANN, I., ROATSCH, M., SCHMITT, M. L., CARLINO, L., PIPPEL, M., SIPPL, W. & JUNG, M. 2012. The role of histone demethylases in cancer therapy. *Mol Oncol*, 6, 683-703.
- HUANG, C., XU, M. & ZHU, B. 2013. Epigenetic inheritance mediated by histone lysine methylation: maintaining transcriptional states without the precise restoration of marks? *Philosophical transactions of the Royal Society of London. Series B, Biological sciences*, 368, 20110332-20110332.
- IZUMI, K. M. & KIEFF, E. D. 1997. The Epstein-Barr virus oncogene product latent membrane protein 1 engages the tumor necrosis factor receptor-associated death domain protein to mediate B lymphocyte growth transformation and activate NF-kappaB. *Proc Natl Acad Sci U S A*, 94, 12592-7.
- JAULIAC, S., LOPEZ-RODRIGUEZ, C., SHAW, L. M., BROWN, L. F., RAO, A. & TOKER, A. 2002. The role of NFAT transcription factors in integrin-mediated carcinoma invasion. *Nat Cell Biol*, 4, 540-4.
- JOHANSEN, E., KOH, E., MOSIALOS, G., TONG, X., KIEFF, E. & GROSSMAN, S. R. 1995. Epstein-Barr virus nuclear protein 2 transactivation of the latent membrane protein 1 promoter is mediated by J kappa and PU.1. *J Virol*, 69, 253-62.
- JOHNSON, S. A., PLEIMAN, C. M., PAO, L., SCHNERINGER, J., HIPPEL, K. & CAMBIER, J. C. 1995. Phosphorylated immunoreceptor signaling motifs (ITAMs) exhibit unique abilities to bind and activate Lyn and Syk tyrosine kinases. *J Immunol*, 155, 4596-603.
- K LEE, D., DEJONG, J., HASHIMOTO, S., HORIKOSHI, M. & G ROEDER, R. 1992. *TFIIA induces conformational changes in TFIID via interactions with the basic repeat.*
- KAGEY, M. H., NEWMAN, J. J., BILODEAU, S., ZHAN, Y., ORLANDO, D. A., VAN BERKUM, N. L., EBMEIER, C. C., GOOSSENS, J., RAHL, P. B., LEVINE, S. S., TAATJES, D. J., DEKKER, J. &

- YOUNG, R. A. 2010. Mediator and cohesin connect gene expression and chromatin architecture. *Nature*, 467, 430-5.
- KAISER, C., LAUX, G., EICK, D., JOCHNER, N., BORNKAMM, G. W. & KEMPKES, B. 1999. The Proto-Oncogene c-myc Is a Direct Target Gene of Epstein-Barr Virus Nuclear Antigen 2. *Journal of Virology*, 73, 4481-4484.
- KALCHSCHMIDT, J. S., GILLMAN, A. C. T., PASCHOS, K., BAZOT, Q., KEMPKES, B. & ALLDAY, M. J. 2016. EBNA3C Directs Recruitment of RBPJ (CBF1) to Chromatin during the Process of Gene Repression in EBV Infected B Cells. *PLoS Pathogens*, 12, e1005383.
- KARPURAPU, M., WANG, D., SINGH, N. K., LI, Q. & RAO, G. N. 2008. NFATc1 targets cyclin A in the regulation of vascular smooth muscle cell multiplication during restenosis. *The Journal of biological chemistry*, 283, 26577-26590.
- KARPURAPU, M., WANG, D., VAN QUYEN, D., KIM, T. K., KUNDUMANI-SRIDHARAN, V., PULUSANI, S. & RAO, G. N. 2010. Cyclin D1 is a bona fide target gene of NFATc1 and is sufficient in the mediation of injury-induced vascular wall remodeling. *J Biol Chem*, 285, 3510-23.
- KATZ, S. G., LABELLE, J. L., MENG, H., VALERIANO, R. P., FISHER, J. K., SUN, H., RODIG, S. J., KLEINSTEIN, S. H. & WALENSKY, L. D. 2014. Mantle cell lymphoma in cyclin D1 transgenic mice with *Bim*-deficient B cells. *Blood*, 123, 884.
- KEMPKES, B., PAWLITA, M., ZIMBER-STROBL, U., EISSNER, G., LAUX, G. & BORNKAMM, G. W. 1995a. Epstein-Barr Virus Nuclear Antigen 2-Estrogen Receptor Fusion Proteins Transactivate Viral and Cellular Genes and Interact with RBP-Jk in a Conditional Fashion. *Virology*, 214, 675-679.
- KEMPKES, B., SPITKOVSKY, D., JANSEN-DÜRR, P., ELLWART, J. W., KREMMER, E., DELECLUSE, H. J., ROTTENBERGER, C., BORNKAMM, G. W. & HAMMERSCHMIDT, W. 1995b. B-cell proliferation and induction of early G1-regulating proteins by Epstein-Barr virus mutants conditional for EBNA2. *Embo j*, 14, 88-96.
- KEMPKES, B., SPITKOVSKY, D., JANSEN-DÜRR, P., ELLWART, J. W., KREMMER, E., DELECLUSE, H. J., ROTTENBERGER, C., BORNKAMM, G. W. & HAMMERSCHMIDT, W. 1995c. B-cell proliferation and induction of early G1-regulating proteins by Epstein-Barr virus mutants conditional for EBNA2. *The EMBO journal*, 14, 88-96.
- KENNEDY, G., KOMANO, J. & SUGDEN, B. 2003. Epstein-Barr virus provides a survival factor to Burkitt's lymphomas. *Proc Natl Acad Sci U S A*, 100, 14269-74.
- KHAN, A., MATHELIER, A. & ZHANG, X. 2018. Super-enhancers are transcriptionally more active and cell type-specific than stretch enhancers. *Epigenetics*, 13, 910-922.
- KHAN, A. & ZHANG, X. 2016. dbSUPER: a database of super-enhancers in mouse and human genome. *Nucleic acids research*, 44, D164-D171.
- KHASNIS, S. 2018. *Investigating the regulation of B cell growth and survival genes by Epstein-Barr virus*. PhD, University of Sussex.
- KIESER, A. & STERZ, K. R. 2015. The Latent Membrane Protein 1 (LMP1). *Curr Top Microbiol Immunol*, 391, 119-49.
- KITAMURA, D., KUDO, A., SCHAAL, S., MULLER, W., MELCHERS, F. & RAJEWSKY, K. 1992. A critical role of lambda 5 protein in B cell development. *Cell*, 69, 823-31.
- KITAMURA, D., ROES, J., KUHN, R. & RAJEWSKY, K. 1991. A B cell-deficient mouse by targeted disruption of the membrane exon of the immunoglobulin mu chain gene. *Nature*, 350, 423-6.
- KLEIN, G., LINDAHL, T., JONDAL, M., LEIBOLD, W., MENEZES, J., NILSSON, K. & SUNDSTROM, C. 1974. Continuous lymphoid cell lines with characteristics of B cells (bone-marrow-derived), lacking the Epstein-Barr virus genome and derived from three human lymphomas. *Proc Natl Acad Sci U S A*, 71, 3283-6.
- KLEIN, U., TU, Y., STOLOVITZKY, G. A., KELLER, J. L., HADDAD, J., JR., MILJKOVIC, V., CATTORETTI, G., CALIFANO, A. & DALLA-FAVERA, R. 2003. Transcriptional analysis of the B cell germinal center reaction. *Proc Natl Acad Sci U S A*, 100, 2639-44.

- KNOX, P. G. & YOUNG, L. S. 1995. Epstein-Barr virus infection of CR2-transfected epithelial cells reveals the presence of MHC class II on the virion. *Virology*, 213, 147-57.
- KOLOVOS, P., KNOCH, T. A., GROSVELD, F. G., COOK, P. R. & PAPANTONIS, A. 2012. Enhancers and silencers: an integrated and simple model for their function. *Epigenetics & Chromatin*, 5, 1.
- KOUZARIDES, T. 2007. Chromatin modifications and their function. *Cell*, 128, 693-705.
- KRAUTLER, N. J., SUAN, D., BUTT, D., BOURNE, K., HERMES, J. R., CHAN, T. D., SUNDLING, C., KAPLAN, W., SCHOFIELD, P., JACKSON, J., BASTEN, A., CHRIST, D. & BRINK, R. 2017. Differentiation of germinal center B cells into plasma cells is initiated by high-affinity antigen and completed by Tfh cells. *J Exp Med*, 214, 1259-1267.
- KUEH, H. Y., CHAMPHEKAR, A., NUTT, S. L., ELOWITZ, M. B. & ROTHENBERG, E. V. 2013. Positive Feedback Between PU.1 and the Cell Cycle Controls Myeloid Differentiation. *Science*, 341, 670.
- KURDISTANI, S. K., TAVAZOIE, S. & GRUNSTEIN, M. 2004. Mapping global histone acetylation patterns to gene expression. *Cell*, 117, 721-33.
- KUROSAKI, T. 1999. Genetic analysis of B cell antigen receptor signaling. *Annu Rev Immunol*, 17, 555-92.
- KÜÇÜK, C., HU, X., JIANG, B., KLINKEBIEL, D., GENG, H., GONG, Q., BOUSKA, A., IQBAL, J., GAULARD, P., MCKEITHAN, T. W. & CHAN, W. C. 2015. Global promoter methylation analysis reveals novel candidate tumor suppressor genes in natural killer cell lymphoma. *Clinical cancer research : an official journal of the American Association for Cancer Research*, 21, 1699-1711.
- LAM, K. P., KUHN, R. & RAJEWSKY, K. 1997. In vivo ablation of surface immunoglobulin on mature B cells by inducible gene targeting results in rapid cell death. *Cell*, 90, 1073-83.
- LAUGESEN, A., HOJFELDT, J. W. & HELIN, K. 2016. Role of the Polycomb Repressive Complex 2 (PRC2) in Transcriptional Regulation and Cancer. *Cold Spring Harb Perspect Med*, 6.
- LENOIR, G. M., VUILLAUME, M. & BONNARDEL, C. 1985. The use of lymphomatous and lymphoblastoid cell lines in the study of Burkitt's lymphoma. *IARC Sci Publ*, 309-18.
- LEVITSKAYA, J., SHARIPO, A., LEONCHIKS, A., CIECHANOVER, A. & MASUCCI, M. G. 1997. Inhibition of ubiquitin/proteasome-dependent protein degradation by the Gly-Ala repeat domain of the Epstein-Barr virus nuclear antigen 1. *Proceedings of the National Academy of Sciences*, 94, 12616-12621.
- LI, N., THOMPSON, S., SCHULTZ, D. C., ZHU, W., JIANG, H., LUO, C. & LIEBERMAN, P. M. 2010. Discovery of selective inhibitors against EBNA1 via high throughput in silico virtual screening. *PLoS One*, 5, e10126.
- LI, Y., KAO, G. D., GARCIA, B. A., SHABANOWITZ, J., HUNT, D. F., QIN, J., PHELAN, C. & LAZAR, M. A. 2006. A novel histone deacetylase pathway regulates mitosis by modulating Aurora B kinase activity. *Genes Dev*, 20, 2566-79.
- LIN, H. & GROSSCHEDL, R. 1995. Failure of B-cell differentiation in mice lacking the transcription factor EBF. *Nature*, 376, 263-267.
- LINDSTROM, M. S. & WIMAN, K. G. 2002. Role of genetic and epigenetic changes in Burkitt lymphoma. *Semin Cancer Biol*, 12, 381-7.
- LING, P. D., RAWLINS, D. R. & HAYWARD, S. D. 1993. The Epstein-Barr virus immortalizing protein EBNA-2 is targeted to DNA by a cellular enhancer-binding protein. *Proceedings of the National Academy of Sciences*, 90, 9237.
- LU, T. X., LIANG, J. H., MIAO, Y., FAN, L., WANG, L., QU, X. Y., CAO, L., GONG, Q. X., WANG, Z., ZHANG, Z. H., XU, W. & LI, J. Y. 2015. Epstein-Barr virus positive diffuse large B-cell lymphoma predict poor outcome, regardless of the age. *Sci Rep*, 5, 12168.
- LUE, J. K. & AMENGUAL, J. E. 2018. Emerging EZH2 Inhibitors and Their Application in Lymphoma. *Curr Hematol Malig Rep*, 13, 369-382.
- LUKIN, K., FIELDS, S., HARTLEY, J. & HAGMAN, J. 2008. Early B cell factor: Regulator of B lineage specification and commitment. *Seminars in immunology*, 20, 221-227.

- MAIER, H., OSTRAAT, R., GAO, H., FIELDS, S., SHINTON, S. A., MEDINA, K. L., IKAWA, T., MURRE, C., SINGH, H., HARDY, R. R. & HAGMAN, J. 2004. Early B cell factor cooperates with Runx1 and mediates epigenetic changes associated with mb-1 transcription. *Nature Immunology*, 5, 1069-1077.
- MAIER, S., SANTAK, M., MANTIK, A., GRABUSIC, K., KREMMER, E., HAMMERSCHMIDT, W. & KEMPKES, B. 2005. A somatic knockout of CBF1 in a human B-cell line reveals that induction of CD21 and CCR7 by EBNA-2 is strictly CBF1 dependent and that downregulation of immunoglobulin M is partially CBF1 independent. *J Virol*, 79, 8784-92.
- MAIER, S., STAFFLER, G., HARTMANN, A., HOCK, J., HENNING, K., GRABUSIC, K., MAILHAMMER, R., HOFFMANN, R., WILMANN, M., LANG, R., MAGES, J. & KEMPKES, B. 2006. Cellular target genes of Epstein-Barr virus nuclear antigen 2. *J Virol*, 80, 9761-71.
- MANCAO, C. & HAMMERSCHMIDT, W. 2007. Epstein-Barr virus latent membrane protein 2A is a B-cell receptor mimic and essential for B-cell survival. *Blood*, 110, 3715-21.
- MANCINI, M. & TOKER, A. 2009. NFAT proteins: emerging roles in cancer progression. *Nat Rev Cancer*, 9, 810-820.
- MARAFIOTI, T., POZZOBON, M., HANSMANN, M. L., VENTURA, R., PILERI, S. A., ROBERTON, H., GESK, S., GAULARD, P., BARTH, T. F., DU, M. Q., LEONCINI, L., MOLLER, P., NATKUNAM, Y., SIEBERT, R. & MASON, D. Y. 2005. The NFATc1 transcription factor is widely expressed in white cells and translocates from the cytoplasm to the nucleus in a subset of human lymphomas. *Br J Haematol*, 128, 333-42.
- MARUO, S., ZHAO, B., JOHANNSEN, E., KIEFF, E., ZOU, J. & TAKADA, K. 2011. Epstein-Barr virus nuclear antigens 3C and 3A maintain lymphoblastoid cell growth by repressing p16INK4A and p14ARF expression. *Proc Natl Acad Sci U S A*, 108, 1919-24.
- MASON, D. Y., CORDELL, J. L., BROWN, M. H., BORST, J., JONES, M., PULFORD, K., JAFFE, E., RALFKIAER, E., DALLENBACH, F., STEIN, H. & ET AL. 1995. CD79a: a novel marker for B-cell neoplasms in routinely processed tissue samples. *Blood*, 86, 1453-9.
- MASON, D. Y., VAN NOESEL, C. J., CORDELL, J. L., COMANS-BITTER, W. M., MICKLEM, K., TSE, A. G., VAN LIER, R. A. & VAN DONGEN, J. J. 1992. The B29 and mb-1 polypeptides are differentially expressed during human B cell differentiation. *Eur J Immunol*, 22, 2753-6.
- MAYRAN, A. & DROUIN, J. 2018. Pioneer transcription factors shape the epigenetic landscape. *Journal of Biological Chemistry*, 293, 13795-13804.
- MBULAITEYE, S. M., PULLARKAT, S. T., NATHWANI, B. N., WEISS, L. M., RAO, N., EMMANUEL, B., LYNCH, C. F., HERNANDEZ, B., NEPPALLI, V., HAWES, D., COCKBURN, M. G., KIM, A., WILLIAMS, M., ALTEKRUSE, S., BHATIA, K., GOODMAN, M. T. & COZEN, W. 2014. Epstein-Barr virus patterns in US Burkitt lymphoma tumors from the SEER residual tissue repository during 1979-2009. *Apmis*, 122, 5-15.
- MCCLELLAN, M. J., KHASNIS, S., WOOD, C. D., PALERMO, R. D., SCHLICK, S. N., KANHERE, A. S., JENNER, R. G. & WEST, M. J. 2012. Downregulation of Integrin Receptor-Signaling Genes by Epstein-Barr Virus EBNA 3C via Promoter-Proximal and -Distal Binding Elements. *Journal of Virology*, 86, 5165-5178.
- MCCLELLAN, M. J., WOOD, C. D., OJENIYI, O., COOPER, T. J., KANHERE, A., ARVEY, A., WEBB, H. M., PALERMO, R. D., HARTH-HERTLE, M. L., KEMPKES, B., JENNER, R. G. & WEST, M. J. 2013. Modulation of Enhancer Looping and Differential Gene Targeting by Epstein-Barr Virus Transcription Factors Directs Cellular Reprogramming. *PLoS Pathog*, 9, e1003636.
- MEDYOUNG, H., ALCALDE, H., BERTHIER, C., GUILLEMIN, M. C., DOS SANTOS, N. R., JANIN, A., DECAUDIN, D., DE THE, H. & GHYSDAEL, J. 2007. Targeting calcineurin activation as a therapeutic strategy for T-cell acute lymphoblastic leukemia. *Nat Med*, 13, 736-41.
- MEDYOUNG, H. & GHYSDAEL, J. 2008. The calcineurin/NFAT signaling pathway: a novel therapeutic target in leukemia and solid tumors. *Cell Cycle*, 7, 297-303.
- MIELE, L. 2011. Transcription factor RBPJ/CSL: A genome-wide look at transcriptional regulation. *Proceedings of the National Academy of Sciences*, 108, 14715.

- MIFSUD, B., TAVARES-CADETE, F., YOUNG, A. N., SUGAR, R., SCHOENFELDER, S., FERREIRA, L., WINGETT, S. W., ANDREWS, S., GREY, W., EWELS, P. A., HERMAN, B., HAPPE, S., HIGGS, A., LEPROUST, E., FOLLOWS, G. A., FRASER, P., LUSCOMBE, N. M. & OSBORNE, C. S. 2015. Mapping long-range promoter contacts in human cells with high-resolution capture Hi-C. *Nat Genet*, 47, 598-606.
- MILLER, C. L., BURKHARDT, A. L., LEE, J. H., STEALEY, B., LONGNECKER, R., BOLEN, J. B. & KIEFF, E. 1995. Integral membrane protein 2 of Epstein-Barr virus regulates reactivation from latency through dominant negative effects on protein-tyrosine kinases. *Immunity*, 2, 155-66.
- MILLER, C. L., LONGNECKER, R. & KIEFF, E. 1993. Epstein-Barr virus latent membrane protein 2A blocks calcium mobilization in B lymphocytes. *Journal of Virology*, 67, 3087.
- MILLER, J. P., IZON, D., DEMUTH, W., GERSTEIN, R., BHANDoola, A. & ALLMAN, D. 2002. The Earliest Step in B Lineage Differentiation from Common Lymphoid Progenitors Is Critically Dependent upon Interleukin 7. *The Journal of Experimental Medicine*, 196, 705.
- MOGNOL, G. P., CARNEIRO, F. R. G., ROBBS, B. K., FAGET, D. V. & VIOLA, J. P. B. 2016. Cell cycle and apoptosis regulation by NFAT transcription factors: new roles for an old player. *Cell Death & Disease*, 7, e2199.
- MORI, M., WATANABE, M., TANAKA, S., MIMORI, K., KUWANO, H. & SUGIMACHI, K. 1994. Epstein-Barr virus-associated carcinomas of the esophagus and stomach. *Arch Pathol Lab Med*, 118, 998-1001.
- MURRAY, P. G. & YOUNG, L. S. 2001. Epstein-Barr virus infection: basis of malignancy and potential for therapy. *Expert Reviews in Molecular Medicine*, 3, 1-20.
- MYERS, L. C., GUSTAFSSON, C. M., HAYASHIBARA, K. C., BROWN, P. O. & KORNBERG, R. D. 1999. Mediator protein mutations that selectively abolish activated transcription. *Proc Natl Acad Sci U S A*, 96, 67-72.
- NAUMOVA, N., SMITH, E. M., ZHAN, Y. & DEKKER, J. 2012. Analysis of long-range chromatin interactions using Chromosome Conformation Capture. *Methods (San Diego, Calif.)*, 58, 10.1016/j.ymeth.2012.07.022.
- NERI, A., BARRIGA, F., KNOWLES, D. M., MAGRATH, I. T. & DALLA-FAVERA, R. 1988. Different regions of the immunoglobulin heavy-chain locus are involved in chromosomal translocations in distinct pathogenetic forms of Burkitt lymphoma. *Proc Natl Acad Sci U S A*, 85, 2748-52.
- NEUBERGER, M. S. 1983. Expression and regulation of immunoglobulin heavy chain gene transfected into lymphoid cells. *Embo j*, 2, 1373-8.
- NIIRO, H. & CLARK, E. A. 2002. Regulation of B-cell fate by antigen-receptor signals. *Nat Rev Immunol*, 2, 945-56.
- NIKOLOV, D. B., HU, S. H., LIN, J., GASCH, A., HOFFMANN, A., HORIKOSHI, M., CHUA, N. H., ROEDER, R. G. & BURLEY, S. K. 1992. Crystal structure of TFIID TATA-box binding protein. *Nature*, 360, 40-6.
- NISHIZUMI, H., HORIKAWA, K., MLINARIC-RASCAN, I. & YAMAMOTO, T. 1998. A double-edged kinase Lyn: a positive and negative regulator for antigen receptor-mediated signals. *The Journal of experimental medicine*, 187, 1343-1348.
- NÄÄR, A. M., TAATJES, D. J., ZHAI, W., NOGALES, E. & TJIAN, R. 2002. Human CRSP interacts with RNA polymerase II CTD and adopts a specific CTD-bound conformation. *Genes & Development*, 16, 1339-1344.
- O'REILLY, L. A., CULLEN, L., VISVADER, J., LINDEMAN, G. J., PRINT, C., BATH, M. L., HUANG, D. C. & STRASSER, A. 2000. The proapoptotic BH3-only protein bim is expressed in hematopoietic, epithelial, neuronal, and germ cells. *Am J Pathol*, 157, 449-61.
- OK, C. Y., PAPHATHOMAS, T. G., MEDEIROS, L. J. & YOUNG, K. H. 2013. EBV-positive diffuse large B-cell lymphoma of the elderly. *Blood*, 122, 328-40.

- OLLILA, J. & VIHINEN, M. 2005. B cells. *The International Journal of Biochemistry & Cell Biology*, 37, 518-523.
- OMORI, S. A. & WALL, R. 1993. Multiple motifs regulate the B-cell-specific promoter of the B29 gene. *Proc Natl Acad Sci U S A*, 90, 11723-7.
- PALSER, A. L., GRAYSON, N. E., WHITE, R. E., CORTON, C., CORREIA, S., BA ABDULLAH, M. M., WATSON, S. J., COTTEN, M., ARRAND, J. R., MURRAY, P. G., ALLDAY, M. J., RICKINSON, A. B., YOUNG, L. S., FARRELL, P. J. & KELLAM, P. 2015. Genome diversity of Epstein-Barr virus from multiple tumor types and normal infection. *J Virol*, 89, 5222-37.
- PANNUTI, A., FOREMAN, K., RIZZO, P., OSIPO, C., GOLDE, T., OSBORNE, B. & MIELE, L. 2010. Targeting Notch to Target Cancer Stem Cells. *Clinical Cancer Research*, 16, 3141.
- PAO, L. I., FAMIGLIETTI, S. J. & CAMBIER, J. C. 1998. Asymmetrical phosphorylation and function of immunoreceptor tyrosine-based activation motif tyrosines in B cell antigen receptor signal transduction. *J Immunol*, 160, 3305-14.
- PARTHUN, M. R. 2007. Hat1: the emerging cellular roles of a type B histone acetyltransferase. *Oncogene*, 26, 5319.
- PASCHOS, K., BAZOT, Q., LEES, J., FARRELL, P. J. & ALLDAY, M. J. 2019. Requirement for PRC1 subunit BMI1 in host gene activation by Epstein-Barr virus protein EBNA3C. *Nucleic Acids Res*, 47, 2807-2821.
- PASCHOS, K., PARKER, G. A., WATANATANASUP, E., WHITE, R. E. & ALLDAY, M. J. 2012. BIM promoter directly targeted by EBNA3C in polycomb-mediated repression by EBV. *Nucleic Acids Research*, 40, 7233-7246.
- PASCHOS, K., SMITH, P., ANDERTON, E., MIDDELDORP, J. M., WHITE, R. E. & ALLDAY, M. J. 2009. Epstein-Barr Virus Latency in B Cells Leads to Epigenetic Repression and CpG Methylation of the Tumour Suppressor Gene Bim. *PLOS Pathogens*, 5, e1000492.
- PENG, M. & LUNDGREN, E. 1992. Transient expression of the Epstein-Barr virus LMP1 gene in human primary B cells induces cellular activation and DNA synthesis. *Oncogene*, 7, 1775-82.
- PETERSON, C. L. & LANIEL, M. A. 2004. Histones and histone modifications. *Curr Biol*, 14, R546-51.
- PHAM, L. V., TAMAYO, A. T., YOSHIMURA, L. C., LIN-LEE, Y.-C. & FORD, R. J. 2005. Constitutive NF- κ B and NFAT activation in aggressive B-cell lymphomas synergistically activates the CD154 gene and maintains lymphoma cell survival. *Blood*, 106, 3940-3947.
- PHILLIPS, J. E. & CORCES, V. G. 2009. CTCF: Master Weaver of the Genome. *Cell*, 137, 1194-1211.
- POLACK, A., HORTNAGEL, K., PAJIC, A., CHRISTOPH, B., BAIER, B., FALK, M., MAUTNER, J., GELTINGER, C., BORNKAMM, G. W. & KEMPKE, B. 1996. c-myc activation renders proliferation of Epstein-Barr virus (EBV)-transformed cells independent of EBV nuclear antigen 2 and latent membrane protein 1. *Proc Natl Acad Sci U S A*, 93, 10411-6.
- PORTAL, D., ZHOU, H., ZHAO, B., KHARCHENKO, P. V., LOWRY, E., WONG, L., QUACKENBUSH, J., HOLLOWAY, D., JIANG, S., LU, Y. & KIEFF, E. 2013. Epstein-Barr virus nuclear antigen leader protein localizes to promoters and enhancers with cell transcription factors and EBNA2. *Proc Natl Acad Sci U S A*, 110, 18537-42.
- PUGLIELLI, M. T., WOISETSCHLAEGER, M. & SPECK, S. H. 1996. oriP is essential for EBNA gene promoter activity in Epstein-Barr virus-immortalized lymphoblastoid cell lines. *Journal of Virology*, 70, 5758.
- PUI, J. C., ALLMAN, D., XU, L., DEROCCO, S., KARNELL, F. G., BAKKOUR, S., LEE, J. Y., KADESCH, T., HARDY, R. R., ASTER, J. C. & PEAR, W. S. 1999. Notch1 expression in early lymphopoiesis influences B versus T lineage determination. *Immunity*, 11, 299-308.
- RADTKE, F., WILSON, A., STARK, G., BAUER, M., VAN MEERWIJK, J., MACDONALD, H. R. & AGUET, M. 1999. Deficient T cell fate specification in mice with an induced inactivation of Notch1. *Immunity*, 10, 547-58.
- RETH, M. 1992. Antigen receptors on B lymphocytes. *Annu Rev Immunol*, 10, 97-121.

- RIETHOVEN, J.-J. M. 2010. Regulatory Regions in DNA: Promoters, Enhancers, Silencers, and Insulators. *In: LADUNGA, I. (ed.) Computational Biology of Transcription Factor Binding*. Totowa, NJ: Humana Press.
- ROBBS, B. K., CRUZ, A. L., WERNECK, M. B., MOGNOL, G. P. & VIOLA, J. P. 2008. Dual roles for NFAT transcription factor genes as oncogenes and tumor suppressors. *Mol Cell Biol*, 28, 7168-81.
- ROUGHAN, J. E. & THORLEY-LAWSON, D. A. 2009. The Intersection of Epstein-Barr Virus with the Germinal Center. *Journal of Virology*, 83, 3968.
- SAINSBURY, S., BERNECKY, C. & CRAMER, P. 2015. Structural basis of transcription initiation by RNA polymerase II. *Nature Reviews Molecular Cell Biology*, 16, 129.
- SAITOH, N., BELL, A. C., RECILLAS-TARGA, F., WEST, A. G., SIMPSON, M., PIKAART, M. & FELSENFELD, G. 2000. Structural and functional conservation at the boundaries of the chicken beta-globin domain. *Embo j*, 19, 2315-22.
- SAKAI, T., TANIGUCHI, Y., TAMURA, K., MINOGUCHI, S., FUKUHARA, T., STROBL, L., ZIMBER-STROBL, U., BORNKAMM, G. & HONJO, T. 1998. Functional Replacement of the Intracellular Region of the Notch1 Receptor by Epstein-Barr Virus Nuclear Antigen 2. *Journal of virology*, 72, 6034-9.
- SCHLICK, S. N., WOOD, C. D., GUNNELL, A., WEBB, H. M., KHASNIS, S., SCHEPERS, A. & WEST, M. J. 2011. Upregulation of the Cell-Cycle Regulator RGC-32 in Epstein-Barr Virus-Immortalized Cells. *PLoS ONE*, 6, e28638.
- SCHOLLE, F., LONGNECKER, R. & RAAB-TRAUB, N. 1999. Epithelial cell adhesion to extracellular matrix proteins induces tyrosine phosphorylation of the Epstein-Barr virus latent membrane protein 2: a role for C-terminal Src kinase. *J Virol*, 73, 4767-75.
- SERFLING, E., AVOTS, A., KLEIN-HESSLING, S., RUDOLF, R., VAETH, M. & BERBERICH-SIEBELT, F. 2012. NFATc1/ α A: The other Face of NFAT Factors in Lymphocytes. *Cell communication and signaling : CCS*, 10, 16-16.
- SHI, J., WHYTE, W. A., ZEPEDA-MENDOZA, C. J., MILAZZO, J. P., SHEN, C., ROE, J. S., MINDER, J. L., MERCAN, F., WANG, E., ECKERSLEY-MASLIN, M. A., CAMPBELL, A. E., KAWAOKA, S., SHAREEF, S., ZHU, Z., KENDALL, J., MUHAR, M., HASLINGER, C., YU, M., ROEDER, R. G., WIGLER, M. H., BLOBEL, G. A., ZUBER, J., SPECTOR, D. L., YOUNG, R. A. & VAKOC, C. R. 2013. Role of SWI/SNF in acute leukemia maintenance and enhancer-mediated Myc regulation. *Genes & development*, 27, 2648-62.
- SHI, Y. 2007. Histone lysine demethylases: emerging roles in development, physiology and disease. *Nat Rev Genet*, 8, 829-33.
- SHI, Y., WANG, X.-X., ZHUANG, Y.-W., JIANG, Y., MELCHER, K. & XU, H. E. 2017. Structure of the PRC2 complex and application to drug discovery. *Acta Pharmacologica Sinica*, 38, 963.
- SHIRAMIZU, B., BARRIGA, F., NEEQUAYE, J., JAFRI, A., DALLA-FAVERA, R., NERI, A., GUTTIEREZ, M., LEVINE, P. & MAGRATH, I. 1991. Patterns of chromosomal breakpoint locations in Burkitt's lymphoma: relevance to geography and Epstein-Barr virus association. *Blood*, 77, 1516.
- SHLYUEVA, D., STAMPFEL, G. & STARK, A. 2014. Transcriptional enhancers: from properties to genome-wide predictions. *Nature reviews. Genetics*, 15, 272-86.
- SINCLAIR, A. J., PALMERO, I., PETERS, G. & FARRELL, P. J. 1994. EBNA-2 and EBNA-LP cooperate to cause G0 to G1 transition during immortalization of resting human B lymphocytes by Epstein-Barr virus. *Embo j*, 13, 3321-8.
- SIONOV, R. V., VLAHOPOULOS, S. A. & GRANOT, Z. 2015. Regulation of Bim in Health and Disease. *Oncotarget*, 6, 23058-23134.
- SKALSKA, L., WHITE, R. E., FRANZ, M., RUHMANN, M. & ALLDAY, M. J. 2010. Epigenetic Repression of p16INK4A by Latent Epstein-Barr Virus Requires the Interaction of EBNA3A and EBNA3C with CtBP. *PLOS Pathogens*, 6, e1000951.
- SKALSKA, L., WHITE, R. E., PARKER, G. A., TURRO, E., SINCLAIR, A. J., PASCHOS, K. & ALLDAY, M. J. 2013. Induction of p16(INK4a) is the major barrier to proliferation when Epstein-Barr

- virus (EBV) transforms primary B cells into lymphoblastoid cell lines. *PLoS Pathog*, 9, e1003187.
- SMITH, E. M., AKERBLAD, P., KADESCH, T., AXELSON, H. & SIGVARDSSON, M. 2005. Inhibition of EBF function by active Notch signaling reveals a novel regulatory pathway in early B-cell development. *Blood*, 106, 1995-2001.
- SPENDER, L. C., CORNISH, G. H., SULLIVAN, A. & FARRELL, P. J. 2002. Expression of Transcription Factor AML-2 (RUNX3, CBF α -3) Is Induced by Epstein-Barr Virus EBNA-2 and Correlates with the B-Cell Activation Phenotype. *Journal of Virology*, 76, 4919-4927.
- SPENDER, L. C., LUCCHESI, W., BODELON, G., BILANCIO, A., KARSTEGEL, C. E., ASANO, T., DITTRICH-BREIHZOLZ, O., KRACHT, M., VANHAESEBROECK, B. & FARRELL, P. J. 2006. Cell target genes of Epstein-Barr virus transcription factor EBNA-2: induction of the p55 α regulatory subunit of PI3-kinase and its role in survival of EREB2.5 cells. *Journal of General Virology*, 87, 2859-2867.
- SPENDER, L. C., WHITEMAN, H. J., KARSTEGEL, C. E. & FARRELL, P. J. 2005. Transcriptional cross-regulation of RUNX1 by RUNX3 in human B cells. *Oncogene*, 24, 1873.
- SPOONER, C. J., CHENG, J. X., PUJADAS, E., LASLO, P. & SINGH, H. 2009. A Recurrent Network Involving the Transcription Factors PU.1 and Gfi1 Orchestrates Innate and Adaptive Immune Cell Fates. *Immunity*, 31, 576-586.
- STADHOUDERS, R., FILION, G. J. & GRAF, T. 2019. Transcription factors and 3D genome conformation in cell-fate decisions. *Nature*, 569, 345-354.
- STAYNOV, D. Z. 2000. DNase I digestion reveals alternating asymmetrical protection of the nucleosome by the higher order chromatin structure. *Nucleic acids research*, 28, 3092-3099.
- STERNER, D. E. & BERGER, S. L. 2000. Acetylation of histones and transcription-related factors. *Microbiol Mol Biol Rev*, 64, 435-59.
- STRASSER, A. 2005. The role of BH3-only proteins in the immune system. *Nat Rev Immunol*, 5, 189-200.
- SVEJSTRUP, J. Q., VICHI, P. & EGLY, J.-M. 1996. The multiple roles of transcription/repair factor TFIIH. *Trends in Biochemical Sciences*, 21, 346-350.
- TAGAWA, H., KARNAN, S., SUZUKI, R., MATSUO, K., ZHANG, X., OTA, A., MORISHIMA, Y., NAKAMURA, S. & SETO, M. 2005. Genome-wide array-based CGH for mantle cell lymphoma: identification of homozygous deletions of the proapoptotic gene BIM. *Oncogene*, 24, 1348-58.
- TAKATA, M., SABE, H., HATA, A., INAZU, T., HOMMA, Y., NUKADA, T., YAMAMURA, H. & KUROSAKI, T. 1994. Tyrosine kinases Lyn and Syk regulate B cell receptor-coupled Ca²⁺ mobilization through distinct pathways. *Embo j*, 13, 1341-9.
- TEMPERA, I., DE LEO, A., KOSENKOV, A. V., CESARONI, M., SONG, H., DAWANY, N., SHOWE, L., LU, F., WIKRAMASINGHE, P. & LIEBERMAN, P. M. 2016. Identification of *MEF2B*, *EBF1*, and *IL6R* as Direct Gene Targets of Epstein-Barr Virus (EBV) Nuclear Antigen 1 Critical for EBV-Infected B-Lymphocyte Survival. *Journal of Virology*, 90, 345.
- THINNES, C. C., ENGLAND, K. S., KAWAMURA, A., CHOWDHURY, R., SCHOFIELD, C. J. & HOPKINSON, R. J. 2014. Targeting histone lysine demethylases - progress, challenges, and the future. *Biochim Biophys Acta*, 1839, 1416-32.
- THORLEY-LAWSON, D. A. 2015. EBV Persistence--Introducing the Virus. *Current topics in microbiology and immunology*, 390, 151-209.
- THORLEY-LAWSON, D. A. & ALLDAY, M. J. 2008. The curious case of the tumour virus: 50 years of Burkitt's lymphoma. *Nat Rev Microbiol*, 6, 913-24.
- TIMMS, J. M., BELL, A., FLAVELL, J. R., MURRAY, P. G., RICKINSON, A. B., TRAVERSE-GLEHEN, A., BERGER, F. & DELECLUSE, H. J. 2003. Target cells of Epstein-Barr-virus (EBV)-positive

- post-transplant lymphoproliferative disease: similarities to EBV-positive Hodgkin's lymphoma. *Lancet*, 361, 217-23.
- TOMKINSON, B., ROBERTSON, E. & KIEFF, E. 1993. Epstein-Barr virus nuclear proteins EBNA-3A and EBNA-3C are essential for B-lymphocyte growth transformation. *J Virol*, 67, 2014-25.
- TONG, X., DRAPKIN, R., REINBERG, D. & KIEFF, E. 1995a. The 62- and 80-kDa subunits of transcription factor IIH mediate the interaction with Epstein-Barr virus nuclear protein 2. *Proceedings of the National Academy of Sciences of the United States of America*, 92, 3259-3263.
- TONG, X., WANG, F., THUT, C. J. & KIEFF, E. 1995b. The Epstein-Barr virus nuclear protein 2 acidic domain can interact with TFIIB, TAF40, and RPA70 but not with TATA-binding protein. *Journal of Virology*, 69, 585-588.
- TORRES, R. M., FLASWINKEL, H., RETH, M. & RAJEWSKY, K. 1996. Aberrant B Cell Development and Immune Response in Mice with a Compromised BCR Complex. *Science*, 272, 1804-1808.
- TRAVIS, A., HAGMAN, J. & GROSSCHEDL, R. 1991. Heterogeneously initiated transcription from the pre-B- and B-cell-specific mb-1 promoter: analysis of the requirement for upstream factor-binding sites and initiation site sequences. *Mol Cell Biol*, 11, 5756-66.
- TZELLOS, S. & FARRELL, P. J. 2012. Epstein-barr virus sequence variation-biology and disease. *Pathogens*, 1, 156-74.
- VAN ATTIKUM, H., FRITSCH, O. & GASSER, S. M. 2007. Distinct roles for SWR1 and INO80 chromatin remodeling complexes at chromosomal double-strand breaks. *The EMBO Journal*, 26, 4113-4125.
- VAN NOESEL, C. J., VAN LIER, R. A., CORDELL, J. L., TSE, A. G., VAN SCHIJNDEL, G. M., DE VRIES, E. F., MASON, D. Y. & BORST, J. 1991. The membrane IgM-associated heterodimer on human B cells is a newly defined B cell antigen that contains the protein product of the mb-1 gene. *The Journal of Immunology*, 146, 3881-3888.
- VENTURA, A., YOUNG, A. G., WINSLOW, M. M., LINTAULT, L., MEISSNER, A., ERKELAND, S. J., NEWMAN, J., BRONSON, R. T., CROWLEY, D., STONE, J. R., JAENISCH, R., SHARP, P. A. & JACKS, T. 2008. Targeted deletion reveals essential and overlapping functions of the miR-17 through 92 family of miRNA clusters. *Cell*, 132, 875-86.
- VOCKERODT, M., MORGAN, S. L., KUO, M., WEI, W., CHUKWUMA, M. B., ARRAND, J. R., KUBE, D., GORDON, J., YOUNG, L. S., WOODMAN, C. B. & MURRAY, P. G. 2008. The Epstein-Barr virus oncoprotein, latent membrane protein-1, reprograms germinal centre B cells towards a Hodgkin's Reed-Sternberg-like phenotype. *J Pathol*, 216, 83-92.
- WALPORT, L. J., HOPKINSON, R. J. & SCHOFIELD, C. J. 2012. Mechanisms of human histone and nucleic acid demethylases. *Curr Opin Chem Biol*, 16, 525-34.
- WALTZER, L., LOGEAT, F., BROU, C., ISRAEL, A., SERGEANT, A. & MANET, E. 1994. The human J kappa recombination signal sequence binding protein (RBP-J kappa) targets the Epstein-Barr virus EBNA2 protein to its DNA responsive elements. *The EMBO journal*, 13, 5633-5638.
- WANG, F., TSANG, S. F., KURILLA, M. G., COHEN, J. I. & KIEFF, E. 1990. Epstein-Barr virus nuclear antigen 2 transactivates latent membrane protein LMP1. *Journal of Virology*, 64, 3407-3416.
- WANG, L., GROSSMAN, S. R. & KIEFF, E. 2000. Epstein-Barr virus nuclear protein 2 interacts with p300, CBP, and PCAF histone acetyltransferases in activation of the LMP1 promoter. *Proceedings of the National Academy of Sciences of the United States of America*, 97, 430-435.
- WANG, Y., WYSOCKA, J., SAYEGH, J., LEE, Y. H., PERLIN, J. R., LEONELLI, L., SONBUCHNER, L. S., MCDONALD, C. H., COOK, R. G., DOU, Y., ROEDER, R. G., CLARKE, S., STALLCUP, M. R., ALLIS, C. D. & COONROD, S. A. 2004. Human PAD4 regulates histone arginine methylation levels via demethylination. *Science*, 306, 279-83.

- WESTHOFF SMITH, D. & SUGDEN, B. 2013. Potential cellular functions of Epstein-Barr Nuclear Antigen 1 (EBNA1) of Epstein-Barr Virus. *Viruses*, 5, 226-40.
- WHITE, R. E., GROVES, I. J., TURRO, E., YEE, J., KREMMER, E. & ALLDAY, M. J. 2010. Extensive Co-Operation between the Epstein-Barr Virus EBNA3 Proteins in the Manipulation of Host Gene Expression and Epigenetic Chromatin Modification. *PLoS ONE*, 5, e13979.
- WHITE, R. E., RAMER, P. C., NARESH, K. N., MEIXLSPERGER, S., PINAUD, L., ROONEY, C., SAVOLDO, B., COUTINHO, R., BODOR, C., GRIBBEN, J., IBRAHIM, H. A., BOWER, M., NOURSE, J. P., GANDHI, M. K., MIDDELDORP, J., CADER, F. Z., MURRAY, P., MUNZ, C. & ALLDAY, M. J. 2012. EBNA3B-deficient EBV promotes B cell lymphomagenesis in humanized mice and is found in human tumors. *J Clin Invest*, 122, 1487-502.
- WHYTE, WARREN A., ORLANDO, DAVID A., HNISZ, D., ABRAHAM, BRIAN J., LIN, CHARLES Y., KAGEY, MICHAEL H., RAHL, PETER B., LEE, TONG I. & YOUNG, RICHARD A. 2013. Master Transcription Factors and Mediator Establish Super-Enhancers at Key Cell Identity Genes. *Cell*, 153, 307-319.
- WIENANDS, J. 2000. The B-cell antigen receptor: formation of signaling complexes and the function of adaptor proteins. *Curr Top Microbiol Immunol*, 245, 53-76.
- WILLIS, S. N. & ADAMS, J. M. 2005. Life in the balance: how BH3-only proteins induce apoptosis. *Curr Opin Cell Biol*, 17, 617-25.
- WILSON, A., MACDONALD, H. R. & RADTKE, F. 2001. Notch 1-deficient common lymphoid precursors adopt a B cell fate in the thymus. *J Exp Med*, 194, 1003-12.
- WOISETSCHLAEGER, M., JIN, X. W., YANDAVALA, C. N., FURMANSKI, L. A., STROMINGER, J. L. & SPECK, S. H. 1991. Role for the Epstein-Barr virus nuclear antigen 2 in viral promoter switching during initial stages of infection. *Proceedings of the National Academy of Sciences of the United States of America*, 88, 3942-3946.
- WOOD, C. D., VEENSTRA, H., KHASNIS, S., GUNNELL, A., WEBB, H. M., SHANNON-LOWE, C., ANDREWS, S., OSBORNE, C. S. & WEST, M. J. 2016. MYC activation and BCL2L1 silencing by a tumour virus through the large-scale reconfiguration of enhancer-promoter hubs. *eLife*, 5, e18270.
- WORKMAN, J. L. 2006. Nucleosome displacement in transcription. *Genes & Development*, 20, 2009-2017.
- WU, D. Y., KALPANA, G. V., GOFF, S. P. & SCHUBACH, W. H. 1996. Epstein-Barr virus nuclear protein 2 (EBNA2) binds to a component of the human SNF-SWI complex, hSNF5/Ini1. *Journal of Virology*, 70, 6020-8.
- YAMADA, T., FISCHLE, W., SUGIYAMA, T., ALLIS, C. D. & GREWAL, S. I. 2005. The nucleation and maintenance of heterochromatin by a histone deacetylase in fission yeast. *Mol Cell*, 20, 173-85.
- YANG, X.-J. & SETO, E. 2008. The Rpd3/Hda1 family of lysine deacetylases: from bacteria and yeast to mice and men. *Nature Reviews Molecular Cell Biology*, 9, 206.
- YANG, X. J. & SETO, E. 2007. HATs and HDACs: from structure, function and regulation to novel strategies for therapy and prevention. *Oncogene*, 26, 5310.
- YOUNG, L., ALFIERI, C., HENNESSY, K., EVANS, H., O'HARA, C., ANDERSON, K. C., RITZ, J., SHAPIRO, R. S., RICKINSON, A., KIEFF, E. & ET AL. 1989. Expression of Epstein-Barr virus transformation-associated genes in tissues of patients with EBV lymphoproliferative disease. *N Engl J Med*, 321, 1080-5.
- YOUNG, L. S. & RICKINSON, A. B. 2004. Epstein-Barr virus: 40 years on. *Nat Rev Cancer*, 4, 757-768.
- YOUNG, R. M. & STAUDT, L. M. 2013. Targeting pathological B cell receptor signalling in lymphoid malignancies. *Nat Rev Drug Discov*, 12, 229-43.
- ZARATIEGUI, M., IRVINE, D. V. & MARTIENSSSEN, R. A. 2007. Noncoding RNAs and gene silencing. *Cell*, 128, 763-76.

- ZHANG, Y., LIU, T., MEYER, C. A., ECKHOUTE, J., JOHNSON, D. S., BERNSTEIN, B. E., NUSBAUM, C., MYERS, R. M., BROWN, M., LI, W. & LIU, X. S. 2008. Model-based Analysis of ChIP-Seq (MACS). *Genome Biology*, 9, R137.
- ZHAO, B., MARUO, S., COOPER, A., M, R. C., JOHANNSEN, E., KIEFF, E. & CAHIR-MCFARLAND, E. 2006. RNAs induced by Epstein-Barr virus nuclear antigen 2 in lymphoblastoid cell lines. *Proc Natl Acad Sci U S A*, 103, 1900-5.
- ZHAO, B., ZOU, J., WANG, H., JOHANNSEN, E., PENG, C.-W., QUACKENBUSH, J., MAR, J. C., MORTON, C. C., FREEDMAN, M. L., BLACKLOW, S. C., ASTER, J. C., BERNSTEIN, B. E. & KIEFF, E. 2011a. Epstein-Barr virus exploits intrinsic B-lymphocyte transcription programs to achieve immortal cell growth. *Proceedings of the National Academy of Sciences*, 108, 14902-14907.
- ZHAO, B., ZOU, J., WANG, H., JOHANNSEN, E., PENG, C. W., QUACKENBUSH, J., MAR, J. C., MORTON, C. C., FREEDMAN, M. L., BLACKLOW, S. C., ASTER, J. C., BERNSTEIN, B. E. & KIEFF, E. 2011b. Epstein-Barr virus exploits intrinsic B-lymphocyte transcription programs to achieve immortal cell growth. *Proc Natl Acad Sci U S A*, 108, 14902-7.
- ZHOU, B., CRON, R. Q., WU, B., GENIN, A., WANG, Z., LIU, S., ROBSON, P. & BALDWIN, H. S. 2002. Regulation of the Murine Nfatc1 Gene by NFATc2. *Journal of Biological Chemistry*, 277, 10704-10711.
- ZHOU, H., SCHMIDT, STEFANIE C. S., JIANG, S., WILLOX, B., BERNHARDT, K., LIANG, J., JOHANNSEN, ERIC C., KHARCHENKO, P., GEWURZ, BENJAMIN E., KIEFF, E. & ZHAO, B. 2015. Epstein-Barr Virus Oncoprotein Super-enhancers Control B Cell Growth. *Cell Host & Microbe*, 17, 205-216.
- ZHUANG, Y., SORIANO, P. & WEINTRAUB, H. 1994. The helix-loop-helix gene E2A is required for B cell formation. *Cell*, 79, 875-884.
- ZUIN, J., DIXON, J. R., VAN DER REIJDEN, M. I. J. A., YE, Z., KOLOVOS, P., BROUWER, R. W. W., VAN DE CORPUT, M. P. C., VAN DE WERKEN, H. J. G., KNOCH, T. A., VAN IJCKEN, W. F. J., GROSVELD, F. G., REN, B. & WENDT, K. S. 2014. Cohesin and CTCF differentially affect chromatin architecture and gene expression in human cells. *Proceedings of the National Academy of Sciences*, 111, 996.

8. Appendices

8.1 Cell line summary

Cell line	EBV Status	Description	Reference
Burkitt's Lymphoma cell lines			
BL31	Negative	EBV negative BL cells derived from a 14 year old male.	Lenoir et al., 1985
BL31 Cell lines	Positive (Latency III)	BL31 cells infected with wild-type recombinant EBV or EBNA 3A, 3B, 3C knock-out and revertants EBVs	Anderton et al., 2008
BL2	Negative	EBV negative BL cells derived from a 7 year old male	Lenoir et al., 1985
BL2 Cell lines	Positive (Latency III)	BL2 cells infected with wild-type recombinant EBV or EBNA 3C knock-out and revertant EBVs	Anderton et al., 2008
Mutu III	Positive (Latency III)	African BL cells derived from a 7 year old black male. Mutu BL drifted spontaneously during culture to express a latency III pattern	Gregory et al., 1990
BL41K3	Negative	BL cells originally derived from a 8 year old male. Transfected with a plasmid expressing a conditionally active ER-EBNA2 fusion protein.	Lenoir et al., 1985 Kempkes et al., 1995
DG75	Negative	BL cells derived from a biopsy taken in 1975 from a 10 year old male	Ben-Bassat et al., 1977
DG75 CBF1KO	Negative	DG75 BL cells where CBF1/RBPJk gene has been deactivated by homologous recombination	Ben-Bassat et al., 1977 Maier et al., 2005

8.1 Cell line summary continued

Cell line	EBV Status	Description	Reference
B cell Lymphoma cell lines			
BJABK3	Negative	African Lymphoma originally classed as BL but lacks Myc translocation. Transfected with a plasmid expressing a conditionally active ER-EBNA2 fusion protein.	Klein et al., 1974 Kempkes et al., 1995
Lymphoblastoid Cell lines (LCL)			
GM12878	Positive (Latency III)	LCL transformed by EBV from the blood of a female donor from European decent	Coriell Cell Repositiries
ER-EB 2.5	Positive (Latency III)	EBV-immortalised LCL expressing a conditionally active ER-EBNA2 fusion protein	Kempkes et al., 1995

8.2 Plasmids used for transient transfections

Plasmid	Description	Company/Generated by
pGL3	Basic luciferase reporter vector	Promega
pSG5	Expression Vector	Stratagene
pSG5 2A	The entire EBNA 2 open reading frame of EBV strain W91 under the control of the SV40 early promoter in the vector pSG5	Gift from Prof. M. Rowe
pCMV-SPORT6 EBF-1	The pCMV_SPORT6 vector expressing EBF-1 under control of the CMV promoter	PlasmidID, Harvard Medical School
pGL3 CD79Ap1p2	A 0.63 kb fragment (approx. -1945 to -1302 relative to the predicted TSS) and a 0.97 kb fragment (approx. -509 to +449 relative to predicted transcription start site) of the CD79A promoter was synthesised by Life Technologies and the resulting 1.6 kb fragment was cloned into pGL3-Basic cut with NheI and HindIII.	Created by Opeoluwa Ojieniyi
pGL3 CD79Ap1	A 0.97 kb fragment (approximately -509 to +449 relative to predicted transcription start site) of the CD79A promoter was synthesised by Life Technologies and cloned into pGL3-Basic cut with XhoI and HindIII.	Created by Opeoluwa Ojieniyi
pGL3 CD79B	A 0.94 kb fragment (approximately -765 to +176 relative to predicted transcription start site) of the CD79B promoter was amplified from genomic DNA and cloned into pGL3-Basic cut with NheI and SacI.	Created by Opeoluwa Ojieniyi
pGL3-NFAT ₃	The pGL3 luciferase reporter vector containing 3 NFAT binding motifs upstream of the luciferase promoter	Clipstone and Crabtree (1992)
pRL TK	A Renilla reporter vector which is co-transfected with the luciferase reporter vector and provides weak constitutive expression of <i>Renilla</i> luciferase	Promega
pRL CMV	A renilla reporter vector which co-transfected with the luciferase reporter vector and provides strong and constitutive expression of <i>Renilla</i> luciferase	Promega

8.3 Antibodies used for Western Blot

Protein	Primary Antibody	Antibody species	Primary antibody dilution	Company/ generated by
EBNA3A	EBNA3A	Sheep polyclonal	1/500	Ex-Alpha Biologicals #F115P
EBNA3B	EBNA3B	Sheep polyclonal	1/500	Ex-Alpha Biologicals #F120P
EBNA3C	E3C A10	Mouse monoclonal	1/300	Prof. M. Rowe
Actin	Actin	Rabbit polyclonal	1/5000	Sigma #A2066
CD79A	CD79A	Rabbit polyclonal	1/100	Cell signalling Technology #3351
CD79B	CD79B	Rabbit polyclonal	1/500	Abcam #175399
NFATC1	NFAT2	Mouse monoclonal	1/1000	Abcam #2796
NFATC2	NFAT1	Mouse monoclonal	1/500	Abcam #2722
LMP1	CS1-4	Mouse monoclonal	1/200	Prof. M. Rowe
EBNA2	PE2	Mouse monoclonal	1/200	Prof. M. Rowe

Secondary Antibody	Secondary Antibody Dilution	Company
Anti-Rabbit-HRP	1/5000	Cell Signalling Technology
Anti-Mouse-HRP	1/5000	Cell Signalling Technology
Anti-Sheep-HRP	1/5000	Cell Signalling Technology

8.4 Antibodies used for CHIP-QPCR

Protein	Antibody	Antibody species	Quantity used (μ g)	Company/ generated by
EBNA2	PE2	Mouse monoclonal	8	M. Rowe
EBF-1	EBF-1	Mouse monoclonal	2	Santa Cruz # SC-137065
H3Ac	Acetyl-Histone H3	Rabbit polyclonal	5	MerckMillipore #06-599
EBNA3C	E3CD8	Mouse monoclonal	8	M. Rowe
EBNA3B	EBNA3B	Sheep monoclonal	8	Ex-Alpha Biologicals #F120P
IgG	Normal mouse IgG	Mouse monoclonal	8	Santa Cruz #sc-2025

Secondary Antibody	Quantity used (μ g)	Company
Rabbit Anti-Mouse IgG	13.5	Dako

8.5 Q-PCR Primers used for mRNA analysis

Description		Sequence (5' - 3')
GAPDH	MW84 F MW85 R	TCAAGATCATCAGCAATGCC CATGAGTCCTTCCACGATACC
CD79A	MW1751 F MW1752 R	CTGCCACCATCTTCCTCCTC GCCACGTGTAGTTGCCATG
CD79B	MW584 F MW585 R	AGCAGAGGAACACGCTGAA AGCCTTGCTGTCATCCTTGT
NFATC1	MW1690 F MW1691 R	GAGGACCAGGAGTTCGACTTC ACGTTGGAGGATGCATAGCC
NFATC2	MW1692 F MW1693 R	ACGAGCTTGACTTCTCCATCC GGCGACCTTATGTGCATTCC
Cp	MW302 F MW303 R	GATCAGATGGCATAGAGACAAGGAC AGGCTGTTTCTTCAGTC
MYC	MW1127 F MW1128 R	TCAAGAGGTGCCACGTCTCC TCTTGGCAGCAGGATAGTCCTT
B-2- Microglobulin	MW1447 F MW1448 R	TTAGCTGTGCTCGCGCTACTCT TGGTTCACACGGCAGGCATACT
BIM	MW1522 F MW1523 R	GCTGTCTCGATCCTCCAGTG GTAAACTCGTCTCCAATACG
PLCy2	MW1944 F MW1945 R	GCCTCAGAGAACCGTGAAAG GGATGGGAAGTACTGCTGGA
CD21	MW1132 F MW1133 R	TCTTGGCTCTCGTCGCAC TTATCACGGTACCAACAGCAATG

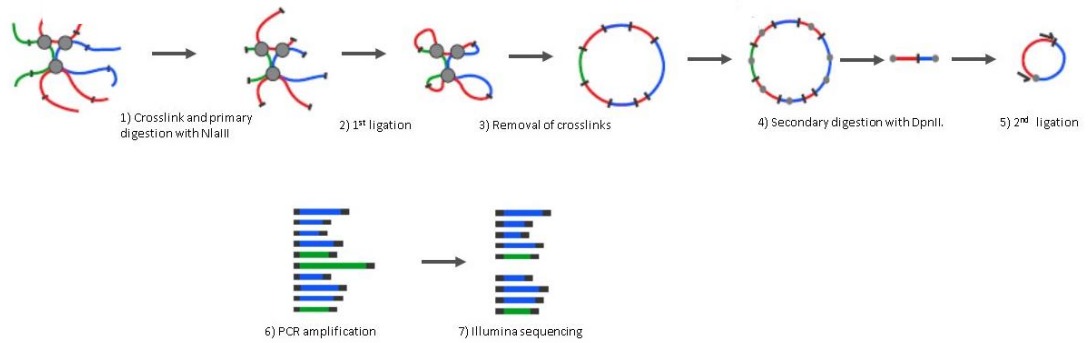
8.6 Q-PCR Primers used for CHIP-QPCR

Gene	Primer	EBNA Peak Relative to TSS	Sequence 5' to 3'
CD79B	MW 578_F	+38 bp	GGACAGAGCGGTGACCAT
	MW 579_R	+38 bp	GTTCTGTACCTGAGAGCAGCAG
NFATC1	MW1714_F	+5 kb	CCTGAGGACTTGACACAGA
	MW1715_R	+5 kb	ACTAGAGCCAGATCACCGGA
	MW1948_F	+36 kb	GAAAGCTCTCAGTTGCCGTG
	MW1949_R	+36 kb	AGCCTCGTTTCTGAAAAGCG
	MW1950_F	+54 kb	ACCTTCAGCTGCTATGGGTT
	MW1951_R	+54 kb	ATGAGGCCAACACCAGCTT
	MW1716_F	+59 kb	TGTGACTCTGAGCTTCTGG
	MW1717_R	+59 kb	AAGGCTGTGGTCCTCTGAAG
	MW1718_F	+65 kb	CAGTCTCGGCTTCATGAGA
	MW1719_R	+65 kb	CGATGGAGTCAGCAGCTAC
	MW1952_F	+73 kb	GAAGGGCTCCAATTGAAAGGG
	MW1953_R	+73 kb	ACACGCTCTGAGGACACG
	MW1720_F	+123 kb	GCTCCACGTACGGCTCTC
	MW1721_R	+123 kb	AGAGGACAGCACAGCAACC
NFATC2	MW1722_R	+142 kb	GCACAATGGCGCTATCTCAG
	MW1723_R	+142 kb	CAGACGGAGCCATCATGTGA
	MW1726_F	+81 kb	GGTGAAGTCTTGACCTCTGCT
	MW1727_R	+81 kb	TATGACGTGCCAGAATCCAGG
	MW1954_F	+16 kb	CTTCGCCGTAATTAAGCAGC
	MW1955_R	+16 kb	AGATGCAGGAAGGAACCAGG
PLCγ2	MW1946_F	+21 kb	CTGCGTCTTCTGCTCCT
	MW1947_R	+21 kb	CATCCTGGAGTGGCTGGTAG

8.7 PCR primers used for 4C and 3C

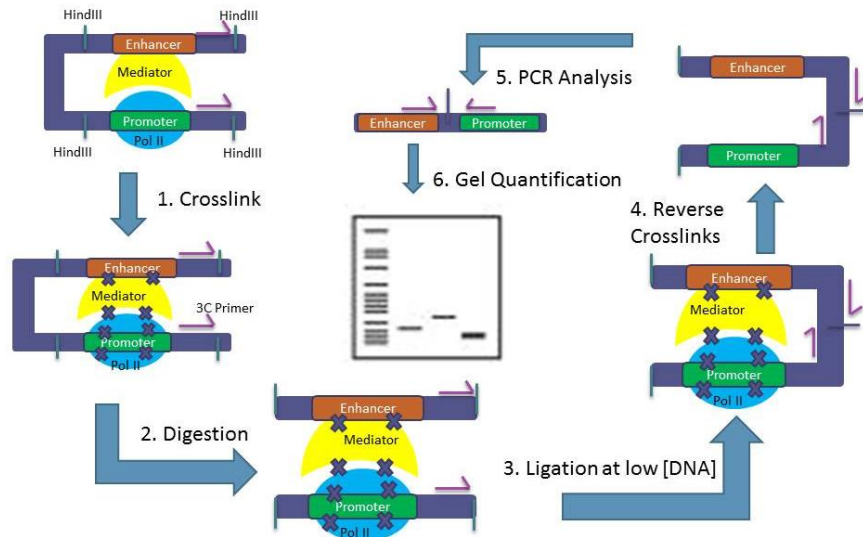
Experiment	ID	Description	Sequence (Illumina sequencing overhang (RED), Unique barcode (Green), 4C ligation product (Black))
4C primers	MYC P5 TSBC02	TSBC02 CGATGT	AATGATACGGCGACCACCGAGAACAACACTCTTTCCCTACACGACGCTCTCCGAT CTCGATGAGCTGCTGGGAGGAGACATG
	MYC P5 TSBC04	TSBC04 TGACCA	AATGATACGGCGACCACCGAGAACAACACTCTTTCCCTACACGACGCTCTCCGAT CTTGACCAAGCTGCTGGGAGGAGACATG
	MYC P5 TSBC05	TSBC05 ACAGTG	AATGATACGGCGACCACCGAGAACAACACTCTTTCCCTACACGACGCTCTCCGAT CTACAGTGAGCTGCTGGGAGGAGACATG
	MYC P5 TSBC06	TSBC06 GCCAAT	AATGATACGGCGACCACCGAGAACAACACTCTTTCCCTACACGACGCTCTCCGAT CTGCCAATAGCTGCTGGGAGGAGACATG
	MYC P5 TSBC07	TSBC07 CAGATC	AATGATACGGCGACCACCGAGAACAACACTCTTTCCCTACACGACGCTCTCCGAT CTCAGATCAGCTGCTGGGAGGAGACATG
	MYC P5 TSBC12	TSBC12 CTTGTA	AATGATACGGCGACCACCGAGAACAACACTCTTTCCCTACACGACGCTCTCCGAT CTCTTGTAAGCTGCTGGGAGGAGACATG
	MYC P7		CAAGCAGAAGACGGCATAACGACCAACGTCCTAACACCTCTAG
3C primers	MW1312	MYC promoter	TGCAGAAGGTCCGAAGAAAG
	MW1330	MYC 168/186 1	GGTTCCTGACACTCCATTCC
	MW1577	MYC 428	GAAGTAGAAGGGACCCAGGC
	MW1369	MYC 566 3	TTGTCATCAGTCTCACGGCA
	MW1540	MYC 1.8	CCAACCTACCTTGTCACCT
	MW1204	BCL2L11 promoter	CATGAAAATGCTCCCCATA
	MW1206	ACOXL promoter	GATTTGAGGCAAGCAGAAGG
	MW1205	ACOXL 1	TGTTGCTTAGGGGATTGGAG
	MW1207	ACOXL 2	ATGTTACCATTGGGCGAAAC
	MW1208	ACOXL 3	CTCAAGTGATCTGCCACCT
	MW1211	BCL2L11 control	TTGCCATGGGTTTAATGTCA
	MW1222	BCL2L11 4	CCCCACAAAACCAACTTCAT
	MW1223	BCL2L11 5	GTGGGAGGTGACTGGATCAT
	MW1224	BCL2L11 6	CCTGAAGACGCAAGAAGACC
	MW1579	BCL2L11 C4	AAGCTGACATCTGGACTCCC
	MW1580	BCL2L11 C3	GGCTCAGTGTCTTTCCTGC
	MW1581	BCL2L11 C2	ACAGGCGTAGAGACCAATGG

8.8 The 4C technique workflow



A simplified flow diagram of the 4C technique 1) Crosslinking of DNA:Protein and protein:protein interactions and primary restriction enzyme digestion, 2) Ligation under dilute conditions, 3) Reverse the crosslinks, 4) Secondary digestion, 5) Ligation under dilute conditions, 6) PCR amplify, 7) Illumina sequencing.

8.9 3C technique workflow



A simplified flow diagram of the 3C technique. 1) Crosslinking of DNA:Protein and protein:protein interactions, 2) restriction enzyme digestion, 3) ligation at low DNA, 4) Reverse the crosslinks, 5) PCR analysis and gel electrophoresis (6)